

File ID 134436
Filename Thesis
Version Final published version (publisher's pdf)

SOURCE (OR PART OF THE FOLLOWING SOURCE):

Type Dissertation
Title Unknitting the black hole : black holes as effective geometries
Author I. Messamah
Faculty Faculty of Science
Year 2009
Pages X, 208
ISBN 978-90-5776-192-8

FULL BIBLIOGRAPHIC DETAILS:

<http://dare.uva.nl/record/304859>

Copyright

It is not permitted to download or to forward/distribute the text or part of it without the consent of the author(s) and/or copyright holder(s), other than for strictly personal, individual use.

UNKNITTING THE BLACK HOLE

BLACK HOLES AS EFFECTIVE GEOMETRIES

UNKNITTING THE BLACK HOLE

BLACK HOLES AS EFFECTIVE GEOMETRIES

ACADEMISCH PROEFSCHRIFT

ter verkrijging van de graad van doctor

aan de Universiteit van Amsterdam

op gezag van de Rector Magnificus

Prof. dr. D.C. van den Boom

ten overstaan van een door het college voor promoties

ingestelde commissie,

in het openbaar te verdedigen in de Agnietenkapel

op dinsdag 9 juni 2009, te 12:00 uur

door

ILIES MESSAMAH

geboren te Bouzina, ALGERIJE

PROMOTIECOMMISSIE

PROMOTOR

Prof. dr J. de Boer

OVERIGE LEDEN

Prof. dr. V. Balasubramanian

Prof. dr. E.A. Bergshoeff

Prof. dr. R.H. Dijkgraaf

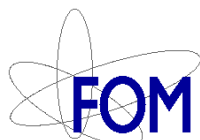
Prof. dr. E.P. Verlinde

Prof. dr. B.Q.P.J. de Wit

Dr. M. Taylor

FACULTEIT DER NATUURWETENSCHAPPEN, WISKUNDE EN INFORMATICA

ISBN 978-90-5776-192-8



This work is part of the research program of the “Stichting voor Fundamenteel Onderzoek der Materie (FOM)”, which is financially supported by the “Nederlandse Organisatie voor Wetenschappelijk Onderzoek (NWO)”.

PUBLICATIONS

This thesis is based on the following publications:

★

- ① Alday, Luis F. and de Boer, Jan and Messamah, Ilies,
What is the dual of a dipole?,
Nucl. Phys. **B746** (2006) 29–57 [hep-th/0511246].
- ② Alday, Luis F. and de Boer, Jan and Messamah, Ilies,
The gravitational description of coarse grained microstates,
JHEP **12** (2006) 063 [hep-th/0607222].
- ③ de Boer, Jan and Denef, Frederik and El-Showk, Sheer and Messamah, Ilies
and Van den Bleeken, Dieter,
Black hole bound states in $AdS_3 \times S^2$,
JHEP **11** (2008) 050 [0802.2257 [hep-th]].
- ④ de Boer, Jan and El-Showk, Sheer and Messamah, Ilies and Van den Bleeken,
Dieter,
Quantizing $\mathcal{N} = 2$ multicenter solutions,
[0807.4556 [hep-th]].
- ⑤ Balasubramanian, Vijay and de Boer, Jan and El-Showk, Sheer and Messamah, Ilies,
Black Holes as Effective Geometries,
Class. Quant. Grav. **25:214004** (2008) [arXiv:0811.0263 [hep-th]].
- ⑥ de Boer, Jan and El-Showk, Sheer and Messamah, Ilies and Van den Bleeken,
Dieter,
To appear.

CONTENTS

Preface	1
I From Black Holes to Microstates	11
1 Four Dimensional Black Holes	15
1.1 Black Holes in General Relativity	15
1.1.1 Black Holes	16
1.1.2 Killing Horizons and Surface Gravity	18
1.2 The Laws of Black Hole Mechanics	18
1.2.1 Kumar Integrals	18
1.2.2 Black Hole Laws	19
1.3 Black Holes as Thermodynamical Objects	20
1.3.1 A Free Scalar Field and Bogoliubov Transformations	20
1.3.2 Hawking Radiation	23
1.4 Consequences of the Black Hole Radiation	27
1.4.1 Black Hole Evaporation and Information Loss	28
1.4.2 Gravity as an Effective Description	28
2 The Fuzzball Machinery	29
2.1 Black Holes of Interest to Us	30
2.1.1 BPS-ness, Linearity and AdS/CFT	30
2.1.2 Beyond AdS/CFT?	34
2.1.3 The Guinea Pigs	35
2.2 Black Hole Ensemble	37
2.2.1 The No-Hair Theorem, Entropy and Geometry	37
2.2.2 At Which Level Can we Trust Our geometries	38
2.3 Phase Space Quantization	39
2.3.1 Solution Space, Phase Space and the Symplectic Form	40
2.3.2 Quantization	42

2.4	Coarse Graining	43
2.4.1	Coarse Graining as an Average	43
2.4.2	Another Possibility: Typical States	44
II	D1-D5 System and Coarse Graining	45
3	The Lunin-Mathur (LM) Geometries	49
3.1	The Five Dimensional “Small” Black Hole	49
3.1.1	The Set-Up	50
3.1.2	The Geometry	50
3.2	The Lunin-Mathur (LM) Geometries	52
3.2.1	Switching to the FP System	52
3.2.2	The LM Geometries	52
3.3	The Symplectic Form and Quantization	53
3.3.1	The Symplectic Form	54
3.3.2	Quantization	55
4	Simple Ensembles and Their Coarse Graining	57
4.1	Interlude: Phase Space Densities	58
4.1.1	Why Phase Space Densities?	58
4.1.2	Wigner vs Husimi Distribution	59
4.2	Mapping States to Geometries	61
4.2.1	From States to Geometries	61
4.2.2	Avoiding Red Traffic Lights	63
4.3	A First Look at Thermodynamical Ensembles	69
4.4	The Survival of the No-Hair Theorem	71
4.5	Thermal Ensembles and Condensation	73
4.6	The “Small” Black Ring	76
4.6.1	Describing the “Condensate” Ensemble	76
4.6.2	The Small Black Ring Effective Geometry	77
4.6.3	Avoiding the No-Hair Theorem	78
4.7	The Conical Defect Metric	79
III	Towards Macroscopic Black Holes in the Fuzzball Realm	83
5	Black Constellations in Four Dimensions	87
5.1	From Ten to Four Dimensions	88
5.1.1	Walking the Path of Reduction	88
5.1.2	The Special Kähler Geometry	90
5.2	Spherical Symmetry and Attractor Flow	93

5.2.1	Supersymmetry and Attractor Flow	93
5.2.2	The One Centered Black Hole	95
5.3	Bubbles and Bound Black Holes	97
5.3.1	More than One Center	97
5.3.2	Useful Properties	98
5.4	BPS States Counting	100
5.4.1	The Family Tree	100
5.4.2	Missing States: Wall Crossing	102
6	Setting the Stage for Fuzzballs	105
6.1	From the Symplectic Form to Quantization	106
6.1.1	Open Strings and Symplectic Form	108
6.1.2	Kähler Geometry and Geometric Quantization	110
6.2	Quantization at Work	114
6.2.1	Behind the Scene: Toric Kähler Manifolds	115
6.2.2	Inviting Fermions to the Party	119
6.2.3	Treasure Hunt: Degeneracy	120
6.3	Simple Bound Black Hole Systems	121
6.3.1	The Two-Center Case	122
6.3.2	The Three-Center Case	123
6.3.3	Comparison to the Split Attractor Flow Picture	129
6.4	Dipole Halos	131
6.4.1	Meet the Dipole Halo	132
6.4.2	Degeneracy Using Attractor Tree	135
6.4.3	Degeneracy Using Toric Techniques	137
6.5	Scaling Solutions and Fuzzballs	140
6.5.1	D6- $\overline{\text{D}6}$ -D0 Crush and its Quantization	141
6.5.2	Not Enough States	142
6.5.3	Beyond Supergravity?	143
6.6	Large Scale Quantum Effects	145
IV	Conclusion and Discussion	149
7	Conclusions	151
7.1	So Far so Good	151
7.2	Looking to the Future	153
V	Appendices	155
A	Squeezed States and Negative Energy Density	157

A.1	Squeezed States	157
A.2	Negative Energy Density	158
B	A Quick Trip in Ten Dimensions	159
B.1	Ten-Dimensional Supergravity	159
B.1.1	Type-IIA Supergravity	160
B.1.2	Type-IIB Supergravity	160
B.2	D-Branes in Supergravity	161
B.2.1	Electric and Magnetic D-Branes	162
B.2.2	The Backreacted Dp-Brane	162
B.3	T and S Dualities	163
B.3.1	T-Duality and Buscher Rules	163
B.3.2	Type-IIB and S-Duality	163
C	The D1-D5 Generating Function	165
C.1	Simple Phase Space Densities	166
C.2	The Monochromatic State	167
C.3	The Generic Thermodynamical Ensemble	168
D	Calabi-Yau Manifolds and String Compactification	169
D.1	From Kähler to Calabi-Yau Manifolds	169
D.2	Cohomology of Calabi-Yau Manifolds	171
D.3	Compactification	171
D.3.1	Some General Remarks on Compactification	172
D.3.2	Type-IIA on a Calabi-Yau	174
E	Adding Fermions	177
E.1	Calculating the determinant	177
E.2	Properties of $A(l)$	178
F	The Three-Center Solution Space	179
	Bibliography	183
	Summary	197
	Samenvatting	201
	Acknowledgements	207

PREFACE

In this thesis, we will try to shed some light on the origin of black hole geometries in the context of the fuzzball proposal. The claim is that black holes are an effective description of an exponentially large number of smooth geometries. These geometries are hardly distinguishable from the black hole geometry outside the black hole horizon, and hence, can be seen as describing the same physics. In other words, these smooth geometries can be thought of as a manifestation of the black hole degrees of freedom whose number should reproduce the black hole entropy.

Though the idea described above is elegant, putting it to work is far from trivial. This is mainly due to the complicated nature of the gravitational equations. A way to overcome such an inconvenience is to appeal to as many symmetries as we need to gain control over our solutions. This is the strategy we will be using in this thesis. We will concentrate on two stringy systems which are tamed by their symmetries. The first one is the D1-D5 system which will be the study material of the second part. As it will be shown subsequently, this system turns out to be a successful testing ground for most of the fuzzball ideas. However, the D1-D5 system comes with a serious drawback; it is not quite a black hole as it has a vanishing horizon area. This motivates us to look for other black hole solutions with a large horizon but still under enough control. Such requirements are satisfied by a special class of black hole solutions of the $\mathcal{N} = 2$ four-dimensional supergravity. These black holes will be the subject of the third part of this thesis. Although, by requiring a large horizon we had to sacrifice simplicity, there are still enough symmetries to address some simple fuzzball questions regarding these black holes.

We close by a discussion about the successes, limitations, and some open questions of this program. Some technical details will be left to the appendices. Before embarking into this fascinating journey to visit our special classes of black holes, we will make a small detour in the first part of this thesis. The latter contains a review of the Hawking radiation of black holes, as well as a discussion of the general philosophy of the fuzzball scenario.

Preface

INTRODUCTION AND MOTIVATION

The beginning of the last century was marked by the emergence of two fascinating theories that led to a revolution in our way of thinking about nature: general relativity and quantum field theory. For a long time, physicists did not worry about the possible incompatibility of the two theories because they had different domains of applicability: general relativity was concerned with large distance physics (planets, galaxies, ...), while quantum field theory dealt with short distances (molecules, atoms, ...). The necessity of reconciling the two theories emerged with the study of quantum field theories in the presence of black holes following the seminal work of Hawking [1]. To the surprise of everybody, black holes seemed at the time to be in conflict with well established and cherished principles of modern physics.

Trying to understand black holes is the main subject of this thesis, but before going into technical details, we will first try to explain in simple words what is the problem with black holes, and what are the ideas explored in this thesis to understand them.

I-BLACK HOLES: CLASSICAL VS SEMI-CLASSICAL

One of the most puzzling objects that general relativity predicts are black holes. Classically, they are boring objects completely fixed once one is given the values of charges at infinity, this is the acclaimed no-hair theorem (See e.g. [2]). This picture changes drastically once quantum effects are taken into account. Black holes behave like thermodynamical objects [3, 1, 4]; they possess entropy, temperature ... etc. This naive “marriage” between classical general relativity and quantum field theory, the so-called “*semi-classical quantum gravity*”, leads to several paradoxes which are:

1-ENTROPY, HORIZON AREA AND HOLOGRAPHY

Entropy, as we know from statistical physics, is a quantity that measures the number of degrees of freedom of a system. According to the no-hair theorem, the entropy of a black hole should be zero. This is in clear conflict with what we have learned from semi-classical analysis: a black hole has an entropy proportional to its horizon area. The situation does not improve in the case where the uniqueness is violated, which happens in five dimensions for example [5, 6]. Even in this case, one still has far less degeneracy to account for the exponential number of black hole states. A possible way out would be to declare that these states are inherently quantum with no classical limit. However, this leaves the question of the entropy not being proportional to a volume, a logical guess based on extensivity, unanswered. To explain such an unexpected property, it was suggested that quantum gravity is holographic in nature [7, 8]: quantum gravity in d dimensions should somehow be equivalent to a field theory without gravity in one dimension less. String theory gives a concrete realization of this idea that goes under the name of “*AdS/CFT correspondence*”, where, gravity (string theory) on AdS spacetime is equivalent to a conformal field theory that lives on the boundary of AdS [9].

2-INFORMATION LOSS PARADOX AND UNITARITY

Classically black holes are greedy objects; nothing escapes once the horizon is crossed. However, quantizing fields in a black hole background shows that the latter thermally radiates [4], and as a consequence, evaporates completely. It turns out that this radiation does not care about the state of the matter that collapsed to form the black hole, which is a potential source of information loss. However, as will be explained in the next chapter, this is due to the limitation of our derivation and is not of a fundamental origin. The other origin of information loss, which should be taken seriously, is the entangled nature of the radiation. In simple words, the radiated particles are correlated with “anti-particles” that fall behind the horizon. The information is lost when the black hole evaporates completely destroying part of the information. As a result, we are faced with the following dilemma:

- Information is lost [10], and one should drop the requirement of unitarity in the presence of gravitation.
- The semiclassical approximation breaks down, and quantum gravity becomes important at scales bigger than the natural Planck scale; see e.g. [11]. Essentially this is because, as we will see later (section 1.3.2), the Hawking radiation depends on the local physics around the black hole horizon. For large enough black holes, the curvature will be small everywhere near the horizon; and

hence, Hawking calculation will remain valid if the quantum effects are not enhanced. As a result, in the absence of such large quantum effects information will be lost after the complete evaporation of the black hole.

String theory, through AdS/CFT, suggests that gravity is unitary but does not shed light on how information is restored yet.

3-WHAT ABOUT THE BLACK HOLE SINGULARITY?

Classically, every black hole has a singularity where the curvature blows up. As a result, general relativity breaks down in a region surrounding this singularity. We do not even know how to formulate physics laws in that region. Even worse, the predictability of physics at a point in spacetime is destroyed whenever these singularities are in the past lightcone of this point. To avoid such a wild behavior, the “*cosmic censorship*” was conjectured [12]: every singularity should be shielded by a horizon that causally disconnects us from it. Sadly, such a conjecture fails in some cases, see e.g. [13, 14]. Another widely accepted way out, which remains to be checked, is that the full theory of quantum gravity should resolve singularities.

II-BLACK HOLES AND STRING THEORY

One of the highly controversial predictions of string theory is the existence of six extra dimensions. Despite that, this turns out to be a key point in black hole physics as we will explain in a moment. Before that, let us first understand how black holes emerge in string theory. To do so, we will take a quick look at the objects described by string theory.

String theory, as its name indicates, is a theory of vibrating strings, which means that its fundamental objects are one-dimensional extended objects. But, strings are not the only extended objects in string theory. A quick way to see that is to study open strings. In principle, one can imagine attaching the ends of the open string to an extended object called a “*D-brane*”. In such a situation, there will be a leak of energy from the open string to the D-brane which already tells us that these D-branes are heavy objects. What this does not tell us is that D-branes carry also a charge like an electron which is true.

All in all, string theory is formulated on a ten-dimensional spacetime and describes on top of strings, the dynamics of a host of extended, charged, and massive objects called “D-branes”. But, what have these properties to do with black holes? To understand that, let us discuss a toy model where we live in a two-dimensional

spacetime \mathbb{R}^2 (time plus a one-dimensional space \mathbb{R}) but string theory is living in one dimension higher [15]. We take the extra dimension to be a circle S^1 , see picture 1. Suppose also that we have a one-dimensional D-brane which we will call a “D1-brane”. Such a D1-brane can be wrapped around the circle S^1 . From our point of view, we cannot see the D1-brane because it lives in an extra dimension that we cannot access directly. Instead, we will observe a point particle in our spacetime. The metamorphosis of this point particle to a black hole happens as follows. Remember that our D1-brane is massive and charged. When we increase the intensity of the gravitational interaction, the D1-brane will try to decrease the size of the S^1 due to gravitational attraction. This process does not go on forever because there is a competing repulsive force due to the charge of the D1-brane. Such a force on the contrary will try to maximize the size of the S^1 . The full spacetime $\mathbb{R}^2 \times S^1$ will stabilize once the two competing forces balance each other for a certain size of the S^1 . Due to such process, the size of the S^1 will not be the same throughout the full spacetime $\mathbb{R}^2 \times S^1$. Such a non-uniform size will manifest itself in our spacetime \mathbb{R}^2 as a curvature (see figure 1). In other words, we will feel a gravitational field as if there is a charged black hole sitting somewhere in our spacetime. This simple story generalizes to the full string theory, where now, the extra dimensions can be very complicated allowing for different kinds of charged black holes.



Figure 1: (Left) A schematic depiction of $\mathbb{R} \times S^1$ the spatial part of spacetime where we live in \mathbb{R} (the thick black line for example) while the extra dimension S^1 (dashed grey) is not visible to us. (Right) A D1-brane (thick grey) is wrapped around the S^1 making its size dependent on where we are on \mathbb{R} . As a result, our visible spacetime \mathbb{R}^2 is curved, which is felt as the presence of an attractive gravitational force. If we put, for example, a particle (small circle in grey) at point p in \mathbb{R} it will roll down as if it was subject to an attractive force. This does not happen in the original spacetime (left).

This is not the end of the story as string theory does more than just generating solutions describing black holes. String theory gives us a nice way to reproduce the entropy of a class of black holes by counting the underlying degrees of freedom [16]. Let us go back to our previous example to understand how this works in a simple set up. The story is more complicated but the idea is very simple; we just add vibrations to our D1-brane. Since these vibrations are living in the non-observed dimension of

spacetime we will not see them. Said differently, we will not be able to distinguish between different black holes associated to the D1-brane wrapping the extra S^1 with different vibration modes. In principle, counting the number of possible modes will give us the statistical explanation of the entropy of our black hole.

Although the idea described above is simple, the actual counting of microstates is more involved. It is true that one can reproduce the right entropy of some black holes this way, but, that does not really explain why is the entropy of a black hole proportional to the horizon area. Neither does this way of approaching black holes shed light on the other paradoxes of black holes. Things become a little bit better using AdS/CFT correspondence [9]. The essence of this correspondence is that “string theory (supergravity) on an AdS_{d+1} spacetime is equivalent to a CFT_d living on the boundary of AdS_{d+1} ”. In this correspondence, black holes are described by a thermodynamical ensemble of CFT states [17], which is characterized by a set of potentials related to the conserved charges carried by the black hole. Since the CFT is extensive, such equivalence between gravity and a CFT living in one dimension lower gives a nice explanation to why the black hole entropy is proportional to a surface. It also suggests that quantum gravity is highly non-local. In principle, one can also argue, using such duality, that information is not lost since CFT is a unitary theory. However, we are still far from completely understanding black holes using AdS/CFT duality due to the limitation of our present understanding of this duality.

For more information about what string theory can and cannot do regarding black hole physics, the reader is urged to consult the literature. By now, there are a lot of good review papers on the subject, see [18, 19, 20, 21, 22, 23, 24, 25, 26, 27, 28, 29, 30, 31] for a sample of them.

III-THE FUZZBALL PROGRAM

Although AdS/CFT taught us many key ideas about black hole physics, at present, its domain of applicability is very restricted due to our ignorance of the full map between bulk and boundary dynamics. To deal with such limitations, Mathur and collaborators suggested the following bright idea [32, 33, 34, 35]: instead of studying the black hole dual states in the CFT, why not study their manifestation in gravity. On general grounds, absence of entropy forces these dual geometries to be smooth. Since the CFT description of a black hole is a thermodynamical ensemble of states, one is tempted to declare that the black hole geometry should be an effective description of the same thermodynamical ensemble of these dual smooth geometries. But, is this the right way to think about black holes? After all, in a fundamental theory we expect to be able to describe a quantum system in terms of pure states.

This should apply to a black hole as well. At first glance, since the black hole carries an entropy, the thermodynamical ensemble description seems to be favorable. But, as we know from statistical physics, the thermodynamical ensemble can be regarded as a technique for approximating the physics of the generic microstate in the microcanonical ensemble with the same macroscopic charges. Thus, one should be able to speak of the black hole as a coarse grained effective description of a generic underlying microstate. Recall that, a typical or generic state in an ensemble is very hard to distinguish from the ensemble average without doing impossibly precise microscopic measurements. The entropy of the black hole is then, as usual in thermodynamics, a measure of the ignorance of macroscopic observers about the nature of the microstate underlying the black hole.

This ambitious program was first undertaken successfully in the case of the D1-D5 system [32, 33, 34, 35]. Then, it was extended to other supergravity solutions with a varied degree of success, for reviews see [36, 37, 11, 38, 39, 40]. We will leave the description of the fuzzball idea to the second chapter and content ourselves here by mentioning the following properties:

- The smooth geometries look indistinguishable from that of the associated black hole outside a compact region around the origin in space where the black hole sits.
- In the class of black holes we will study, the naive black hole geometry develops an infinite throat near its horizon in contrast to microstate geometries which have a finite deep throat, see picture 2. The incident quantum gets trapped inside the throat for a long time, but, eventually reflects off the tip of the throat and escapes to the outer region of the geometry in a process similar to the thermal radiation of a black hole. It is clear that in such a process information is not lost.
- Quantum effects are enhanced and seen at distances of the order of the horizon radius much larger than the natural Plank length. This allows for a better chance to understand the breakdown of semi-classical calculation as the horizon cannot be described by the naive vacuum state.
- Black hole singularity is an emergent phenomenon.

Despite these tantalizing properties, a good formulation of the fuzzball conjecture is still lacking. The idea that black holes are simply effective descriptions of underlying horizon-free objects is confusing because it runs counter to well-established intuitions in effective field theory. Most importantly, the idea that near the horizon of a large black hole the curvatures are small and hence so are the effects of quantum gravity is in clear conflict with the claim above that quantum effects become important at the horizon. A little thought reveals that such large quantum effects

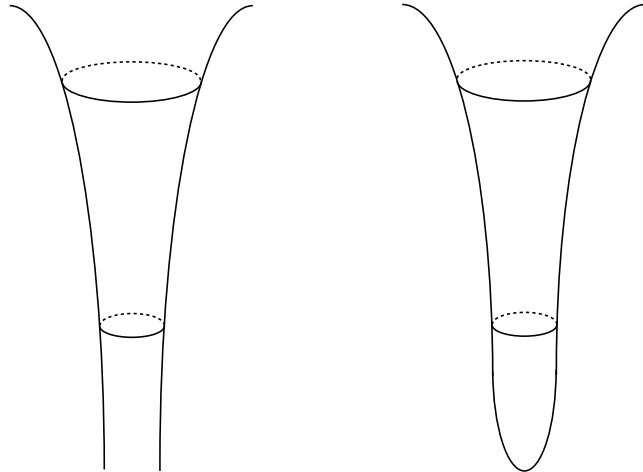


Figure 2: (Left) The infinite throat of the naive black hole geometry. **(Right)** A finite smoothly cupped throat of a smooth geometry

are not that strange. Remember that quantum mechanics discretizes the phase space into \hbar -sized cells. It could happen that points belonging to the same cell describe states that differ from each other macroscopically. We will leave a thorough discussion of such subtleties and potential misconception to the conclusion at the end of this thesis.

IV-THE ORGANIZATION OF THE THESIS

This thesis is divided into three parts:

- The first part discusses background material. It starts by a reminder about four dimensional black holes building up to give a rough idea about Hawking radiation. In the second chapter, ideas about phase space quantization and coarse graining are explained.
- The second part deals with the D1-D5 system and its coarse graining. We start by a description of the system and its solution in the first chapter of this part. Then, coarse graining of simple thermodynamical ensembles of these geometries is discussed in the second chapter of this part of the thesis.
- The third part concerns the four dimensional $\mathcal{N} = 2$ multi-black hole solutions.

We start with a description of these solutions and discuss their most important properties in the first chapter of this part. Then, a phase space quantization of these solutions is described in the second chapter of this part of the thesis.

- We close by a conclusion discussing open issues about the fuzzball program and future directions of investigation. Some technicalities are left to the appendices.

We tried to be very basic in the first part of the thesis. The only required background materials to hopefully follow the discussion in this part are: general relativity, quantum field theory and statistical physics. Our apologies for the advanced reader. The last two parts on the other hand are meant for advanced readers. In those parts the reader is assumed to have elementary notions of string theory like D-branes, supergravity, and also differential geometry, though, we will spend sometime explaining some background material that is not widely known, such as phase space densities (fourth chapter) and geometric quantization (sixth chapter). We will try our best to specify at the beginning of each chapter what background is needed to understand it.

Part I

From Black Holes to Microstates

PRELUDE

Before discussing the main subject of this thesis we will first take a quick detour and discuss briefly some background material. As was advocated in the introduction, the main theme of this thesis is black holes and some of their already raised paradoxes. The idea here is to give a quick look at the problems and the tools that we will use later on to address these problems. We are going to be very brief leaving most of the details to the literature.

In the first chapter, we start by a light description of four dimensional black hole solutions and their laws of mechanics. At this stage, an analogy with the laws of thermodynamics is already visible at the level of formulas. This will be promoted to a physical equivalence after the study of the massive scalar field in the background of a black hole. We close this chapter by discussing the implications of such analogy.

The second and last chapter in this part of the thesis is about phase space quantization and coarse graining. These will be our primary tools for the application of the fuzzball proposal. Emphasis will be on general ideas leaving some details to the subsequent chapters.

CHAPTER 1

FOUR DIMENSIONAL BLACK HOLES

This chapter is an attempt to summarize what is known about black holes in general relativity and semi-classical quantum gravity. We start by reviewing standard four-dimensional black holes: Schwarzschild and Kerr-Newman black holes. Then, a summary of the laws of black hole mechanics will be given suggesting the possible thermodynamical nature of black holes which closes the classical side of the story. Although a full quantum theory of gravity is still out of reach, one can still see some glimpses of its effects by resorting to semi-classical quantum gravity. Following this line of thoughts, we are going to quantize a free scalar field in a black hole background. This leads to the Hawking radiation of black holes making the thermodynamical nature of black holes physical. We close this chapter by discussing some implications of the Hawking radiation.

In this chapter familiarity with general relativity and black holes is assumed. The reader is also required to be familiar with canonical quantization of field theories in flat spacetime.

1.1 BLACK HOLES IN GENERAL RELATIVITY

As opposed to the other fundamental interactions, gravity distinguishes itself by treating spacetime as a dynamical entity. As a result, generalizations of well established notions in Mink spacetime are not that trivial as we will see later. In the

following, we are going to describe quickly the Schwarzschild and Kerr-Newmann black holes. This section follows closely [2]. For more details the reader is encouraged to consult standard books on general relativity.

1.1.1 BLACK HOLES

The first exact solution to the vacuum Einstein equation $R_{\mu\nu} = 0$ was found by Schwarzschild. This solution is spherically symmetric and it turns out to be describing a black hole. The metric is given by

$$ds^2 = - \left(1 - \frac{2M}{r}\right) dt^2 + \left(1 - \frac{2M}{r}\right)^{-1} dr^2 + r^2(d\theta^2 + \sin^2\theta d\varphi^2), \quad (1.1)$$

where M is a free parameter that equals the mass of the black hole. A strange thing seems to happen at $r = r_h = 2M$ where naively the metric degenerates. Finiteness of the Ricci scalar at r_h reveals that such degeneracy is nothing more than an artifact of the chosen coordinates. The surface defined by $r = r_h$ is called a “horizon” (or “event horizon”) and marks a “point of no return”; if one crosses it, he is forced to crush into the singularity at $r = 0$ where the curvature R blows up. This can be seen easily by drawing the associated Penrose diagram, see picture 1.1.

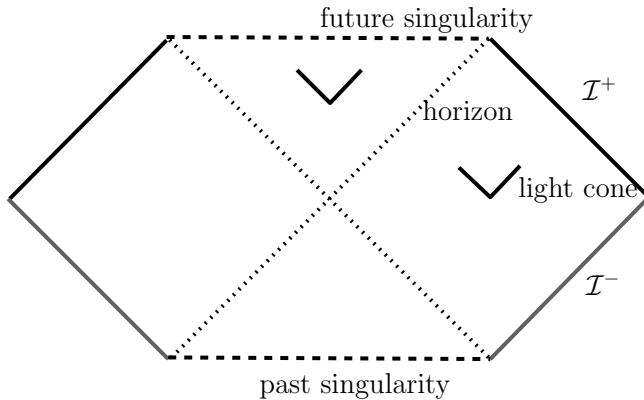


Figure 1.1: The Penrose diagram of the fully extended Schwarzschild black hole. \mathcal{I}^+ (black) and \mathcal{I}^- (grey) are future and past lightlike infinity respectively. The horizon is depicted in a dotted line. The future and past singularities are depicted in dashed lines. The small wedges represent future directed light cones.

A generalization of the Schwarzschild black hole is the Kerr-Newman one which is charged and rotating. This is a solution of the vacuum Einstein-Maxwell theory

$$S = \frac{1}{16\pi} \int d^4x \sqrt{-g} (R - F_{\mu\nu} F^{\mu\nu}) . \quad (1.2)$$

The Kerr-Newman black hole metric and Maxwell one-form read

$$ds^2 = -\frac{\Delta}{\Sigma} (dt - a \sin^2 \theta d\varphi)^2 + \frac{\sin^2 \theta}{\Sigma} [adt - (r^2 + a^2) d\varphi]^2 + \frac{\Sigma}{\Delta} dr^2 + \Sigma d\theta^2 , \quad (1.3)$$

$$A = \frac{1}{\Sigma} (Q r (dt - a \sin^2 \theta d\varphi) - P \cos \theta [a dt - (r^2 + a^2) d\varphi]) , \quad (1.4)$$

where

$$\Sigma = r^2 + a^2 \cos^2 \theta , \quad (1.5)$$

$$\Delta = r^2 - 2M r + a^2 + (P^2 + Q^2) , \quad (1.6)$$

and $a = J/M$, J is the angular momentum, M is the mass, Q is the electric charge, and P is the magnetic charge. One of the striking results in general relativity concerning black holes is

The No-Hair Theorem If (M, g) is an asymptotically flat stationary vacuum Einstein-Maxwell spacetime that is non-singular on and outside an event horizon, then (M, g) is a member of the three-parameter Kerr-Newman family of black holes described above.

where stationary means that there exists a timelike Killing vector. Before moving on, let us pause for a moment to point out an important difference between the Schwarzschild black hole and the more general Kerr-Newman black one. We have seen that the Schwarzschild black hole has two special spacetime regions: the singularity which for the Kerr-Newman black hole sits at $r = 0$ and $\theta = \pi/2$, and, the horizon whose counterpart for Kerr-Newman is located at the zeros of Δ . The latter being a second order polynomial in r (1.6) leads to three possibilities: two horizons, one horizon or no horizon at all. The second possibility is very special and the corresponding black hole is called “extremal”. A class of them can be embedded in a very special class of solutions to supergravity theories called BPS solutions (see section 2.1.1). These are solutions that preserve a fraction of the supersymmetries of the full theory. They (and their five dimensional cousins) will play an important role in the bulk of the thesis. The third possibility above (no horizon) suggests that there is a naked singularity. The existence of such a naked singularity will destroy the predictability of the future given initial data on a spacelike hypersurface. Based on the behavior of physically reasonable matter and in order to avoid such disaster, Penrose suggested the [12]

Cosmic Censorship Principle Under suitable physical conditions, naked singularities cannot form from a gravitational collapse in an asymptotically flat spacetime that is not singular on an initial spacelike hypersurface.

Proving or disproving this conjecture is one of the important open questions in general relativity. Actually, there are some gravitational collapse scenarios where the end result is a naked singularity. For a thorough discussion on the status of the cosmic censorship principle see e.g. [13, 14] and references therein.

1.1.2 KILLING HORIZONS AND SURFACE GRAVITY

Null hypersurfaces enjoy a lot of peculiar properties and play an important role in the study of the causal structure of spacetime. An important class of these surfaces are Killing horizons. These are null hypersurfaces \mathcal{H} that admit a normal Killing vector ξ . It can be shown that on \mathcal{H} , ξ satisfies

$$\xi^\nu \nabla_\nu \xi^\mu = \kappa \xi^\mu, \quad (1.7)$$

where ξ is normalized appropriately in the asymptotic flat region. κ is called the surface gravity. Our interest in Killing horizons is twofold

- Usually black hole horizons are Killing horizons.
- κ is a constant on the horizon and it will play the role of a temperature.

1.2 THE LAWS OF BLACK HOLE MECHANICS

The laws of black hole mechanics are obtained by studying the reaction of the solution to perturbations of its parameters (Mass, angular momentum, charge ...). Our first task then will be to define what we mean by these quantities. This is not as simple as it sounds because gravity does carry energy which makes it hard to distinguish black hole contributions from gravity ones. Luckily, there is a well defined prescription for asymptotic flat solutions of direct interest to us.

1.2.1 KUMAR INTEGRALS

Using the analogy with the ambiguity in defining the potential energy in classical mechanics, we are going to choose a reference geometry for which the mass, charge, and angular momentum are set to zero. For asymptotically flat black holes, the flat

Minkowski spacetime does the job. There are different methods to put this convention into work. A covariant formulation goes under the name of Kumar integrals which is as follows. Given a Killing vector ξ , for a spacelike hypersurface Σ one defines the conserved quantity

$$Q_\xi(\Sigma) = \frac{c}{16\pi} \int_\Sigma dS_\mu g^{\mu\rho} \nabla_\nu \nabla_\rho \xi^\nu , \quad (1.8)$$

provided that $J^\mu(\xi) = g^{\mu\rho} R_{\rho\nu} \xi^\nu$ vanishes on the boundary of Σ . In the equation above S_μ is the normal vector to Σ and c is a constant. For example, the energy (angular momentum) is evaluated using the Killing vector that generates time translations (space rotations) and choosing $c = -2$ ($c = 1$) respectively. These values of the constant c are chosen so that one ends up with the right normalization of mass and angular momentum.

1.2.2 BLACK HOLE LAWS

The following laws are specific to asymptotically flat black holes. We will be a little bit loose here, for exact formulation and proofs see [2].

Zeroth Law κ , the surface gravity is a constant on the horizon.

First Law The perturbation of a stationary black hole with mass M , charge Q and angular momentum J satisfies

$$\delta M = \frac{\kappa}{8\pi} \delta A + \Omega_h \delta J + \Phi_h \delta Q \quad (1.9)$$

where κ is the surface gravity, A is the area of the horizon, Ω_h is the angular velocity, and Φ_h is the electric surface potential.

Second Law The area of the horizon of an asymptotically flat spacetime is a non-decreasing function of time.

These laws are analogous to thermodynamics laws if one identifies the temperature (the entropy) with the surface gravity κ (respectively, the horizon area A). At this level, the resemblance is just in terms of formulas and seems not to have any sort of physical explanation whatsoever. After all, black holes are black objects, they do not radiate and they do not have hair. The status changes drastically when field theory is quantized in a black hole background, which we will turn to in the following section.

1.3 BLACK HOLES AS THERMODYNAMICAL OBJECTS

Diffeomorphism invariance of gravity theories leads to an ambiguity in defining time. Such an ambiguity triggers a chain of contamination all the way to the definition of creation/annihilation operators as will be explained below (subsection 1.3.1). Generically, there will be a mixing between creation/annihilation operators that are constructed starting from different choices of time. This is precisely the origin of Hawking radiation of black holes. The transformation that governs the mixing between these operators is called the “*Bogoliubov transformations*”.

In the following, we will start by discussing a free scalar field in a stationary curved background. This will shed light on the origin of Bogoliubov transformations and their physical consequences. As an application, we will deal with the Schwarzschild black hole background. Even if the full analytic solution is out of reach, by studying the asymptotic behavior of the solution (the asymptotic flat region and the horizon) we can derive the Hawking radiation. The material in this section follows very closely [41].

1.3.1 A FREE SCALAR FIELD AND BOGOLIUBOV TRANSFORMATIONS

Our aim at the end is the derivation of the Hawking radiation; i.e., particle creation by a black hole. To understand this phenomenon, we first need to specify the definition of particles. Armed with our knowledge from flat Minkowski spacetime, we will quantize a free scalar field in a curved spacetime. It turns out that the generalization of the notion of particles to curved spacetimes is in general ambiguous, which leads to Bogoliubov transformations.

CURVED BACKGROUND

Going from a flat to a curved background involves the task of covariantizing formulas. In the following, we are going to restrict ourselves to stationary spacetimes which admit a timelike Killing vector ∂_t . The associated coordinate will be our time coordinate t . By choosing the other spatial coordinates judiciously, one can always bring the metric to the form

$$ds^2 = -h(dt + \omega)^2 + h_{ij}dx^i dx^j, \quad (1.10)$$

where h , h_{ij} and $\omega = \omega_i dx^i$ depend only on the spatial coordinates x^i . Such a rewriting of the metric supplements us with a nice separation between temporal t

and spatial copordinates x^i , which allows us to perform a canonical quantization of our free scalar field. The action of the scalar field reads

$$S = \int dt L, \quad L = \int d^3x \sqrt{-g} \frac{1}{2} (g^{\mu\nu} \partial_\mu \phi \partial_\nu \phi + \mu^2 \phi^2), \quad (1.11)$$

where $g = \det g_{\mu\nu}$ is the determinant of $g_{\mu\nu}$, and $g^{\mu\nu}$ is the inverse of the metric $g_{\mu\nu}$. As usual in the canonical quantization approach, one defines the conjugate momentum as

$$\pi = \frac{\delta L}{\delta (\partial_t \phi)} = \sqrt{-g} g^{0\mu} \partial_\mu \phi. \quad (1.12)$$

Then, one requires that the field ϕ and its conjugate momentum π , promoted now to Hermitian operators, to satisfy the following equal-time commutation relations

$$[\phi(x, t), \phi(y, t)] = [\pi(x, t), \pi(y, t)] = 0, \quad [\phi(x, t), \pi(y, t)] = i\delta^3(x - y), \quad (1.13)$$

where $\delta^3(x - y)$ satisfies

$$\int d^3x \delta^3(x - y) f(x) = f(y),$$

for any scalar function $f(x)$. The transition from quantum fields to particles goes through creation/annihilation operators, which are defined as follows. One starts by constructing a basis for the solution space of the scalar wave equation, given below (equation 1.23). A convenient way to find a basis is to require it to be orthonormal with respect to a well defined innerproduct. Generalizing the one used in the flat spacetime case, the Klein-Gordon innerproduct, to general backgrounds gives

$$\langle f, h \rangle = i \int_{\Sigma} d\Sigma_\mu \sqrt{-g} g^{\mu\nu} (f^* \partial_\nu h - h \partial_\nu f^*), \quad (1.14)$$

which can be proved to be independent of the Cauchy surface “ Σ ” when f and h are solutions to the wave equation (1.23) given below. This is the equivalent statement of time independence of the Klein-Gordon innerproduct in the flat spacetime case. For stationary metrics (1.10) “ Σ ” can be chosen to be the spatial part $\{x^i\}$ of spacetime. In this case, the innerproduct simplifies to

$$\langle f, g \rangle = i \int d^3x \sqrt{\tilde{h}} (f^* \partial_t g - g \partial_t f^*), \quad (1.15)$$

where \tilde{h} is the determinant of the induced spatial metric ($\tilde{h}_{ij} = h_{ij} - h\omega_i\omega_j$). Furthermore, in view of characterizing particles by their energy (mass) we want to isolate the time dependence of our wave functions. A nice guess stemmed from the flat spacetime experience is to use frequencies; solutions of the form $f(x, t) = f(x) e^{-i\omega t}$. There is a well defined generalization of frequencies to a stationary spacetime called

a “*Killing frequency*”. The latter is defined with respect to the timelike Killing vector which is in our case ∂_t .

Before going on with our discussion, we need to address a small subtlety here. There is a redundancy in the solution space of (1.23) due to the reality of the wave equation. As is custom in quantum field theory, we will use the positive frequency $\omega > 0$ solutions to define the needed operators. To complete the picture, one uses the Hermitian conjugates of the already constructed operators. For example, our scalar field will have the following expansion

$$\phi = \sum_f (a(f) f + a^\dagger(f) f^*) , \quad (1.16)$$

where f is the positive frequency part of a complete basis of solutions to (1.23) that satisfy $\langle f, f' \rangle = \delta_{f,f'}$, \sum_f is a sum/integral over all possible f ’s, and $a(f)$ ($a^\dagger(f)$) are the annihilation (respectively, creation) operator as they satisfy

$$[a(f), a(h)] = -\langle f, h^* \rangle = 0 , \quad (1.17)$$

$$[a^\dagger(f), a^\dagger(h)] = -\langle f^*, h \rangle = 0 , \quad (1.18)$$

$$[a(f), a^\dagger(h)] = \langle f, h \rangle = \delta_{f,h} . \quad (1.19)$$

To get these commutators, we used (1.13), (1.12) and the inverse of (1.16) which is given, using the orthonormality of f ’s, by

$$a(f) = \langle f, \phi \rangle , \quad a^\dagger(f) = -\langle f^*, \phi \rangle . \quad (1.20)$$

We are now ready to define the notion of particles. First, we define the vacuum state $|0\rangle$ as the unique state annihilated by all the annihilation operators

$$\forall f ; \quad a(f) |0\rangle = 0 . \quad (1.21)$$

Particles are then constructed by the action of an appropriate combination of creation operators on the vacuum $|0\rangle$. For example, a particle with “characteristic” f is given by

$$|f\rangle = a^\dagger(f) |0\rangle . \quad (1.22)$$

FREQUENCY AMBIGUITY AND BOGOLIUBOV TRANSFORMATION

The definition of particles above starts to be problematic when our timelike Killing vector is not globally well defined. This happens in the case of spacetimes with a horizon such as black holes. Before discussing the special case of the Schwarzschild black hole, let us look for general lessons to be learned.

Creation and annihilation operators are defined through equation (1.20) given a basis of solutions to the wave equation

$$\frac{1}{\sqrt{-g}} \partial_\mu (\sqrt{-g} g^{\mu\nu} \partial_\nu) \phi - \mu^2 \phi = 0. \quad (1.23)$$

Suppose that our timelike Killing vector is not globally well defined. This means that, there are at least two patches where the expression of the Killing vector differs. On the overlap we have two notions of time leading to two different basis of positive frequency solutions f and h

$$\phi = \sum_f (a(f) f + a^\dagger(f) f^*), \quad (1.24)$$

$$\phi = \sum_h (a(h) h + a^\dagger(h) h^*). \quad (1.25)$$

Using the definitions of creation and annihilation operators (1.20), one finds

$$a(f) = \sum_h \langle f, h \rangle a(h) + \sum_h \langle f, h^* \rangle a^\dagger(h), \quad (1.26)$$

$$a^\dagger(f) = \sum_h \langle h^*, f \rangle a(h) + \sum_h \langle h, f \rangle a^\dagger(h), \quad (1.27)$$

which are called Bogoliubov transformation. An important consequence of the mixing between creation and annihilation operators in this kind of transformation is the ambiguity in defining the vacuum, which leads to particle production. To see this, let us calculate the average number of particles of type f “ $N(f) = a^\dagger(f) a(f)$ ” in the h -vacuum “ $|0(h)\rangle$ ” defined as $a(h) |0(h)\rangle = 0$. One easily finds using (1.26, 1.27)

$$\langle 0(h) | N(f) | 0(h) \rangle = \sum_h |\langle f, h^* \rangle|^2. \quad (1.28)$$

This relation clarifies what we mean by particle creation, the h -vacuum is unstable against emission of particles of type f .

1.3.2 HAWKING RADIATION

As a quantum physicist, one would like to know the answer to the following question “*during the collapse of matter field in a state $|\psi\rangle$ to become a black hole, what will be the response of an observer at asymptotic infinity long after the black hole forms?*” During the collapse there will be different modes that get excited. The modes near the would be horizon, just before the black hole forms, are special as they can escape to infinity at the cost of spending a long time to overcome the strong gravitational field. By the time these modes reach infinity, there will be a black hole that has

been formed ages ago. This suggests that we will measure radiation, even after the formation and stabilization of the black hole. On the contrary, if the original state is the vacuum, one would have expected that no radiation should be measured. This conclusion turns out to be erroneous as was first shown by Hawking [1]. The reason resides in the difference between the definition of positive frequencies for the horizon and the observer. This leads to particle creation as explained above.

In the following, we are going to discuss the case of a free scalar field in the background of the Schwarzschild black hole. We are going to follow closely [41]. For another approach following the original work of Hawking, see [42]. Our starting point will be the Schwarzschild metric (1.1) written in different coordinate systems

$$ds^2 = - \left(1 - \frac{r_h}{r}\right) dt^2 + \left(1 - \frac{r_h}{r}\right)^{-1} dr^2 + r^2 (d\theta^2 + \sin^2 \theta d\varphi^2) \quad (1.29)$$

$$= - \left(1 - \frac{r_h}{r}\right) (dt^2 - dr_*^2) - r^2 (d\theta^2 + \sin^2 \theta d\varphi^2) \quad (1.30)$$

$$= - \left(1 - \frac{r_h}{r}\right) dudv + r^2 (d\theta^2 + \sin^2 \theta d\varphi^2), \quad (1.31)$$

where $r_h = 2M$ is the horizon radius, $r_* = r + r_h \ln(r/r_s - 1)$ is the Regge-Wheeler radial coordinate, and $u = t - r_*$ ($v = t + r_*$) is the outgoing (respectively, ingoing) null coordinate. Taking advantage of the spherical symmetry of the problem, one decomposes ϕ in spherical harmonics as

$$\phi(t, r, \theta, \varphi) = \sum_{l,m} \frac{\psi_{l,m}(t, r)}{r} Y_m^l(\theta, \varphi), \quad (1.32)$$

which reduces the wave equation (1.23) to [41]

$$(\partial_t^2 - \partial_{r_*}^2 + V_{l,m}(r)) \psi_{l,m} = 0, \quad (1.33)$$

where

$$V_{l,m}(r) = \left(1 - \frac{r_h}{r}\right) \left(\frac{r_s}{r^3} + \frac{l(l+1)}{r^2} + \mu^2\right). \quad (1.34)$$

We are mainly interested in the observer region (asymptotic infinity), and the horizon region. In the observer region ($r \rightarrow \infty$ or $r_* \rightarrow \infty$), the potential goes to μ^2 . In this case, solutions with positive frequency will be of the form $\xi(r_*) \exp(-i\omega t)$. On the other hand, near the horizon ($r_* \rightarrow -\infty$ or $r - r_h \rightarrow r_h e^{r_*/r_h}$) the potential vanishes exponentially. In this case, the solutions are of the form $f(u) + g(v)$.

Jumping ahead of ourselves, suppose that our observer measures an outgoing wave packet narrowly peaked around a frequency ω . Its form will be $P \sim \exp(-i\omega t)$. Ultimately we want to evaluate

$$\langle N(P) \rangle = \langle \psi | a^\dagger(P) a(P) | \psi \rangle, \quad (1.35)$$

where, for a normalized wave packet P , the operator $a(P)$ is given by (1.20)

$$a(P) = \langle P, \phi \rangle , \quad (1.36)$$

evaluated on a Cauchy surface Σ_f corresponding to $t = t_f$. Due to our ignorance about $|\psi\rangle$ except at earlier times, we need to propagate P backward in time. Ideally, one needs to rewind the evolution until before the formation of the black hole. However, as has been shown first by Unruh [43], it is enough to go back in time until $t = t_i$ long after the black hole formed and long before the measurements. The backward time evolved wave packet P will split, at certain stage, to two components the reflected one R with support asymptotic infinity, and a transmitted one T whose support is a narrow region just above the horizon, see picture 1.2. In the language of creation/annihilation operators, one has

$$a(P) = a(T) + a(R) , \quad (1.37)$$

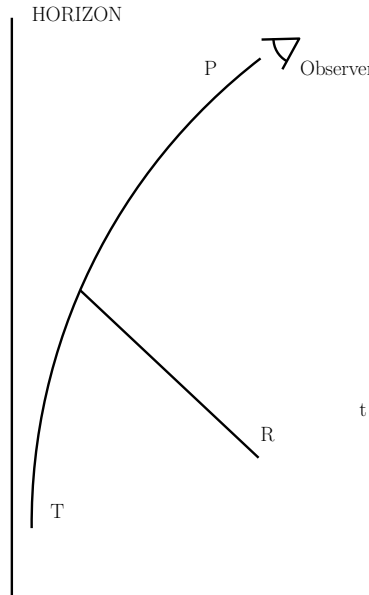


Figure 1.2: The observer measures a wave packet P narrowly peaked around the frequency ω . When this wave packet is evolved backward in time, it splits into two wave packets: T with support just above the horizon of the black hole, and R with support asymptotic infinity.

where now the evaluation is done with respect to the Cauchy surface Σ_i corresponding to $t = t_i$ using that the Klein-Gordon innerproduct is independent of the chosen Cauchy surface. Based on the conservation of the Killing frequency in stationary spacetimes, and that we assumed the absence of incoming radiation at $t = t_i$, one

concludes that $a(R)|\psi\rangle = 0$. So our number of particles $N(P)$ (1.35) reduces to

$$\langle N(P) \rangle = \langle \psi | a^\dagger(T) a(T) | \psi \rangle , \quad (1.38)$$

where T has the form $T \sim \exp(-i\omega u)$. Suppose that $|\psi\rangle$ is the vacuum state of the collapsing matter. This singles out the proper time of an in-falling observer τ as a preferred time coordinate. We need then to decompose T into two parts: the negative frequencies and the positive ones with respect to τ . Assuming that the infalling observer crosses the horizon at $\tau = 0$, one finds that

$$T \sim \exp\left(i\frac{\omega}{\kappa} \log[-\tau]\right) ; \quad \tau < 0 , \quad (1.39)$$

and zero otherwise, where $\kappa = 1/(2r_h)$ is the surface gravity of the black hole. T has both positive and negative τ -frequencies because it vanishes on the horizon, otherwise, it will be identically zero everywhere. Next, we use the result that a bounded analytic function in the lower half plane has purely positive frequencies following Unruh [44]. First, we construct the positive/negative frequency extension of T from $\tau < 0$ to $\tau > 0$ giving

$$T_\pm = T(-\tau) e^{\mp\pi\omega/\kappa} . \quad (1.40)$$

Then, we define a new wave packet that has support only inside the horizon by $\tilde{T}(\tau) = T(-\tau)$. The argument above shows that the positive/negative frequency components of T are

$$T^+ = \frac{T + e^{-\pi\omega/\kappa} \tilde{T}}{1 - e^{-2\pi\omega/\kappa}} , \quad (1.41)$$

$$T^- = \frac{T + e^{+\pi\omega/\kappa} \tilde{T}}{1 - e^{+2\pi\omega/\kappa}} . \quad (1.42)$$

We are almost there. The only missing link in the chain is the identity

$$a(T) = a(T^+) + a(T^-) = a(T^+) - a^\dagger([T^-]^*) . \quad (1.43)$$

The last part of this identity comes about because in our definitions of creation/annihilation operators, we used always the positive frequency part of the basis. One can think about it as having a complex scalar field where T^+ and T^- are related to the particle and its anti-particle. The vacuum $|\psi\rangle$ is defined by

$$a(T^+) |\psi\rangle = a([T^-]^*) |\psi\rangle = 0 . \quad (1.44)$$

Now it is a matter of plugging the equations derived until now in the equation (1.38) to get

$$\langle N(P) \rangle = \frac{\langle T, T \rangle}{e^{2\pi\omega/\kappa} - 1} , \quad (1.45)$$

where we used that $\langle T, \tilde{T} \rangle = 0$ (they have different supports), $\langle \tilde{T}, \tilde{T} \rangle = -\langle T, T \rangle$ and some properties of the innerproduct (1.15). This is just a thermal state at the Hawking temperature $T_H = (\kappa/2\pi)$ multiplied by the grey-body factor $\Gamma = \langle T, T \rangle$.

THE HORIZON VACUUM VS THE OBSERVER VACUUM

To get a better understanding of the Hawking radiation process, let us compare the horizon vacuum $|\psi\rangle$ with the observer vacuum $|0\rangle$. It is easy to show, using (1.44) and the relations (1.41, 1.42), that

$$\left[a(T) - e^{-\pi\omega/\kappa} a^\dagger(\tilde{T}^*) \right] |\psi\rangle = 0, \quad (1.46)$$

$$\left[a(\tilde{T}^*) - e^{-\pi\omega/\kappa} a^\dagger(T) \right] |\psi\rangle = 0, \quad (1.47)$$

whereas the vacuum $|0\rangle$ satisfies

$$a(T) |0\rangle = a(\tilde{T}^*) |0\rangle = 0. \quad (1.48)$$

It is not hard to check that (1.46, 1.47) are satisfied given (1.48) and

$$|\psi\rangle = \left(1 - e^{-2\pi\omega/\kappa}\right)^{1/2} \exp\left(e^{-\pi\omega/\kappa} a^\dagger(T) a^\dagger(\tilde{T}^*)\right) |0\rangle, \quad (1.49)$$

which can be interpreted as follows. A pair of particle and anti-particle is spontaneously created near the horizon. The particle escapes to infinity where it can be measured, and the anti-particle disappears behind the horizon. Despite being a pure albeit entangled state, the information that the observer gathers corresponds only to the incoming particles. So, as far as the black hole is there, the best the observer can do is to describe the $|\psi\rangle$ state as a density matrix by tracing over the anti-particles. This leads to the following matrix

$$\rho = \left(1 - e^{-2\pi\omega/\kappa}\right) \sum_n e^{-2\pi\omega/\kappa} |n\rangle\langle n|, \quad (1.50)$$

where $|n\rangle$ stands for a state with n particles. The above density matrix describes a thermal canonical ensemble at the Hawking temperature. We end this section with a small remark of relevance later. The vacuum $|\psi\rangle$ can also be seen as a vacuum squeezed state (Appendix A). The reason is that the equations (1.47, 1.48) look precisely like equation (A.6) in appendix A.

1.4 CONSEQUENCES OF THE BLACK HOLE RADIATION

After the discovery of the black hole radiation, the physics of black holes entered a new era marked by unresolved or partially resolved puzzles. The information loss paradox occupies the top of the list. On the other hand, the thermodynamical nature of black holes is taken as an indication that the black hole geometry could be just an effective description of an underlying microscopic system. Following this line of thoughts, Ted Jacobson [45] derived the Einstein equations assuming the thermodynamical properties of black holes generalized to local horizons.

1.4.1 BLACK HOLE EVAPORATION AND INFORMATION LOSS

There are two different sources of information loss in the background of a black hole. The first one is the information about the collapsed matter after they cross the horizon. After all, the horizon delimits a region that is causally disconnected from the outside. The other source involves the entangled nature of the vacuum near the horizon (1.49). This state remains pure as far as the black hole is there: the missing information are, in principle, stored behind the horizon even if we cannot access them. However, the black hole does evaporate leading to the disappearance of all the stored information. But, *why does a black hole evaporate in the first place?* Roughly, this happens because the black hole loses its mass through Hawking radiation due to the conservation of total energy. This leads to a decrease in the horizon area through backreaction. Because the radiation does not depend on the black hole, this process continues until all the mass is converted into energy. This conclusion seems counter intuitive as the black hole does eat particles in the process of radiation and so its mass should increase. This last observation is misleading because the energy density of our field near the horizon is negative [46, 47]. This is not so strange because, as we have noted at the end of section 1.3.2, the local vacuum state of the horizon is a squeezed state, and we know that these kind of states have always a region in space where their energy density is negative. See appendix A for an example in the flat spacetime .

1.4.2 GRAVITY AS AN EFFECTIVE DESCRIPTION

One of the main lessons that we learned from statistical mechanics is that thermodynamical systems are an effective description of an underlying complex microscopic system where most of the details are ignored. In this paradigm the entropy is a measure of the number of degrees of freedom accessible to the system. As black holes behave like thermodynamical systems, one cannot help himself but wonder: “*could black holes be an effective description of some sort?*”. Answering this question is the main interest of this thesis following ideas stemmed from the fuzzball proposal. The short answer seems to be yes, however, the access to the details of the underlying ensemble changes drastically depending on the black hole under study. We leave the details to the bulk of this thesis (part II and III).

CHAPTER 2

THE FUZZBALL MACHINERY

The central subject of this thesis is the investigation of the idea that black holes are effective descriptions of some underlying microscopic system. We will study how concretely is this realized in the fuzzball scenario. In such scenario, this microscopic system will be some subset of all possible smooth supergravity solutions with the same asymptotic quantum numbers as the black hole. From now on, we will call these smooth geometries “*black hole states*”. Furthermore, these states are assigned different weights depending on the nature of the black hole under study. The black hole states with their weights define an ensemble that we call, henceforth, “*the black hole ensemble*”.

In this chapter we will try to explain some basic concepts of the fuzzball scenario that we will be using later on in this thesis. We will be using the strong analogy between black hole ensembles and thermodynamical ensembles, a result of AdS/CFT duality [17]. We will first start by describing and motivating the kind of black holes we are interested in. Then, we will elaborate on the black hole ensemble setting up the stage for subsequent concepts. After that, we will specify the common characteristics of black hole states, leaving details to specific examples discussed later on in this thesis. A first test that a black hole ensemble should pass is to reproduce the entropy of the associated black hole. This leads us to our next task: to figure out a way to count black hole states. Our approach will be to quantize the phase space of the associated smooth solutions. Another test of the black hole ensemble is that after coarse graining, one should get an effective geometry that resembles, to a great precision, the one of the black hole outside the horizon. Where by coarse graining we mean a process where insignificant “microscopic” details are washed away. Explaining how to do coarse graining will be the subject of the last section of

this chapter.

In this chapter the reader is assumed to be familiar with statistical physics, group theory, quantum field theory and spinor representation.

2.1 BLACK HOLES OF INTEREST TO US

So far, we were not that clear about which black holes are we going to study. It is time to lift the curtains on our main protagonists. We will do that step by step. First, we are going to motivate why are we interested in BPS black holes. Then, we will spell out our preferred class of black holes and explain their special status, for the fuzzball program, among their cousins.

2.1.1 BPS-NESS, LINEARITY AND ADS/CFT

As alluded to earlier, our winning horse in dealing with the complicated nature of gravity dynamics is symmetries. Although spherical and axial symmetries were powerful enough to allow for exact solutions to the Einstein and Einstein-Maxwell theories, we will be needing an even stronger symmetry for our considerations: supersymmetry. This is a symmetry that links fermions with bosons. The goal of this subsection is to give a taste of the most important qualities of supersymmetry that we will be needing in the remaining of this thesis.

Reviewing supersymmetry and its beautiful structure is not the intended goal of this subsection. The interested reader should consult standard books on the subject e.g [48, 49, 50, 51]. We will be practical in our exposition here, restricting ourselves to describing the needed supersymmetry properties that will be used in subsequent sections and chapters of this thesis. We will start by introducing the supersymmetry algebra. After that, we are going to introduce one of the most important notions in this thesis: BPS states and some of their most useful properties. At the end, we will mention some quick words about our “black holes” that we will study later on, leaving more details to the second and third parts of the thesis.

EXTENDED SUPERSYMMETRY AND BPS STATES

Conservation laws play an important role in the search for the fundamental laws of particle interactions. Thanks to Noether theorem, these conservation laws are ultimately connected to global symmetries of the Lagrangian. During the mid of the last century two classes of symmetries were in the heart of the development

of high energy physics: external and internal symmetries. On one hand, we have Poincaré symmetries acting on spacetime, hence the name external. These symmetries manifest themselves through the conservation of energy, momenta and angular-momenta. On the other hand, internal symmetries were put forward to explain the absence of some interaction channels that cannot be accounted for by spacetime considerations. When supplemented with locality, internal symmetries give rise to gauge theories.

In the 1960's, physicists attempted to combine both classes of symmetries by trying to find a non-trivial symmetry that can fuse both of them. Such efforts accumulated in the Coleman-Mandula no go theorem [52], which asserts that such a non-trivial symmetry does not exist given generic and simple assumptions. Of importance to us, the assumption that physical symmetries are described by Lie groups i.e. restricting to commutation relations between the different generators of the symmetries. The story took a different turn when the last assumption was dropped [53] i.e. include anti-commutation relations in the algebra of symmetries. In such cases, it was possible to construct a non-trivial combination of internal and external symmetries. Since anti-commuting variables are associated with fermions, the anti-commuting generators \mathcal{Q} are fermionic and hence map bosons to fermions and vice versa. Such a symmetry is called “*supersymmetry*”. The Coleman-Mandula no go theorem then restricts the spin of \mathcal{Q} to be $1/2$.

The fermionic generators, \mathcal{Q} , called also “*supercharges*”, have the structure of multiplets \mathcal{Q}_α^a where α is a spinor index and a is a multiplet label, as they are $1/2$ -spin representation of the Lorentz group. If \mathcal{N} the number of multiplets is bigger than one we have an extended supersymmetry. The latter plays an important role in what follows as it allows for a spacial class of massive representations of the supersymmetry algebra, called “*BPS-states*”, which we will turn to now.

For the sake of the arguments, we will restrict ourselves to $\mathcal{N} = 2$ supersymmetry in four dimensions. In this case we have eight supercharges \mathcal{Q}_α^a and $(\mathcal{Q}_\alpha^a)^\dagger$, which are taken to be in the two-dimensional Weyl (called also “*chiral*”) representation, where α is a spinor index and takes the values 1 and 2. The part of the supersymmetry algebra that we will be needing is:

$$\{\mathcal{Q}_\alpha^a, (\mathcal{Q}_\beta^b)^\dagger\} = \sigma_{\alpha\beta}^\mu P_\mu \delta_b^a, \quad \{\mathcal{Q}_\alpha^a, \mathcal{Q}_\beta^b\} = \epsilon_{\alpha\beta} \epsilon^{ab} \mathcal{Z}, \quad \{(\mathcal{Q}_\alpha^a)^\dagger, (\mathcal{Q}_\beta^b)^\dagger\} = \epsilon_{\alpha\beta} \epsilon^{ab} \bar{\mathcal{Z}}, \quad (2.1)$$

where $\sigma^0 = -\mathbb{I}_{2 \times 2}$, σ^i ; $i = 1, 2, 3$ are the Pauli matrices, $\epsilon_{\alpha\beta}$ is the totally anti-symmetric tensor where $\epsilon_{12} = -1$, and \mathcal{Z} is a complex number called a “*central charge*”. In general, we will have instead of \mathcal{Z} an operator which commutes with all operators in the supersymmetry algebra.

For massive representations and by going to the center of mass frame $P = (-M, \vec{0})$,

positivity of the operators $\mathcal{O}_\alpha^\pm = \{a_\alpha^\pm, (a_\alpha^\pm)^\dagger\}$ defined as

$$a_\alpha^\pm = \mathcal{Q}_\alpha^1 \pm \epsilon_{\alpha\beta} (\mathcal{Q}_\beta^2)^\dagger , \quad (2.2)$$

implies that $M \geq |\mathcal{Z}|$. As a result, the mass of field representations of the supersymmetry algebra are bounded from below by $|\mathcal{Z}|$. Such a bound is called the “BPS bound” and it is saturated by a special class of states called “BPS states”. It is clear from the way we derived the bound that these states are annihilated by two out of the four supercharges. In such a situation the BPS state is called 1/2-BPS. In general, we will have other kinds of BPS states according to the number of independent linear combinations of supercharges that annihilate them.

ESTIMATING THE NUMBER OF BPS STATES

In a supersymmetric theory, fields come in multiplets as they are representations of the supersymmetry algebra, in accordance with the general lore that fields in a quantum field theory are representations of the global symmetries of the Lagrangian. One of the powerful results of supersymmetry is that the number of fermions and bosons in a multiplet is the same. This is a straightforward result of the first commutator in (2.1), and the fact that P_μ is a one-to-one operator. Taking advantage of such pairing, Witten showed in a fascinating paper [54] that one can define a parameter-dependant weighted sum over states that is invariant under a continuous change of this parameter, provided that supersymmetry is not broken.

For the sake of the argument, we will restrict ourselves in the following to one supercharge and its Hermitian conjugate. One has the following commutators

$$\{\mathcal{Q}, \mathcal{Q}^\dagger\} = \mathcal{E}, \quad [\mathcal{Q}, \mathcal{E}] = [\mathcal{Q}^\dagger, \mathcal{E}] = 0 , \quad (2.3)$$

where \mathcal{E} is the energy. The first equation is a special case of (2.1), and the other two were not mentioned earlier as they did not play a role in the previous argument. It is easy now to show that the following weighted sum, usually called an “index”,

$$I(\beta) = \text{Tr}_{\text{states}} (-1)^F e^{-\beta \mathcal{E}} , \quad (2.4)$$

where F is the fermion number, and β is some continuous parameter, does not receive contributions from states that are not annihilated by the supercharges. Suppose the inverse is true, there exists a states $|\psi\rangle$ that contributes to $I(\beta)$ such that $\mathcal{Q}|\psi\rangle \neq 0$ and $\mathcal{Q}^\dagger|\psi\rangle \neq 0$. By acting with a supercharge on this state, one can generate another state $|\chi\rangle$ with the wrong fermion number and the same energy, a consequence of (2.3). In doing so, we managed to construct a state $|\chi\rangle$ whose contribution exactly cancels the contribution of $|\psi\rangle$. According to this argument,

the only contributing states to the index $I(\beta)$ are the ones that are annihilated by supercharges, which, according to the first equation in (2.3), have zero energy. We will call such states “ground states”.

Suppose now that, for some reason, by changing the parameter β some ground states cease to be so. These states should leave the ground state in fermion-boson pairs to preserve supersymmetry. Hence using the argument before, the change in the index $I(\beta)$ vanishes. One concludes then, that $I(\beta)$ is invariant under a continuous change in β as promised.

There are generalizations of the simple index (2.4) where, instead of one parameter β , we have a parameter space \mathcal{M}_β , and the weights are chosen such that the only contributing states belong to a specific class of BPS states. These generalized indices are sometimes called “*elliptic genera*”. Unfortunately, it turns out that BPS states annihilated by at most four supercharges do suffer a discrete jumps in the their index [55]. This happens at specific values of the continuous parameters β_i that enter in the definition of the index. These special values of β_i define a co-dimension one hypersurface in \mathcal{M}_β which is called a “*wall of marginal stability*”. In some cases, like the 1/2-BPS sector of $\mathcal{N} = 2$ four-dimensional supergravity of interest to us, there are ways to quantify such a jump [30] (see also section 5.4).

Making the supersymmetry local, forces us to study gravity at the same time. Such theories are called “*supergravity*” theories. In this case one can construct BPS solutions that have only bosonic excitations, which are the class of solutions that we will be dealing with. But, how is that possible? Naively one would think that supersymmetry transformations will turn on fermionic degrees of freedom. The trick is that these BPS solutions exist whenever there is a supersymmetry transformation parameter ϵ , that does not generate fermionic degrees of freedom when acting on the bosonic fields of the BPS solution. In other words, this spinor ϵ , called a “*Killing spinor*”, is such that the variations of fermions ψ under supersymmetry transformations vanish $\delta_\epsilon \psi = 0$, for the given values of the bosonic fields of the BPS solution. In the following, we will be calling the equation $\delta_\epsilon \psi = 0$ the “*Killing spinor constraints*”.

Our interest in these BPS-solutions is threefold:

- i- Generically, and for enough preserved supersymmetries, the index gives the actual number of BPS states. In such a situation, the number of BPS states is invariant under continuous variations of parameters baring walls of marginal stability. This will play an important role in the arguments of section 2.3 below.
- ii- On the technical level, and at least for the class of theories we will be dealing with, these solutions are much simpler than the non-BPS ones for the following reason. We have already seen that the gravity field equations are second

order non-linear differential equations, which makes them hard to solve. The simplification that BPS solutions bring is that, the Killing spinor constraint is first order. In some cases, a further simplification does occur: solving the set of field equations and Killing spinor constraints in the right order linearizes the equations to be solved at each step. The non-linearity manifests itself in a source term that depends only on solutions to the equations of the previous steps. This happens in the examples we will be studying in the next two parts of the thesis. Using this strategy, a large number of smooth solutions with the same asymptotic quantum numbers as a black hole was built, opening the door for a fuzzball study of such solutions.

- iii- The Last motivation comes from totally different considerations. A powerful tool to study properties of black holes in string theory is AdS/CFT duality [9]. This duality asserts the equivalence of string theory (gravity) on AdS_{d+1} backgrounds and a CFT_d living on the boundary of AdS_{d+1} . A way to get such backgrounds is to take a decoupling limit of a certain class of black holes that includes BPS ones. This decoupling limit amounts to decoupling the physics in the near horizon region of the black hole from that of the asymptotically flat region by scaling the appropriate Planck length, l_p , to decouple the asymptotic gravitons from the bulk. At the same time one needs to scale appropriate spatial coordinates with powers of l_p to keep the energies of some excitations finite. Two lessons learned in the AdS/CFT duality will be of importance to us in what follows. On one hand, it has been shown that “*BPS black holes behave like thermodynamical ensembles [17], even though they do not Hawking radiate*”. The chemical potentials of such ensembles, including the temperature, are just parameters to describe the black hole ensemble without any physical meaning. On the other hand, it is only in the realm of AdS/CFT duality that one can really be confident that the fuzzball scenario might be after all a correct way to think about black holes. We already mentioned that black holes are described by thermodynamical ensembles of states on the CFT side. The AdS/CFT duality then tells us that these states, if they are accessible in gravity, should be given in terms of smooth geometries.

2.1.2 BEYOND AdS/CFT?

Although considerations in AdS/CFT were the origin of the fuzzball program [32, 33, 34, 35], we would like to weaken such dependence if not get rid of it. The hope at the end is to apply coarse graining ideas to realistic black holes (without supersymmetry) for which AdS/CFT as we know it now is not applicable. Although we cannot, for the moment, disregard the AdS/CFT because some of the building

blocks we are going to use are well established in this duality (such as the thermodynamical nature of BPS black holes and general characterization of black hole states, see section 2.2), we are not going to use AdS/CFT explicitly in the following. We should always keep in the back of our mind that, in the cases we are interested in, we can embed the whole discussion in an AdS/CFT duality frame. Such a duality then supplements us with the missing building blocks that we will be needing.

Another point of view would be that the fuzzball paradigm, as we are going to use it, is complementary to AdS/CFT. The former can explore questions beyond the reach of the latter. As an example, the fuzzball conjecture predicts that quantum effects in gravity gets enhanced to large distances (horizon size) [56], completely unseen by the AdS/CFT. Such enhancement opens the door to re-question the applicability of local effective field theories whenever gravity is around even if the curvature is small everywhere.

2.1.3 THE GUINEA PIGS

We will be dealing in the bulk of this thesis with two kinds of black holes: the D1-D5 “small” black holes in five dimensions (part II) and the $\mathcal{N} = 2$ four dimensional 1/2-BPS black holes (part III). The word “small” in small black hole means that the horizon area of the black hole vanishes if one is using the two derivative effective action. It was shown that, including higher order terms will generate a proper albeit small horizon [57, 58, 59, 60, 61, 26].

We are interested in these systems mainly because they are among few that have known large space of smooth solutions with the same asymptotic charges as a black hole. Actually, smooth solutions exist provided we go one dimension higher: six for the D1-D5 and five of the $\mathcal{N} = 2$ black holes. The uplift of the D1-D5 system is still described using type-IIB string theory, however, the uplift of the $\mathcal{N} = 2$ black holes is now described using M-theory. This is a consequence of the fact that type-IIA string theory is the compactification of the eleven-dimensional M-theory over an S^1 whose radius is related to type-IIA coupling constant: the M-theory is the large coupling limit of type-IIA where the S^1 circle decompactifies. As a result, if one compactifies type-IIA on a Calabi-Yau, the resulting physics is equivalent to compactifying M-theory on the same Calabi-Yau $\times S^1$. This relation allows us to map four-dimensional solutions to a special class of five dimensional solutions that have a $U(1)$ isometry. This map goes under the name of “4d-5d uplift” [62, 63]. Since we are keeping the $U(1)$ isometry, going back and forth between five and four dimensions will not affect the number of states. Based on this observation, we will be studying the four dimensional solutions in this thesis.

Another reason behind our interest in these class of solutions is that we can embed them in an asymptotic $\text{AdS}_3 \times S^d$ spacetime, with, $d = 3$ for the uplifted six-dimensional D1-D5 solutions e.g. [24] and $d = 2$ for the uplifted five-dimensional 1/2-BPS black holes [64]. Such embedding makes us confident about the possible applicability of the fuzzball ideas to these class of solutions.

From a different perspective, the study of the D1-D5 system is physically interesting as one can hope to describe the so called “*small black rings*” [65] using an appropriate thermodynamical ensemble of the D1-D5 states [66]. We have already explained the use of the word small but what about the word black ring? and why are they interesting? Black rings are the first gravity solutions with a horizon whose topology is not a sphere [5, 6]. They are five dimensional solutions with a horizon that is topologically $S^2 \times S^1$ instead of S^3 . These black rings are the first known gravity solutions that violate the no-hair theorem [67]. The hair of these black rings is a local non-conserved charge, called the “*dipole charge*”, that is not visible at the asymptotic flat region. Even though we cannot measure these dipole charges at infinity, we can still find their imprint as they enter in the first law of thermodynamics of black rings [67, 68]. Such a non expected role of dipoles makes them special as, based on general grounds, they should enter somehow in the characterization of the black ring ensemble.

The D1-D5 small black ring carries a non-trivial angular momentum in contrast to the naive D1-D5 small black hole. In the presence of this angular momentum, the D1-D5 system starts to look like a ring rather than a point-like object in five dimensions [69, 33]. Therefore, it is expected that such a system, D1-D5 with angular momentum, will describe a black ring with a small horizon [65, 70, 71, 72] when higher order terms are included in the gravity action, in the same spirit as the small D1-D5 black hole develops a small horizon.

On the negative side of the story, both our classes of solutions (D1-D5 and $\mathcal{N} = 2$ four dimensional 1/2-BPS black holes) suffer from some drawbacks. The D1-D5, as was mentioned before, corresponds to a five dimensional solution with vanishing horizon area which raises doubts about its possible usefulness to realistic black holes i.e. black holes with large classical horizon. On the other hand, the $\mathcal{N} = 2$ four-dimensional 1/2-BPS solutions include such large black holes, but due to the small amount of preserved supersymmetries (only four supercharges), they are technically more demanding. Certainly for these class of solutions there is much work that still needs to be done.

Historically, the D1-D5 system was the main inspiration of the whole fuzzball program and by far the most fruitful testing ground of the fuzzball ideas (see [36, 37, 11, 38, 39, 40] and references therein). This is mainly due to the high supersymmetry that the system preserves, eight preserved supercharges. However, the first

class of solutions that was subject to coarse graining considerations [73] describes the 1/2-BPS sector of type-IIB supergravity on $AdS_5 \times S^5$. These solutions go under the name of “Lin-Lunin-Maldacena geometries” (LLM in short) [74]. These are the simplest solutions to deal with as they preserve sixteen supercharges. Despite that, there is no known large black hole that preserves the same symmetries. We will not mention this system beyond this point. On the other hand, the $\mathcal{N} = 2$ black holes are still in the beginning of the journey (see [38, 39, 40] and references therein).

2.2 BLACK HOLE ENSEMBLE

Black holes are solutions of gravity theories with the metric playing the role of the fundamental field. This suggests that the black hole states might be characterized by their geometry. This is not entirely obvious and seems to fail for 1/4-BPS black holes. For the moment, let us forget about this failure leaving the discussion it deserves to the third part of this thesis and proceed with the general idea.

2.2.1 THE NO-HAIR THEOREM, ENTROPY AND GEOMETRY

As we have seen in the first chapter, black holes have an entropy that is in clear clash with the no hair theorem. The latter states that the metric is completely fixed given stationarity and a small number of fixed charges at infinity. A familiar situation that bears a lot of resemblance to the black hole is thermodynamics. There, the system is also characterized by few parameters (temperature, energy, pressure, ...). Still the statement that such a system has a non-zero entropy does not raise any objections. This is because we know that Newtonian mechanics is the “fundamental” theory, and thermodynamics is just an effective description. In this realm, the entropy is a measure of the degrees of freedom that the thermodynamical system can access. Given such success, one is tempted to repeat the same philosophy for the black hole. However, things are not that trivial.

Let us restrict ourselves to the Schwarzschild black hole for the sake of the argument. Such a black hole emerges in the context of general relativity where the metric is the sole field. The no-hair theorem states that, given the mass, the geometry is unique. In other words, if general relativity is the fundamental theory this seems to be the end of the story.

An ambitious idea that the fuzzball proposal seems to suggest is that the classical picture of the region behind the horizon is not the right one. We do not have a clear notion of geometry there, the spacetime is fuzzy which is the origin of the name

coined by Mathur to such proposal, “the fuzzball proposal” [32, 33, 34, 35]. Such a drastic change in our way of perceiving black holes goes against our intuition from classical gravity, and even worse, from the point of view of effective field theory. The gravity objection to such picture is that the horizon is a global concept, locally there is nothing special about it. While the effective field theory objection is due to the intuition that for a large horizon with a small curvature everywhere, there will not be any drastic change of the classical picture due to quantum effects. However, quantum mechanics outruns such objections by appealing to the discrete nature of the quantum phase space. Remember that, due to the uncertainty principle, the classical phase space is discretized to \hbar -sized cells. All the states that belong to the same cell are indistinguishable classically. If these classically indistinguishable solutions differ from each other over large distances in the real spacetime, they will manifest large macroscopic quantum effects. We will see an example of such effects in the following two parts of the thesis.

In the fuzzball scenario, our starting point is an ensemble of geometries with the following characteristics:

- The pure state geometries are smooth everywhere as the existence of a singularity is expected to lead to an entropy as follows. Naked singularities are unpleasant objects as they destroy the predictability of physics even long distances far away. So, one expects that they will be shielded by a horizon once higher order corrections are included. This suggests, following general considerations for black holes, that such solutions will have an entropy proportional to the area of this horizon. As such, they should be seen as a sub-ensemble rather than a pure state. We can sometimes relax the smoothness requirement to include solutions with zero entropy.
- The smooth geometries should carry the same asymptotic charges as a black hole. In some cases refinements of this condition will be needed. We will see some examples in the next two parts of the thesis. Although we do not know a precise general enough formulation of these refinements, a natural proposal would be to include all the quantities that appear in the first law of black holes.
- A weight that depends on the black hole under consideration is associated, in principle, to each smooth geometry.

2.2.2 AT WHICH LEVEL CAN WE TRUST OUR GEOMETRIES

The fuzzball scenario with its unorthodox ideas is subject to some criticism that we will not discuss all of it here. For more details see [36, 11, 75, 40] and the conclusions at the end of the thesis. We have already discussed the large quantum

effects objection in the previous subsection. The other objection that we are going to address here concerns the possible deference in the results of measurements done with respect to the black hole ensemble effective geometry, or with respect to the naive black hole geometry. If these were so, then the usual black hole could not be a good effective description, and there would be a massive violation of our usual expectations from effective field theory. Fortunately, one can show that in *any* scenario where the entropy of a black hole has a statistical interpretation in terms of states in a microscopic Hilbert space, the variance of finitely local observables over the Hilbert space will be suppressed by a power of e^{-S} [76]. Thus, even if the microstates of a black hole are realized in spacetime as some sort of horizon free bound states, finitely local observables with finite precision, of the kind that are accessible to semiclassical observers, would fail to distinguish between these states. Indeed, the semiclassical observer, having finite precision, might as well take an ensemble average of the observables over the microstates, as this would give the same answer. The ensemble of microstates gives a density matrix with entropy S , and will be described in spacetime as a black hole geometry. In this sense, the black hole geometry will give the effective description of measurements made by semiclassical observers.

Even with this positive situation, one can still question the validity of describing the black hole ensemble using an effective geometry. In general, one is not sure that such geometry will be free of regions with a large curvature, and hence, will not be trustworthy. Unfortunately, such a possibility is non-vanishing as typical states tend to have such problems. In such a situation, one should be careful about the kind of questions he is asking. Presumably, a corrected version of this effective geometry will be the honest effective description of the black hole ensemble.

2.3 PHASE SPACE QUANTIZATION

After we (partially) specified our black hole ensemble, we need a way to count the number of states among other things. We are going to do so by quantizing the space of solutions. Among the reasons to follow such approach is that the counting of states will be more transparent. We will also be able to evaluate quantum effects in view of identifying the scales at which they become important. By doing so, we will be able to check when does classical geometry break down. A third reason is that by having an associated quantum Hilbert space, one can hope to coarse grain.

It turns out that, the space of solutions in the cases of interest to us, comes equipped with a symplectic form. This allows us to use the so called “*covariant phase space quantization*” to quantize our systems. In such an approach, we will quantize the actual space of solutions rather than the fluctuations around these solutions. This

is equivalent to the study of Landau levels of an electron in a large magnetic field, which amounts to neglecting quadratic terms while keeping the linear term in momentum.

2.3.1 SOLUTION SPACE, PHASE SPACE AND THE SYMPLECTIC FORM

Shifting the quantization from phase space to solution space relies on two fundamental observations:

- On general grounds, one can identify the space of solutions of a general field theory with its canonical phase space. Heuristically, this is because a given point in the phase space, comprised of a configuration and associated momenta, can be translated into an entire history by integrating the equations of motion against this initial data. Likewise, by fixing a spatial foliation, any solution can be translated into a unique point in the phase space by extracting configuration and momentum from the solution evaluated on this spatial slice.
- The existence of a symplectic form on the space of solutions that can be derived starting from the Lagrangian. This is an old idea [77], see also [78] for an extensive list of references and [79, 80, 81, 82] for more recent work. In the case of Lagrangians that only depend on the fields and their derivatives $\mathcal{L} = \mathcal{L}(\phi_a, \partial\phi_a)$, which is the class of Lagrangians we will be working with, this symplectic form is given by

$$\omega = \int d\Sigma_l J^l; \quad J^l = \delta \left(\frac{\partial \mathcal{L}}{\partial \partial_l \phi_a} \right) \wedge \delta\phi_a, \quad (2.5)$$

where the integration is over an initial Cauchy surface and δ is the exterior derivative in field space.

An important subtlety in our application of such quantization approach is that we will not quantize the entire solution space, but rather, a subspace of the solutions with a certain amount of preserved supersymmetry (see part II and III of the thesis).

In general, quantizing a subspace of the phase space will not yield the correct physics, as it is not clear that the resultant states do not couple to states coming from other sectors. It is not even clear that a given subspace will be a symplectic manifold with a non-degenerate symplectic pairing. As discussed in [83], we expect the latter to be the case only if the solutions belonging to the subspace have a non-trivial momentum. For gravitational solutions we thus expect stationary but not static solutions to possibly yield a non-degenerate phase space. This is because the canonical momenta of these class of solutions are non-vanishing. To see this,

we will discuss the metric part of the solution. We start by putting the metric in the canonical form [84]

$$ds^2 = -N^2 dt^2 + f_{ij} (dx^i + N^i dt) (dx^j + N^j dt), \quad (2.6)$$

where x^i ; $i = 1, 2, 3$ span the spatial part of the metric. This separation of time t and space allows us to define the canonical momenta dual to the components of the spatial part of the metric f_{ij} . These turn out to be given by [84]

$$\pi^{ij} = \sqrt{-g} f^{ik} f^{jl} (\Gamma_{kl}^t - f^{mn} \Gamma_{mn}^t f_{kl}), \quad (2.7)$$

where f^{ij} is the inverse of f_{ij} i.e $f^{ij} f_{jk} = \delta_k^i$ which is different from g^{ij} the spatial part of the inverse of the metric (2.6), and $\Gamma_{\mu\nu}^\rho$ is the usual Christoffel connection. In the case of a stationary metric, the coordinates t and $\{x^i\}$ can be chosen such that the functions N , f_{ij} and N^i entering in the expression of the metric (2.6) are independent of time t . In this case we have non-trivial momenta π^{ij} if Γ_{ij}^t is non-vanishing, which in turn requires N^i to be different from zero. The last condition fails in the case of a static metric. Therefore, in the case of stationary but non-static metric we do have non-trivial dual momenta.

This still does not address the issue of consistency as states in the Hilbert space derived by quantizing solutions along a constrained submanifold of the phase space might mix with modes transverse to the submanifold. When the submanifold corresponds to the space of BPS solutions one can argue, however, that this should not matter. The number of BPS states is invariant under continuous deformations that do not cross a wall of marginal stability or induce a phase transition. Thus, if we can quantize the solutions in a regime where the interaction with transverse fluctuations is very weak, then, the energy eigenstates will be given by perturbations around the states on the BPS phase space. Although, these will change character as parameters are varied, the resultant space should be isomorphic to the Hilbert space obtained by quantizing the BPS sector alone. In some cases, nailing precisely the regime where the interaction of BPS states with transverse fluctuations is weak, harbors a lot of subtleties that we are not going to discuss here. However, there is a much quicker argument in favor of the safety of restricting the quantization to the BPS submanifold. Our approach consists of enforcing the BPS-constraints at the classical level then quantize the resultant constrained system. The other, more correct, way of quantization is to quantize the full space of solutions then enforce the BPS-constraints on the resultant quantum states. Most of the time, these two approaches are the same. For an example of the relation between states obtained by considering the BPS sector of the fully quantized Hilbert space and the states obtained by quantizing just the BPS sector phase space see [85].

Let us emphasize that the validity of this decoupling argument depends on what questions one is asking. If we were interested in studying dynamics, then, we would

have to worry about how modes on the BPS phase space interact with transverse modes. For the purpose of enumerating or determining general properties of states, however, as we have argued, it should be safe to ignore these modes.

2.3.2 QUANTIZATION

So far we spoke about the symplectic form in the classical theory, how do we proceed to the quantum theory? The symplectic form encodes the quantum information through its connection with the Poisson bracket as follows. In the phase space, the canonical Poisson bracket is given by

$$\{q^a, p^b\} = \delta^{ab}.$$

This can be encoded in the symplectic form $\Omega = dp^a \wedge dq^a$. Now, given a coordinateization x^α of the phase space, the symplectic form becomes

$$\Omega = \omega_{\alpha\beta} dx^\alpha \wedge dx^\beta; \quad \omega_{\alpha\beta} = \frac{1}{2} \left(\frac{\partial p^a}{\partial x^\alpha} \frac{\partial q^a}{\partial x^\beta} - \frac{\partial q^a}{\partial x^\alpha} \frac{\partial p^a}{\partial x^\beta} \right). \quad (2.8)$$

It is easy to see from the equation above that, the Poisson bracket of x^α and x^β is just the inverse of the $\omega_{\alpha\beta}$. Explicitly

$$\{x^\alpha, x^\beta\} = \frac{1}{2} \omega^{\alpha\beta}. \quad (2.9)$$

The only missing connection to the quantum theory is then, to replace the Poisson bracket by the (anti-)commutator following the standard canonical quantization procedure.

The next step in the quantization is to construct the Hilbert space. Unfortunately, this is not so trivial and depends on the case under consideration (e.g [86]). The fundamental issue is to distinguish coordinates from momenta by picking a *polarization*. In the cases we are going to discuss, two approaches are followed

- The D1-D5 system: this case turns out to be easy as one gets a harmonic oscillator algebra. This allows us to introduce creation/annihilation operators leading to the Hilbert space as in the standard way [87, 88].
- The four dimensional multi-center black hole solutions: in this case we resort to geometric quantization techniques (see for example [89, 90, 91]). We defer a small discussion about this approach to the sixth chapter.

2.4 COARSE GRAINING

In principle, we have succeeded in constructing the Hilbert space of black hole states. However, we do not know yet what is the relation between our classical black hole and these states. To get some insight about this connection, a possible thing to do is to look for a typical state among the semi-classical states. This should be the closest we could get to reproduce the naive black hole physics. However this notion (typical state) usually needs an “average” state to be defined. The latter may also be seen as a close cousin of our black hole. The golden question that begs for an answer is: *suppose that we are given a black hole and its ensemble. Suppose also that somehow we have succeeded in finding the average/typical state of the ensemble. Can we treat the three geometries: average state geometry, typical state geometry, and the black hole geometry as being the same when we coarse grain?*? If the answer is yes than we can confirm that the black hole is an effective description of its ensemble. But what do we mean by “coarse graining”? In this process we have in mind a measuring device with a limited resolution Δ . Due to such limitation any measurements with deference less than Δ will be registered as the same. This is called “coarse graining”.

2.4.1 COARSE GRAINING AS AN AVERAGE

The only way to evaluate averages, that we know of, is when there is a linearity in the system under consideration. Since gravity equations are non-linear, it is not clear how to “average” over geometries. Luckily, in the cases we are going to deal with, our geometries are completely fixed given a set of harmonic functions. In this class of solutions we are offered with a suitable coarse graining procedure, we simply smear these Harmonic functions against appropriate weights. Of course, this is not the end of the story as one has to make sure that the resulting average geometry does solve the original equations of motion at least asymptotically, and is free of pathologies such as closed timelike curves (CTC in short) and regions of high curvature.

To carry on such averaging in practice, we need to specify the weights of the different “geometries” that enter the process of averaging. Such weights have two origins. The first one is classical, and has to do with the nature of the ensemble under study. In the case of black holes these weights will be thermodynamical weights, because of the total body of evidence gathered so far that indicates that black holes behave like thermodynamical ensembles. The second contribution is quantum in nature for the following reason. We are in principle evaluating the average in the quantum theory, but, we want to recast the result in terms of classical quantities (like the geometry) living in the phase space. This transition between quantum Hilbert space to classical phase space can be achieved using the phase space densities, see for

example the review [92] and references there in to the original literature. We will defer the rightful discussion of such a concept to the fourth chapter, section 4.1, as this average procedure will be carried out only for the D1-D5 system. Unfortunately, it is not clear how to extend such an operation to the more interesting $\mathcal{N} = 2$ four-dimensional 1/2-BPS black holes. This is because, as we will see later, we seem to not have enough states to account for a finite fraction of the entropy.

2.4.2 ANOTHER POSSIBILITY: TYPICAL STATES

As we pointed out before, another coarse graining candidate is typical states. A typical state in an ensemble is one for which the expectation values of macroscopic observables agree, to within the observable accuracy, with the average of the observable in the entire ensemble. Obviously, this definition depends on the appropriate notions of macroscopic observables and observable accuracy. Given a typical state, we can try to map it directly to a solution of supergravity (this may still be a formidable task), after which, one still needs to verify that the resulting geometry has no pathologies such as closed timelike curves and regions with Planck size curvature. Such typical states can be useful in the case of the $\mathcal{N} = 2$ four-dimensional supergravity to study the physics of 1/2-BPS black holes, though, we are not going to do so in this thesis.

Part II

D1-D5 System and Coarse Graining

PRELUDE

The study of simple systems and toy models plays an important role in discovering new concepts in physics as well as checking them. Following this line of thoughts, we are going to study the D1-D5 system under the microscope of the fuzzball program. The importance of this system is twofold. On one hand, we already know a great deal of its field theory dual (see for example [24] and references there in). This gives us a solid reference point to which we can turn to for comparison, inspiration, and guidance. On the other hand, the large symmetry that this system enjoys allows us to be explicit in our discussion. This can help us understand better how to apply the fuzzball ideas developed so far, and also shed some light on the possible limitations of their applicability.

We will start by reviewing the D1-D5 system and its naive ten dimensional geometry. Then, we will describe its space of solutions (called also “solution space”), which is comprised of what is known as the “Lunin-Mathur” geometries (LM in short). This space of solutions will be our working material in the remaining of this part of the thesis. After that, a quick review of the solution space quantization and the resulting Hilbert space will follow.

The last chapter of this part of the thesis will deal mainly with coarse graining. Due to the simple structure of the D1-D5 Hilbert space, we can average over geometries. The resulting effective geometries look exactly like the associated black objects except around the “origin”, where the geometry becomes smooth instead of being singular. During the process we uncover a version of the no-hair theorem. It turns out that the effective description loses almost all information about the thermodynamical ensemble it describes, except for three quantum numbers that we understand very well. We will see that it is possible to put extra hair whenever the dual quantum system behaves like a Bose-Einstein condensate. As an example, we will treat a simple case associated to the “small” black ring. We close this chapter by showing that it is not possible to construct conical defect metrics with an arbitrary opening angle. Some technical manipulations will be left to appendix C.

CHAPTER 3

THE LUNIN-MATHUR (LM) GEOMETRIES

The D1-D5 system was and still is an active laboratory for different ideas and aspects of quantum gravity in string theory. In order to better understand it, using AdS/CFT duality, Mathur and collaborators ended up suggesting an unorthodox idea that was baptized the “fuzzball” program [32, 33, 34, 35]. In this chapter we will try to describe this fertile system leaving the study of the implications of the fuzzball ideas when applied to this system to the next chapter.

We will start by describing the stringy/brane construction of the D1-D5 system. Then, by using T and S duality we will be able to construct the most general D1-D5 supergravity solution through its connection with the FP system. The latter describes the closed fundamental string (F) which carries a momentum charge (P) as a traveling wave. Finally, we will discuss the quantization of this solution space.

Familiarity with string theory is assumed throughout this chapter. See appendix B for a summary of our conventions.

3.1 THE FIVE DIMENSIONAL “SMALL” BLACK HOLE

The simplest stringy system that bears a lot of resemblance to black holes is the so called “two charges system”. A prototype is the D1-D5 system which, after back reaction, describes a five dimensional black hole with zero horizon area. Because of the last property it is dubbed a “small” black hole. We are going to describe the

brane set-up, and its ten dimensional backreacted geometry in the following. We will be very brief in our survey, for more details see e.g [93] and references there in.

3.1.1 THE SET-UP

We start with type-IIB string theory on $\mathcal{M}^{(1,4)} \times S^1 \times X_4$, where $\mathcal{M}^{(1,4)}$ is a non-compact five dimensional spacetime and X_4 is either a T^4 or K_3 . In the following, we will have T^4 in our mind as it allows us to be explicit. Things should carry on to K_3 with slight changes. In the above geometry, the size of the S^1 is much bigger than the size of X_4 , which is itself much bigger than the typical string scale so that we can trust supergravity to leading order. Such scale hierarchy allows us to compactify on X_4 reducing every thing to a six dimensional supergravity theory. The latter will be the frame work in the next chapter.

Among the fields of type-IIB supergravity, we are going to turn on the dilaton ϕ and, of all possible R-R forms, the two-form $C^{(2)}$ corresponding to the D1 and the D5 D-branes. Furthermore, we are going to wrap N_5 D5 branes on $S^1 \times T^4$ and N_1 D1 branes on S^1 . Since we do not want to keep track of the position of the D1 in the internal space T^4 , we are going to uniformly distribute the D1-branes on this space. This is called “smearing”.

3.1.2 THE GEOMETRY

To construct the supergravity solution that corresponds to the D1-D5 system, we need to solve the equations of motion coming from the action (section B.1.2)

$$S = \frac{1}{2\kappa_0^2} \int d^{10}x (-G)^{1/2} \left(e^{-2\phi} [R + 4(\nabla\phi)^2] - \frac{1}{12} dC^{(2)} \wedge *dC^{(2)} \right), \quad (3.1)$$

where we should be careful when dealing with $C^{(2)}$ because it describes both D1 and D5 branes. We should require that

$$\int_{T^4 \times S^3} *dC^{(2)} \sim Q_1, \quad \int_{S^3} dC^{(2)} \sim Q_5, \quad (3.2)$$

where Q_1 (Q_5) is the D1 (respectively, D5) charge, and S^3 is a three-sphere that sits at large radius on the spatial part of $\mathcal{M}^{(1,4)}$. We should also require the existence of a Killing spinor predicted by the probe brane analysis. In such analysis, the string coupling constant that sets the strength of gravity is very small. This means that the geometry will not feel the presence of the D-branes. As a result, the non-compact part of the space, $\mathcal{M}^{(1,4)}$, will be the flat five-dimensional Minkowski spacetime. In

such a situation, one can use the physics of open strings ending on the D1 and/or D5 branes to study the D1-D5 system.

In the following, we are not going to use the strategy outlined before. Instead, we are going to take advantage of the explicit form of the solutions describing the response of spacetime to the existence of D-branes (section B.2). In some cases, one can apply a simple algorithm to figure out the metric of orthogonally intersecting branes called the “harmonic function rule” [94, 95]. The D1-D5 system does satisfy the requirements needed to apply such an algorithm that we are going to describe in some detail. Essentially, each D-brane solution is characterized by a harmonic function H that depends on the non-smeared transverse directions. In the string frame, it enters in the metric as $H^{-1/2}$ in front of the parallel directions and as $H^{1/2}$ in front of the transverse directions (see section B.2). The full solution then contains all the associated harmonics as if each D-brane exists on its own. In the case of the D1-D5 system the solution reads [93]

$$\begin{aligned} ds^2 &= \frac{1}{\sqrt{f_1 f_5}} [-dt^2 + dy^2] + \sqrt{f_1 f_5} (dr^2 + r^2[d\theta^2 + \cos^2 \theta d\phi^2 + \sin^2 \theta d\psi^2]) + e^{\Phi} d\mathbf{z}^2, \\ e^{2\Phi} &= \frac{f_1}{f_5}, \quad f_i = 1 + \frac{Q_i}{r^2}, \\ G^{(3)} &= dC^{(2)} = Q_5 \sin 2\theta d\theta \wedge d\phi \wedge d\psi - \frac{2Q_1}{r^3 f_1^2} dr \wedge dt \wedge dy, \end{aligned} \quad (3.3)$$

where y is the coordinate along S^1 , and $\{z^i\}$ are the T^4 coordinates. We use throughout the remaining of this part of the thesis boldface notations to indicate four-dimensional vectors. Innerproducts are also understood in expressions like $|\mathbf{F}|^2$. It can be checked that this geometry when reduced to five dimensions describes a black hole with vanishing horizon area [96]

$$A \sim \lim_{r \rightarrow 0} \left(r^3 \sqrt{\frac{Q_1 Q_5}{r^4}} \right) = 0.$$

As for the supersymmetries, one can either start from the zero string coupling limit (probe D-branes in flat spacetime), or solve the Killing spinor equations [93, Appendix: D]. In both cases, the conclusion is that the Killing spinors of the D1-D5 system satisfy the following two projections [93]

$$\Gamma_{\hat{t}} \Gamma_{\hat{y}} \epsilon = -i\epsilon^*, \quad \Gamma_{\hat{t}} \Gamma_{\hat{y}} \prod_{i=1}^4 \Gamma_{\hat{z}_i} \epsilon = -i\epsilon^*, \quad (3.4)$$

where the hat stands for flat local frame directions.

3.2 THE LUNIN-MATHUR (LM) GEOMETRIES

The reduction of the solution described above to six dimensions describes the geometry of an effective string wrapped around the S^1 . This suggests that we can construct other solutions by including the possibility of a non-trivial profile. The story is not as simple as it sounds because we should make sure that we are not adding an extra charge by doing so. Using the large duality group that the D1-D5 system has, [69, 35, 97] managed to construct a generalization of the solution (3.3) by mapping it to a fundamental string carrying a right (or left) momentum, called FP system [98, 99, 100]. Such a construction is the subject of this section.

3.2.1 SWITCHING TO THE FP SYSTEM

There are different duality chains that map a D1-D5 system to an FP one. A possible chain is [97]

$$\begin{pmatrix} \text{D1}(y) \\ \text{D5}(y, \{z_i\}) \end{pmatrix} \xrightarrow{\text{S}} \begin{pmatrix} \text{F1}(y) \\ \text{NS5}(y, \{z_i\}) \end{pmatrix} \xrightarrow{\text{T}_y} \begin{pmatrix} \text{P}(y) \\ \text{NS5}(y, \{z_i\}) \end{pmatrix} \xrightarrow{\text{S}} \begin{pmatrix} \text{P}(y) \\ \text{D5}(y, \{z_i\}) \end{pmatrix} \xrightarrow{\prod_i \text{T}_{z_i}} \begin{pmatrix} \text{P}(y) \\ \text{D1}(y) \end{pmatrix} \xrightarrow{\text{S}} \begin{pmatrix} \text{P}(y) \\ \text{F1}(y) \end{pmatrix}, \quad (3.5)$$

where T_* stands for T-duality in the “*” direction and S stands for S-duality (section B.3). At the end, we get an FP system whose general supergravity solution is well known [98, 99, 100]

$$ds^2 = H(\mathbf{x}, v) (-du dv + K(\mathbf{x}, v) dv^2 + 2A_i(\mathbf{x}, v) dy_i dv) + d\mathbf{x}^2 + d\mathbf{z}^2, \quad (3.6)$$

$$b_{uv} = -g_{uv} = \frac{1}{2} H(\mathbf{x}, v), \quad b_{vi} = -g_{vi} = -H(\mathbf{x}, v) A_i(\mathbf{x}, v), \quad e^{-2\phi} = H^{-1}(\mathbf{x}, v),$$

where $b_{\mu\nu}$ is the NS-NS B-field, $g_{\mu\nu}$ is the metric, $v = t - y$ and $u = t + y$ are null coordinates. The functions $H(\mathbf{x}, v)$, $K(\mathbf{x}, v)$ and $A_i(\mathbf{x}, v)$ depend on $\mathbf{F}(v)$, the profile of the string in the following way

$$H^{-1}(\mathbf{x}, v) = 1 + \frac{Q}{|\mathbf{x} - \mathbf{F}(v)|^2}, \quad K(\mathbf{x}, v) = \frac{Q |\dot{\mathbf{F}}(v)|^2}{|\mathbf{x} - \mathbf{F}(v)|^2}, \quad A_i(\mathbf{x}, v) = -\frac{Q \dot{F}_i(v)}{|\mathbf{x} - \mathbf{F}(v)|^2}, \quad (3.7)$$

where the dot in $\dot{\mathbf{F}}$ stands for derivative with respect to v .

3.2.2 THE LM GEOMETRIES

To get the most general D1-D5 geometry, we need to undo the chain of dualities described above. One slight complication comes from the explicit dependence of the

profile \mathbf{F} on y (through v) which is used as a T-duality direction. To apply the rules given in section B.3 we need to smear our string over v . In practice, this amounts to integrating the functions H^{-1}, K and A_i over v . Going through the reverse of the chain of dualities (3.5) leads us to the following D1-D5 solution generalizing (3.3)

$$ds^2 = \frac{1}{\sqrt{f_1 f_5}} [-(dt + A)^2 + (dy + B)^2] + \sqrt{f_1 f_5} d\mathbf{x}^2 + \sqrt{f_1/f_5} d\mathbf{z}^2, \\ e^{2\Phi} = \frac{f_1}{f_5}, \quad C = \frac{1}{f_1} (dt + A) \wedge (dy + B) + \mathcal{C}, \quad (3.8)$$

where:

$$dB = *_4 dA, \quad dC = - *_4 df_5, \quad A = \frac{Q_5}{L} \int_0^L \frac{F'_i(s) ds}{|\mathbf{x} - \mathbf{F}(s)|^2}, \\ f_5 = 1 + \frac{Q_5}{L} \int_0^L \frac{ds}{|\mathbf{x} - \mathbf{F}(s)|^2}, \quad f_1 = 1 + \frac{Q_5}{L} \int_0^L \frac{|\mathbf{F}'(s)|^2 ds}{|\mathbf{x} - \mathbf{F}(s)|^2}, \quad (3.9)$$

where the Hodge star $*_4$ is defined with respect to the flat four-dimensional non-compact space spanned by $\{x^i\}$. We have also switched v to s as it is now just a parameter, and the prime in \mathbf{F}' stands for derivative with respect to s . These solutions (3.8) are asymptotically $\mathbb{R}^{1,4} \times S^1 \times T^4$ and they are parametrized in terms of a closed curve $x_i = F_i(s)$ with $0 \leq s \leq L$. In the sequel, we are going to ignore oscillations in the T^4 direction as well as fermionic excitations; for a further discussion of these degrees of freedom see [101, 102]. The D1 (D5) charge Q_1 (respectively, Q_5) satisfy

$$L = \frac{2\pi Q_5}{R}, \quad Q_1 = \frac{Q_5}{L} \int_0^L |\mathbf{F}'(s)|^2 ds. \quad (3.10)$$

The first relation is a result of the identification of the D5 with the F1 through duality. In terms of charges, Q_5 corresponds to the winding number of the fundamental string. The second relation seems more involved though its origin is very simple. It is due to the identification of the D1 charge with the momentum running around the fundamental string which is given by $F'(s)$. It turns out that these geometries are smooth if the profile \mathbf{F} does not self-intersect and has an everywhere non vanishing derivative \mathbf{F}' [97]. The last comment we want to mention here is that the Killing spinors of these geometries satisfy the same projection (3.4) [93]. The only difference resides in the vielbeins, which means that asymptotically they preserve the same supersymmetries.

3.3 THE SYMPLECTIC FORM AND QUANTIZATION

So far, we have succeeded in constructing a large class of smooth solutions (3.8) that look asymptotically like the naive D1-D5 one (3.3), except that they have a non

zero angular momentum given by:

$$J_{ij} = \frac{Q_5 R}{L} \int_0^L (F_i F'_j - F_j F'_i) \, ds , \quad (3.11)$$

where R is the coordinate radius of the S^1 . It can be checked that $J \leq N_1 N_5$ in agreement with an upper bound on possible quantum numbers, dubbed the stringy exclusion principle in [17]. The N_1 (N_5) stand for the number of D1 (respectively, D5) branes. Their relation with the charges Q_1 and Q_5 is given by

$$N_1 = \frac{g_s}{V_4} Q_1, \quad Q_5 = g_s N_5 , \quad (3.12)$$

where V_4 is the coordinate volume of T_4 , and g_s is the string coupling constant.

We want to quantize this space of solutions following the general scheme described in section 2.3. First, we will sketch how to get the symplectic form [87, 88]. Then, we will construct the associated Hilbert space.

3.3.1 THE SYMPLECTIC FORM

In evaluating the symplectic form of the solution space described above, we can either use its form (2.5) and evaluate its restriction directly [87], or, we can take advantage of the symmetries of our solutions to reduce the amount of work that has to be done [88]. We are going to follow the latter as it is simpler and does not need any long calculations except to fix an overall prefactor.

The idea relies on a simple observation regarding the equivalence of the Hamiltonian flows of the total Hamiltonian system (\mathcal{H}, Ω) on our solution space and the flow of its restriction (h, ω) on the same solution space. The next input that we are going to use, is that our solutions (3.8) are time independent. We start by writing down the Hamiltonian equations corresponding to the curve \mathbf{F}

$$\frac{dF_i}{dt} = \{F_i, h\} , \quad (3.13)$$

where $\{, \}$ is the Poisson bracket that we want to specify using the time independence property. The latter tells us that the only non trivial acceptable equations are of the form

$$\frac{dF_i}{dt} = \alpha \frac{dF_i}{ds} , \quad (3.14)$$

where α is a constant. This is because \mathbf{F} enters in the solution (3.8) through integration over s (see equation (3.9)). Next, we need to evaluate the restriction of the

Hamiltonian to our solution space. This can be done using the expression of energy in the asymptotic flat spacetime. The restricted Hamiltonian turns out to be [88]

$$h = \frac{R V_4}{g_s^2} \left(\frac{Q_5}{L} \int_0^L |\mathbf{F}'|^2 ds + Q_5 \right) = \frac{R V_4}{g_s^2} (Q_1 + Q_5) , \quad (3.15)$$

where in the last equation we used (3.10). This is in perfect agreement with the fact that our solutions are BPS. Using this explicit expression, it is easy to see that the only possible form of the Poisson bracket which is consistent with equations (3.13) and (3.14) is

$$\{F_i(s), F'_j(\tilde{s})\} = \pi \mu^2 \delta_{ij} \delta(s - \tilde{s}) , \quad (3.16)$$

where μ is a constant that cannot be fixed by these general considerations. Looking carefully at some simple examples, [88] showed that μ takes the form:

$$\mu = \frac{g_s}{R\sqrt{V_4}} . \quad (3.17)$$

For completeness, we will write down explicitly the symplectic form

$$\omega = \frac{1}{2\pi\mu^2} \int \delta F'(s) \wedge \delta F(s) ds . \quad (3.18)$$

3.3.2 QUANTIZATION

After finding the Poisson bracket (3.16), we can go ahead and construct our Hilbert space. Taking advantage of the periodicity of \mathbf{F} , we can expand it in oscillators as

$$\mathbf{F}(s) = \mu \sum_{k=1}^{\infty} \frac{1}{\sqrt{2k}} \left(\mathbf{c}_k e^{i \frac{2\pi k}{L} s} + \mathbf{c}_k^\dagger e^{-i \frac{2\pi k}{L} s} \right) , \quad (3.19)$$

where we have promoted \mathbf{F} to an operator. One can invert this expression to get \mathbf{c}_k and \mathbf{c}_k^\dagger in terms of \mathbf{F} using the orthonormality of the different oscillator modes. Now, it is a matter of plugging in these expressions into the commutator that one gets from the Poisson bracket (3.16) through canonical quantization. After things settle down, we get the following non-vanishing commutator between \mathbf{c}_k and \mathbf{c}_l^\dagger

$$\left[c_k^i, (c_l^j)^\dagger \right] = \delta^{ij} \delta_{kl} , \quad (3.20)$$

where i, j are spacetime indices corresponding to the non-compact spatial part x^i and k, l correspond to the level of the oscillator.

Before constructing our Hilbert space, let us pause for a moment and discuss a subtlety that we have ignored until now. The expansion (3.19) is not the most

general one. We have already chosen a gauge where we set the constant term in $\mathbf{F}(s)$ to zero. This is because we can absorb such a constant by shifting the origin of the coordinates \mathbf{x} which does not change our solution (3.8, 3.9). In a sense, by doing so we decoupled the translation modes of our system. Of course, this is not the only gauge one can choose. The only condition that one should respect is invariance under the shift symmetry $s \rightarrow s + \delta s$ (section 4.2.2). As a matter of fact, [103, 104] made another choice based on holographic considerations to treat the decoupled version of our solutions.

Our Hilbert space is not the full Fock space that is comprised of all states that can be built by the action of all possible combinations of the creation operators \mathbf{c}_k^\dagger on the vacuum state $|0\rangle$, as the profile \mathbf{F} should satisfy the constraint (3.10). The latter, when expressed in terms of the operators $\mathbf{c}_k, \mathbf{c}_k^\dagger$, becomes

$$N \equiv N_1 N_5 = \frac{L}{(2\pi)^2} \frac{1}{\mu^2} \left\langle \int_0^L :|\mathbf{F}'(s)|^2: ds \right\rangle = \sum_{k=1}^{\infty} k \left\langle \mathbf{c}_k^\dagger \mathbf{c}_k \right\rangle. \quad (3.21)$$

So our Hilbert space is spanned by

$$|\psi\rangle = \prod_{i=1}^4 \prod_{k=1}^{\infty} (c_k^{i\dagger})^{N_{k_i}} |0\rangle, \quad \sum k N_{k_i} = N, \quad (3.22)$$

where $|0\rangle$ is the vacuum state that is annihilated by all the annihilation operators c_k^i .

CHAPTER 4

SIMPLE ENSEMBLES AND THEIR COARSE GRAINING

In this chapter, we are going to explore some simple ensembles of the D1-D5 states and their effective geometries. In the examples we are going to discuss, the weights of the D1-D5 states in the ensemble under study can be parametrized by giving a density matrix. Since we are looking for an effective geometry description of these ensembles, we will be led to discuss the phase space counter part of the defining density matrix. This is the so called “*phase space density*” [92] (section 4.1). Having that at our disposal allows us to propose a map from quantum states to geometries (section 4.2), opening the possibility to look for the effective geometry description of D1-D5 ensembles.

Since our Hilbert space is constrained (3.21), we should take into account such a constraint in the definition of our density matrix. This is very much like dealing with a microcanonical ensemble. In some cases, we will switch to the canonical ensemble description as it is easier to deal with. For large quantum numbers, we expect that the two descriptions will give the same physics at leading order. For a thorough discussion on this point see section 4.2.2. We start by the ensemble that associates the same weight to all the states. Dealing with its canonical ensemble version allows us to derive its effective geometry description. This turns out to be approximately the D1-D5 naive geometry except in a region around the origin (section 4.3). After that, we will discuss a simple yet an interesting class of thermodynamical ensembles (section 4.4). In this class of ensembles, each oscillator c_{k^i} is occupied thermally with a temperature β_k^i . It turns out that most of the details of the ensemble disappear leaving behind three quantum numbers with well understood physics (section

4.4). However, to arrive at this conclusion we overlooked an important physical phenomenon: the Bose-Einstein condensate (section 4.5). As we will see, when the temperatures defining a toy model ensemble are tuned appropriately, a condensation of specific modes can be induced (section 4.5). Finding out the geometric description of such condensates will be the subject of the next-to-last section (section 4.6). In the last section (section 4.7), we will set foot on a path to construct a metric that describes a conical defect with an arbitrary deficit angle whose existence was ruled out based on regularity requirements [97, appendix: C]. We will try to relax such a requirement by looking for an effective description of a specific ensemble of (possibly non-smooth) metrics.

Throughout this chapter familiarity with quantum mechanics and statistical physics is assumed.

4.1 INTERLUDE: PHASE SPACE DENSITIES

As is well known, the uncertainty principle destroys the classical notion of phase space as coordinates and their conjugate momenta cannot be defined at the same time. Since ultimately we want to deal with geometries which are –in our set up– points in a phase space, we would like to have an approximate quantum description of a phase space. It turns out that such a description can be achieved with the help of the “phase space density” (see [92] and references there in). Explaining this concept and its use is the subject of this section.

4.1.1 WHY PHASE SPACE DENSITIES?

Quantum mechanics, as we know it, is a set of abstract rules; “*axioms*” which gives a recipe for results to be expected from carrying out an experiment. Due to its probabilistic nature, the average of measured quantities are nicely expressed as expectation values of the associated operators. Usually, in such a process, these operators are integrated against probabilities that are expressed in terms of either position coordinates or dual momenta but not both. Such a traditional approach is clearly not applicable when we want to treat the phase space as a whole. This is precisely the case we are dealing with, because the geometries (3.8) are points in a phase space. Another physical situation where such a treatment is very welcome is statistical mechanics. This was the reason behind Wigner’s suggestion to reformulate Schrödinger’s quantum mechanics in a way such that coordinates and momenta are treated on the same footing [105]. This proposal goes under the name of “*phase space density*” approach.

Statistical and quantum mechanics share the same probabilistic nature though these probabilities have different origins: the probability in statistical mechanics originates in our ignorance about the full details of our system on the contrary to quantum mechanics whose probabilistic nature is of a fundamental origin. This clearcut difference does not forbid us from migrating some technical tools from statistical to quantum mechanics. Let us follow this line of thoughts and see what we can learn.

A particle (or a statistical system) in the quantum theory is described by giving its density matrix ρ . The result of any measurement can be seen as an expectation value of an appropriate operator which is given explicitly by

$$\langle \mathcal{O} \rangle_\rho = \text{Tr}(\rho \mathcal{O}) . \quad (4.1)$$

This is reminiscent of classical statistical mechanics where the measurements are averages of appropriate quantities using some statistical distribution $w(p, q)$

$$\langle \mathcal{O} \rangle_w = \int dp dq w(p, q) \mathcal{O}(p, q) , \quad (4.2)$$

where the integration is over the full phase space. One can wonder at this point if it is possible to construct a density $w(p, q)$ so that one can rewrite equation (4.1) as equation (4.2). The answer is affirmative: for every density matrix ρ there is an associated phase space distribution w_ρ such that the following equality holds for all operators A

$$\int dp dq w_\rho(p, q) A(p, q) = \text{Tr}(\rho A(\hat{p}, \hat{q})) . \quad (4.3)$$

In defining the phase space density $w_\rho(p, q)$, there is a subtlety that needs to be addressed. This will be the subject of the next subsection.

4.1.2 WIGNER VS HUSIMI DISTRIBUTION

Recall that in the quantum theory we have to face the question of operator ordering. This comes about because the operators \hat{q} and their dual momenta \hat{p} do not commute with each other. This means that the distribution w_ρ should somehow include information about the chosen order of \hat{p} and \hat{q} . As a result, there does not exist a unique phase space distribution. However, for semi-classical states, which by definition are states for which the classical limit is unambiguous, $w_\rho(p, q)$ should be independent of the choice of ordering prescription in the classical limit as well, so this is not actually much of a problem for these class of states.

Wigner was the first one to introduce a phase space density [105]. His motivation was the study of quantum corrections to classical statistical mechanics. This distribution is commonly known right now as the “Wigner distribution” and is given

by

$$w(p, q) \sim \int dy \langle q - y | \rho | q + y \rangle e^{2ipy}, \quad (4.4)$$

where ρ is the quantum density matrix. It turns out that such a distribution corresponds to Weyl ordering [92], given by the prescription:

$$\hat{\mathcal{O}}(\hat{q}, \hat{p}) = \int d\sigma d\tau \alpha(\sigma, \tau) e^{i(\sigma \hat{q} + \tau \hat{p})}, \quad (4.5)$$

where the hats in \hat{q}, \hat{p} stand for operators and $\alpha(\sigma, \tau)$ is the Fourier transform of the classical quantity $\mathcal{O}(q, p)$.

Wigner distribution suffers from the fact that it is not positive-definite in general. It is also quite sensitive to the physics at a quantum scale [92, 73], as it usually has fluctuations of order \hbar . Another drawback of this distribution is that it is difficult to work with from a computational standpoint.

These issues stimulate us to look for another distribution. We need to have a good requirement so that we can narrow down the possible candidates. Going back to our starting point, “phase space quantization”, supplements us with a possible starting point. Remember that we want to be able to map states to geometries which are points in phase space. This suggests to look for a smooth distribution that can get us close enough to the notion of a point in phase space. A possible candidate is a Gaussian with width \hbar , which is the best we can do according to the uncertainty principle. However, these distributions should not be associated to any quantum state. If this was the case, then, quantum mechanics will be a small deformation of classical mechanics which we know is not the case: Quantum mechanics is fundamentally different from classical mechanics. There is however a special class of states, the so called “semi-classical states”, for which quantum mechanics measurements reduce to the classical ones in the limit $\hbar \rightarrow 0$ limit. These are the class of states we wish to associate a Gaussian distribution of width \hbar to them.

Finding semi-classical states is usually far from trivial, but fortunately our Hilbert space is similar to the one of a Harmonic oscillator. And luckily enough, we know precisely what we mean by a semi-classical state in this case. These are the so called “coherent states” $|z\rangle$ defined by:

$$|z\rangle = e^{-|z|^2/2} e^{z a^\dagger} |0\rangle; \quad a|z\rangle = z|z\rangle. \quad (4.6)$$

Using the properties of such states, a natural guess for the sought after distribution is the projection on the associated coherent state. This is not a δ -function as we all know that the coherent states are not orthonormal. Indeed their innerproduct is given by

$$\langle z|w\rangle = \exp\left[-\frac{1}{2}|z-w|^2\right], \quad (4.7)$$

which clearly shows that our distribution reduces to a Gaussian centered around a classical solution when evaluated on a semi-classical state. It can be checked that, after re-introducing \hbar and normalizing the distribution, in the $\hbar \rightarrow 0$ limit this distribution reduces to a δ -function.

Our starting point is then a distribution that, in the case of a Harmonic oscillator, projects a state $|\psi\rangle$ on coherent states:

$$Hu_\psi(z) = |\langle\psi|z\rangle|^2. \quad (4.8)$$

This is the so called “*Husimi distribution*” [92, 73]. To prove that such a distribution is appropriately normalized, we use the over-completeness relation of coherent states

$$\int d^2z |z\rangle\langle z| = \mathbb{I}, \quad (4.9)$$

where $d^2z = -i/(2\pi)dz \wedge d\bar{z}$, which is the convention we are going to use in the remaining of this chapter. It can be shown that the Husimi distribution is always smooth and positive definite [92]. The price to be payed for these nice properties is that the average of classical quantities, using Husimi distribution, corresponds to anti-normal ordered operators [92, 73]. This is a result of the following general identity

$$\int d^2z Hu_\psi(q, p) z^m \bar{z}^n = \langle\psi| a^m (a^\dagger)^n |\psi\rangle, \quad (4.10)$$

where we used (4.8), (4.6) and its Hermitian conjugate, and finally (4.9). In the following, we are going to use the Husimi distribution because of its nice properties mentioned above. It turns out also that dealing with such distribution is a lot easier technically than the Wigner distribution.

4.2 MAPPING STATES TO GEOMETRIES

We succeeded above in constructing a dictionary between states in the Hilbert space and distributions in the classical phase space. This will allow us to carry on an averaging process for our LM geometries (3.8, 3.9) starting from our Hilbert space (3.22, 3.19). Describing such a process will be the subject of this section.

4.2.1 FROM STATES TO GEOMETRIES

The first step towards the implementation of coarse graining will be to construct a map from states to solutions through an adaptation of the Husimi distribution to the

phase space (3.19, 3.10). Given a state, or more generically a density matrix

$$\rho = \sum_i |\psi_i\rangle\langle\psi_i|, \quad (4.11)$$

we wish to associate to it a density on phase space. The phase space is given by the space of classical curves (section 3.2.2), which we will parametrize as (note that d and \bar{d} are now complex numbers, not operators as in (3.19))

$$\mathbf{F}(s) = \mu \sum_{k=1}^{\infty} \frac{1}{\sqrt{2k}} \left(\mathbf{d}_k e^{i \frac{2\pi k}{L} s} + \bar{\mathbf{d}}_k e^{-i \frac{2\pi k}{L} s} \right), \quad (4.12)$$

and which obey the classical constraint (3.10).

We now propose to associate to a density matrix of the form (4.11) a phase space density of the form [106]

$$f(d, \bar{d}) = \sum_i \prod_k e^{-|\mathbf{d}_k|^2} \langle 0 | e^{\mathbf{d}_k \mathbf{c}_k} |\psi_i\rangle \langle\psi_i| e^{\bar{\mathbf{d}}_k \mathbf{c}_k^\dagger} |0\rangle. \quad (4.13)$$

This is just the Husimi distribution described in the previous section (equation 4.8). Notice that this phase space density, as written, is a function on a somewhat larger phase space as d, \bar{d} do not have to obey (3.10). Let us ignore this issue for the moment and return to it later. As an example, the distribution corresponding to a generic state

$$|\psi\rangle = \prod_{k=1}^{\infty} \frac{1}{\sqrt{N_{k_i}!}} (c_k^{i\dagger})^{N_{k_i}} |0\rangle,$$

can be easily computed to be

$$f(d, \bar{d}) = \prod_{k,i} e^{-d_k^i \bar{d}_k^i} \frac{(d_k^i \bar{d}_k^i)^{N_{k_i}}}{N_{k_i}!}. \quad (4.14)$$

The density (4.13) has the property that for any function $g(d, \bar{d})$

$$\int \int_{d, \bar{d}} f(d, \bar{d}) g(d, \bar{d}) = \sum_i \langle\psi_i| :g(c, c^\dagger):_A |\psi_i\rangle, \quad (4.15)$$

where $: \mathcal{O} :_A$ is the anti-normal ordered operator associated to \mathcal{O} , and $\int_{d, \bar{d}}$ is an integral over all variables \mathbf{d}_k . This is just a straightforward generalization of (4.10).

As expected, (4.13) associates to a coherent state a density which is a Gaussian centered around a classical curve (see section 4.1.2), which totally agrees with the usual philosophy that coherent states are the most classical states. It is then clear that given a classical curve (4.12), we wish to associate to it the density matrix

$$\rho = P_N \prod_k e^{-|\mathbf{d}_k|^2} \left(e^{\mathbf{d}_k \mathbf{c}_k} |0\rangle\langle 0| e^{\bar{\mathbf{d}}_k \mathbf{c}_k^\dagger} \right) P_N, \quad (4.16)$$

where P_N is the projector onto the actual Hilbert space of states of energy N as defined in (3.22). Because of this projector, the phase space density associated to a classical curve is not exactly a Gaussian centered around the classical curve, but, there are some corrections due to the finite N projections. Obviously, these corrections will vanish in the $N \rightarrow \infty$ limit.

Since the harmonic functions appearing in (3.9) can be arbitrarily superposed, we finally propose to associate to (4.11) the geometry defined using the functions

$$\begin{aligned} f_5 &= 1 + \frac{Q_5}{L} \int_0^L \int_{d,\bar{d}} \frac{f(d, \bar{d}) ds}{|\mathbf{x} - \mathbf{F}(s)|^2}, \\ f_1 &= 1 + \frac{Q_5}{L} \int_0^L \int_{d,\bar{d}} \frac{f(d, \bar{d}) |\mathbf{F}'(s)|^2 ds}{|\mathbf{x} - \mathbf{F}(s)|^2}, \\ A_i &= \frac{Q_5}{L} \int_0^L \int_{d,\bar{d}} \frac{f(d, \bar{d}) \mathbf{F}'_i(s) ds}{|\mathbf{x} - \mathbf{F}(s)|^2}. \end{aligned} \quad (4.17)$$

See [107] for a discussion about the validity of such proposal for a generic state. As we have already mentioned at the end of section 3.2.2, the geometries corresponding to a classical curve are regular provided $|\mathbf{F}'(s)|$ is not vanishing and the curve is not self-intersecting [97]. In our setup, we sum over continuous families of curves which generically smooths the singularities. The price that one pays for this is that the solutions will no longer solve the vacuum type-IIB equations of motion, instead a small source will appear on the right hand side of the equations. We defer a discussion on this point to section 4.2.2 below.

4.2.2 AVOIDING RED TRAFFIC LIGHTS

We will first take care of some subtleties and inconveniences, that otherwise will make our lives complicated, before going further and discuss the effective geometric description of some simple ensembles.,

CANONICAL VS MICROCANONICAL ENSEMBLE

The first subtlety that we need to address is that we wish to study the phase space of curves of fixed length. The phase space of curves of arbitrary length is very easy, it simply equals to that of an infinite set of harmonic oscillators. The length of the curve is measured by some operator \hat{N} . The constraint $\hat{N} = N$ is however first class in the language of Dirac, because $[\hat{N}, \hat{N}] = 0$ (or in classical language, the length Poisson commutes with itself). First class constraints generate a gauge invariance. In

in the present case, the operator \hat{N} also generates a gauge invariance, which is simply the shift of the parametrization of the curve,

$$\mathbf{F}(s) \rightarrow \mathbf{F}(s + \delta s) . \quad (4.18)$$

This follows immediately from the commutation relations of \hat{N} with the oscillators.

Therefore, we have two possibilities:

- We can either forget about the length constraint, and include an extra factor $\exp(-\beta\hat{N})$ in the calculations, where we choose β such that the expectation value of \hat{N} is precisely N . This would be like doing a canonical ensemble, and for many purposes this is probably a very good approximation.
- Or, we can insist on fixing the length taking into account the gauge invariance. Therefore, once we include the length constraint, it is impossible to distinguish curves whose parametrization is shifted by a constant. In particular, the only meaningful quantities to compute are those of gauge invariant operators such as f_1 , f_5 and A .

If we insist on fixing the length of the curve \mathbf{F} , we also need to improve the map we discussed above a little bit: we need to project the measure (4.13) on loop space onto the submanifold of phase space of curves of fixed length. It is not completely trivial to determine the right measure. To get an idea we will do the simple example of two oscillators.

We consider \mathbb{C}^2 with the usual measure. We wish to restrict to the submanifold $N = a_1|z_1|^2 + a_2|z_2|^2$, and we wish to gauge fix the $U(1)$ symmetry that maps $z_k \rightarrow e^{i\epsilon a_k} z_k$. What is the measure that we should use? In general, if we have a three-manifold with a $U(1)$ action, and we gauge fix this $U(1)$ the measure on the gauge-fixed two-manifold is simply the induced measure as long as the $U(1)$ orbits are normal to the gauge fixed two-manifold. As a result, integrating a gauge-invariant operator over the gauge fixed two-manifold is the same as integrating it over the entire three-manifold, but dividing by the length of the $U(1)$ orbit through each point. Call the length of this orbit at the point P , $\ell(P)$. On the three-manifold (given by $N = a_1|z_1|^2 + a_2|z_2|^2$) we have the induced measure $d^4x\delta(f)|df|$, with $|df|$ the norm of the differential df , and $f = 0$ is the defining equation of the three-manifold. So, all in all we can write the integral of a gauge invariant quantity A on the two-dimensional submanifold as

$$\int d^4x A(x) \frac{\delta(f)|df|}{\ell(P)} . \quad (4.19)$$

The length of the $U(1)$ orbit is rather tricky, for general a_1, a_2 the orbits do not even close. So, we will assume that these numbers are integers. Then, up to an overall

constant that depends only on a_i , the length of the orbit is almost everywhere

$$\ell(P) = \sqrt{\sum a_i^2 |z_i|^2}, \quad (4.20)$$

with some pathologies if some of the z_i vanish.

Interestingly enough, we now see that $|df|$ and $\ell(P)$ cancel each other. Thus, the only modification in the measure will be to include an extra delta function of the form

$$\delta(N - \sum_k k d_k \bar{d}_k), \quad (4.21)$$

in phase space density. As long as we integrate gauge invariant quantities, this will yield the right answer. Thus, in (4.13) and in (4.14) we should include the appropriate delta function.

Inserting the delta function is just like passing from a canonical to a microcanonical ensemble. For many purposes, the difference between the two is very small, and not relevant as long as we consider the classical gravitational equations of motion only. We will therefore, in the remainder of this chapter, work predominantly in the canonical picture, commenting on the difference with the (more precise) microcanonical picture when necessary.

THE GHOST OF OPERATOR ORDERING

We have already pointed out that our phase space density corresponds to anti-normal ordered operators. As our theory behaves like a 1+1 dimensional field theory, such a prescription will lead to infinities. To get rid of such unwanted behavior, we resort to calculating normal ordered quantities. To further motivate such decision, we note that everything we do is limited by the fact that our analysis is in classical gravity, and therefore, can at best be valid up to quantum corrections.

But, how do we proceed to implement such a modification? One can for example use another distribution that guarantees normal ordering. However, such a distribution suffers from a lot of problems, and is not appropriate for all density matrices [92]. Instead, we are going to adopt the following procedure. We just rewrite our normal ordered operator in terms of anti-normal ordered ones, and use the classical expression of the latter in evaluating the left hand side of (4.15). As an example, let us verify (3.21). The implementation of our prescription for $|\mathbf{F}'(s)|^2$ simply amounts to the replacement:

$$d_k^i \bar{d}_k^i \rightarrow d_k^i \bar{d}_k^i - 1. \quad (4.22)$$

We will continue to write expressions like $|\mathbf{F}'(s)|^2$ in order to not clutter the notation, but always keep in mind that a modification according to our prescription to get rid

of infinities is implemented. Using (4.22), it is then easy to show that (3.21) is satisfied. Indeed, (4.22) is equivalent to the following condition

$$Q_1 = \frac{Q_5}{L} \int_0^L \int_{d,\bar{d}} f(d, \bar{d}) |\mathbf{F}'(s)|^2 ds , \quad (4.23)$$

and this is satisfied as a consequence of $\sum kN_{k_i} = N_1 N_5$. More explicitly

$$\begin{aligned} \frac{Q_5}{L} \int_0^L \int_{d,\bar{d}} f(d, \bar{d}) |\mathbf{F}'(s)|^2 ds &= \frac{Q_5}{L} \int_{d,\bar{d}} f(d, \bar{d}) \left(\mu^2 \frac{4\pi^2}{L^2} L \sum_{k=1}^{\infty} k (d_k^i \bar{d}_k^i - 1) \right) \\ &= \mu^2 \frac{4\pi^2}{L^2} Q_5 \left(\sum_k k N_{k_i} \right) = Q_1 . \end{aligned} \quad (4.24)$$

To go from the first line to the second we have used the following identity

$$\int_{d,\bar{d}} (dd\bar{d})^k e^{-dd\bar{d}} = 2 \int_0^\infty dr r^{2k+1} e^{-r^2} = k! . \quad (4.25)$$

SEMI-CLASSICAL VALIDITY

The last red light we need to take care of is that the average will no longer solve the vacuum type-IIB equations of motion, instead, a small source will appear on the right hand side of the equations. Since these sources are subleading in the $1/N$ expansion and vanish in the classical limit, they are in a regime where classical gravity is not valid and they may well be cancelled by higher order contributions to the equations of motion. To have an idea about these sources, let us study the circular profile.

Classical Treatment We consider the following profile

$$F^1(s) = a \cos \frac{2\pi q}{L} s, \quad F^2(s) = a \sin \frac{2\pi q}{L} s, \quad F^3(s) = F^4(s) = 0 , \quad (4.26)$$

which describes a circular curve winding q times around the origin in the 12-plane. In order to simplify our discussion, we focus on the simplest harmonic function f_5 . Plugging (4.26) into (3.8), it is straightforward to compute

$$f_5 = 1 + \frac{Q_5}{\sqrt{(x_1^2 + x_2^2 + x_3^2 + x_4^2 + a^2)^2 - 4a^2(x_1^2 + x_2^2)}} , \quad (4.27)$$

where the value of a is fixed by the condition (3.10) to be

$$Q_1 = Q_5 \left(\frac{2\pi q}{L} a \right)^2 .$$

In order to evaluate the various integrals, it will be convenient to Fourier transform the x -dependence. Using

$$\frac{1}{|\mathbf{x}|^2} = \frac{1}{4\pi^2} \int d^4u \frac{e^{i\mathbf{u}\cdot\mathbf{x}}}{|\mathbf{u}|^2}, \quad (4.28)$$

we can write f_5 in the following equivalent way

$$\begin{aligned} f_5^{clas} &= 1 + \frac{Q_5}{4\pi^2} \int d^4u \frac{e^{i\mathbf{u}\cdot\mathbf{x}}}{|\mathbf{u}|^2} J_0(a\sqrt{u_1^2 + u_2^2}) \\ &= 1 + J_0\left(a\sqrt{-\partial_1^2 - \partial_2^2}\right) \frac{Q_5}{|\mathbf{x}|^2}. \end{aligned} \quad (4.29)$$

Writing f_5 in this somewhat formal way has the advantage of being more easily compared to the quantum expression obtained below. As explained in appendix C, the other harmonic functions can be obtained from the “generating harmonic function”

$$f_v = Q_5 J_0 \left(a \sqrt{\left(\frac{2\pi q}{L} v_2 + i\partial_1 \right)^2 + \left(\frac{2\pi q}{L} v_1 - i\partial_2 \right)^2} \right) \frac{1}{|\mathbf{x}|^2}. \quad (4.30)$$

For example, putting $v_1 = v_2 = 0$ immediately reproduces (4.29). The geometry can be written in a more familiar form by performing the following change of coordinates

$$\begin{aligned} x_1 &= (r^2 + a^2)^{1/2} \sin \theta \cos \varphi, & x_2 &= (r^2 + a^2)^{1/2} \sin \theta \sin \varphi, \\ x_3 &= r \cos \theta \cos \psi, & x_4 &= r \cos \theta \sin \psi. \end{aligned} \quad (4.31)$$

In terms of these coordinates, the harmonic functions $f_{1,5}$ become

$$f_5 = 1 + f_v|_{v=0} = 1 + \frac{Q_5}{r^2 + a^2 \cos^2 \theta}, \quad f_1 = 1 - \partial_{v^i} \partial_{v^i} f_v|_{v=0} = 1 + \frac{Q_1}{r^2 + a^2 \cos^2 \theta}. \quad (4.32)$$

As a consistency check, we notice that $\square f_5$ is a delta function with a source at the location of the classical curve, to be precise

$$\square |\mathbf{x} - \mathbf{F}(s)|^{-2} = -4\pi^2 \delta^{(4)}(\mathbf{x} - \mathbf{F}(s)).$$

One indeed finds

$$\begin{aligned} \square f_5 &= -\frac{Q_5}{4\pi^2 L} \int_0^L ds \int d^4u e^{i\mathbf{u}\cdot(\mathbf{x}-\mathbf{F}(s))} \\ &= -\frac{Q_5 4\pi^2}{L} \int_0^L ds \delta(x_1 - a \cos \frac{2\pi q}{L} s) \delta(x_2 - a \sin \frac{2\pi q}{L} s) \delta(x_3) \delta(x_4) \\ &= -4\pi^2 Q_5 \delta(x_1^2 + x_2^2 - a^2) \delta(x_3) \delta(x_4). \end{aligned} \quad (4.33)$$

Quantum Treatment In a quantum theory, it is impossible to arbitrarily localize wave packets in phase space. Therefore, in the quantum theory we expect to obtain a profile that is something like a minimal uncertainty Gaussian distribution spread around the classical curve. If we take the classical circular curve (4.26), then associate to it the density matrix (4.16), and subsequently the phase space density (4.13), we find out that

$$f(d, \bar{d}) = \frac{\left(d_q^+ \bar{d}_q^+\right)^{N/q}}{(N/q)!} e^{-\sum_l d_l^\pm \bar{d}_l^\mp}, \quad (4.34)$$

where we used the notation: $d_k^\pm = (d_k^1 \pm d_k^2)/\sqrt{2}$. We have ignored the delta function (4.21) here and expect (4.34) to be valid for large values of N/q . It is therefore better thought of as a semi-classical profile rather than the full quantum profile.

The distribution above, (4.34), is similar to (C.15) in appendix C. This observation allows us to borrow the results derived there. For example (C.11) reads in this case

$$f_5 = 1 + \frac{Q_5}{4\pi^2} \int d^4u \frac{e^{i\mathbf{u}\cdot\mathbf{x}}}{|\mathbf{u}|^2} e^{\frac{\mu^2}{4q}(u_1^2 + u_2^2)} \int_0^\infty d\rho \frac{\rho^{2N/q+1}}{(N/q)!} e^{-\rho^2} J_0\left(\mu \frac{1}{\sqrt{q}} \sqrt{u_1^2 + u_2^2} \rho\right), \quad (4.35)$$

where $\rho = |d_q^+|$. The ρ integration is easily done using the identity

$$L_n(x) = \frac{e^x}{n!} \int_0^\infty e^{-t} t^n J_0(2\sqrt{tx}) dt, \quad (4.36)$$

with L_n the Laguerre polynomial of order n . At the end, we are left with the following expression for f_5 (see also (C.18))

$$f_5^{quantum} = 1 + L_{N/q} \left(\frac{a^2}{4N/q} (\partial_1^2 + \partial_2^2) \right) \frac{Q_5}{|\mathbf{x}|^2}. \quad (4.37)$$

Notice that, beside the approximation of ignoring the δ function (4.21) in the distribution, this result is exact in N/q . In order to relate both results recall that

$$L_n(x) = \sum_{m=0}^n \frac{(-1)^m n!}{(n-m)!(m!)^2} x^m,$$

which allows to find the following expansion for large values of N/q

$$L_{N/q} \left(\frac{a^2 \rho^2}{4N/q} \right) = J_0(a\rho) - \frac{1}{N/q} \frac{a^2 \rho^2}{4} J_2(a\rho) + \dots. \quad (4.38)$$

From this, we see explicitly that in the limit $N/q \gg 1$ the quantum geometry coincides with the classical one. More precisely, around asymptotic infinity the harmonic functions can be written as a series expansion in a^2/r^2 . If we focus on a given term

a^{2p}/r^{2p} for some fixed (but arbitrarily large) p , then, the coefficient of such term tends to the classical coefficient as N/q tends to infinity. Note, however, that for finite N/q the quantum harmonic function is a finite order polynomial in a^2/r^2 (of degree N/q) which contains a large number of terms that are singular at the origin (and that will re-sum only in the strict N/q infinite limit). These divergences at $r = 0$ may sound like a disaster, but they are actually unphysical and due to the fact that we ignored the delta function (4.21) in the distribution (4.34). Including the delta function will impose a cutoff on the ρ integral in (4.35), and since all singular terms are due to the large ρ behavior of the integrand in (4.35), the cutoff will remove the singularities in f_5 .

From this discussion, it is clear that we can trust our semi-classical computation provided N/q is large and we do not look at the deep interior of the solution.

As for the case of the classical curve, it is instructive to compute $\square f_5$ for this case

$$\square f_5 = -4\pi^2 Q_5 \delta(x_3) \delta(x_4) A(x_1, x_2), \quad (4.39)$$

$$A(x_1, x_2) = \int_0^\infty d\rho \rho J_0(\sqrt{x_1^2 + x_2^2} \rho) L_{N/q} \left(\frac{a^2 \rho^2}{4N/q} \right). \quad (4.40)$$

Until here we have not used any approximation. Using identity (4.36), and approximating $\exp(\frac{a^2 \rho^2}{4N/q}) \approx 1$, one obtains

$$A(x_1, x_2) = \frac{e^{-(N/q)(r^2/a^2)} \left([N/q] [r^2/a^2] \right)^{N/q}}{(N/q-1)! a^2}, \quad (4.41)$$

with $r^2 = x_1^2 + x_2^2$. In the limit $N/q \rightarrow \infty$, $A(x_1, x_2)$ approaches $\frac{\delta(r^2/a^2-1)}{a^2}$, and the classical and quantum results agree. For large N/q , $A(x_1, x_2)$ is approximately a Gaussian around $r^2 \approx a^2$, and width $1/\sqrt{N/q}$. Indeed, using Stirling's formula

$$A(x_1, x_2) \approx \frac{\sqrt{N/q}}{\sqrt{2\pi}} e^{-(N/q)(r^2/a^2-1)} (r^2/a^2)^{N/q}. \quad (4.42)$$

So, the quantum geometry corresponds to a solution of the equations of motion in presence of smeared sources. The width of the smeared source goes to zero in the limit $N/q \rightarrow \infty$, as expected.

4.3 A FIRST LOOK AT THERMODYNAMICAL ENSEMBLES

We managed above to lay out the tools to tackle the question of thermodynamical ensembles effective description. The simplest ensemble would be our full Hilbert space (3.22) equally weighted. This is believed to be describing a massless BTZ black

hole [106, 40] after taking a decoupling limit. We propose that such an ensemble is describing, in the full geometry, the small five dimensional black hole after reducing the six dimensional metric over the U(1) parametrized by y in (3.8).

In principle, one should consider a microcanonical ensemble with states of fixed level

$$\hat{N}|\psi\rangle \equiv \sum_k k c_k^{i\dagger} c_k^i |\psi\rangle = N|\psi\rangle .$$

We will, instead, consider a canonical ensemble, since in the large N limit the difference between the two should vanish. In the following, we are going to ignore the i -index in some equations where it does not play any role to avoid cluttered equations. The corresponding thermal ensemble is characterized by the following density matrix

$$\rho = \sum_{N_k, \tilde{N}_k} \frac{|N_k\rangle\langle N_k| e^{-\beta\hat{N}} |\tilde{N}_k\rangle\langle \tilde{N}_k|}{\text{Tr } e^{-\beta\hat{N}}} , \quad (4.43)$$

where $|N_k\rangle$ is a generic state labelled by collective indices N_k

$$|N_k\rangle = \prod_k \frac{1}{\sqrt{N_k!}} (c_k^\dagger)^{N_k} |0\rangle ,$$

and we have chosen a normalization so that $\langle N_k | \tilde{N}_k \rangle = \delta_{N_k, \tilde{N}_k}$. The value of the potential β has to be adjusted such that $\langle \hat{N} \rangle = N$. It is clear that

$$\rho = \prod_n \rho_n, \quad \rho_n = (1 - e^{-k\beta}) \sum_{n=0}^{\infty} e^{-nk\beta} |k, n\rangle\langle k, n| , \quad (4.44)$$

with $|k, n\rangle = \frac{1}{\sqrt{n!}} (c_k^\dagger)^n |0\rangle$. Then, the full distribution will simply be the product

$$f(d, \bar{d}) = \prod_k f_{d_k, \bar{d}_k}^{(k)} ,$$

with

$$f_{d_k, \bar{d}_k}^{(k)} = (1 - e^{-k\beta}) e^{-d_k \bar{d}_k} \sum_{n=0}^{\infty} \frac{e^{-nk\beta}}{n!} (d_k \bar{d}_k)^n = (1 - e^{-k\beta}) \exp(-(1 - e^{-k\beta}) d_k \bar{d}_k) . \quad (4.45)$$

This is a special case of (C.19), where, in this case $\beta_k^\pm = k\beta$. In the present case, the generating function f_v reads (C.24)

$$f_v = Q_5 e^{-\frac{\mu^2}{8} \left(\frac{2\pi}{L}\right)^2 \mathcal{N} |\mathbf{v}|^2} \frac{1 - e^{-\frac{\mu^2}{\mathcal{N}^2} x^2}}{x^2} . \quad (4.46)$$

where,

$$\mathcal{N} = 4 \sum_k k \frac{e^{-\beta k}}{1 - e^{-\beta k}} , \quad \mathcal{D} = 4 \sum_k \frac{1}{k} \frac{e^{-\beta k}}{1 - e^{-\beta k}} . \quad (4.47)$$

Using the expression (4.46), it is easy to evaluate the different harmonic functions and one-forms (3.9) that enter in the characterization of our solution (3.8), to be

$$f_5 = 1 + Q_5 \frac{1 - e^{-\frac{2}{\mu^2 \mathcal{D}} x^2}}{x^2}, \quad f_1 = 1 + Q_1 \frac{1 - e^{-\frac{2}{\mu^2 \mathcal{D}} x^2}}{x^2}, \quad A_i = 0, \quad (4.48)$$

The only remaining step is to express \mathcal{D} in terms of \mathcal{N} , which is itself fixed in this ensemble to be $N = N_1 N_5$. In the thermodynamical limit $\beta \ll 1$, the expressions (4.47) above become

$$\mathcal{N} \approx \frac{2\pi^2}{3} \frac{1}{\beta^2}, \quad \mathcal{D} \approx \frac{2\pi^2}{3} \frac{1}{\beta}, \quad (4.49)$$

which gives $\mathcal{D} \approx \pi \sqrt{2N/3}$.

A final comment is in order. The geometry obtained differs from the *naive* D1-D5 geometry (3.3) by an exponentially suppressed correction that renders it smooth at $x = 0$. Following [33, 36], we could put a stretched horizon at the point where this exponential factor becomes of order one, so that the metric deviates significantly from the classical D1-D5 one. We could also interpret this radius as the scale where quantum effects start to become important. Thus, using this criterion we find for the radius of the stretched horizon

$$r_0 \approx \frac{\mu}{\beta^{1/2}}, \quad (4.50)$$

with a corresponding entropy that is different from the one of the mixed state from which the geometry was obtained ($S = N^{1/2}$). This does not contradict any known laws of physics, and in addition, we should remember that the notion of stretched horizon depends on the choice of the observer. It is quite likely that for a suitable choice of the observer, the entropy of the stretched horizon agrees with the entropy obtained from the dual CFT. For a further discussion of this point see [106, 108].

4.4 THE SURVIVAL OF THE NO-HAIR THEOREM

As was already mentioned (see section 2.1.3), the no-hair theorem fails in five dimensions [67]. This is due to a new class of solutions called black rings [5, 6] whose horizon has an $S^2 \times S^1$ topology. The violation of the no-hair theorem is due to a local charge called a “dipole charge”, which is not visible at the asymptotic infinity. Such a dipole charge is mysterious as it enters in the generalization of the first law of black hole mechanics to black rings [67, 68]. This suggests that such a black hole hair i.e. dipole charge, should be visible in the definition of any possible ensemble that might describe black rings.

The D1-D5 system gives us a good opportunity to address the possibility of describing a black ring as an effective geometry of an appropriate ensemble. This is because,

as we have already discussed (section 2.1.3), the D1-D5 system allows for a small version of black ring,s the so called “small black ring” [65, 70, 71, 72]. We will leave the characterization of the small black ring ensemble to the next section (section 4.5), and the derivation of its effective geometry to section 4.6. In this section, we will deal with a much pressing question, *could one put hair on black holes by putting more information in the weights defining the D1-D5 ensemble?*

To address this question, let us be completely generic and assume that each oscillator c_{k^i} is occupied thermally with a temperature β_k^i . The latter is a function of k in general. In case we want such ensemble to be a small deformation of the thermal ensemble, discussed in the previous section, at large occupation number, the temperatures β_k will take the form

$$\beta_k = \sum_{n=-1}^{\infty} \beta_n k^{-n}. \quad (4.51)$$

One of the quantum numbers that we want to turn on is the angular momentum, as it can be measured at asymptotic infinity. Since we have restricted ourselves to a non-trivial profile in the four non-compact directions x^i , the best we can do is to have rotations in the (12) and (34)-planes. It is easy to see, using the form of the angular momentum (3.11), that we will have such rotations once we have different temperatures $(\beta^a)_k^{\pm}$ for the oscillator $(c^a)_k^{\pm}$; $a = 1, 2$ defined as:

$$(c^1)_k^{\pm} = \frac{1}{\sqrt{2}} (c_k^1 \pm i c_k^2), \quad (c^2)_k^{\pm} = \frac{1}{\sqrt{2}} (c_k^3 \pm i c_k^4).$$

A further simplification that we are going to adopt in the following is to set the two temperatures $(\beta^a)_k^{\pm}$; $a = 1, 2$ equal. This will allow us to get analytical expressions for the averages (4.17). In the following, we are going to suppress the superscript a as it does not play any role.

We are led then to consider a distribution that is the product of

$$f_k(d, \bar{d}) = (1 - e^{-\beta_{k^+}}) (1 - e^{-\beta_{k^-}}) \exp(-(1 - e^{-\beta_{k^+}})|d_k^+|^2 - (1 - e^{-\beta_{k^-}})|d_k^-|^2). \quad (4.52)$$

Using (C.20, C.4), such a distribution leads to

$$f_5 = Q_5 \frac{1 - e^{-\frac{2|\mathbf{x}|^2}{\mu^2 D}}}{|\mathbf{x}|^2}, \quad (4.53)$$

$$f_1 = Q_1 \left(\frac{1 - e^{-\frac{2|\mathbf{x}|^2}{\mu^2 D}}}{|\mathbf{x}|^2} - \frac{J^2}{4N\mu^4 D^2} e^{-\frac{2|\mathbf{x}|^2}{\mu^2 D}} \right), \quad (4.54)$$

$$A = \frac{\mu^2 J R}{2} \left(2 \frac{e^{-\frac{2|\mathbf{x}|^2}{\mu^2 D}}}{\mu^2 D} - \frac{1 - e^{-\frac{2|\mathbf{x}|^2}{\mu^2 D}}}{|\mathbf{x}|^2} \right) (\cos^2 \theta d\phi + \sin^2 \theta d\psi), \quad (4.55)$$

where $(|\mathbf{x}|, \theta, \phi, \psi)$ are spherical coordinates for \mathbb{R}^4 , in terms of which, the Euclidean metric of \mathbb{R}^4 reads $ds^2 = dr^2 + r^2(d\theta^2 + \cos^2 \theta d\phi^2 + \sin^2 \theta d\psi^2)$.

We see that, rather surprisingly, the geometry depends only on few quantum numbers J , D explicitly and N through its relation with Q_5 i.e. $N = N_1 N_5$. In terms of the temperatures, these quantum numbers are given by the relations (C.21, C.22, C.23) which we re-quote here:

$$N = 2 \sum_k k \left(\frac{e^{-\beta_{k+}}}{1 - e^{-\beta_{k+}}} + \frac{e^{-\beta_{k-}}}{1 - e^{-\beta_{k-}}} \right), \quad (4.56)$$

$$J = 2 \sum_k \left(\frac{e^{-\beta_{k+}}}{1 - e^{-\beta_{k+}}} - \frac{e^{-\beta_{k-}}}{1 - e^{-\beta_{k-}}} \right), \quad (4.57)$$

$$D = 2 \sum_k \frac{1}{k} \left(\frac{e^{-\beta_{k+}}}{1 - e^{-\beta_{k+}}} + \frac{e^{-\beta_{k-}}}{1 - e^{-\beta_{k-}}} \right). \quad (4.58)$$

As a result, the information carried by the geometry is much less than that carried by the ensemble of microstates. In fact, only N and J are visible at infinity while D sets the size of the “core” of the geometry. We interpret this as a manifestation of the no-hair theorem for black holes.

The quantum number D defined above has similar properties as the dipole charge. Surprisingly enough, it is the same one proposed in [66] to describe the CFT dual of the “small” black ring dipole charge. This suggests that any general enough density matrix will describe a small black ring. Unfortunately, a quick look at the geometry reveals the failure of such proposal. At this point, we should be very careful before completely dismissing such a proposal because we have negelected –in the discussion above– a very interesting physical phenomenon: the Bose-Einstein condensation. As we will show in the next section, such a phenomenon does occur in our class of thermodynamical ensembles discussed in this section. We will leave the geometric interpretation of such condensate to section 4.6.

4.5 THERMAL ENSEMBLES AND CONDENSATION

Quantum mechanics being the ruler of the microscopic world does not mean that its footprints cannot be seen at the macroscopic level. A famous example of such imprint is superfluidity and superconductivity. In the heart of these phenomena lies the Bose-Einstein condensate. This happens because bosons tend to occupy the same state with increasing probability as their number increases. In the extreme case, it could happen that macroscopically many bosons will occupy the same ground state. This is exactly the notion of Bose-Einstein condensate. The signal of such a

condensate is the blowing up of the occupation number of the associated mode in our ensemble.

In this section, we will try to study the possibility of the occurrence of a Bose-Einstein condensate in the class of ensembles discussed previously. Ultimately, we are looking for an ensemble whose effective description is a small black ring. Since the latter is characterized by three quantum numbers: mass, angular momentum and dipole charge, we will study the simplest toy model that can accommodate for three independent quantum numbers. We already know the part that will reproduce the mass and angular momentum. For the dipole charge, one can use the quantum number D (4.58), found in the previous section, as a first guess. After all, this is the only extra quantum number that appears in the general case, and it does share the same properties as the dipole charge. In the following, we are going to forget for a moment about our Hilbert space and possible geometric interpretation of the results to be derived here. Such an interpretation will be the subject of the next section.

The partition function we want to study is given by

$$\mathcal{Z} = \text{Tr}_{\mathcal{H}}(e^{-\beta H + \mu J + \nu D}), \quad (4.59)$$

where $\mu, \nu \sim \beta$. The Hilbert space \mathcal{H} consists of a Fock space built out of $(d+2)$ free oscillators α_{-n}^{\pm} and α_{-n}^i , $i = 1, \dots, d$, carrying the following charges [66]

$$[H, \alpha_{-n}^{\pm}] = n \alpha_{-n}^{\pm}, \quad [H, \alpha_{-n}^i] = n \alpha_{-n}^i, \quad (4.60)$$

$$[J, \alpha_{-n}^{\pm}] = \pm \alpha_{-n}^{\pm}, \quad [J, \alpha_{-n}^i] = 0, \quad [D, \alpha_{-n}^{\pm}] = \frac{1}{n} \alpha_{-n}^{\pm}. \quad (4.61)$$

The charge of the other oscillators with respect to D will not be relevant for the discussion below, but will be relevant for the subleading behavior of the entropy. The definition of the operator D is chosen to mimic the expression of the quantum number D in (4.58).

Let us focus on the α^+ oscillator, its contribution to the partition function is

$$\log \mathcal{Z} = - \sum_{n=1}^{\infty} \log (1 - e^{-n\beta + \mu + \nu/n}) = \sum_{n=1}^{\infty} \mathcal{C}_n, \quad (4.62)$$

where \mathcal{C}_n can be rewritten as

$$\mathcal{C}_n = \sum_{l=1}^{\infty} \frac{e^{-n l \beta}}{l} \left(\sum_{j,k=0}^{\infty} \frac{(\mu l)^j (l \nu/n)^k}{j! k!} \right) = \sum_{j,k=0}^{\infty} \frac{\mu^j \nu^k}{j! k! n^k} \text{Li}_{1-j-k}(e^{-\beta n}). \quad (4.63)$$

After changing variables $k + j = s$, and summing over $0 \leq j \leq s$, we get

$$\mathcal{C}_n = \sum_{s=0}^{\infty} \text{Li}_{1-s}(e^{-\beta n}) \frac{(\nu + n\mu)^s}{n^s s!}. \quad (4.64)$$

Up to this point, the above computation is exact. In order to proceed, we approximate, in the limit $\beta \ll 1$, the polylogarithm Li_{1-s} for $s \geq 1$ by

$$Li_{1-s}(e^{-\beta n}) \approx \frac{(s-1)!}{\beta^s n^s}. \quad (4.65)$$

Then,

$$\tilde{\mathcal{C}}_n = \sum_{s=1}^{\infty} Li_{1-s}(e^{-\beta n}) \frac{(\nu + n\mu)^s}{n^s s!} \approx -\log \left(1 - \frac{\mu}{n\beta} - \frac{\nu}{n^2\beta}\right). \quad (4.66)$$

The contribution from $s = 0$ can be taken care of separately, and the sum over n can easily be performed and it gives the usual term depending only on β . Taking into account all the oscillators, we get

$$\log \mathcal{Z} \approx \frac{(d+2)\pi^2}{6\beta} - \sum_{n=1}^{\infty} \log \left(1 - \frac{\mu}{n\beta} - \frac{\nu}{n^2\beta}\right). \quad (4.67)$$

The first term here is obtained by summing over all “d+2” oscillators, but the second term is due only to α^+ . There are similar μ, ν -dependent terms for the other oscillators as well, but the reason for not including their contribution will become clear momentarily. Computing the level N , the average angular momenta J , and the average dipole charge D from (4.67), we get

$$N = -\frac{\partial \log \mathcal{Z}}{\partial \beta} = \frac{1}{\beta} \left(\frac{(d+2)\pi^2}{6\beta} + \mu J + \nu D \right), \quad (4.68)$$

$$J = \frac{\partial \log \mathcal{Z}}{\partial \mu} = \sum_{n=1}^{\infty} \frac{n}{n^2\beta - n\mu - \nu}, \quad (4.69)$$

$$D = \frac{\partial \log \mathcal{Z}}{\partial \nu} = \sum_{n=1}^{\infty} \frac{1}{n^2\beta - n\mu - \nu}. \quad (4.70)$$

The expression for J appears to diverge, but that is due to the approximation that we made. If we include the contribution from α_{-n}^+ , which is similar to that of α^+ in (4.67) except that μ is replaced by $-\mu$, the expression for J will be convergent. This α^- contribution will not be relevant for most of what follows though. The expressions for J, D are at first sight of order $\sqrt{N} \sim \beta^{-1}$. To see this we need to include the contribution from α^- in J . In order for J, D to be of order N , one term in the sum must be very large; if this happens for the term with $n = q$ then in order to have $J, D \sim N$ we need that

$$q^2 - q\mu' - \nu' \sim \beta \ll 1, \quad (4.71)$$

where $\mu' = \mu/\beta$ and $\nu' = \nu/\beta$. Notice that, this will imply condensation of modes with $n = q_3$. Indeed

$$\langle 0 | \alpha_{-n}^+ \alpha_n^+ | 0 \rangle = \frac{e^{\beta(-n+\mu'+\nu'/n)}}{1 - e^{\beta(-n+\mu'+\nu'/n)}}, \quad (4.72)$$

which has a pole at $n = q$ for $q^2 - q\mu' - \nu' = 0$. Obviously, the combination $n^2 - n\mu' - \nu'$ has to be greater than 0 for all n , otherwise the thermodynamical system is ill-defined. If we also require that this quantity has a minimum obeying (4.71) at $n = q$, we find

$$\mu' \approx 2q, \quad \nu' \approx -q^2. \quad (4.73)$$

With these values of μ', ν' , the term with $n = q$ will dominate the sum that appears in the partition function in (4.67). If we keep only this term together with the other contribution π^2/β , we can compute the entropy and find

$$S = \beta(N - \mu'J - \nu'D) + \log \mathcal{Z} \sim \frac{1}{\beta} \sim \sqrt{N - \mu'J - \nu'D} = \sqrt{N - qJ}. \quad (4.74)$$

This scales exactly like the small black ring entropy for a general dipole charge q [66]!

What we have here is similar to the Bose-Einstein condensate with a slight difference. Instead of a macroscopically large number of bosons occupying the ground state, as is the case in the Bose-Einstein condensate, the condensate state in our case can be chosen to be any excited state, provided we tune the temperatures β, μ and ν appropriately as explained around equation (4.71).

4.6 THE “SMALL” BLACK RING

We argued successfully in the previous section that, one should be careful when dealing with general thermodynamical ensembles of the kind discussed in section 4.4, as condensates of certain modes may appear. The aim of this section is to shed some light on the possible geometric manifestation of such condensates. First, we are going to describe the kind of density matrix that can describe a thermodynamical ensemble with a condensate. Then, we are going to turn on our machinery, developed so far, to translate this density matrix to a geometry.

4.6.1 DESCRIBING THE “CONDENSATE” ENSEMBLE

When a condensate occurs, a part of all possible degrees of freedom freezes in the condensate state leaving a reduced thermal ensemble. To be concrete let us treat the situation described in the previous section where J oscillators a_{-q}^+ have condensed leaving a thermal ensemble of effective level $N - qJ$. It is easy to see that, the density matrix associated with such a system will be the thermal one (4.43) in the

excited state $|q, J\rangle$. Explicitly:

$$\rho = \sum'_{N_k, \tilde{N}_k} \frac{|N_k\rangle\langle N_k| e^{-\beta \tilde{N}} |\tilde{N}_k\rangle\langle \tilde{N}_k|}{\text{Tr } e^{-\beta \tilde{N}}} \otimes |q^+, J\rangle\langle q^+, J|, \quad (4.75)$$

where the prime in \sum' means that the sum does not include states coming from the oscillator a_{-q}^+ , and we use the notation $|N, k\rangle$ to denote the state $|N, k\rangle = \frac{1}{\sqrt{N!}} (a_{-k})^N |0\rangle$. In the following, we use the index q to denote quantities related to the special oscillator $a_{\pm q}^+$ to avoid messy formulas. A careful look at the density matrix above reveals that it is just a tensor product between the thermal one (section 4.3) and the one associated with the circular profile (section 4.2.2). This inevitably leads to a phase space density that is the product of the ones associated to each component. The only task that we are left with here is to combine the two calculations. For example, the phase space density is a combination of (4.34) and (4.45). It reads

$$\rho = e^{-|d_q|^2} \frac{|d_q|^{2J}}{J!} \prod'_k (1 - e^{-k\beta}) \exp [-(1 - e^{-k\beta}) |d_k|^2]. \quad (4.76)$$

4.6.2 THE SMALL BLACK RING EFFECTIVE GEOMETRY

It is time now to discuss the effective geometry description of the density matrix (4.75), given above, using our general rule (4.17). It is enough to evaluate the generating function f_v given by (C.1), which turns out to be:

$$f_v = Q_5 L_J \left(\frac{\mu^2}{4q} \left[\left(\frac{2\pi q}{L} v_2 + i\partial_1 \right)^2 + \left(\frac{2\pi q}{L} v_1 - i\partial_2 \right)^2 \right] \right) e^{-\frac{\mu^2 \pi^2 |v|^2}{2L^2} (N - qJ)} \frac{1 - e^{-\frac{2|\mathbf{x}|^2}{\mu^2 D}}}{|\mathbf{x}|^2}, \quad (4.77)$$

where $D = \pi\sqrt{2/3}(N - qJ)^{1/2}$, which indicates that the geometry is purely expressed in terms of the macroscopic quantities N, J and q . The form (4.77) that f_v takes above is easily understood as follows. The condensate behaves as the circular profile (section 4.2.2) so the integral over d_q, \bar{d}_q can be evaluated in a completely analogous way giving rise to the Laguerre polynomial above. The extra terms look the same as the thermal contribution (4.46). The reason we have $N - qJ$ above instead of N is due to the restricted level of our thermal part as a result of condensation.

We would like to make contact between this geometry and the geometry corresponding to small black rings studied in [66]. As we will see, in the limit of large quantum numbers both geometries reproduce the same asymptotics.

In order to see this, first note that the exponential factor $e^{-\frac{2|\mathbf{x}|^2}{\mu^2 D}}$ will not contribute (as it vanishes faster than any power at asymptotic infinity). Secondly, one has the

formal expansion

$$L_J \left(\frac{\mu^2}{4q} \mathcal{O} \right) = J_0(\mu \sqrt{\frac{J}{q}} \mathcal{O}^{1/2}) + \dots \quad (4.78)$$

In order to estimate the validity of this approximation, we can think of \mathcal{O} as being proportional to $1/|x|^2$. On the other hand, $\mu \sqrt{J/q}$ can be roughly interpreted as the radius of the black ring (see [6, 66], where this parameter is called R). Hence, this approximation is valid for large values of J at a fixed distance compared to the radius of the ring.

Using the above approximations, and the change of coordinates (4.31), it is straightforward to compute the harmonic functions

$$f_5 = 1 + \frac{Q_5}{r^2 + \mu^2 \frac{J}{q} \cos \theta}, \quad f_1 = 1 + \frac{Q_1}{r^2 + \mu^2 \frac{J}{q} \cos \theta}. \quad (4.79)$$

This result could have been guessed based on the observation that, up to the exponentially suppressed terms, which we got rid of because we are mainly interested in the asymptotics, the generating function (4.77) is similar to the one of the circular profile (C.18). In this situation, and for large quantum numbers, the “quantum” geometry reduces to the classical one as argued in section (4.2.2). This means that under our assumptions, the effective geometry of the condensate ensemble should be similar to (4.32) which is the case. Hence, in this approximation the geometry reduces exactly to that of the small black ring studied in [66].

Let us summarize the key points that the ensemble characterized by the density matrix (4.75) share with an ensemble that could describe a small black ring. First of all, the statistical entropy of the ensemble (4.74) is the same as the entropy of the small black ring with dipole charge q and angular momentum J [66]. The second important property is that its effective geometry description is the same as the naive geometry of a small black ring at large distances. Based on such key points, one is confident to declare that the density matrix (4.75) is the right thermodynamical description of a small black ring with dipole charge q and angular momentum J .

4.6.3 AVOIDING THE NO-HAIR THEOREM

We have seen that the existence of a condensate changes drastically the thermodynamical ensemble, and hence, its corresponding effective geometry. One would like to know what will happen to generic ensembles and the associated no-hair theorem discussed in section 4.4. One would expect that by tuning the temperatures, it will be possible to condense one (like in the small black ring case) or more oscillators. If this happens, we should perform a more elaborate analysis than what have

been done previously in section 4.4. Naively, one would guess that the generating function now will take the form of multiple Laguerre polynomials with differential operator arguments acting on the generating function of the naive D1-D5 thermal ensemble (4.46).

From the geometry point of view, we expect that the effective geometrical description to correspond to concentric small black rings. In this case the configuration will depend on more quantum numbers than just N, J, D , in particular we will find solutions where the small black rings carry arbitrary dipole charges. Thus, once we try to put hair on the small black hole by tuning chemical potentials appropriately, we instead find a phase transition to a configuration of concentric small black rings, each of which still is characterized by just few quantum numbers.

4.7 THE CONICAL DEFECT METRIC

We have already seen that coarse graining over simple thermodynamical ensembles gave rise to effective geometries that look like known geometries far away from the origin. The aim of this section is to shed some light on the claim of [97] appendix C, where it is shown that there is no conical defect metric with arbitrary opening angles. Our aim here is to answer the following question: “*is there a phase space density of D1-D5 geometries that gives as an effective description a conical defect metric with arbitrary opening angles after coarse graining?*”

In this section, a decoupling limit is assumed e.g. [93], which amounts in practice to deleting the “1” from the definition of f_i (3.3, 3.9). The end result is a geometry which is asymptotically $AdS_3 \times S^3$. The starting point is the supersymmetric conical metric [109, 110]

$$\frac{ds^2}{N} = -(r^2 + \gamma^2) \frac{dt^2}{R^2} + r^2 \frac{dy^2}{R^2} + \frac{dr^2}{r^2 + \gamma^2} + d\theta^2 + \cos^2 \theta (d\psi + \gamma \frac{dy}{R})^2 + \sin^2 \theta (d\varphi + \gamma \frac{dt}{R})^2, \quad (4.80)$$

where N is the AdS radius, and $2\pi\gamma$ is the opening angle. It is well known that every supersymmetric conical metric is defined by its angular momentum and N . The metric (4.80) is precisely identical to the metric that we would have found in the near-horizon limit in section 4.2.2, if we would also have computed the one-forms A, B and evaluated (3.8), see e.g. [97] for a detailed discussion. The relation between γ and q works out to be $\gamma = 1/q$. The construction in section 4.2.2 therefore provides a conical defect metrics with q integer, but for q non-integer the construction in section 4.2.2 fails. The reason is that the classical curve $\mathbf{F}(s)$ needs to satisfy $\int_0^L \mathbf{F}(s) ds = 0$, as $\mathbf{F}(s)$ does not have a zero-mode, and this is only true if q is an integer and the curve closes.

In order to try to construct a more general conical defect metric, we first notice that according to the δ -function in (4.33), the source for the metric has to be contained in a circle of radius a in the x_1, x_2 -plane. The most general source term satisfying these requirements is

$$F_1(s) = a \cos[f(s)], \quad F_2(s) = a \sin[f(s)], \quad F_3(s) = F_4(s) = 0, \quad (4.81)$$

where $f(s)$ is some arbitrary function which has to satisfy

$$\int_0^L e^{if(s)} ds = 0, \quad (4.82)$$

because $\mathbf{F}(s)$ does not contain a zero-mode. In addition, the metric (4.80) is invariant under rotations in the x_1, x_2 -plane. To accomplish this, we need to coarse grain over all $U(1)$ rotations of (4.81). This is most easily done by introducing polar coordinates $x_1 + ix_2 = ue^{i\varphi}, x_3 + ix_4 = ve^{i\psi}$, so that the $U(1)$ average can be expressed as

$$\begin{aligned} f_5 &= \frac{Q_5}{2\pi L} \int_0^{2\pi} d\xi \int_0^L \frac{ds}{|ue^{i\varphi} - ae^{if(s)+i\xi}|^2 + v^2}, \\ f_1 &= a^2 \frac{Q_5}{2\pi L} \int_0^{2\pi} d\xi \int_0^L \frac{f'(s)^2 ds}{|ue^{i\varphi} - ae^{if(s)+i\xi}|^2 + v^2}, \\ A &= -a \frac{Q_5}{2\pi L} \int_0^{2\pi} d\xi \int_0^L \frac{if'(s)e^{if(s)+i\xi} ds}{|ue^{i\varphi} - ae^{if(s)+i\xi}|^2 + v^2}. \end{aligned} \quad (4.83)$$

The constraint (3.10) on the curve now reads

$$Q_1 = a^2 \frac{Q_5}{2\pi L} \int_0^{2\pi} d\xi \int_0^L f'(s)^2 ds = \frac{a^2 Q_5}{L} < f'^2 >. \quad (4.84)$$

Here and in the following by $< g(s) >$ we simply mean

$$< g(s) > = \int_0^L g(s) ds. \quad (4.85)$$

It is straightforward to evaluate the integrals in (4.83) to get

$$f_5 = \frac{Q_5}{h}, \quad f_1 = \frac{Q_1}{h}, \quad A = a Q_5 \left(\frac{< f' >}{L} \right) \left(\frac{u^2 + v^2 + a^2 - h}{2h} \right) d\varphi, \quad (4.86)$$

with $h^2 = (u^2 + v^2 + a^2)^2 - 4a^2 u^2$. In order to put it in a form which resembles the conical defect one as much as possible, one has to make the following change of coordinates (4.31)

$$u^2 = (r^2 + a^2) \sin^2 \theta, \quad v = r \cos \theta. \quad (4.87)$$

Using these new coordinates, the various functions appearing in (3.8) become

$$f_5 = \frac{Q_5}{r^2 + a^2 \cos^2 \theta}, \quad f_1 = \frac{Q_1}{r^2 + a^2 \cos^2 \theta}, \quad \mathcal{C} = -\frac{Q_5 r^2 \sin^2 \theta}{r^2 + a^2 \cos^2 \theta} d\psi \wedge d\varphi, \quad (4.88)$$

$$A = \alpha \frac{a\sqrt{Q_1 Q_5}}{r^2 + a^2 \cos^2 \theta} \sin^2 \theta d\varphi, \quad B = -\alpha \frac{a\sqrt{Q_1 Q_5}}{r^2 + a^2 \cos^2 \theta} \cos^2 \theta d\psi, \quad (4.89)$$

where

$$\alpha^2 = a^2 \frac{Q_5}{Q_1} \left(\frac{\langle f' \rangle}{L} \right)^2 = \frac{1}{L} \left(\frac{\langle f' \rangle^2}{\langle f'^2 \rangle} \right),$$

is a constant introduced for later convenience. Plugging these values into the expression of the metric (3.8) gives

$$ds_4^2 = (r^2 + a^2 \cos^2 \theta) \left(\frac{dr^2}{r^2 + a^2} + d\theta^2 \right) + r^2 \cos^2 \theta d\psi^2 + (r^2 + a^2) \sin^2 \theta d\varphi^2. \quad (4.90)$$

Next, we rescale r by a factor of $\frac{\sqrt{Q_1 Q_5}}{R}$, and define $\gamma = \alpha \frac{2\pi}{\langle f' \rangle}$, and after some straightforward algebraic manipulations, we end up with

$$\begin{aligned} \frac{ds^2}{\sqrt{Q_1 Q_5}} &= -(r^2 + \gamma^2) \left(\frac{dt}{R} \right)^2 + r^2 \left(\frac{dy}{R} \right)^2 + \frac{dr^2}{r^2 + \gamma^2} \\ &\quad + \left(d\theta^2 + \sin^2 \theta (d\varphi - \alpha \gamma \frac{dt}{R})^2 + \cos^2 \theta (d\psi - \alpha \gamma \frac{dy}{R})^2 \right) \\ &\quad + \frac{(1 - \alpha^2)\gamma^2}{r^2 + \gamma^2 \cos^2 \theta} (\sin^2 \theta d\Sigma_1^2 + \cos^2 \theta d\Sigma_2^2), \\ \frac{C}{Q_5} &= (r^2 + \gamma^2 \cos^2 \theta) \frac{dt}{R} \wedge \frac{dy}{R} + \frac{\alpha^2 \gamma^2 - r^2 \sin^2 \theta}{r^2 + \gamma^2 \cos^2 \theta} d\psi \wedge d\varphi \\ &\quad - \alpha \gamma \left(\cos^2 \theta \frac{dt}{R} \wedge d\psi + \sin^2 \theta \frac{dy}{R} \wedge d\varphi \right), \end{aligned} \quad (4.91)$$

where we defined

$$\begin{aligned} d\Sigma_1^2 &= \sin^2 \theta d\varphi^2 + (r^2 + \gamma^2 \cos^2 \theta) \left(\frac{dt}{R} \right)^2, \\ d\Sigma_2^2 &= -\cos^2 \theta d\psi^2 + (r^2 + \gamma^2 \cos^2 \theta) \left(\frac{dy}{R} \right)^2. \end{aligned}$$

This metric is a conical defect metric for $\alpha = 1$. So, the question is which values of γ are compatible with $\alpha = 1$. To analyze this, we recast the constraints on $f(s)$ for $\alpha = 1$ here

$$\int_0^L e^{if(s)} ds = 0, \quad \left(\int_0^L f'(s) ds \right)^2 = L \int_0^L (f'(s))^2 = \left(\frac{2\pi}{\gamma} \right)^2. \quad (4.92)$$

However, according to Schwarz's inequality,

$$\left(\int_0^L f'(s) ds \right)^2 \leq L \int_0^L (f'(s))^2 , \quad (4.93)$$

for integrable functions $f'(s)$ with equality if and only if $f'(s)$ is a constant. Thus, $\alpha \leq 1$, and $\alpha = 1$ only if $f'(s) = \text{const}$. Interestingly, the metric (4.91) is in general a perfectly acceptable metric, since $\alpha \leq 1$ is precisely the condition for the absence of CTC's as one can derive using the results in [6]. If $\alpha = 1$ then $f'(s) = \text{const}$ together with (4.92) imply that $f(s) = 2\pi ks/L$, for some nonzero integer k , and $\gamma = 1/k$. We can therefore indeed only construct conical defect metrics with $\gamma = 1/k$, where k is an integer. For k noninteger, we find a bound on α

$$\alpha^2 \leq \left[\frac{1}{\gamma} \right]^2 \gamma^2 , \quad (4.94)$$

with $[x]$ the largest integer less than or equal to x . Indeed, we cannot come arbitrarily close to a non-integer conical defect metric in this way.

Such a negative result raises the following puzzle. Even though conical defects with any opening angle are treated on the same footing in gravity, “quantum” gravity seems to restrict the possible opening angles to a specific class, $\theta = 2\pi/n$, where n is an integer. It is not clear at all why such a distinction occurs. Is it some non-trivial effect of quantization? or can there be a gravity mechanism that will select such a class of conical defects? An answer to this question will inevitably shed more light on the status of geometries in quantum gravity.

Part III

Towards Macroscopic Black Holes in the Fuzzball Realm

PRELUDE

With all the exciting results and successes in the D1-D5 system, one is more confident that the fuzzball considerations might be, after all, an important window into black hole physics. Although we cannot, with our actual technology, study realistic black holes, we can however make small steps toward such a goal. Our task is then to weaken the differences between the D1-D5 system and the more down to earth black holes. Unfortunately, as things stand now, looking at non-BPS black holes is not a good option. Some progress in this direction was made in [111, 112, 113, 114, 115], however, it is still in its very early stages. In this thesis, we opt to the option of reducing the amount of preserved supersymmetry without breaking it completely. We should also keep in mind that we would like to have BPS black holes with a large macroscopic horizon. Such requirements are met by some 1/2-BPS black holes of the $\mathcal{N} = 2$ four-dimensional supergravity. These BPS black holes and their multi-center cousins will be the study material of this part of the thesis.

We start by a quick review of the construction of these solutions. After quick words about how to get the four dimensional supergravity effective action, we describe the multi-center BPS solutions. Some of their most important properties will be also discussed. At the end, we are going to quickly review the wall crossing formula developed in [30], that we will be needing in the sixth chapter.

In the second chapter of this part of the thesis, we are going to develop a quantization procedure for our gravity solutions. Unfortunately, due to the complicated nature of the solutions we are dealing with, our success will be very limited. Luckily enough, we can still quantize a solution space that was argued to be dual to a D4-D0 black hole [116, 117, 118]. However, we seem to get far less entropy than the expected one from supergravity. We close by giving some free field arguments to why restricting ourselves to just gravity will probably not be enough to account for the needed degeneracy to reproduce the entropy of this class of black holes.

CHAPTER 5

BLACK CONSTELLATIONS IN FOUR DIMENSIONS

Driven by our search for black holes that are close enough to realistic ones, but still under enough control, we are led to study $\mathcal{N} = 2$ four-dimensional supergravity [119]. The latter turns out to be describing type-II string theories compactified on Calabi-Yau threefolds. Although, smooth solutions can exist only when we uplift to $\mathcal{N} = 1$ five-dimensional supergravity [120], these solutions can be traced back to four dimensional multi-center solutions [121, 122, 123] through the 4d-5d connection [62, 63]. This connection is a result of the equivalence of type-IIA on a Calabi-Yau and M-theory on the same Calabi-Yau $\times S^1$. As a result, when uplifting four-dimensional solutions to five dimensions, the resulting solutions have a $U(1)$ isometry. Since all the known five-dimensional smooth solutions have a $U(1)$ isometry, moving up or down in dimensions does not have any effect on the number of states. This allows us to restrict our attention to the four-dimensional solutions [124]. The basic example of a four-dimensional solution that becomes smooth when it is uplifted to five dimensions is the solution describing a D6-brane. The four-dimensional solution is singular, whereas the five dimensional uplift is a smooth solution known as the “Taub-Nut geometry”.

This chapter is a short summary of what is known about multi-center black hole solutions to the $\mathcal{N} = 2$ four-dimensional supergravity theory. As usual, we will be very brief inviting the interested reader to check the literature. See for example [119, 125, 96, 22, 27, 30, 126] and references therein. See also the references mentioned throughout this chapter.

We start by reviewing the construction of the four dimensional action. Then, we discuss the simplest BPS black hole solution i.e. the static spherically symmetric one. In the process, we uncover a famous behavior of the scalar fields which is known as the “*attractor mechanism*” [127]. It turns out that there are other BPS solutions that are essentially a bound state of many black holes [121, 122, 123]. Such solutions do not exist always and may disappear when we cross co-dimension one hypersurfaces in the moduli space of scalar fields. These hypersurfaces are called “*walls of marginal stability*”. The final section will deal with characterizing the possibility of the disappearance of multi-center black holes by a generalization of the attractor mechanism to these new solutions [122]. Along the way, we will be able to count the number of states that have disappeared using the wall crossing formula [30].

Familiarity with string theory, differential geometry and compactification is assumed. Some concepts about these subjects are summarized in appendices B and D.

5.1 FROM TEN TO FOUR DIMENSIONS

To get the four dimensional action, one starts with the ten dimensional one (B.1), then reduces over a Calabi-Yau threefold. The derivation of the massless field content of our four dimensional theory is carried out in appendix D, section D.3.2. A further simplification that we are going to take advantage of, is that by restricting ourselves to the two derivative effective action, supersymmetry restricts the allowed interactions between hypermultiplets and vectormultiplets to gravitational ones [119]. Since the hypermultiplets enter in the action through their derivative, we can put them to constants and decouple them. As a consequence, the black hole solutions we will derive are characterized by the vectormultiplets. For example, the dilaton will be a constant throughout this part of the thesis as it belongs to the universal hypermultiplet. For a discussion of the inclusion of hypermultiplets in the study of black holes see [128]. A quick look at the four-dimensional massless fields that one gets after reducing over a Calabi-Yau threefold (section D.3.2) reveals that, all we need to know about the Calabi-Yau is its even-cohomology and its complexified Kähler form.

5.1.1 WALKING THE PATH OF REDUCTION

In this section we will go through the main steps in deriving the bosonic part of the four-dimensional action. As explained in appendix D section D.3.2, the vectormultiplets are in one to one correspondence with the basis elements of $H^{(0,0)}$ and

$H^{(1,1)}$ cohomology of the Calabi-Yau threefold X . String theory requires an integer version of these cohomology groups which is defined only of real cohomology. Since the Calabi-Yau we will be working with has no $H^{(2,0)}$, $H^{(1,0)}$ and $H^{(0,1)}$ cohomologies (see equation D.11), we can identify $H^{1,1}(X, \mathbb{C})$ with $H^{(2)}(C, \mathbb{R})$. Let α_A ; $A = 1, \dots, h^{1,1}$ be a harmonic basis for the $H^{(2)}(X, \mathbb{Z})$ cohomology, and let us call $1 = \alpha_0$ the generator of the $H^{(0)}(X, \mathbb{Z})$ cohomology. We will collectively denote by α_Λ ; $\Lambda = 0, 1, \dots, h^{1,1}$ the harmonic basis of $H^{(0)}(X, \mathbb{Z}) \oplus H^{(2)}(X, \mathbb{Z})$ cohomology.

Following the discussion in section D.3.2, we parametrize the ten-dimensional fields as follows:

$$C^{(1)} = A^0(x) \alpha_0, \quad C^{(3)} = A^A(x) \alpha_A, \quad B + i J = (b^A(x) + i j^A(x)) \alpha_A, \quad (5.1)$$

where $C^{(1)}$ and $C^{(3)}$ are the ten-dimensional RR-forms, J is the Kähler form, and j^A parametrize the Kähler deformations of the metric (section D.3.2). To carry out the reduction of (B.1) to four dimensions, we need to know the action of $*_{10}$ and the form of $\sqrt{-G} R_{10}$. First, we go to the Einstein frame by rescaling the metric G_s as $G_E = e^{-\phi/2} G_s$. Next, using that the ten-dimensional metric G takes the following bloc diagonal form $G = g_M \oplus g_X$, where g_X is the Kähler metric of the Calabi-Yau (section D.3.1), one concludes that $*_{10} = *_M *_X$. The evaluation of the scalar curvature R_{10} simplifies drastically as a result of the bloc diagonal form of the ten-dimensional metric and the Ricci-flatness of Calabi-Yau manifolds i.e. $R_{i\bar{j}} = 0$. Let us also introduce the following quantities for later convenience

$$D_{ABC} = \int_X \alpha_A \wedge \alpha_B \wedge \alpha_C, \quad j_{AB} = \int_X \alpha_A \wedge \alpha_B \wedge J = D_{ABC} j^C, \quad (5.2)$$

$$j_A^2 = \int_X \alpha_A \wedge J \wedge J = D_{ABC} j^B j^C, \quad j^3 = \int_X J \wedge J \wedge J = D_{ABC} j^A j^B j^C.$$

Notice that D_{ABC} is the intersection number of three four-cycles β^A that are Poicaré dual to the forms α_A . We are now almost in the position of getting the reduced four-dimensional effective action. First, we plug the expressions (5.1) in the action (B.1) (after going to the Einstein frame). Then, we perform the integration over the Calabi-Yau to get [129, 130, 131]

$$2S = \int \mathcal{R} * 1 - \int (\text{Im } \mathcal{N}_{\Lambda\Sigma}(t) F^\Lambda \wedge *F^\Sigma + \text{Re } \mathcal{N}_{\Lambda\Sigma}(t) F^\Lambda \wedge F^\Sigma + G_{AB} dt^A \wedge *d\bar{t}^B), \quad (5.3)$$

where $F^\Lambda = dA^\Lambda$ is the field strength of the Abelian gauge field A^Λ , $t^A = b^A + i j^A$ is the complexified Kähler moduli, and [131]

$$G_{AB} = \frac{3}{2j^3} \int_X \alpha_A \wedge * \alpha_B = -\frac{3}{2} \left(\frac{j_{AB}}{j^3} - \frac{3}{2} \frac{j_A^2 j_B^2}{(j^3)^2} \right) = -\frac{\partial}{\partial t^A} \frac{\partial}{\partial \bar{t}^B} \ln \left(\frac{4}{3} j^3 \right), \quad (5.4)$$

whereas the expression of $\mathcal{N}_{\Lambda\Sigma}$ is given below in (5.14). To get the expression of G_{AB} above we used that [132, 129]:

$$*_X \alpha_A = -J \wedge \alpha_A + \frac{3}{2} \frac{j_A^2}{j^3} J \wedge J , \quad (5.5)$$

which can be derived using that the volume-form of the Calabi-Yau is given by

$$dv_X = \frac{1}{6!} J \wedge J \wedge J , \quad (5.6)$$

and that α_A is harmonic i.e. closed and co-closed. It is clear from (5.4) that the scalar moduli space is Kähler. However, this is not the end of the story, as supersymmetry requirements tell us that this manifold should be special Kähler, see e.g. [129, 133, 134]. Discussing the whole geometric structure of special Kähler manifolds is beyond the scope of this thesis, we will content ourselves by introducing some practical formulas that we will be needing later on.

5.1.2 THE SPECIAL KÄHLER GEOMETRY

It turns out that all the information about the action (5.3) can be nicely expressed in terms of a single function \mathcal{F} called the “*prepotential*”. Before spelling out formulas, let us first go back to the integer even-cohomology of the Calabi-Yau threefold. First, we are going to enlarge the cohomology we worked with so far ($H^{(0,0)} \oplus H^{(1,1)}$) to include $H^{(2,2)} \oplus H^{(3,3)}$. The absence of the $H^{(3,1)}$ and the $H^{(1,3)}$ cohomologies allows us to identify $H^{(2,2)}(X, \mathbb{C})$ with $H^{(4)}(X, \mathbb{R})$. Furthermore, we will choose the harmonic basis of $H^{(4)}(X, \mathbb{Z})$ ($H^{(6)}(X, \mathbb{Z})$) denoted by α^A ; $A = 1, \dots, h^{1,1}$ (respectively, α^0) such that

$$\int_X \alpha_\Lambda \wedge \alpha^\Sigma = \delta_\Lambda^\Sigma , \quad (5.7)$$

where $\Lambda = 0, 1, \dots, h^{1,1}$. In the following, we are going to abbreviate $H^{(2n)}(X, \mathbb{Z})$ by $H^{(2n)}$. We will also denote by H^* the total even-cohomology of the Calabi-Yau

$$H^* = H^{(0)} \oplus H^{(2)} \oplus H^{(4)} \oplus H^{(6)} .$$

It turns out that the even-cohomology H^* comes equipped with a skew-symmetric pairing $\langle \cdot, \cdot \rangle$ between its elements, that appears naturally in supergravity. It is defined as follows; first, we expand each element Γ of H^* in the harmonic basis α_Λ , α^A as

$$\Gamma = \Gamma^0 \alpha_0 + \Gamma^A \alpha_A + \Gamma_A \alpha^A + \Gamma_0 \alpha^0 . \quad (5.8)$$

To this element, $\Gamma \in H^*$, we will associate a new element, $\tilde{\Gamma} \in H^*$, defined as

$$\tilde{\Gamma} = \Gamma^0 \alpha_0 - \Gamma^A \alpha_A + \Gamma_A \alpha^A - \Gamma_0 \alpha^0 . \quad (5.9)$$

The skew-symmetric pairing is then given by

$$\langle \Gamma, \Delta \rangle = \int_X \Gamma \wedge \tilde{\Delta} = -\Gamma^0 \Delta_0 + \Gamma^A \Delta_A - \Gamma_A \Delta^A + \Gamma_0 \Delta^0. \quad (5.10)$$

The last bit of information we need concerns the scalars t^A . Since we want to treat the whole H^* , we need to have $2(1 + h^{1,1})$ complex scalars. Following the same strategy as above, let us first extend the scalar content so it becomes in one to one correspondence with basis elements of $H^{(0)} \oplus H^{(2)}$, and call these scalars X^Λ ; $\Lambda = 0, 1, \dots, h^{1,1}$. The latter turn out to be describing the same physics if they are multiplied by the same complex number, in agreement with the actual number of physical degrees of freedom t^A . X^Λ are called projective coordinates and we choose them such that, if $X^0 \neq 0$ then $t^A = X^A/X^0$. The needed “dual” scalars Y_Λ to cover the whole H^* turn out to be given in terms of X^Λ through a single function \mathcal{F} called the prepotential. The new scalars Y_Λ are given by $Y_0 = -\partial\mathcal{F}/\partial X^0 = -\mathcal{F}_0$ and $Y_A = \partial\mathcal{F}/\partial X^A = \mathcal{F}_A$. In the large Calabi-Yau volume limit, the prepotential is given by

$$\mathcal{F} = -\frac{1}{6} \frac{D_{ABC} X^A X^B X^C}{X^0}. \quad (5.11)$$

For the modification of this expression to include instanton corrections, see e.g. [135, 136].

We are now ready to discuss the special Kähler geometry underlying the $\mathcal{N} = 2$ four-dimensional supergravity. A special kähler geometry is characterized by the existence of a holomorphic section Ω_{hol} of H^* such that the Kähler potential $\mathcal{K} = -\ln(4j^3/3)$ of the Kähler metric (5.4) is given by

$$e^{-\mathcal{K}} = i \langle \Omega_{hol}, \bar{\Omega}_{hol} \rangle = i \left[\bar{X}^\Lambda \mathcal{F}_\Lambda - X^\Lambda \bar{\mathcal{F}}_\Lambda \right]. \quad (5.12)$$

The last expression corresponds to the rewriting of \mathcal{K} in terms of the scalars X^Λ . It is easy to see that Ω_{hol} can be written as:

$$\Omega_{hol} = X^\Lambda \alpha_\Lambda - \mathcal{F}_A \alpha^A + \mathcal{F}_0 \alpha^0 = -e^{t^A \alpha_A}. \quad (5.13)$$

The last expression in the equation above is a formal one and is valid for $X^0 = -1$. Since supersymmetry relates $h^{1,1}$ combinations of the gauge fields A^Λ to the scalars t^A as they belong to the same multiplet (see the end of section D.3.2), one expects that the metric $\mathcal{N}_{\Lambda\Sigma}$ will be expressed in terms of \mathcal{F} and X^Λ only. This turns out to be true and the expression reads [119]

$$\mathcal{N}_{\Lambda\Sigma} = \bar{\mathcal{F}}_{\Lambda\Sigma} + 2i \frac{\text{Im}(\mathcal{F}_{\Lambda\Lambda'}) X^{\Lambda'} \text{Im}(\mathcal{F}_{\Sigma\Sigma'}) X^{\Sigma'}}{\text{Im}(\mathcal{F}_{\Lambda'\Sigma'}) X^{\Lambda'} X^{\Sigma'}}, \quad (5.14)$$

where $\mathcal{F}_\Lambda = \partial_\Lambda \mathcal{F}$ and $\mathcal{F}_{\Lambda\Sigma} = \partial_\Lambda \partial_\Sigma \mathcal{F}$.

In the following, it will be more useful to work with a normalized version of Ω_{hol} defined as

$$\Omega = e^{\mathcal{K}/2} \Omega_{hol} = -\frac{1}{\sqrt{4j^3/3}} e^{(b^A + ij^A) \alpha_A} . \quad (5.15)$$

Notice that, under Kähler transformations $\mathcal{K} \rightarrow \mathcal{K} + f + \bar{f}$, Ω_{hol} transforms like $\Omega_{hol} \rightarrow e^{-f} \Omega_{hol}$. This transformation motivates us to introduce a covariant derivative acting on Ω as:

$$\mathcal{D}_A \Omega = \left(\partial_A + \frac{1}{2} [\partial_A \mathcal{K}] \right) \Omega , \quad (5.16)$$

such that Ω and $\mathcal{D}_A \Omega$ transform in the same way under Kähler transformations. It turns out that $\{\Omega, \mathcal{D}_A \Omega, \bar{\mathcal{D}}_A \bar{\Omega}, \bar{\Omega}\}$ constitute an ‘‘orthonormal’’ basis for H^* with respect to the skew-symmetric pairing (5.10) as they satisfy

$$\langle \Omega, \bar{\Omega} \rangle = -i , \quad \langle \mathcal{D}_A \Omega, \bar{\mathcal{D}}_B \bar{\Omega} \rangle = G_{AB} , \quad \langle \Omega, \mathcal{D}_A \Omega \rangle = 0 . \quad (5.17)$$

Using this new basis, it is easy to work out the decomposition of an arbitrary element Γ of H^* to be

$$\Gamma = 2 \operatorname{Im} (\bar{\mathcal{Z}}(\Gamma) \Omega - G^{AB} \bar{\mathcal{D}}_A \bar{\mathcal{Z}}(\Gamma) \mathcal{D}_B \Omega) , \quad (5.18)$$

where G^{AB} is the inverse of G_{AB} and $\mathcal{Z}(\Gamma)$ is the central charge of Γ given by

$$\mathcal{Z}(\Gamma) = \langle \Gamma, \Omega \rangle = \frac{1}{\sqrt{4j^3/3}} \left(\frac{t^3}{6} \Gamma^0 - \frac{t_A^2}{2} \Gamma^A + t^A \Gamma_A - \Gamma_0 \right) . \quad (5.19)$$

The easiest way to understand the reason behind calling such a combination a central charge is to study the action of a supersymmetric probe brane Γ in a $\mathcal{N} = 2$ four-dimensional background, which we will write down in a moment. Before doing so, we need to introduce a new element in $H^* \otimes \Omega^{(2)}(\mathcal{M}^{(1,3)})$, where $\Omega^{(2)}(\mathcal{M}^{(1,3)})$ stands for the space of two-forms in $\mathcal{M}^{(1,3)}$ the four-dimensional non-compact part of our ten-dimensional geometry. Taking advantage of the form of the gauge field part in (5.3), we introduce the following even-form

$$F = F^\Lambda \alpha_\Lambda - G_A \alpha^A + G_0 \alpha^0 , \quad (5.20)$$

where G_Λ is defined by

$$G_\Lambda = \operatorname{Re} \mathcal{N}_{\Lambda\Sigma} F^\Sigma + \operatorname{Im} \mathcal{N}_{\Lambda\Sigma} * F^\Sigma , \quad (5.21)$$

The signs in (5.20) are chosen such that the gauge field part of the action (5.3) is written as

$$S_F = \frac{1}{2} \int \langle F_{(0,2)}, F_{(4,6)} \rangle , \quad (5.22)$$

where a four dimensional wedge product is understood in the expression above, and the even forms $F_{(0,2)}$ and $F_{(4,6)}$ are given by:

$$F_{(0,2)} = F^\Lambda \alpha_\Lambda , \quad F_{(4,6)} = -G_A \alpha^A + G_0 \alpha^0 . \quad (5.23)$$

Using the expression (5.20) and that $\alpha^\Lambda, \alpha_\Lambda$ are harmonic, the Bianchi identity and the gauge field equations can be combined in the equation $dF = 0$. The latter implies the conservation of the following charge

$$\Gamma = \frac{1}{4\pi} \int F = p^\Lambda \alpha_\Lambda + q_\Lambda \alpha^\Lambda, \quad (5.24)$$

where p^0 is due to a D6-brane wrapping the whole Calabi-Yau X , $\{p^A\}$ are due to a D4-brane wrapping the four-cycle dual to the two-form $\beta^{(2)} = p^A \alpha_A$, $\{q_A\}$ are due to a D2-brane wrapping the two-cycle dual to the four-form $\beta^{(4)} = q_A \alpha^A$ and q_0 is the D0-brane charge.

The equation $dF = 0$ can be solved locally to give $F = dA$. The components A^Λ, A_Λ of A in the harmonic basis of H^* are the four dimensional Maxwell fields. Strictly speaking we have only $h^{1,1} + 1$ independent fields as a result of the relation (5.21). The components A^Λ, A_Λ of A are essentially the electric and magnetic parts of the physical Maxwell field. Using the field A , the action of a supersymmetric probe brane Γ in a $\mathcal{N} = 2$ four-dimensional background is given by [137]

$$S_{probe} = - \int |\mathcal{Z}(\Gamma)| ds + \frac{1}{2} \int \langle \Gamma, A \rangle, \quad (5.25)$$

where s is the line element of the particle. It is clear that the first term is a mass term i.e. the corresponding central charge giving the needed explanation as promised. The second term is like an electron-monopole interaction term, and will play an important role in the multi-center solutions (section 5.3).

5.2 SPHERICAL SYMMETRY AND ATTRACTOR FLOW

In the following, we are going to spell out the simplest 1/2-BPS black hole solution to (5.3) and some of its most important properties. This solution is the static spherically symmetric 1/2-BPS black hole.

5.2.1 SUPERSYMMETRY AND ATTRACTOR FLOW

Requiring supersymmetry puts a lot of constraints on our solution [138, 139]. Restricting ourselves further to static spherically symmetric solutions fixes the metric to be of the form

$$ds^2 = -e^{2U(r)} dt^2 + e^{-2U(r)} d\vec{x}^2, \quad (5.26)$$

where r is the radial coordinate in the spatial part \mathbb{R}^3 . Spherical symmetry also reduces the information about the scalar moduli t^A and the gauge fields A^Λ to 1 +

$h^{1,1}$ unknown functions that depend only on r [122]. These functions are U and t^A . We will not go through the whole derivation of solution here. The interested reader should consult [122] for details. Rather, we will outline the strategy and describe some important properties of the solution.

The idea of [122] is to take advantage of the staticity and the spherical symmetry of the problem to reduce the action (5.3) to an effective one-dimensional action that depends only on $\tau = 1/r$. Then, one solves the field equations that result from this effective action. Such procedure is in general illegal. Rather, one should first find the equations of motion of the action (5.3) then, reduce them over the sphere using our ansatz. This generally gives rise to more equations than what one gets using the resulting effective action. Luckily for us, it was checked in [122] that solving the effective field equations is enough in the case we are dealing with. A further simplification that [122] used is time independence of our solution. Basically, they rewrote the effective action they got after reducing (5.3) over a sphere S^2 as a sum of a square and a boundary term. Then, they used that the Hamiltonian of the system equals the Lagrangian multiplied by (-1) due to time independence to derive the BPS equations. According to supersymmetry, these equations should minimize the energy and hence, are equivalent in this case to the vanishing of the square term in the effective action. These equations turn out to be given by [122]:

$$\text{Im} (\partial_A \mathcal{K} \dot{t}^A) + \dot{\xi} = 0, \quad 2\partial_\tau (e^{-U} \text{Im} [e^{-i\xi} \Omega]) = -\Gamma, \quad (5.27)$$

where \mathcal{K} is the Kähler potential (5.12), the charge “vector” Γ is defined in (5.24), and ξ is the phase of the central charge $\mathcal{Z}(\Gamma)$ defined in (5.19).

The equations (5.27) are equivalent to the Killing spinor equations. They describe a one parameter flow of t^A in the moduli space. They are called the “*attractor flow*” equations [127]. One can show that during such a flow, the norm of the central charge $|\mathcal{Z}(\Gamma)|$ is a decreasing function of τ , and it reaches its minimum with respect to varying all moduli t^A at $\tau \rightarrow \infty$. This implies that the value of $|\mathcal{Z}(\Gamma)|_{\tau=\infty} = |\mathcal{Z}(\Gamma)|_{\min}$ is completely fixed by the value of Γ independently from the values of the moduli t^A at $\tau = 0$. This phenomenon is called the “*attractor mechanism*” [140, 141]. It can happen that there is more than one minimum of $|\mathcal{Z}(\Gamma)|$. In such cases, one can end up in any one of them. In this situation, the attractor flow is said to have “multiple-bassins of attraction”. Such phenomenon can occur only in singular regions of moduli space [142, 143]. Throughout the remaining of this thesis, we will assume that we are “far” from such singular regions.

It turns out that $\tau = \infty$ ($r = 0$) describes a *horizon* of the black hole as $e^{-U} \sim |\mathcal{Z}(\Gamma)|_\infty \tau \rightarrow \infty$, [122]. Such a behavior allows us to calculate the associated entropy of the black hole, which turns out to be fixed by $\mathcal{Z}(\Gamma)$

$$S(\Gamma) = \pi |\mathcal{Z}(\Gamma)|_{\min}^2. \quad (5.28)$$

This is good news because due to the attractor mechanism, the entropy of a black hole depends only on the charges and does not care about the value of the moduli in the asymptotic flat region. This is in agreement with the no-hair theorem.

5.2.2 THE ONE CENTERED BLACK HOLE

We are more or less ready to construct our static spherically symmetric solution. We are going to describe the different steps leading to the solution leaving the details to the literature. We will be following [123] and [122] where the whole solution was expressed in terms of a single function Σ called the “*entropy function*”. Its explicit expression was first derived in [144], in the special case of the large Calabi-Yau volume limit.

The idea is to take advantage of the attractor flow equations (5.27), while using at the same time different properties of Ω , $\mathcal{D}_A \Omega$ and their complex conjugates (5.17). First, one formally solves the second equation in (5.27) as:

$$2 e^{-U} \operatorname{Im} (e^{-i\xi} \Omega) = -\Gamma \tau + 2 \operatorname{Im} (e^{-i\xi} \Omega)_{\tau=0} \equiv -H. \quad (5.29)$$

The trick that allows us to construct the solution is to rewrite all our fields (metric, moduli t^A , and Maxwell one-forms A^Λ) in terms of this new function H . Taking the skew-symmetric pairing of this equation with Ω gives

$$e^{-2U} = |\mathcal{Z}(H)|^2 \equiv \Sigma(H). \quad (5.30)$$

To get the expressions for t^A , one first plugs (5.30) back into (5.29) to get the imaginary part of t^A . Then, taking the pairing of (5.29) with $\mathcal{D}_A \Omega$ gives their real part [123]. Combining both gives:

$$t^A = \frac{H^A - i \partial_{H_A} \Sigma(H)}{H^0 + i \partial_{H_0} \Sigma(H)}. \quad (5.31)$$

The only remaining unknown fields to be found are the Maxwell one-forms A^Λ . They turn out to be given by [123]:

$$A^\Lambda = \epsilon \partial_{H_\Lambda} \ln \Sigma(H) dt - p^\Lambda \cos \theta d\phi, \quad (5.32)$$

where $\epsilon = -1$ for $\Lambda = 0$ and $+1$ otherwise. The only remaining thing to do now is to express $\Sigma(H)$ in terms of H^Λ . Using that the former is a homogeneous function of degree two [123], and its asymptotic expression near the horizon $\tau \rightarrow \infty$, one concludes that

$$\Sigma(H) = \frac{1}{\pi} S(H), \quad (5.33)$$

where $S(H)$ is the same function that gives the black hole entropy when we replace H by the corresponding Γ . In general, figuring out such a function is a hard task and depends strongly on the form of the prepotential \mathcal{F} (5.13). In the case of a cubic prepotential (5.11), using the expression for $S(\Gamma)$ derived in [144], our static spherically symmetric BPS black hole solution reads

$$\begin{aligned}
 ds^2 &= -\frac{1}{\Sigma} dt^2 + \Sigma d\vec{x}^2, \quad t^A = \frac{H^A}{H^0} + \frac{y^A}{Q^{3/2}} \left(i\Sigma - \frac{L}{H^0} \right), \\
 A^0 &= -\frac{L}{\Sigma^2} dt + \mathcal{A}^0, \quad A^A = \frac{H^A L - Q^{3/2} y^A}{H^0 \Sigma^2} dt + \mathcal{A}^A, \\
 H &= \frac{\Gamma}{r} - 2 \operatorname{Im} (e^{-i\xi} \Omega)_{r=\infty}, \quad d\mathcal{A}^\Lambda = \star dH^\Lambda, \\
 \Sigma &= \sqrt{\frac{Q^3 - L^2}{(H^0)^2}}, \quad Q^3 = \left(\frac{1}{3} D_{ABC} y^A y^B y^C \right), \\
 L &= (H^0)^2 H_0 + \frac{1}{3} D_{ABC} H^A H^B H^C - H^0 H^A H_A,
 \end{aligned} \tag{5.34}$$

where \star is the flat three-dimensional \mathbb{R}^3 Hodge star, and y^A are solutions to the following equation

$$D_{ABC} y^B y^C = -2 H^0 H_A + D_{ABC} H^B H^C. \tag{5.35}$$

From the explicit expression of the metric and Σ above (5.34), it is clear that a solution will not exist if Σ^2 is negative. Since Σ is roughly the modulus square of the central charge $\mathcal{Z}(\Gamma)$ where the charge Γ is replaced now by H (5.30), one expects that the existence of the solution has something to do with $\mathcal{Z}(\Gamma)$. This turns out to be true, where, [143] showed that there are three possibilities

- $|\mathcal{Z}(\Gamma)|_{min} \neq 0$, a black hole of charge Γ exists.
- $|\mathcal{Z}(\Gamma)|_{min} = 0$ at a regular point in moduli space, the solution does not exist.
- $|\mathcal{Z}(\Gamma)|_{min} = 0$ at a singular point in moduli space, more analysis is needed to decide whether the solution exists or not.

The second point led to the following puzzle. Some known microscopic BPS states at weak coupling (D-brane states) do not have a strong coupling counterpart i.e. supergravity solution. Such a situation is confusing as the dilaton lives in the hypermultiplets moduli-space (section D.3.2), which as we argued in the beginning of this chapter has nothing to do with our solutions. The resolution of such puzzle will be the subject of the next section.

5.3 BUBBLES AND BOUND BLACK HOLES

It was realized in [122, 145] (for an earlier attempt see [146]), that there are other 1/2-BPS solutions to the action (5.3) which describe a bound state of black holes. They may not exhaust the list of all possible BPS-solutions to $\mathcal{N} = 2$ four dimensional supergravity as they are stationary. These solutions play an important role on different fronts. On top of making the map between microscopic and macroscopic degrees of freedom richer and more subtle e.g. [147, 148, 30], they also describe candidate geometries for black hole states [124, 118, 56]. Although, smooth solutions can only appear when we uplift to five dimensions e.g. [38] (through [62, 63]), the number of these states –as things stand right now– is the same. Furthermore, it was shown in [64] that the uplift can be embedded in an asymptotic $\text{AdS}_3 \times S^2$ spacetime, which opens the possibility to apply AdS/CFT duality considerations to these solutions. The latter can be seen as normalizable deformations of AdS_3 , which, according to the AdS/CFT dictionary, should be mapped to states in the dual CFT theory. Such identification can be seen as another argument for the possible applicability of the fuzzball considerations to these supergravity solutions.

In the following, we are going to discuss these solutions and some of their important properties following [122, 85, 123]. We will be very brief in our exposition as the intermediate steps become a bit technical very quickly inviting the unsatisfied reader to check the literature.

5.3.1 MORE THAN ONE CENTER

Based on our intuition from the probe brane action (5.25), the metric this time will not be static any more. This comes about because of the “electron-monopole” interaction term $\langle \Gamma, A \rangle$. So our starting point will be the following metric ansatz:

$$ds^2 = -e^U (dt + \omega)^2 + e^{-U} d\vec{x}^2, \quad (5.36)$$

where ω is a one-form on the base space \mathbb{R}^3 . The existence of such term, and the dependence of the solution on the vector \vec{x} and not only on its norm r as in the one center case, makes the BPS analysis more involved. [122] managed to derive the following BPS equations

$$2e^{-U} \text{Im} (e^{-i\xi} \Omega) = -H, \quad *d\omega = \langle dH, H \rangle, \quad (5.37)$$

$$A = 2e^U \text{Re} (e^{-i\xi} \Omega) dt + \mathcal{A}, \quad *d\mathcal{A} = dH, \quad (5.38)$$

which clearly generalize (5.27). In this generic case, ξ is the phase of the total central charge $\mathcal{Z}(\Gamma)$ where $\Gamma = \sum_a \Gamma_a$, whereas H is a generic harmonic function

that, in the case of many center \vec{x}_a , takes the form

$$H = \sum_a \frac{\Gamma_a}{r_a} - 2 \operatorname{Im} (e^{-i\xi} \Omega)_{\infty} , \quad (5.39)$$

where $r_a = |\vec{x} - \vec{x}_a|$. The derivation of the solution describing a multi-center black holes uses the same strategy as before, where most of the intermediate steps remain valid. At the end, and in the case of a cubic prepotential, the following solution is found

$$\begin{aligned} ds^2 &= -\frac{1}{\Sigma} (dt + \omega)^2 + \Sigma d\vec{x}^2 , \quad t^A = \frac{H^A}{H^0} + \frac{y^A}{Q^{3/2}} \left(i\Sigma - \frac{L}{H^0} \right) , \\ A^0 &= -\frac{L}{\Sigma^2} dt + \mathcal{A}^0 , \quad A^A = \frac{H^A L - Q^{3/2} y^A}{H^0 \Sigma^2} dt + \mathcal{A}^A , \\ H &= \frac{\Gamma}{r} - 2 \operatorname{Im} (e^{-i\xi} \Omega)_{r=\infty} , \quad d\mathcal{A}^\Lambda = \star dH^\Lambda , \quad \star d\omega = \langle dH, H \rangle , \quad (5.40) \\ \Sigma &= \sqrt{\frac{Q^3 - L^2}{(H^0)^2}} , \quad Q^3 = \left(\frac{1}{3} D_{ABC} y^A y^B y^C \right) , \\ L &= (H^0)^2 H_0 + \frac{1}{3} D_{ABC} H^A H^B H^C - H^0 H^A H_A , \end{aligned}$$

where \star is the flat three-dimensional \mathbb{R}^3 Hodge star, and y^A are solutions to (5.35). As before, the solution is valid if $\Sigma^2 > 0$. We will postpone the discussion about this point to the next section, and turn now to the description of two of the most important properties of these solutions.

5.3.2 USEFUL PROPERTIES

The solutions described above distinguish themselves from their one-center cousins by two properties which are:

BUBBLE CONSTRAINTS

In the derivation of the solution (5.40), we have neglected an important issue. The existence of the one-form ω is not always trivial. This is because, its defining equation (5.37) combined with the expression of H (5.39) puts constraints on the possible positions of the different centers. Using that $d^2 = 0$, and that $\Delta H = \sum_a \Gamma_a \delta^3(\vec{x} - \vec{x}_a)$, leads to the following important constraint on the inter-center distances

$$\sum_{b,b \neq a} \frac{\langle \Gamma_a, \Gamma_b \rangle}{r_{ab}} = \langle h, \Gamma_a \rangle ; \quad \forall a , \quad (5.41)$$

where we used the short hand notation $h = -2 \operatorname{Im} (e^{-i\xi} \Omega)_\infty$. These equations are not all independent. To check that note, using the expression of h and the definition of ξ , that the sum of the equations (5.41) is trivial. This can be seen as factoring out the center of mass degrees of freedom. In the case of N centers, one ends up with a $2(N - 1)$ -dimensional space of solutions (called also solution space). The dimension being even will turn out to be important for the considerations of the next chapter.

Having such “bubble” equations complicates our lives. We have to check that the solutions r_{ab} are physically acceptable; all of them are positive and they should satisfy the triangle inequalities. Such complications, on top of the requirement that $\Sigma^2 > 0$, makes a systematic study of such solutions intractable. However, [147, 30] conjectured a simpler way to overcome this murky situation. This will be the subject of the next section.

ANGULAR-MOMENTUM

As was already mentioned around (5.36), these solutions are stationary but not static. This is due to the presence of cross terms encoded by ω . It is clear from its defining equation that its origin resides in the non-trivial angular momentum generated by the electron-monopole interaction. It can be easily shown by studying the asymptotics of the metric around the flat background that, there is a non-trivial angular momentum given by:

$$\vec{J} = \frac{1}{4} \sum_{a \neq b} \frac{\langle \Gamma_a, \Gamma_b \rangle}{r_{ab}} \vec{x}_{ab}, \quad (5.42)$$

where $\vec{x}_{ab} = \vec{x}_a - \vec{x}_b$ and $r_{ab} = |\vec{x}_{ab}|$. Note that the normalization of J above is chosen such that after quantization, J will be quantized in half integer units. The existence of such angular momentum will play an important role in the discussion of the symplectic form in section 6.1.1. Using the constraints (5.41), one can show that the norm of \vec{J} is given by [56]

$$|J| = \frac{1}{2} \sqrt{- \sum_{a < b} \langle h, \Gamma_a \rangle \langle h, \Gamma_b \rangle r_{ab}^2}. \quad (5.43)$$

This formula will be useful in section 6.3.3 where we will compare the number of states that we will get from quantizing the supergravity solutions to the number that one expects based on the wall crossing formula.

5.4 BPS STATES COUNTING

So far, we have reviewed a class of four dimensional solutions, but, these solutions are relatively complicated and it is non-trivial to determine if they are well-defined everywhere. In particular, the entropy function Σ , that appears in the solution involves a square root and may take imaginary values in some regions (when uplifted to five dimensions this can lead to closed timelike curves [63] [149] [150]). In [122] and [30], a simplified criterion was proposed for the well behavedness of such solutions which we will now briefly relate.

5.4.1 THE FAMILY TREE

In [122], a conjecture is proposed whereby pathology-free solutions are those with a corresponding *attractor flow tree* in the moduli space. The latter is a graph in the Calabi-Yau moduli space beginning at the moduli at infinity, $t^A|_\infty$, and ending at the attractor points for each center. The edges correspond to single center flows towards the attractor point for the sum of charges further down the tree. Vertices can occur where single center flows (for a charge $\Gamma = \Gamma_1 + \Gamma_2$) cross walls of marginal stability where the central charges are all aligned ($|Z(\Gamma)| = |Z(\Gamma_1)| + |Z(\Gamma_2)|$). The actual flow of the moduli $t^A(\vec{x})$ for a multi-centered solution will then be a thickening of this graph (see [122], [30] for more details). According to the conjecture, a given attractor flow tree will correspond to a single connected set of solutions to the equations (5.41), all of which will be well-behaved. An example of such a flow is given in figure 5.1.

As mentioned before, the main purpose of the attractor flow tree is to allow us to determine if a solution is well defined. For a single centered black hole, the entropy function Σ undergoes a monotonic flow from infinity to the horizon. At infinity the value of Σ depends on the choice of moduli (boundary conditions), while at the horizon it flows to a fixed value depending only on the charges, as the moduli are fixed by the attractor mechanism. Spherical symmetry dictates that the moduli depend only on a radial variable, so, the flow through moduli space is indeed just a single line from the moduli at infinity to the attractor value. If Σ should become imaginary somewhere along this flow, the solution would suffer from pathologies. However, since the flow is monotonic, it need only be checked at its initial (the moduli at infinity) and final points (the attractor point).

For a multi-centered system, the moduli depend on three variables and the flow is no longer monotonic in a straightforward way (it is not even a one dimensional tree but rather a “fat graph”). By assuming that solutions could be built constructively by bringing in centers from infinity, [122] was able to conjecture that even for

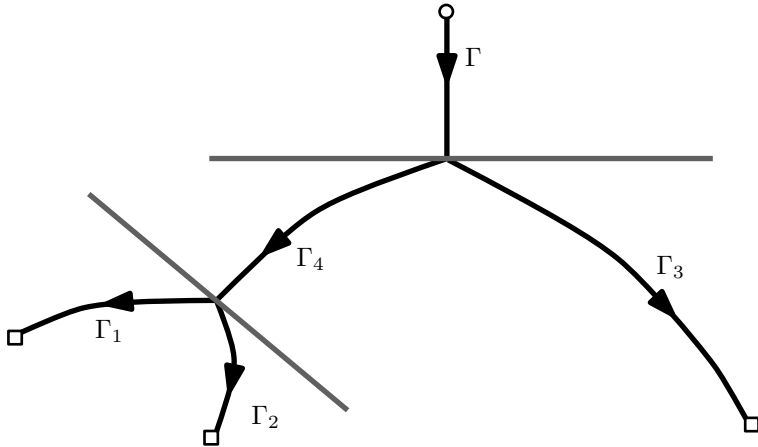


Figure 5.1: Three centered attractor flow tree. The system is composed of three center of charge Γ_1 , Γ_2 and Γ_3 and the moduli at infinity are at the value labelled by the black circle. Each leg of the tree above represents a single center flow towards the attractor value associated with the total charge below that point. Thus the first flow is towards the attractor point for $\Gamma = \Gamma_1 + \Gamma_2 + \Gamma_3$. After the first split the flows are towards the attractor points for charges Γ_3 and $\Gamma_4 = \Gamma_1 + \Gamma_2$. In each case the split occurs along walls of marginal stability (thick grey lines). The first, horizon, line of MS corresponds to $|Z(\Gamma)| = |Z(\Gamma_3)| + |Z(\Gamma_4)|$ while the second is for $|Z(\Gamma_4)| = |Z(\Gamma_1)| + |Z(\Gamma_2)|$.

multi-centered configurations we can study a flow *tree* in the moduli space (recall the actual flow will be a “fat” version of this) and study each leg of the flow to check for pathologies. The conjecture is then that if the tree exists (each leg is pathology free) then the full solution is actually well behaved (see [122, 147] for more details). There is considerable evidence for this conjecture [122, 85, 147, 30], and our computation in sections 6.3.3 and 6.4 will provide even further support.

The intuition behind this proposal is based on studying the two-center solution for charges Γ_1 and Γ_2 . The constraint equations (5.41) imply that when the moduli at infinity are moved near a wall of marginal stability (where Z_1 and Z_2 are parallel), the centers are forced infinitely far apart

$$r_{12} = \frac{\langle \Gamma_1, \Gamma_2 \rangle}{\langle h, \Gamma_1 \rangle} = \frac{\langle \Gamma_1, \Gamma_2 \rangle |Z_1 + Z_2|}{2 \operatorname{Im}(\bar{Z}_2 Z_1)} \Big|_{\infty}. \quad (5.44)$$

In this regime, the actual flows in moduli space are well approximated by the split attractor trees since the centers are so far apart that the moduli will assume single-center behavior in a large region of spacetime around each center. Thus, in this regime the conjecture is well motivated. Varying the moduli at infinity continuously

should not alter the BPS state count, which corresponds to the quantization of the two center moduli space, so unless the moduli cross a wall of marginal stability we expect solutions smoothly connected to these to also be well defined. Extending this logic to the general N center case requires an assumption that it is always possible to tune the moduli such that the N centers can be forced to decay into two clusters that effectively mimic the two-center case. There is no general argument that this should be the case but one can run the logic in reverse, building certain large classes of solutions by bringing in charges pairwise from infinity, and this can be understood in terms of attractor flow trees. It is clear that not all solutions can be constructed in this way. For example, for some set of charges Γ_a , it could happen that the constraint equations (5.41) allow for solutions where the centers approach each other arbitrarily closely. These class of solutions cannot be constructed using the strategy explained above. For more discussion on this point, the reader should consult [147].

5.4.2 MISSING STATES: WALL CROSSING

For generic charges, the attractor flow conjecture also provides a way to determine the entropy of a given solution space. The idea is that the entropy of a given total charge is the sum of the entropy of each possible attractor flow tree associated with it. Thus, the partition function receives contributions from all possible trees associated with a given total charge and specific *moduli at infinity*. An immediate corollary of this is that, as emphasized in [30], the partition function depends on the asymptotic moduli. As the latter are varied, certain attractor trees will cease to exist; specifically, a tree ceases to contribute when the moduli at infinity cross a wall of marginal stability (MS) for its first vertex, $\Gamma \rightarrow \Gamma_1 + \Gamma_2$, as is evident from (5.44).

For two-center solutions, one can determine the entropy most easily near marginal stability where the centers are infinitely far apart. In this regime, locality suggests that the Hilbert state contains a product of three factors [30]

$$\mathcal{H}(\Gamma_1 + \Gamma_2; t_{ms}) \supset \mathcal{H}_{\text{int}}(\Gamma_1, \Gamma_2; t_{ms}) \otimes \mathcal{H}(\Gamma_1; t_{ms}) \otimes \mathcal{H}(\Gamma_2; t_{ms}) . \quad (5.45)$$

One should be a little bit more careful as attractor flow trees do not *have* to split at walls of marginal stability. Generally, in such cases there will be other contributions to $\mathcal{H}(\Gamma_1 + \Gamma_2; t_{ms})$ as well. In the following, we will be assuming that such split does happen keeping in mind subtleties aforementioned.

Since the centers move infinitely far apart as t_{ms} is approached, we do not expect them to interact in general. There is, however, a conserved angular momentum carried in the electromagnetic fields sourced by the centers, and this also yields a non-trivial multiplet of quantum states. Thus, the claim is that \mathcal{H}_{int} is the Hilbert

space of a single spin J multiplet where $J = \frac{1}{2}(|\langle \Gamma_1, \Gamma_2 \rangle| - 1)$. The unusual (-1) in the definition of J comes from quantizing additional fermionic degrees of freedom [85] [56]. $\mathcal{H}(\Gamma_1)$ and $\mathcal{H}(\Gamma_2)$ are the Hilbert spaces associated with BPS brane excitations in the Calabi-Yau, and their dimensions are given in terms of a suitable entropy formula for the charges Γ_1 and Γ_2 valid at t_{ms} .

Thus, if the moduli at infinity were to cross a wall of marginal stability for the two-center system above, the associated Hilbert space would cease to contribute to the entropy (or the index). A similar analysis can be applied to a more general multi-centered configuration like that in figure 5.1 by working iteratively down the tree, and treating subtrees as though they correspond to single center with the combined total charge of all their nodes. The idea is, once more, that we can cluster charges into two clusters by tuning the moduli and then treat the clusters effectively like individual charges. We can then iterate these arguments within each cluster. This counting argument mimics the constructive one for building the solutions by bringing in charges from infinity, and is hence, subject to the same caveats, discussed above.

Altogether, the above ideas allow us to determine the entropy associated with a particular attractor tree, which by the split attractor flow conjecture, corresponds to a single connected component of the solutions space. The entropy of a tree is the product of the angular momentum contribution from each vertex (i.e. $|\langle \Gamma_1, \Gamma_2 \rangle|$, the dimension of \mathcal{H}_{int}) times the entropy associated to each node. When we want to compare against the number of states derived from quantizing the classical phase space, as we are going to do in the next chapter, the latter factor (from the nodes) will not be included as it is not visible in the supergravity solutions.

In the next chapter, we will show that it is also possible –in some cases– to quantize the solution space directly and to match the entropy so derived with the entropy calculated using the split attractor tree. This provides a non-trivial check of both calculations.

CHAPTER 6

SETTING THE STAGE FOR FUZZBALLS

So far, we have described a rich family of four dimensional BPS states that asymptotically look like a single center black hole (5.3). It will be very interesting if one could choose a subset of all these possible solutions and declare them to be black hole states. As was already mentioned at several places, although for smoothness considerations one needs to go one dimension higher we are not going to do so here. Our space of solutions that we will be working with, will be the set of all possible center positions \vec{x}_a subject to the constraint (5.41). Unfortunately, due to the complicated nature of our space of solutions, things are not as concrete as was the case in the D1-D5 system. Actually, what we have been able to do is to quantize a special class of all possible $\mathcal{N} = 2$ BPS solutions. This is a first step toward an implementation of the fuzzball ideas to a 1/2-BPS macroscopically large black hole of the $\mathcal{N} = 2$ four-dimensional supergravity.

This chapter will deal mainly with quantizing the $\mathcal{N} = 2$ four-dimensional solution space. Although, the latter is very complicated and might have a rich topology, we managed to carry out the quantization in some simple cases. These are the three-center (section 6.3) and the so called “*dipole halo solutions*” (section 6.4). Our results agree with what one expects from wall-crossing considerations when the latter is applicable (section 5.4.2). In the cases where the wall-crossing considerations fail, like in the case of scaling solutions (section 6.3.2), our quantization gives a prediction of the number of BPS states.

Eventhough the class of solutions we managed to quantize is very restricted, a

special case of the dipole halo systems turns out to be very interesting (section 6.5). These are dipole halos that develop a scaling behavior. It was argued that such solutions can be seen as a geometric manifestation of D4-D0 black hole states [116, 117, 118]. Unfortunately, after counting the number of BPS states of these class of solutions, we seem to get far less entropy than the corresponding entropy of the D4-D0 with the same total charges. As a result, we are facing two possibilities: either there are other supergravity solutions that we did not include in our counting and these will account for the missing states, or we need stringy degrees of freedom to reach the needed number of states. We are inclined to believe the second possibility. We will present an estimate of an upper limit on the possible supergravity BPS states in section 6.5.3 in support of our claim.

Before diving into the details of these exciting results, we start by constructing the symplectic form which gives us a clear criterion to when a solution space is a phase space. Armed with this, we go ahead and describe the quantization method we will be using. This is the so called “*geometric quantization*”. Some details will be left to appendices E and F.

In this chapter, the reader is assumed to have some knowledge of differential geometry and two-dimensional conformal field theory.

6.1 FROM THE SYMPLECTIC FORM TO QUANTIZATION

In this section, we will study the general features of the quantization approach that we will use, later on, to quantize a special class of our solution spaces (5.40), where the centers positions \vec{x}_a are subject to the bubble constraint (5.41). Following the general approach discussed in section 2.3, we need to derive the restriction of the symplectic form (2.5) to our solution space. Due to the complicated nature of both the supergravity action (5.3) and our solution space, we will take another approach to get the symplectic form relying on open/closed string duality. We will be using the dual open string picture of our multi-center solutions to derive our symplectic form.

Let us try to describe in simple words what kind of field theory one gets in the open string picture. We will be sketchy in the following, for more details see [85]. The story is a little bit involved but its spirit is simple as we will describe now. Remember that the multi-center solutions describe the geometry response to a set of D-branes that wrap different cycles inside the compact Calabi-Yau. These D-branes are characterized by the the charge vector Γ_a , where a labels the different centers, as described below (5.24). In the open string picture, we start with the same D-brane configuration as the one of our gravity solution, however, we will not backreact these

D-branes. In other words, we go to a regime where the gravitational interaction is so weak that the geometry will not feel the presence of these D-branes. This can be achieved by decreasing the string coupling constant.

Summarizing, in the open string picture we have the same brane configuration as in the gravity side, but now the background geometry is a Calabi-Yau times a four-dimensional Minkowski spacetime. Each stack of these D-branes Γ_a , that generates the charge of the center (a), contributes a $U(N_a)$ gauge field where N_a is the greatest common factor of the component of Γ_a in the harmonic basis $\alpha_\Lambda, \alpha^\Lambda$ of H^* . On top of these gauge fields, we have fields that describe open strings stretching between different stacks of D-branes i.e. open strings stretching between the stacks described by Γ_a and Γ_b where $a \neq b$. After reducing this theory over the Calabi-Yau, one ends up with a one-dimensional theory with a couple of $U(N_a)$ gauge fields and fields that transform in the (fundamental, anti-fundamental) representation of $U(N_a) \times U(N_b)$ where $a \neq b$. Such a theory is called “*quiver quantum mechanics*” (QQM in short) [85].

After deriving the symplectic form from the dual quiver quantum mechanics, one has to study to modification of such symplectic form once the string coupling constant is increased. Usually, this is quiet non-trivial, but luckily in our case, the terms in the quiver quantum mechanics action that contribute to the symplectic form are protected. It turns out that they do not receive neither perturbative nor non-perturbative corrections beyond one-loop [85, 56]. Motivated by this non-renormalization theorem [85], we propose that the same symplectic from should be derivable from the supergravity action following the logic in [151] (see also [81] and references therein). This will be further confirmed by an exact agreement of our state counting with Denef and Moore’s wall-crossing formula [56]. Actually we can recognize a term in the supergravity action that might lead to the same symplectic form as in the open string picture. However, there are other terms in the supergravity action besides this term. So we can rephrase our conjecture in the following way: the other putative terms contributing to the symplectic form from supergravity cancel, or only change the normalization as has been seen in [151].

To proceed further, we need to choose a polarization to split our phase space in coordinates and momenta in order to be able to quantize it. Unfortunately, there is no universal strategy to accomplish this. However, the examples we are going to discuss later on (sections 6.3, 6.4 and 6.5) come with a common beautiful mathematical structure that allows us to quantize them in a particularly nice way. Their solution spaces turn out to be “*toric Kähler*” (see section 6.2.1 for some general facts about such geometries). In these cases we can use *geometric quantization* approach, see e.g. [152, 89, 90, 91], to carry out our quantization.

This section is subdivided into two parts. In the first one, we are going to summarize

the derivation of the symplectic form [56]. While we are going to discuss some key points of geometric quantization in the second part.

6.1.1 OPEN STRINGS AND SYMPLECTIC FORM

The symplectic form can, in principle, be derived from the supergravity action as was done, for instance, in [151]. In our case, however, it is far more tractable to take a different approach [56]. As discussed in [85], the four dimensional multi-centered solutions can also be analyzed in the probe approximation by studying the quiver quantum mechanics of D-branes in a multi-centered supergravity background. Moreover, a non-renormalization theorem [85] implies that the terms in the quiver quantum mechanics Lagrangian linear in the velocities do not receive corrections, either perturbatively or non-perturbatively beyond one-loop. We can use this fact to calculate the symplectic form in the probe regime and extend it to the fully back-reacted solution; this is because, for time-independent solutions, the symplectic form depends only on the terms in the action linear in the velocity.

For this approach to be consistent it is necessary that the BPS solution space, which we interpret as a phase space, of the four-dimensional supergravity theory, as well as that of the probe theory, all match. This follows from the fact that they are all governed by the same equation, (5.41) [85]. For instance, one can see that a probe brane of charge Γ_a in the background generated by a charge Γ_b is forced off to infinity as a wall of marginal stability is approached [85], analogous to what was described around equation (5.44) for the corresponding supergravity solution.

In [56], the symplectic form on the solution space is determined. We will not review the derivation in detail but simply note that it arises from the term coupling the probe brane to the background gauge field, $\dot{x}^i A_i$, giving

$$\omega = \frac{1}{2} \sum_p \delta x_p^i \wedge \langle \Gamma_p, \delta \mathcal{A}^i(x_p) \rangle . \quad (6.1)$$

where \mathcal{A} is the “spatial” part of the gauge field given by (5.40)

$$d\mathcal{A} = \star dH , \quad (6.2)$$

with the “ \star ” above is the flat three-dimensional Hodge star. This descends naturally to the spatial part of the 4-d gauge field. Using the definition of \mathcal{A} , we can further manipulate this expression [56] and put it in the form

$$\omega = \frac{1}{4} \sum_{p \neq q} \langle \Gamma_p, \Gamma_q \rangle \frac{\epsilon_{ijk} (\delta(x_p - x_q)^i \wedge \delta(x_p - x_q)^j) (x_p - x_q)^k}{|\mathbf{x}_p - \mathbf{x}_q|^3} . \quad (6.3)$$

This is a two form on the $(2N-2)$ -dimensional solution space which is a submanifold of \mathbb{R}^{3N-3} defined by (5.41). Moreover, one can show that, on this submanifold, this form is closed and, in the cases we will investigate below, non-degenerate. Thus, it endows the solution space with the structure of a phase space. Note that, as anticipated, the center of mass degrees of freedom do not appear in the symplectic form above and hence decouple in the quantization of the system.

Although the constraint equations (5.41) are invariant under global $SO(3)$ rotations, these are nonetheless (generically) degrees of freedom of the system, and this is reflected in the symplectic form. If we contract (6.3) with the vector field that generates rotations around the 3-vector n^i (i.e. we take $\delta x_{pq}^i = \epsilon^{ijk} n^j x_{pq}^k$), then the symplectic form reduces to

$$\omega \rightarrow n^i \delta J^i , \quad (6.4)$$

where J^i are the components of the angular momentum vector defined in (5.42).

This is nothing more than the statement that the components J^i are the conjugate momenta associated to global $SO(3)$ rotations. In general, the symplectic form on any of our phase spaces will have terms like the above coming from the global $SO(3)$ rotations, in addition to terms depending on other degrees of freedom. This does not hold for solution spaces with unbroken rotational symmetries, such as solution spaces containing only collinear centers or a single center. In these cases some $SO(3)$ rotations act trivially, they do not correspond to genuine degrees of freedom nor do they appear in the symplectic form. We close this subsection by noting that (6.4) implies that solution spaces with $\vec{J} = \vec{0}$ everywhere will have a degenerate symplectic form, and therefore, will not constitute a proper phase space. This happens when all the intersection products between charges vanish ($\langle \Gamma_a, \Gamma_b \rangle = 0 ; \forall a, b$). In such situations, the centers are free to move anywhere and hence they are not bound. These systems are not amenable to quantization using the methods that will be developed in this chapter.

In situations like these, one could try to include small velocities for the centers in order to arrive at a well-defined phase space. It is clearly an interesting question whether this modified system will give rise to BPS states upon quantization. Superficially, the momenta increase the energy while leaving the charges invariant, and they therefore violate the BPS condition. However, if the Hilbert space has a continuous spectrum of momenta, it is possible that there is a BPS bound state at zero momentum in the spectrum. This is difficult to analyze in general, but in our case, we do not expect this to happen, at least not in asymptotically AdS spaces, since AdS effectively provides a box and will therefore put an IR cutoff on the admissible momenta. Thus our proposal is that solution spaces with a degenerate symplectic form should not be thought of as describing proper BPS bound states.

This immediately leads to another issue; namely, we know that, for example, N D0-branes can form a marginal bound state [153, 154], but the symplectic form for such a configuration (for example in the presence of a D4-brane) would vanish identically. This clearly conflicts with the statements of the preceding paragraph.

We would like to argue that the resolution of this inconsistency lies in the fact that the marginal bound state of D0-branes cannot be understood purely from a low-velocity expansion. Rather, the presence of the non-Abelian degrees of freedom is essential for the bound state to exist. This is supported both by the analysis of [154], as well as by the size of the bound state (see e.g. [155]). Again, it would be interesting to explore this further. In this chapter, we will take the point of view that a solution containing a marginal bound state of e.g. N D0-branes should be counted separately from a similar solution where the marginal bound state has been replaced by N individual D0-branes. This will be crucial for identifying the number of states of the non-scaling dipole-halo solution, that we will get using our quantization method, with the number of states predicted by wall-crossing formula (section 6.4).

6.1.2 KÄHLER GEOMETRY AND GEOMETRIC QUANTIZATION

Classical physics being our daily life experience is well understood. However, going to the *micro*-world requires a new theory with its own “rules of the game”, this is “*quantum mechanics*”. Unfortunately, the only part that we really understand in quantum mechanics is its limit which is classical physics. Since, in our search for a quantum theory we are trying to build a theory starting from its limit not the other way around, it makes it a challenging task and possibly with a non-unique prescription. After all, the only criterion that we have to check if we got the right quantum mechanics theory, or not, is by confronting its predictions to the results of experiments. In the following, we will be giving a taste of one of the possible approaches to quantization, the so called “*geometric quantization*”. We will be following closely [89].

Geometric quantization is a perfect example of “*the beauty and the beast*” i.e. its fundamental ideas are elegant and simple, however, things become quickly mathematically more demanding. Fortunately, as far as counting degrees of freedom is concerned, which is what we will be doing, the elegant part is more than enough. Geometric quantization builds on the symplectic structure of classical physics which will be the subject of the next subsection. A discussion of the first step towards quantization, the so called “*prequantization*” will follow. In this step, an attempt to construct the Hilbert space will be carried out. This space turns out to be *too large* and needs to be “*halved*”. In such a procedure, a polarization will be chosen that

distinguishes coordinates from momenta. In our cases of interest, a natural polarization will be favorable. This is the “*holomorphic*” (called also “*Kähler*”) polarization which is suitable for Kähler manifolds.

LINKING CLASSICS TO QUANTUM: SYMPLECTIC GEOMETRY

We have already mentioned very briefly the connection between classical physics and symplectic geometry in section 2.3.2. In the Hamiltonian formulation of classical physics, the dynamics is governed by a function \mathcal{H} called the “Hamiltonian”, while the degrees of freedom of the system parametrize a space called the “phase space”. A central element in such formulation is the Poisson bracket $\{\cdot, \cdot\}$, which can be nicely encoded in a symplectic form ω (section 2.3.2).

All in all, we have a $(2n)$ -dimensional manifold M called phase space, equipped with a non degenerate closed symplectic form ω . Using the latter, we can associate to functions f on the phase space a vector field X_f , known as the “*Hamiltonian vector field*” of f , as follows

$$i_{X_f} \omega \equiv \omega(X_f, \cdot) = -df, \quad (6.5)$$

where i_{X_f} stands for a contraction of ω by X_f . Due to closure of ω , X_f generates a flow on M that preserves ω i.e. $\mathcal{L}_{X_f} \omega = 0$, where \mathcal{L}_X is the Lie derivative along the vector X . The symplectic form ω provides a skew-symmetric pairing between functions in M through (6.5) given by

$$\{f, g\} = \omega(X_f, X_g). \quad (6.6)$$

This is the acclaimed Poisson bracket. The laws of classical physics read

$$\frac{df}{dt} = \{\mathcal{H}, f\} = X_{\mathcal{H}} f, \quad (6.7)$$

where \mathcal{H} is the Hamiltonian. One last important identity that will play a key role in the following is that it can be proven easily that

$$[X_f, X_g] = X_{\{f, g\}}, \quad (6.8)$$

where $[\cdot, \cdot]$ is the Lie bracket.

Let us close this section by specifying what we mean by quantization, see e.g [89, 86]. In such a process, we are looking for a map \mathcal{Q} from real functions f in $C^\infty(M)$ to self-adjoint operators $\mathcal{Q}(f)$ that satisfy:

C1. \mathbb{R} -linearity: $\forall r \in \mathbb{R}, \forall f, g \in C^\infty(M); \quad \mathcal{Q}(r f + g) = r \mathcal{Q}(f) + \mathcal{Q}(g).$

- C2. The constant function is mapped to the identity operator.
- C3. The operator $\mathcal{Q}(f)$ is self adjoint if f is real.
- C4. The quantum condition: $[\mathcal{Q}(f), \mathcal{Q}(g)] = -i \hbar \mathcal{Q}(\{f, g\})$
- C5. $\{\mathcal{Q}(f_1), \dots, \mathcal{Q}(f_n)\}$ is a complete set of operators if $\{f_1, \dots, f_n\}$ is a complete set of observables

It turns out that we cannot satisfy the last two conditions (C4.) and (C5.) for all functions f_i at the same time, see e.g. [89, 86]. To get out from this unfortunate situation, we should look for a weak version of one of these two conditions (or both).

Two widely known approaches to remedy such a conflict are *deformation* and *geometric quantization*. The first one tries to modify (C4.) above by higher order terms in \hbar keeping the last requirement, while the second approach –of interest to us– weakens the last condition (C5.) by requiring (C4.) to hold for a restricted class of functions. In the following, we are going to skim over the main steps of geometric quantization leaving details to the literature, see for example [89, 86] and references there in. Our aim is to reach a point where we can count, or even give explicit expressions of quantum states.

PREQUANTIZATION

An important observation that will ignite the whole geometric quantization machinery is the similarity between (6.8) and the quantum condition (C4). This suggests to associate to the observable f the differential operator, $-i \hbar X_f$, in the quantum theory. However, this turns out to fail the test of (C2.), as any constant function is mapped to the zero vector field (not identity operator). Some logical simple modifications of our first proposal, keeping in mind conditions (C1–C4), leads to the following “*prequantum*” assignment to a classical observable f

$$f \longrightarrow \mathcal{PQ}(f) = -i \hbar \mathcal{D}(X_f) + f , \quad (6.9)$$

where \mathcal{D} can be seen as some sort of a covariant derivative which reads for a local trivialization of $\omega = d\theta$

$$\mathcal{D} = d - \frac{i}{\hbar} \theta . \quad (6.10)$$

We should stress here that the prequantum assignment (6.9) does not work for all functions f . For a discussion on this point see e.g. [89, 86] and references therein. We will turn to this issue after introducing the notion of “*polarization*” below. For now, we proceed with our exposition keeping in mind this issue. Putting the assignment (6.9, 6.10) in the appropriate mathematical language brings us to the following definition of the prequantization [89].

A **prequantization** of a symplectic manifold (M, ω) is a pair $(\mathcal{L}, \mathcal{D})$, where \mathcal{L} is a complex Hermitian line bundle over M , and \mathcal{D} is a compatible connection with curvature ω . The “itprequantum Hilbert space” is the completion of the space of square integrable smooth sections of \mathcal{L} with the natural integration measure $\omega^n/(n)!$.

Since line bundles \mathcal{L} are classified by their first Chern class $c_1 \in H^2(M, 2\pi\mathbb{Z})$ which can be represented by the curvature form of any connection on \mathcal{L} , a necessary and sufficient condition for the possibility of prequantization is that $\omega/2\pi$ represents an integral cohomology class.

POLARIZATION

Although our prequantization was natural and cute, our prequantum Hilbert space is too large. This is because our declared states are square integrable functions on the whole phase space which is in clear contradiction with the uncertainty principle. This comes about because such freedom in constructing functions allows us to cook up very localized ones. As a result, we need a way to half our phase space. Such a procedure is called choosing a *polarization*. A way of doing this is to choose a n -dimensional sub-bundle P of the complexified tangent bundle $T_c M$ of M and pick states ψ that are *covariantly* constant.

$$\forall X \in P : \quad \mathcal{D}(X)\psi = 0 . \quad (6.11)$$

This cannot be done in general. Actually, such a condition requires, using that $[\mathcal{D}(X), \mathcal{D}(Y)]\psi = 0$, that P is integrable and Lagrangian i.e.

$$\forall X, Y \in P ; \quad [X, Y] \in P \quad \text{and} \quad \omega(X, Y) = 0 . \quad (6.12)$$

In our case of interest where the phase space is a Kähler manifolds (see section D.1), there is a natural polarization called the “Kähler polarization”. One starts by choosing complex coordinates such that ω is the Kähler form (D.5), locally

$$\omega = i\partial\bar{\partial}\mathcal{K} , \quad (6.13)$$

where

$$\partial = dz^k \wedge \frac{\partial}{\partial z^k} , \quad \bar{\partial} = d\bar{z}^{\bar{k}} \wedge \frac{\partial}{\partial \bar{z}^{\bar{k}}} ,$$

and z^k are complex coordinates. Equation (6.13) allows us to choose $\theta = i\bar{\partial}\mathcal{K}$ or $\theta = -i\partial\mathcal{K}$. We are ready to define our polarization:

The “**holomorphic**” (Kähler) polarization P is spanned by the vectors $\partial/\partial z^k$. Using the choice $\theta = -i\partial\mathcal{K}$, which vanishes on P , reduces the condition (6.11) to just holomorphicity i.e. $\mathcal{D}|_P = \bar{\partial}$. As a result, in the case of a Kähler manifold it is

natural to require that our states are holomorphic sections. This is the result we are going to use in the following.

Unfortunately, geometric quantization comes with some drawbacks. We will only very briefly discuss one problem which is of relevance to us. For a thorough discussion on other shortcomings of geometric quantization see [86] and references therein. As was mentioned in the second chapter of this thesis, section 2.3, one of the important reasons we decided to perform a quantization of our space of solutions was to check the scales at which quantum effects become important. One way to proceed to find such scales is to evaluate the variance of different semi-classical observables in the resulting Hilbert space, and see when they become large. In such a strategy, we will need, on top of the quantum states, an adequate definition of quantum operators that are associated to these observables. We have already alluded below equation (6.10), and when we defined what we mean by quantization, that geometric quantization procedure, specifically the rule (6.9, 6.10), is not applicable for all classical functions f . It turns out that, in general, it works only for functions that depend linearly on the wrong polarization [89, 86]. For example, in our case of Kähler polarization, the prescription we gave in this section for quantization works for functions of the form $f(z, \bar{z}) = g(z) + \bar{z}h(z)$. For some special classes of phase spaces, like being Kähler which is the case of interest to us, there is an involved prescription to extend the rule (6.9, 6.10) to quadratic functions in \bar{z} i.e. $f(z, \bar{z}) = g(z) + \bar{z}h(z) + \bar{z}^2l(z)$. For more details, the reader should consult [89, 86] and references therein.

What we should take from this section about quantization is that, in the case of phase spaces with symplectic form ω that are Kähler, the geometric quantization approach leads to

- The Hilbert space is the completion of the space of integrable holomorphic section of a line bundle whose first Chern class is ω .
- For linear functions in \bar{z} , the associated quantum operator is given by (6.9, 6.10).

6.2 QUANTIZATION AT WORK

We are ready to start the quantization of our space of solutions defined by (5.40) subject to (5.41). Strictly speaking, our quantization works only for centers that do not carry intrinsic degrees of freedom as it does not see them. However, we can still apply the same procedure of quantization in general, where one can see our approach as quantizing the external degrees of freedom only.

The spaces of solutions we managed to quantize turn out to share the same underlying mathematical features [56, 156], that make them toric Kähler manifolds. These solution spaces, being Kähler, allow us to use geometric quantization techniques developed in the previous section to quantize them. Furthermore, our life is made simpler as mathematician have devised a simple way to construct the needed complex coordinates, and the Kähler potential, in the case of toric Kähler manifolds [157, 158, 159], [160, 161].

A complication that we need to take care of is the inclusion of fermions. These arise because the open string picture [85] requires the addition of fermionic degrees of freedom in order to account for all the BPS states. This is because, in the open string description, the centers are described by $\mathcal{N} = 4$, $d=1$ supersymmetric quiver quantum mechanics (QQM), with the position of each center encoded in the scalars of a vector multiplet, and the latter also includes fermionic components which must be accounted for in any quantization procedure. It turns out that one can summarize the fermionic contribution into a modification of the line bundle whose holomorphic sections are our states. This modification of the line bundle can in turn be encoded in a modification of the integration measure.

In the following, we start by introducing toric Kähler manifolds building up to reach the construction of complex coordinates and the Kähler potential. Then, we will deal with the question of fermionic degrees of freedom. At the end, we combine all the knowledge developed to derive constraints on a set of “integers” n_i that encode the sought after number of states. Some details are left to the appendix E.

6.2.1 BEHIND THE SCENE: TORIC KÄHLER MANIFOLDS

Our starting point in describing our solution spaces was a symplectic point of view. It is however more convenient for geometrical quantization to have a Kähler description, which can always be made in the case of a symplectic toric manifold. The main results in this subsection are the expressions (6.19, 6.20) for the complex coordinates and Kähler potential in terms of the symplectic coordinates on a symplectic toric manifold. Before giving these formulas, we review some of the basics of symplectic toric manifolds and symplectic toric orbifolds.

POLYTOPES

As is customary, we will refer to the convex hull of a finite number of points in \mathbb{R}^n as a *polytope*. The boundary of such a polytope is itself the union of various lower dimensional polytopes that are called *faces*. In particular, a zero-dimensional face

is called a *vertex*, a one-dimensional face an *edge*, and a $(n - 1)$ -dimensional face a *facet*. Note that we can view any polytope as the intersection of a number of affine half spaces in \mathbb{R}^n . A polytope P can thus be uniquely characterized by a set of inequalities, namely $\vec{x} \in P$ if and only if $\forall a = 1, \dots, m$

$$\langle \vec{c}_a, \vec{x} \rangle \geq \lambda_a \Leftrightarrow \sum_j c_{ai} x_i \geq \lambda_a , \quad (6.14)$$

where m is the number of facets. It is clear that $m \geq n + 1$ otherwise we will not have a compact polytope. Given a polytope we will call the set $\vec{c}_a \in \mathbb{Z}^n$, given by the inward pointing normals to the various facets, the *normal fan*.

An n -dimensional polytope is called a “*Delzant polytope*” if it satisfies the following three conditions

- **simplicity:** In each vertex exactly n edges meet,
- **rationality:** Each of the n edges that meet at the vertex p is of the form $p + tu_i$, with $t \in \mathbb{R}^+$, and $u_i \in \mathbb{Z}^n$,
- **smoothness:** For each vertex the u_i form a \mathbb{Z} -basis of \mathbb{Z}^n .

The polytope is called “*rational*” instead of Delzant if we replace, in the third condition, the requirement of a \mathbb{Z} -basis by that of a \mathbb{Q} -basis.

SYMPLECTIC TORIC MANIFOLDS

Before giving the precise technical definition of a symplectic toric manifold, let us first sketch the idea. Roughly speaking, a toric manifold is a \mathbb{T}^n fibration over a given n -dimensional polytope, such that at each facet a single $U(1)$ inside the \mathbb{T}^n shrinks to zero size. On the intersections of the different facets multiple $U(1)$ ’s collapse, e.g. at the vertices all circles have shrunk. On the interior of the polytope the toric manifold is simply of the form $P^\circ \times \mathbb{T}^n$, and the full toric manifold is a compactification of this space. On the interior there is, thus, a standard set of coordinates of the form (x_i, θ_i) , with $x_i \in P^\circ$, and $\theta_i \in \mathbb{T}$, and the manifold comes with a standard symplectic form

$$\omega = \sum_i dx_i \wedge d\theta_i . \quad (6.15)$$

It is of course rather non-trivial that this manifold can be smoothly compactified, but when the polytope is Delzant, it is the case. Let us now state the above ideas more precisely.

A *symplectic toric manifold* is a compact connected $2n$ -dimensional symplectic manifold (M, ω) , that allows an effective Hamiltonian action of an n -dimensional torus

\mathbb{T}^n . Remember that, the action of a Lie group on a symplectic manifold is called Hamiltonian if there exists a *moment map* μ , from the manifold to the dual Lie algebra, that satisfies

$$d\langle \mu(p), X \rangle = \omega(\cdot, \tilde{X}) , \quad (6.16)$$

with $p \in M$, X is a generator of the Lie algebra, and \tilde{X} is the corresponding vectorfield. Furthermore, the moment map should be equivariant with respect to the group action, i.e. $\mu(g(p)) = \text{Ad}_g^* \circ \mu(p)$, with Ad^* the coadjoint representation.

By a theorem of Delzant [162], every symplectic toric manifold is uniquely characterized by a Delzant polytope. Given a symplectic toric manifold the corresponding polytope is given by the image of the moment map. To conversely reconstruct the manifold from the polytope is slightly more involved and relies on the technique of symplectic reduction, we refer readers interested in further details to e.g. [157]. Note that the normal fan of the polytope is identical to the *fan* that is used to characterize toric varieties in algebraic geometry, see e.g. [163] for a nice introduction. This can be useful to identify a symplectic manifold given by a polytope, and furthermore, provides an embedding in projective spaces.

TORIC KÄHLER MANIFOLDS

What will be of use to us is that Delzant's construction also associates a set of canonical complex coordinates to every symplectic toric manifold, effectively implying that every closed symplectic toric manifold is actually a Kähler manifold. As the states that we will count are holomorphic sections, we will describe now the construction of a natural set of complex coordinates, be it without proofs or motivation. Those can be found in references [158, 159].

As mentioned above (6.14), any polytope P is characterized by a set of inequalities. Given this combinatorial data of the polytope, one can define the associated functions

$$l_a(x) = \sum_i c_{ai} x_i - \lambda_a , \quad l_\infty = \sum_{i,a} c_{ai} x_i , \quad (6.17)$$

which are everywhere positive on P . Using these functions one can define a 'potential' as follows

$$g(x) = \frac{1}{2} \sum_a l_a(x) \log l_a(x) . \quad (6.18)$$

In case the polytope is Delzant, it is shown in [158] that this potential can be used to define good complex coordinates on the toric manifold as follows

$$z_i = \exp \left(\frac{\partial}{\partial x_i} g(x) + i\theta_i \right) . \quad (6.19)$$

Furthermore, a Kähler potential for the corresponding Kähler metric $\omega(\cdot, J\cdot)$ is given by

$$\mathcal{K} = \sum_a \lambda_a \log l_a(x) + l_\infty. \quad (6.20)$$

It follows from the construction of [158, 159] that \mathcal{K} is the Legendre transform of g , i.e. $\mathcal{K}(z) = \frac{\partial g}{\partial x}x - g(x)$. This can be used to derive that

$$(\det \partial_i \partial_{\bar{j}} \mathcal{K})^{-1} = \exp \left(2 \sum_i \frac{\partial g}{\partial x_i} \right) \det \frac{\partial^2 g}{\partial x_i \partial x_j}, \quad (6.21)$$

which will be a useful formula later when we discuss the inclusion of fermions.

TORIC ORBIFOLDS

As we will also consider quotients of symplectic toric manifolds by a permutation group in this chapter, it will be necessary to introduce the generalization of the above construction of complex coordinates to that of symplectic toric orbifolds. This is because, modding out a manifold by the action of a permutation group leads to a space that belongs to a class of spaces called “orbifolds”. As in the manifold case, a *symplectic toric orbifold* is a $2n$ -dimensional symplectic orbifold that allows a Hamiltonian \mathbb{T}^n action. As was shown in [160], such symplectic toric orbifolds are in one to one correspondence to labeled rational polytopes. Such a labeled rational polytope is nothing but a rational polytope with a natural number attached to each facet. The label m_a denotes that the a ’th facet is a \mathbb{Z}_{m_a} singularity. Again, the explicit construction of the toric orbifold from the labeled polytope is rather involved and we refer those who are interested to [160]. The labeled polytope corresponding to the quotient of a symplectic toric manifold by a group respecting the torus action, is however easy to find. It is given by the quotient of the original polytope, where we attach a label m to each facet that is a \mathbb{Z}_m fixed point under the group action.

Given a labeled rational polytope, one can construct complex coordinates on the toric orbifold in a way similar to the manifold case. The functions l_a from (6.17) are generalized to [160, 161]

$$l_a(x) = m_a \left(\sum_i c_{ai} x_i - \lambda_a \right), \quad l_\infty = \sum_{i,a} m_a c_{ai} x_i, \quad (6.22)$$

where m_a is the label attached to the facet orthogonal to the vector \vec{c}_a . The construction of the complex coordinates and the kähler potential from these functions then carries on analogously to (6.19,6.20). Notice that one can recover the previous case (no orbifolding) by setting $m_a = 1; \forall a$. In order to keep the discussion as general as possible, we will be using the toric orbifold formulas in the following.

6.2.2 INVITING FERMIONS TO THE PARTY

Naively, our phase space is given by the coordinates, \vec{x}_p , subject to the constraint (5.41), which parametrize the space of purely bosonic BPS solutions. But we know from the open string picture that this is not quite true, as we need to include fermions in order to account of all BPS states [85]. Since we expect to see the same number of BPS states in both the open and closed descriptions, and since the bosonic phase spaces in both cases match exactly (and the symplectic forms agree in view of the non-renormalization theorem discussed above), we may ask what the closed string analog of the fermions in the QM is?

Consider our phase space: the coordinates, \vec{x}_p , subject to the constraint (5.41), parametrize the space of purely bosonic BPS solutions but, for each such solution, we may still be able to excite fermions if doing so is allowed by the equations of motion. If we consider only infinitesimal fermionic perturbations of the bosonic solutions, then the former will always appear linearly in the equations of motion, acted on by a (twisted) Dirac operator. Thus fermions which are zero modes of this operator may be excited without altering the bosonic parts of the solution (to first order).

Determining the actual structure of these zero modes is quite non-trivial. A natural guess is that the bosonic coordinates of the centers must be augmented by fermionic partners (making the solution space a superspace), as is argued in [164, 165] where there is no potential. The fact that the bosonic coordinates are constrained by a potential complicates the problem in our case, so we will simply posit the simplest and most natural guess and justify it, *a posteriori*, by reproducing the right degeneracy as expected based on the split attractor conjecture [30].

Thus, we will posit that the full solution space is actually the total space of the spin bundle over the Kähler phase space. The correct phase space densities are now harmonic spinors on the original phase space [166]. Recall (see e.g. [167]) that on a Kähler manifold \mathcal{M} there is a canonical Spin^c structure where the spinors take values in $\Lambda^{0,*}(\mathcal{M})$. To define a spin structure, we need to take a square root of the canonical bundle $K = \Lambda^{N,0}(\mathcal{M})$ and twist $\Lambda^{0,*}(\mathcal{M})$ by that. We also need to remember that the bosonic part of the wave functions were sections of a line bundle, \mathcal{L} . Thus altogether, the spinors on the solution space are given by sections of

$$\mathcal{L} \otimes \Lambda^{0,*}(\mathcal{M}) \otimes K^{1/2}. \quad (6.23)$$

The Dirac operator is given by

$$D = \bar{\partial} + \bar{\partial}^*, \quad (6.24)$$

and we have to look for zero modes of this Dirac operator. These are precisely the harmonic spinors on \mathcal{M} , and therefore, the BPS states correspond to $H^{(0,*)}(\mathcal{M}, \mathcal{L} \otimes$

$K^{1/2}$). By the Kodaira vanishing theorem [168], $H^{(0,n)}(\mathcal{M}, \mathcal{L} \otimes K^{1/2})$ vanishes unless $n = 0$. This is true provided \mathcal{L} is “very ample”, which means in our case that we should be working with large quantum numbers $\langle \Gamma_a, \Gamma_b \rangle$. Thus, finally, the BPS states are given by the global holomorphic sections of $\mathcal{L} \otimes K^{1/2}$.

To find the number of BPS states following the geometric quantization approach, we have to make sure that in the innerproduct we use the norm appropriate for $\mathcal{L} \otimes K^{1/2}$ which is

$$\text{measure} \sim e^{-\mathcal{K}} (\det \partial_i \partial_{\bar{j}} \mathcal{K})^{-1/2} \omega^n, \quad (6.25)$$

where ω is the symplectic form (6.3) on the solution space, and n is the dimension of the polytope (half the dimension of the solution space). The modification of the natural measure, $\omega^n/n!$, used in the definition of the norm when we discussed the prequantum Hilbert space (subsection 6.1.2) comes about because we are integrating over sections of a non-trivial line bundle. The extra terms encode the transformation rules of the sections. For toric Kähler manifolds we find, after some manipulations using (6.20), (6.18), (6.22), (6.21) and (E.1), that

$$\text{measure} \sim \prod_{a=1}^m l_a^{(\sum_{i=1}^n m_a c_{ai} - 1)/2 - m_a \lambda_a}, \quad (6.26)$$

where \sim stands for equality up to an overall smooth non-vanishing term. This is because, as we will see later, the number of “normalizable” sections is controlled by the singularity structure and the zeros of (6.25).

6.2.3 TREASURE HUNT: DEGENERACY

We collected all the needed mathematical background to address the question of counting “BPS”-states. Remember that, according to geometric quantization, we should be looking for holomorphic sections that are normalizable with respect to the measure (6.25, 6.26). A basis of such sections is given by $\{\prod_i z_i^{n_i}\}$, where z_i are complex coordinates given in our case by (6.19) and n_i , are either integers or half-integers depending on the form of the integrand in (6.27) below. Essentially, one wants the integrand to be free of branch cuts due to possible square roots that can appear as a result of $\sqrt{\det \partial_i \partial_{\bar{j}} \mathcal{K}}$. The number of states will be given by the number of possibilities to choose $\{n_i\}$ so that the integral

$$\mathcal{N}_{n_i} \sim \int e^{-\mathcal{K}} \sqrt{\det \partial_i \partial_{\bar{j}} \mathcal{K}} \prod_i |z_i|^{2n_i} \omega^n, \quad (6.27)$$

converges. To proceed further we notice that:

- Since our solution space is toric, one can integrate the $U(1)$ fibers trivially.

- The solution spaces we will quantize will either be compact or can be compactified by adding a harmless boundary. The latter happens in the case of scaling solutions or at walls of threshold stability (section 6.3.2). As a result, divergence of the integral (6.27) can only occur when the integrand becomes singular in the domain of integration.
- It is easy to see that the term ω^n does neither vanish nor diverge in the domain of integration using its simple form given by (6.15).

These observations allow us to conclude that the integral (6.27) is convergent as far as its integrand without ω^n is free from singularities. Using now the formulas (6.26), (6.19), (6.18) and (6.22), the potential problematic part in the integrand of (6.27) reads

$$\prod_{a=1}^m l_a^{\sum_{i=1}^n (n_i + 1/2) m_a c_{ai} - (m_a \lambda_a + 1/2)} . \quad (6.28)$$

It is clear from this expression that the absence of singularities translates to the requirement that the set of (half-)integers $\{n_i\}$ should be chosen such that

$$\sum_{i=1}^n (n_i + 1/2) m_a c_{ai} - (m_a \lambda_a + 1/2) > -1 . \quad (6.29)$$

The degeneracy then will be given by the number of all possible ways to choose $\{n_i\}$ such that (6.29) is satisfied.

So our main task in the following is to calculate the symplectic form ω given by (6.3), then construct the polytope associated to the solution space. This can be achieved by choosing appropriate coordinates such that ω takes the form $\omega = \sum_i dx_i \wedge d\theta_i$, where θ_i are the U(1) fiber directions. Finally, we use the formula (6.29) to figure out the number of states.

6.3 SIMPLE BOUND BLACK HOLE SYSTEMS

In this section, we start by “quantizing” the simplest systems possible; the two and three-center solutions. It turns out that these spaces of solutions are toric Kähler manifolds which allow us to use the techniques developed in the previous section. We will be explicit about the different steps of quantization in these two examples to illustrate the general framework discussed in the previous section.

6.3.1 THE TWO-CENTER CASE

The two-center case is easy to describe. There is only a regular boundstate for $\langle \Gamma_1, \Gamma_2 \rangle \neq 0$ and $\langle h, \Gamma_p \rangle \neq 0$, and the constraint equations immediately tell us that x_{12} is fixed and given by

$$x_{12} = \frac{\langle h, \Gamma_1 \rangle}{\langle \Gamma_1, \Gamma_2 \rangle}. \quad (6.30)$$

In other words, $\vec{x}_1 - \vec{x}_2$ is a vector of fixed length but its direction is not constrained. The solution space is simply the two-sphere, and the symplectic form is proportional to the standard volume form on the two-sphere. In terms of standard spherical coordinates it is given by

$$\omega = \frac{1}{2} \langle \Gamma_1, \Gamma_2 \rangle \sin \theta \, d\theta \wedge d\phi \sim j \sin \theta \, d\theta \wedge d\phi = -d(j \cos \theta) \wedge d\phi, \quad (6.31)$$

where $j = |J|$. Comparing this expression with (6.15) suggests to choose $x = j \cos \theta$, which clearly satisfies $-j \leq x \leq j$. As a result, our solution space S^2 is a toric Kähler manifold with the associated polytope given by

$$j - x \geq 0, \quad j + x \geq 0. \quad (6.32)$$

Let us proceed with the quantization of the two-center solution space. We start with the construction of the complex variable z using the general formula (6.19). We get in this case

$$z^2 = \frac{1 + \cos \theta}{1 - \cos \theta} e^{2i\phi}. \quad (6.33)$$

Next, the Kähler potential corresponding to ω can be shown to be

$$\mathcal{K} = -2j \log(\sin \theta) = -j \log\left(\frac{z\bar{z}}{(1+z\bar{z})^2}\right). \quad (6.34)$$

The holomorphic coordinate z represents a section of the line-bundle \mathcal{L} (over S^2 , the solution space) whose first Chern class equals $\omega/(2\pi)$. The Hilbert space consists of normalizable holomorphic sections of this line bundle, and a basis of these is given by $\psi_m(z) = z^m$. Taking fermions into account (section 6.2.2), the norm of ψ_m is

$$|\psi_m|^2 \sim \int d\text{vol} e^{-\mathcal{K}} \sqrt{\det \partial_i \partial_j \mathcal{K}} |\psi_m(z)|^2, \quad (6.35)$$

where $d\text{vol}$ is the volume form induced by the symplectic form. In our case, we therefore find

$$|\psi_m|^2 \sim \int d\cos \theta \, d\phi (1 + \cos \theta)^{|J|-1+m} (1 - \cos \theta)^{|J|-m}, \quad (6.36)$$

and clearly ψ_m only has a finite norm if: $-|J| \leq m < |J|$. The total number of states equals $2|J|$, which is in agreement with the wall-crossing formula [30] (see also section 5.4.2). This result is the same as (6.29) applied to this case of two-center solution.

6.3.2 THE THREE-CENTER CASE

The three-center case is the next non-trivial solution space. Already at this level some new physics emerge. This is the possibility to have “*scaling*” solutions, which play a distinguished role in trying to construct the geometries of black hole states. These scaling solutions correspond to the case where it is possible for the centers to be arbitrarily close to each other. This section contains three parts. We start by a description of the three-center solution space, some details are left to appendix F. Then, the quantization procedure is described. At the end, a comparison with wall crossing formula [30] will be discussed.

DESCRIBING THE SOLUTION

The three-center solution space is four dimensional. Placing one center at the origin (fixing the translational degrees of freedom) leaves six coordinate degrees of freedom, but, these are constrained by two equations. This leaves four degrees of freedom, of which three correspond to rotations in $SO(3)$ and one of which is related to the separation of the centers.

The constraint equations take the form

$$\frac{a}{u} - \frac{b}{v} = \frac{\Gamma_{12}}{r_{12}} - \frac{\Gamma_{31}}{r_{31}} = \langle h, \Gamma_1 \rangle =: \alpha, \quad (6.37)$$

$$\frac{b}{v} - \frac{c}{w} = \frac{\Gamma_{31}}{r_{31}} - \frac{\Gamma_{23}}{r_{23}} = \langle h, \Gamma_3 \rangle =: -\beta, \quad (6.38)$$

in a self-evident notation. The nature of the solution space simplifies considerably if either α or β vanish, so let us first consider this case. If both vanish, there is an overall scaling degree of freedom and the centers are unbound. This corresponds to a degenerate symplectic form, and is thus, not amenable to quantization using the methods described in this chapter. We have already argued that most likely quantizing these solutions by adding velocities will probably not lead to BPS states (see section 6.1.1 for more details).

For definiteness, we will take $\alpha = 0$; in this case $\sum_p \langle h, \Gamma_p \rangle = 0$ which implies $\langle h, \Gamma_2 \rangle = \beta$. Thus from (5.42) we find

$$\vec{J} = \frac{\beta}{2} r_{23} \hat{z}, \quad (6.39)$$

with \hat{z} defined to be parallel to $\vec{x}_2 - \vec{x}_3$.

The solution has an angular momentum vector \vec{J} directed between the centers 2 and 3, and the direction of this vector defines an S^2 in the phase space which we

will coordinatize using θ and ϕ . The third center is free to rotate around the axis defined by this vector (since this does not change any of the inter-center distances) providing an additional $U(1)$, which we will coordinatize by an angle σ , fibred non-trivially over the S^2 . Finally, the angular momentum has a length, which may be bounded from both below and above, and this provides the final coordinate in the phase space, $j = |\vec{J}|$. This construction is perhaps not the most obvious one from a spacetime perspective but, as we will see, in these coordinates the symplectic form takes a simple and convenient form. When $\alpha = 0$ it is clear from (6.39) that j is a good coordinate on the solution space but, this is not immediately obvious for the more complicated case of $\alpha \neq 0$. This is nonetheless true and, as shown in appendix F, this is always a good coordinatization of the three center solution space (though for $\alpha \neq 0$ the relation between $(j, \sigma, \theta, \phi)$ and the coordinates \vec{x}_p is not as straightforward).

Before quantizing these solution spaces, let us first spend some time describing some physically important special cases of them: the so called “*scaling solutions*” and “*solutions at walls of marginal stability*”.

SCALING SOLUTIONS

As noted in [169] and [30], for certain choices of charges it is possible to have points in the solution space where the centers approach each other arbitrarily closely. Moreover, this occurs for any choice of moduli so it is, in fact, a property of the charges alone. As a consequence, it is not clear how to understand them in the context of attractor flows; the techniques we develop in this chapter provide an alternative method to quantize these solutions that applies even when the attractor tree does not allow us to determine the number of states.

Such solutions occur as follows. We take the leading behavior of inter-center distances to be $r_{ab} \sim \lambda \Gamma_{ab}$ for $\lambda \ll 1$. Clearly, this is only possible if there exists an ordering of the a, b indices such that $\Gamma_{ab} > 0$, and if the positive Γ_{ab} satisfy the triangle inequality. In general it is not clear if the solution exists once higher order terms in λ are included. However, a detailed analysis of the three-center case in appendix F shows that this is true.

We will in general refer to such solutions as *scaling solutions* meaning, in particular, supergravity solutions corresponding to $\lambda \sim 0$. The space of supergravity solutions continuously connected (by varying the \vec{x}_p continuously) to such solutions will be referred to as *scaling solution spaces*. We will, however, occasionally lapse and use the term scaling solution to refer to the entire solution space connected to a scaling solution. We hope the reader will be able to determine, from the context, whether a specific supergravity solution or an entire solution space is intended.

These scaling solutions are interesting because (a) they exist for all values of the moduli; (b) the coordinate distances between the centers go to zero; and (c) an infinite throat forms as the scale factor in the metric blows up as λ^{-2} . Combining (b) and (c) we see that, although the centers naively collapse on top of each other, the actual metric distance between them remains finite in the $\lambda \rightarrow 0$ limit. In this limit, an infinite throat develops looking much like the throat of a single center black hole with the same charge as the total charge of all the centers. Moreover, as this configuration exists at any value of the moduli, it looks a lot more like a single centered black hole (when the latter exists) than generic non-scaling solutions which do not exist for all the values of the moduli at infinity (see section 5.4). On the intuitive level, one can understand such distinction as follows. For non-scaling solutions, there is a minimum inter-center distance which, in principle, allows us to distinguish the different centers as we approach them. On the other hand, for the scaling solutions the centers disappear into the deep throat which makes it harder and harder to distinguish them from a single center black hole.

Unlike the throat of a normal single center black hole the bottom of the scaling throat has non-trivial structure. If the charges, Γ_a , do not carry intrinsic entropy (e.g. D6's with Abelian flux) then the five-dimensional uplifts of these solutions will yield smooth solutions in some duality frame and the throat will not end in a horizon but will be everywhere smooth, even at the bottom of the throat. Outside the throat, however, such solutions are essentially indistinguishable from single center black holes. Thus, such solutions have been argued to be ideal candidate black hole states geometries corresponding to single center black holes.

BARELY BOUND CENTERS

For certain values of charges and moduli it is possible for some centers to move off to infinity. Although this would normally signal the decay of any associated states (as happens, for instance, for two centers at a wall of marginal stability [122]) one can argue that this is not always the case [56]. In particular, it is important to distinguish between cases when centers are forced to infinity (marginal stability) versus those where there is simply an infinite (flat) direction in the solution space (threshold stability; see [64, Appendix B]). Although the first case clearly signals the decay of a state, in the second case, when centers move off to infinity along one direction of the solution space but may also stay within a finite distance in other regions of the solution space, it is still possible to have bound states. Quite essential to this argument is the fact that in some cases, although the solution space may seem naively non-compact (in the standard metric on \mathbb{R}^{2N-2}), its symplectic volume is actually finite and it admits normalizable wave-functions whose expectation values can be argued to be finite [56, section 7]. There are also cases with unbound centers

where the symplectic form on the solution space is degenerate and, in such cases, it is not clear if there is a bound state. See section 6.1.1 for a thorough discussion on this point.

QUANTIZATION

Following the discussion above (see also appendix F), we parametrize the three-center solution space by the coordinates j, σ, θ and ϕ . However, for the purpose of deriving the symplectic form, it turns out to be more convenient to work momentarily with the variables J^i and σ , where σ represents an angular coordinate for rotations around the \mathbf{J} -axis. Obviously, σ does not correspond to a globally well-defined coordinate, but rather should be viewed as a local coordinate on an S^1 -bundle over the space of allowed angular momenta. Ignoring this fact for now, the rotation $\delta x_p^i = \epsilon^{iab} n^a x_p^b$ that we used in (6.4) corresponds to the vector field

$$X_n = \frac{n^i J^i}{|J|} \frac{\partial}{\partial \sigma} + \epsilon^{ijk} n^j J^k \frac{\partial}{\partial J^i} . \quad (6.40)$$

The second term is obvious, as \mathbf{J} is rotated in the same way as the \mathbf{x}_p . The first term merely states that there is also a rotation around the \mathbf{J} -axis given by the component of n in the \mathbf{J} -direction. The final result in (6.4) therefore states that

$$\omega(X_n, m^i \frac{\partial}{\partial J^i}) = n^i m^i , \quad \omega(X_n, \frac{\partial}{\partial \sigma}) = 0 . \quad (6.41)$$

It is now easy to determine that

$$\omega(\frac{\partial}{\partial J^i}, \frac{\partial}{\partial J^j}) = \epsilon_{ijk} \frac{J^k}{|J|^2} , \quad \omega(\frac{\partial}{\partial J^i}, \frac{\partial}{\partial \sigma}) = -\frac{J^i}{|J|} . \quad (6.42)$$

Denoting $|\vec{J}|$ as j , and parametrizing J^i in terms of j and the standard spherical coordinates θ, ϕ , the symplectic form defined by (6.42) becomes

$$\omega = j \sin \theta \, d\theta \wedge d\phi - dj \wedge d\sigma . \quad (6.43)$$

However, we clearly made a mistake since this two-form is not closed. The mistake was that σ was not a well-defined global coordinate but rather a coordinate on an S^1 -bundle. We can take this into account by including a parallel transport in σ when we change J^i . The result at the end of the day is that the symplectic form is modified to

$$\omega = -d(j \cos \theta) \wedge d\phi - dj \wedge d\sigma . \quad (6.44)$$

This very simple form of the symplectic form explains why it is more natural to work with the coordinates j, σ, θ and ϕ . However, in order to quantize the solution space,

we have to understand what the range of the variables is. Since θ, ϕ are standard spherical coordinates on S^2 , ϕ is a good coordinate but degenerates at $\theta = 0, \pi$. The magnitude of the angular momentum vector j is bounded as can be seen from (F.2). By carefully examining the various possibilities in the three-center case (see appendix F), one finds that generically j takes values in an interval $j \in [j_-, j_+]$, where $j = j_-$ or $j = j_+$ only if the three centers lie on a straight line. An exceptional case is if $j_- = 0$, implying that the three centers can sit arbitrarily close to each other as seen in appendix F. Note that this latter case corresponds exactly to the scaling solutions described above.

As we mentioned before, at $j = j_-$ and $j = j_+$ the centers align, and rotations around the J -axis act trivially. In other words, at $j = j_{\pm}$ the circle parametrized by σ degenerates. Actually, we have to be quite careful in determining exactly which $U(1)$ degenerates where. Fortunately, what we have here is a toric Kähler manifold, with the two $U(1)$ actions given by translations in ϕ and σ , and we can use results in the theory of toric Kähler manifolds from section 6.2.1 to describe the quantization of this space. We have to distinguish two cases: $j_- = 0$ which corresponds to a scaling point inside the solution space, and $j_- > 0$ where the scaling point is absent.

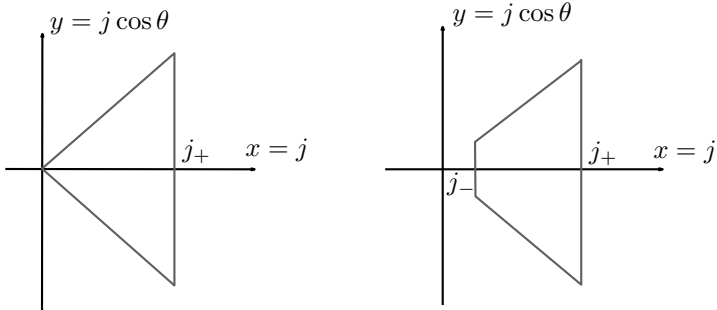


Figure 6.1: (Left) The polytope for $j_- = 0$. (Right) The polytope for $j_- > 0$.

The Non Scaling Case We start by defining $x = j$, and $y = j \cos \theta$, to be two coordinates on the plane. Then the ranges of the variables x and y are given by

$$x - j_- \geq 0, \quad j_+ - x \geq 0, \quad x - y \geq 0, \quad x + y \geq 0. \quad (6.45)$$

Together, these four inequalities define a Delzant polytope in \mathbb{R}^2 which completely specifies the toric manifold (see section 6.2.1). At the edges a $U(1)$ degenerates, at the vertices both $U(1)$'s degenerate. The geometry and quantization of the solution space can be done purely in terms of the combinatorial data of the polytope (see figure 6.1). To proceed we assume that all three centers carry different charges; if two centers carry identical charges, one needs to take into account their indistinguishability, quantum mechanically, and take a quotient of the corresponding solution space. We will not consider this possibility in the remainder.

In order to quantize our space of solution, we start by the construction of complex coordinates following (6.19). Up to irrelevant numerical factors, they are given by

$$\begin{aligned} z^2 &= j^2 \sin^2 \theta \frac{j - j_-}{j_+ - j} e^{2i\sigma} \\ w^2 &= \frac{1 + \cos \theta}{1 - \cos \theta} e^{2i\phi} \end{aligned} \quad (6.46)$$

and the Kähler potential ends up being equal to

$$\mathcal{K} = j_- \log(j - j_-) - j_+ \log(j_+ - j) + 2j. \quad (6.47)$$

A basis for the Hilbert space is given by wave functions $\psi_{m,n} = z^m w^n$. To find the range of n, m we look at the norm (6.25)

$$\int e^{-2r} \frac{(j_+ - r)^{j_+ - 1}}{(r - j_-)^{j_-}} \left(r^2 \sin^2 \theta \left(\frac{r - j_-}{j_+ - r} \right) \right)^n \left(\frac{1 + \cos \theta}{1 - \cos \theta} \right)^{m+1/2} r dr d\cos \theta, \quad (6.48)$$

where we disregarded an overall non-vanishing smooth function. This norm is finite if, $j_- \leq n < j_+$, and, $-n \leq m + \frac{1}{2} \leq n$, leading to the following number of states

$$\mathcal{N} = (j_+ - j)(j_+ + j_-). \quad (6.49)$$

which is in agreement with the wall crossing formula as we will show below in section 6.3.3. One can check easily that the same result is obtained using (6.29).

The Scaling Case As was done in the non-scaling case, we must first construct the appropriate polytope for these solutions (see figure 6.1). The only property that differentiates these solution spaces is that $j_- = 0$ (this is the *scaling point*). As a result, the associated polytope differs slightly from the non-scaling one; for instance, the first inequality in (6.45) is redundant. This may seem to be a small modification, but, it actually changes the topology of the solution space as follows. Remember that, for fixed j and σ there is an S^2 that we parametrized by θ and ϕ . Taking the limit from non-scaling to scaling corresponds to the limit $j \rightarrow 0$, which leads to the vanishing of this S^2 .

Using the coordinates $x = j$ and $y = j \cos \theta$ as before, the scaling solution's polytope is defined by

$$j_+ - x \geq 0, \quad x + y \geq 0, \quad x - y \geq 0. \quad (6.50)$$

The construction of the complex coordinates is achieved through the function g (6.18). They turn out to be given by

$$z_1^2 = \frac{j^2 \sin^2 \theta}{j_+ - j} e^{2i\sigma}, \quad z_2^2 = \frac{1 + \cos \theta}{1 - \cos \theta} e^{2i\phi}. \quad (6.51)$$

Note that the complex variable z_1 in this case is not the naive $j_- \rightarrow 0$ limit of the non-scaling complex variable counterpart z given by the first equation in (6.46). The wave functions that belong to the Hilbert space are the ones that have a finite norm (6.27), which in this case reads

$$|\psi_{n,m}|^2 \sim \int e^{-j} (j_+ - x)^{j_+ - 1 - n} j^{2n+1} (1 + \cos \theta)^{n+(m+1/2)} (1 - \cos \theta)^{n-(m+1/2)} dj d\cos \theta. \quad (6.52)$$

Requiring that the norm is finite imposes the following restrictions

$$0 \leq n \leq j_+ - 1, \quad -n \leq m + 1/2 \leq n, \quad (6.53)$$

which can be reproduced using (6.29). So the number of states is given by

$$\mathcal{N} = j_+^2.$$

Unfortunately, we cannot compare this prediction to the result obtained from the wall-crossing formula, because it is not clear how to treat scaling solutions within the framework of the attractor flow conjecture [30]. On the other hand, this proves the usefulness of the tools we developed in this chapter as they provide the only known way to compute the number of BPS states for scaling solutions.

Another important property that is worth mentioning is that the probability density, given by the integrand of (6.52), vanishes at $j = 0$. This suggests that, although classically the coordinate locations of the centers can be arbitrarily close together, quantum mechanically this is not true anymore. The probability that the centers sit on top of each other is zero, which implies that there is a minimum non-vanishing expected inter-center distance. Since the depth of the throat is related to the coordinate distance between the centers, it follows that the throat will be effectively capped off once quantum effects are taken into account [56].

6.3.3 COMPARISON TO THE SPLIT ATTRACTOR FLOW PICTURE

In the previous subsections we computed the number of states corresponding to the position degrees of freedom of a given set of bound black hole centers. The approach

we developed amounts essentially to calculating the appropriate symplectic volume of the solution space. To count the total number of BPS states of a given total charge, one needs to take into account the fact that the different black hole centers may themselves carry internal degrees of freedom and that there may be many multi-center realizations of the same total charge. In the special case, however, when all the centers have no internal degrees of freedom, the only states that one can get are position degrees of freedom. In this case it is interesting to compare the number of states obtained in our approach, using geometric quantization, with the number obtained by considering jumps at walls of marginal stability as in [30] (see also section 5.4.2).

To make this comparison, we use the attractor flow conjecture which states that, to each component of solution space there corresponds a unique attractor flow tree. Given a component of solution space, we can calculate its symplectic volume and hence the number of states. Given the corresponding attractor flow tree, we can calculate the degeneracy using the wall crossing formula of [30] (equation (6.54) below).

As mentioned before, in the two-center case we get a perfect agreement between the two calculations. This is not so surprising because both approaches are, in fact, counting the number of states in an angular momentum multiplet with $j = \frac{1}{2}\langle\Gamma_1, \Gamma_2\rangle - \frac{1}{2}$. Furthermore, there is no ambiguity in specifying the split attractor tree. Things become more interesting in the three-center case where there are now naively three attractor trees for a given set of centers. According to the attractor flow conjecture, only one tree should correspond to any given solution space.

Let us consider the three-center attractor flow tree depicted in figure 5.1. For the given charges, Γ_1 , Γ_2 , and Γ_3 , there are three possible trees, but in terms of determining the relevant number of states, the only thing that matters is the branching order. In figure 5.1 the first branching is into charges Γ_3 and $\Gamma_4 = \Gamma_1 + \Gamma_2$, so the degeneracy associated with this split is $|\langle\Gamma_4, \Gamma_3\rangle|$, and the degeneracy of the second split is $|\langle\Gamma_1, \Gamma_2\rangle|$, giving a total number of states

$$\mathcal{N}_{\text{tree}} = |\Gamma_{12}| |\langle\Gamma_{13} + \Gamma_{23}\rangle|, \quad (6.54)$$

where we have adopted an abbreviated notation, $\Gamma_{ij} = \langle\Gamma_i, \Gamma_j\rangle$.

To compare this with the number of states arising from geometric quantization of the solution space, (6.49), we need to determine j_+ and j_- . As described in Appendix F, j_+ and j_- correspond to two different collinear arrangements of the centers and, in a connected solution space, there can be only two such configurations. To relate this to a given attractor flow tree, we will assume that we can tune the moduli to force the centers into two clusters as dictated by the tree. For the configuration in figure 5.1, for instance, this implies we can move the moduli at infinity close to the first

wall of marginal stability (the horizon dark blue line) which will force Γ_3 very far apart from Γ_1 and Γ_2 . In this regime, it is clear that the only collinear configurations are $\Gamma_1\text{-}\Gamma_2\text{-}\Gamma_3$ and $\Gamma_2\text{-}\Gamma_1\text{-}\Gamma_3$; it is not possible to have Γ_3 in between the other two charges. Since j_+ and j_- always correspond to collinear configurations, they must, up to signs, each be one of

$$j_1 = \frac{1}{2}(\Gamma_{12} + \Gamma_{13} + \Gamma_{23}), \quad (6.55)$$

$$j_2 = \frac{1}{2}(-\Gamma_{12} + \Gamma_{13} + \Gamma_{23}). \quad (6.56)$$

j_+ will correspond to the larger of j_1 and j_2 , and j_- to the smaller but, from the form of (6.49), we see that this does not effect \mathcal{N} as it depends only on $|j_1^2 - J_2^2|$. Thus

$$\mathcal{N} = |(j_1 - j_2)(j_1 + j_2)| = |\Gamma_{12}| |\Gamma_{13} + \Gamma_{23}|, \quad (6.57)$$

which nicely matches (6.54).

Let us make some further remarks on the results derived here. The scaling solutions corresponding to $\lambda \rightarrow 0$ have $j_- = 0$ even if the centers do not align at this point. Therefore, the connection to the wall crossing formula breaks down. The procedure of geometric quantization itself, however, is well defined for these solutions. The curvature scales always stay small allowing us to trust the supergravity solutions. Thus, one can see the resulting degeneracy as a reliable prediction.

6.4 DIPOLE HALOS

Although the three-center case showed various interesting features, however, one would like to find other systems for which the quantization described in section 6.2 is applicable. After all, our main motivation was the study of systems which can be possibly related to black hole states. A first step in this direction would be to find quantizable systems with an exponentially large number of states. Luckily, there is a multi-center solution that, in some regime of charges, can be argued to be close enough to a single centered black hole [116, 117, 118]. These are a special class of what was called “*dipole halo*” solutions in [56]. The latter correspond to a purely fluxed D6- $\overline{\text{D}6}$ pair (hence the name dipole) bound with an arbitrary number of anti-D0’s (which explains the halo appellation). Depending on the sign of the B-field, these D0’s bind to the D6 or anti-D6 respectively. When we take the B-field to be zero at infinity, the system is at the wall of threshold stability and the D0’s are free to move in the equidistant plane between the D6 and anti-D6. This system and its behavior under variations of the asymptotic moduli was studied in detail in appendix B of [64].

These dipole halo systems come in two variations, scaling and non-scaling dipole halos, depending on the regime of their charges. As we will argue later on, the scaling regime corresponds to $j \rightarrow 0$. By maximizing $\cos \theta_a$'s in (6.62) below, it is clear that the scaling behavior can only be present if the total D0 charge N satisfies $N \geq I/2$, where $I = -\langle \Gamma_6 \Gamma_{\bar{6}} \rangle$.

Before discussing the interesting scaling dipole solutions, we first quantize the non-scaling ones. Our aim in studying such solution spaces is twofold. On one hand, it will be a nice opportunity to deal with orbifold toric geometry and check the validity of (6.29). On the other hand, since the solution space does not develop a scaling behavior, we can compare the degeneracy we get to the one expected from the wall crossing formula.

6.4.1 MEET THE DIPOLE HALO

As the number of states will be independent of the asymptotic moduli, as long as we don't cross a wall of marginal stability, we are free to choose them such that the solution space has its simplest form. The symplectic form on the solution space is most easily calculated at the line of threshold stability discussed in the subsection “barely bound centers” of section 6.3.2. In our example, this corresponds to $B|_{\infty} = 0$ [64]. The dipole halo system is comprised of:

- The dipole part: this is a pair of purely fluxed D6 and $\overline{\text{D}6}$ with charges

$$\Gamma_6 = e^{\frac{1}{2} p^A \alpha_A} = \alpha_0 + \frac{1}{2} p^A \alpha_A + \frac{1}{8} D_{ABC} p^A p^B \alpha^C + \frac{1}{48} D_{ABC} p^A p^B p^C, \quad (6.58)$$

$$\Gamma_{\bar{6}} = -e^{-\frac{1}{2} p^A \alpha_A} = -\alpha_0 + \frac{1}{2} p^A \alpha_A - \frac{1}{8} D_{ABC} p^A p^B \alpha^C + \frac{1}{48} D_{ABC} p^A p^B p^C, \quad (6.59)$$

where we used the Harmonic basis $\alpha_{\Lambda}, \alpha^{\Lambda}; \Lambda = 0, 1, \dots, h^{1,1}$ of H^* , the even-cohomology of the Calabi-Yau threefold (see section 5.1.2), and $D_{ABC} = \int_{\text{CY}} \alpha_A \alpha_B \alpha_C$. In the following, we will use the shorthand notation $\Gamma_6 = (1, \frac{p}{2}, \frac{p^2}{8}, \frac{p^3}{48})$, and $\Gamma_{\bar{6}} = (-1, \frac{p}{2}, -\frac{p^2}{8}, \frac{p^3}{48})$ for the purely fluxed D6 and $\overline{\text{D}6}$ charges. It is clear from the choice of the flux of the D6 and $\overline{\text{D}6}$ that, the total D6 charge vanishes whereas the total D4 charge is $p^A; A = 1, \dots, h^{1,1}$. That is the reason behind using dipole in the name of such system.

- The halo part: this corresponds to a set of D0's with charges $\Gamma_a = (0, 0, 0, -q_a)$ with all the q_a positive and $\sum_a q_a = N$. These D0's do not talk to each other, hence the name halo. Their positions are constrained through their interaction with the D6 and $\overline{\text{D}6}$.

The positions of D0's, D6, and $\bar{D6}$ are constrained by (5.41), which reduces in the present case to:

$$-\frac{q_a}{r_{6a}} + \frac{q_a}{r_{\bar{6}a}} = 0, \quad (6.60)$$

$$-\frac{I}{r_{6\bar{6}}} + \sum_a \frac{q_a}{r_{6a}} = -\beta. \quad (6.61)$$

Here $I = -\langle \Gamma_6, \Gamma_{\bar{6}} \rangle = \frac{p^3}{6}$ is given in terms of the total D4-charge p of the system, and $\beta = \langle \Gamma_6, h \rangle$ with $I, \beta > 0$. From the first line we indeed see that the D0's lie in the plane equidistant from the D6 and $\bar{D6}$, as we are at the line of threshold stability, and so we can simply write $r_a := r_{6a} = r_{\bar{6}a}$.

An explicit expression for the symplectic form (6.3) can be obtained using the following coordinate system. We define an orthonormal frame $(\hat{u}, \hat{v}, \hat{w})$ fixed to the D6- $\bar{D6}$ pair, such that the D6- $\bar{D6}$ lie along the w axis and with the D0's lying in the u - v plane. Rotations of the system can then be interpreted as rotations of the $(\hat{u}, \hat{v}, \hat{w})$ frame with respect to a fixed $(\hat{x}, \hat{y}, \hat{z})$ frame. We will parametrize the position of the w axis (D6- $\bar{D6}$ line) by two angles, (θ, ϕ) as shown in figure 6.2. We can furthermore specify the location of the a 'th D0 with respect to D6- $\bar{D6}$ pair by two additional angles, (θ_a, ϕ_a) . The first angle, θ_a , is the one between $\vec{x}_{6\bar{6}}$ and \vec{x}_{6a} , while ϕ_a is a polar angle in the u - v plane (see figure 6.2). Our $2N + 2$ independent coordinates on solution space are thus $\{\theta, \phi, \theta_1, \phi_1, \dots, \theta_N, \phi_N\}$. The angular momentum, $j(\theta_a, \phi_a)$, is a function of the other coordinates rather than an independent coordinate (when $N = 1$, it can be traded for θ_1 as demonstrated in the general three center case), and is given by

$$j = \frac{I}{2} - \sum_a q_a \cos \theta_a. \quad (6.62)$$

Using this explicit coordinatization, it is straightforward though tedious to evaluate the symplectic form (6.3). The result is relatively simple:

$$\omega = -\frac{1}{4}d \left[2j \cos \theta d\phi + 2 \sum_a q_a \cos \theta_a d\sigma_a \right], \quad (6.63)$$

with d denoting the exterior derivative. Note that, as is manifest from our angular coordinatization, we are still in the toric setting with each additional center introducing an additional $U(1)$ coordinate. Note also that, for a single D0 this reduces to (6.44) when θ_1 is traded for j .

In case $N \geq I/2$, it is possible to combine a sufficient number of centers and form a scaling throat. We will restrict ourselves here to the non-scaling case $I/2 > N$, leaving the more interesting scaling regime to the next section.

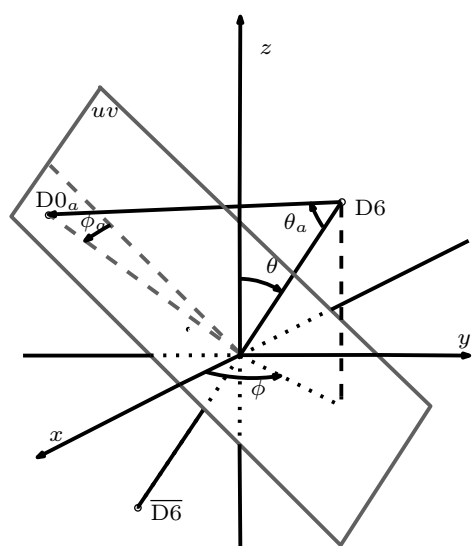


Figure 6.2: The coordinate system used to derive the $D6\overline{D6}$ - N $D0$ symplectic form. The coordinates (θ, ϕ) define the orientation of the \hat{w} -axis with respect to the fixed, reference, $(\hat{x}, \hat{y}, \hat{z})$ axis. The $D6\overline{D6}$ lie along the \hat{w} axis (with the origin between them) and the $D0$'s lie on the $\hat{u}\hat{v}$ plane at an angle ϕ_a from the \hat{u} -axis. The radial position of each $D0$ in the $\hat{u}\hat{v}$ plane is encoded in the angle θ_a (between $\vec{x}_{6\bar{6}}$ and \vec{x}_{6a}).

6.4.2 DEGENERACY USING ATTRACTOR TREE

In the following, we are going to combine the wall-crossing formula and solution space considerations to count the number of states of the dipole halo system. The essential idea in this approach is that, by playing with moduli at infinity we can deform our dipole halo tree $\{\Gamma_2, \{\Gamma_1, N\Gamma_\star\}\}$ to a halo one corresponding to the charge Γ_1 surrounded by n_a centers carrying the charges $a\Gamma_\star$ plus a far away center Γ_2 . The former system $\{\Gamma_1, N\Gamma_\star\}$ will be called a “halo” in the following. In doing so, we reduced our task of counting the BPS states to evaluating the number of states D_N^{halo} coming from the halo part $\{\Gamma_1, N\Gamma_\star\}$. To find this number of states we resort to solution space considerations. By knowing this number, the total degeneracy will be

$$D_N = (\langle \Gamma_2, \Gamma_1 \rangle + N\langle \Gamma_2, \Gamma_\star \rangle) D_N^{\text{halo}}. \quad (6.64)$$

Note that to derive this degeneracy, we use the attractor flow conjecture which only works for non-scaling solutions, so for scaling solutions we will have to resort to other methods. For other values of the moduli, the center Γ_2 will be closer to the halo and deform it. In certain cases, it can even deform so much that the topology of the split changes to $\{\Gamma_1, \{\Gamma_2, N\Gamma_\star\}\}$. Such a change can happen when crossing a wall of threshold stability [64, 30], and in that case the number of states does not change (even though the topology of the tree changes).

The halo configurations are characterized by a split tree of the form $\{\Gamma_1, N\Gamma_\star\}$ with $N = \sum_a q_a n_a$, where n_a is the number of centers of charge $q_a \Gamma_\star$. As all q_a and n_a are positive integers, every halo of total charge $N\Gamma_\star$ thus corresponds to a specific partitioning of N and vice versa. It follows straightforwardly from the constraint equations (5.41) that all the Γ_i centers orbit Γ_1 at the same distance $r_{1i} = l$, given by

$$l = \frac{\langle \Gamma_\star, \Gamma_1 \rangle}{\langle h, \Gamma_\star \rangle}.$$

Note that this radius is independent of the different a_i . Furthermore, all the centers Γ_i can be placed arbitrarily on this sphere surrounding Γ_1 as they do not interact among each other.

So, for a halo configuration of m orbiting centers, the solution space is simply the product of m identical S^2 ’s. When quantizing this system we have to take into account that in case some $a_i = a_j$, the corresponding centers should be treated as indistinguishable particles and we will have to quotient by the appropriate permutation group. As all centers in the Halo are independent, there is a standard way to get the degeneracy. Let us sketch the idea in the simplest case of a halo consisting of N equally charged centers, i.e all $a_i = 1$. Given that the N particles are independent and identical, the Hilbert space for all the particles is nothing but the

(anti-)symmetrized product of the one particle Hilbert space, i.e $\mathcal{H}_N = \mathcal{H}_1^N / S_N$. By the definition of \mathcal{H}_1 , this is the space of sections of \mathcal{L}_1^N / S_N , where \mathcal{L}_1 is the one-particle line bundle. So, we can take the one particle (2-center) solution space and construct a multi-particle wave function on it.

The single particle wave function is a section of a line-bundle \mathcal{L} on S^2 , the position space of the electron. The line bundle \mathcal{L} has Euler number $|\langle \Gamma_1, \Gamma_* \rangle|$. This is because the highest Chern character of a line bundle is the first one. To generalize this to N particles, we have to tensor the bundle N times and (anti-)symmetrize due to indistinguishability. The Euler number of the resulting line bundle then gives the number of sections, i.e. the number of states. It is more convenient to summarize these numbers for different N in terms of a generating function. Such a generating function for Euler numbers of the symmetric product of a line bundle was given in e.g. [170]. The only difference with the discussion there is that, in our case, the line bundles are fermionic in nature. Taking this point into account properly, following e.g. [171], gives the following generating function

$$\sum_N d_N q^N = (1 + q)^{|\langle \Gamma_1, \Gamma_* \rangle|}, \quad (6.65)$$

where d_N stands for the Euler number of the N^{th} symmetric product \mathcal{L}^N / S_N . Newton's binomial expansion yields

$$d_N = \binom{|\langle \Gamma_1, \Gamma_* \rangle|}{N}. \quad (6.66)$$

The fact that the different centers in the halo behave like fermions results in an upper bound of $|\langle \Gamma_1, \Gamma_* \rangle|$ for the number of such centers; this is nothing but Pauli's exclusion principle at work.

The generating function (6.65) can be generalized to include halos given by an arbitrary partition $\{n_a\}$ of N , i.e. $N = \sum_a a n_a$, where n_a is the number of centers carrying the same charge $\Gamma_a = a \Gamma_*$. It is not hard to see that the generating function including such arbitrary partitions is given by

$$\sum_N D_N^{\text{halo}} q^N = \prod_{k>0} (1 + q^k)^{k |\langle \Gamma_1, \Gamma_* \rangle|}, \quad (6.67)$$

where D_N is the degeneracy of all halos with total charge $N \Gamma_*$. The degeneracies can be found by expanding the product:

$$D_N = \sum_P \prod_a \binom{a |\langle \Gamma_1, \Gamma_* \rangle|}{n_a}, \quad (6.68)$$

where the sum is over all possible partitions $P = \{n_a\}$ of N i.e. $N = \sum_a a n_a$. This agrees with the fact that the total degeneracy of a given partition is the product of

the degeneracies of each group of identical terms in the partition. The degeneracies of such a group of identical halo charges was exactly what we calculated in (6.65) to be a binomial coefficient.

We close this subsection by the following remark. The formula (6.67) is similar to (5.6) in [30], but, there are also some obvious differences. The first one comes from the fact that [30] is calculating an index while we are counting the number of states without relative signs. The second difference is that we are neglecting the degeneracies associated to internal degrees of freedom of each individual center.

6.4.3 DEGENERACY USING TORIC TECHNIQUES

In the following, we are going to use the same toric techniques as in the previous sections to calculate the number of states associated to the non-scaling D6- $\overline{\text{D}6}$ -D0 dipole halo, i.e. those for which $N < I/2$. From the associated symplectic form (6.63), one easily reads the toric coordinates to be

$$y = j \cos \theta, \quad x_a = q_a \cos \theta_a \geq 0. \quad (6.69)$$

Because some of the centers can be identical, we need to orbifold our polytope by the appropriate symmetric group. Before treating the configuration given by a generic partitioning $\{q_a\}$ of N i.e. $N = \sum_a n_a q_a$, let us focus on the simple case of n centers carrying the same D0 charge, $-q$, so that $N = q n$. In this case the labelling of the facets (section 6.2.1) turns out to be

- four facets with label 1 given by
 - i) the facet $x_1 = 0$,
 - ii) the facet $x_a = q$,
 - iii) the facet $y = \frac{I}{2} - \sum_a x_a$,
 - iv) the facet $y = -\frac{I}{2} + \sum_a x_a$,
- $(n - 1)$ facets with label 2 given by
 - v) the facets $x_{a+1} - x_a = 0$, for $a = 1, \dots, n - 1$.

Given this labelled polytope, we can then again construct the corresponding complex coordinates following the strategy outlined in section 6.2.1. In this case we have

$$\begin{aligned}
 z_0^2 &\sim \frac{I/2 + y - \sum_a x_a}{I/2 - y - \sum_a x_a} e^{2i\sigma_0}, \\
 z_1^2 &\sim \frac{1}{(I/2 + y - \sum_a x_a)(I/2 - y - \sum_a x_a)} \frac{x_1}{(x_2 - x_1)^2} e^{2i\sigma_1}, \\
 z_n^2 &\sim \frac{1}{(I/2 + y - \sum_a x_a)(I/2 - y - \sum_a x_a)} \frac{(x_n - x_{n-1})^2}{(q - x_n)} e^{2i\sigma_n}, \\
 z_i^2 &\sim \frac{1}{(I/2 + y - \sum_a x_a)(I/2 - y - \sum_a x_a)} \left(\frac{x_i - x_{i-1}}{x_{i+1} - x_i} \right)^2 e^{2i\sigma_i}, \quad i = 2, \dots, n-1.
 \end{aligned} \tag{6.70}$$

The next step is to construct the Kähler potential, which turns out to be equal to

$$\begin{aligned}
 \mathcal{K} = & -\frac{I}{2} \ln \left(\frac{I}{2} + y - \sum_a x_a \right) \left(\frac{I}{2} - y - \sum_a x_a \right) \\
 & -2 \sum_a x_a + x_n - x_1 - q \ln(q - x_n).
 \end{aligned} \tag{6.71}$$

A basis for the Hilbert space is then given by normalizable functions $\psi_m = \prod_{i=0}^n z_i^{m_i}$, where the norm is given by (6.25). In addition, $\det \partial_i \partial_j g$ turns out to be given by

$$\det \partial_i \partial_j g \sim \left(\frac{I}{2} + y - \sum_a x_a \right)^{-1} \left(\frac{I}{2} - y - \sum_a x_a \right)^{-1} (x_1)^{-1} (q - x_n)^{-1} \prod_{a=1}^{n-1} (x_{a+1} - x_a)^{-1}.$$

The study of the normalizability of ψ_m reveals the following constraint on the possible exponents $m = (m_i)$:

$$\begin{aligned}
 0 \leq m_1 < m_2 < \dots < m_n < q, \\
 -\left(\frac{I-1}{2} - \sum_a (m_a + \frac{1}{2})\right) \leq m_0 + \frac{1}{2} \leq \left(\frac{I-1}{2} - \sum_a (m_a + \frac{1}{2})\right),
 \end{aligned} \tag{6.72}$$

where n is the number of D0-centers carrying charge q , in perfect agreement with the restriction of (6.29) to this case. The total number of normalizable states is thus

$$d_{n,q} = \sum_{m=n(n-1)/2}^{(I-n-1)/2} b_m^n(q) [(I-n) - 2m], \tag{6.73}$$

where the coefficient $b_m^n(q)$ is the number of ways to write m as a sum of n strictly ordered positive integers all smaller than q .

Let us now generalize the simple example of n equally charged D0-centers to an arbitrary partition of N . We will label the different groups of equally charged centers by an index a , and the charge of individual centers in this group by q_a (i.e. $q_a \neq q_b$

if and only if $a \neq b$). With n_a we then denote the number of centers with charge q_a so that the total D0-charge N carried by the D0 centers is given by

$$N = \sum_a n_a q_a .$$

Labeling the centers in a given group a by an additional index $i = 1, \dots, n_a$, we can simply generalize the conditions (6.72) by applying them to each group of equally charged centers separately. The conditions on the powers $m^a = (m_i^a)$ then become

$$\begin{aligned} 0 &\leq m_1^a < m_2^a < \dots < m_{n_a}^a < q_a , \\ - \left[\frac{I-1}{2} - \sum_{a,i} (m_i^a + \frac{1}{2}) \right] &\leq m_0 + \frac{1}{2} \leq \left[\frac{I-1}{2} - \sum_{a,i} (m_i^a + \frac{1}{2}) \right] . \end{aligned} \quad (6.74)$$

A first step towards counting all possible states with total charge N in D0-centers is to count the degeneracy for a fixed partitioning of N . The number of solutions to the constraints (6.74) is given by

$$\begin{aligned} d_{\{n_a, q_a\}} &= \sum_{\text{all allowed } m_i^a} \left[I - 2 \sum_{a,i} \left(m_i^a + \frac{1}{2} \right) \right] \\ &= I \prod_a \binom{q_a}{n_a} - 2 \sum_{\text{all allowed } m_i^a} \sum_{i,a} \left(m_i^a + \frac{1}{2} \right) . \end{aligned} \quad (6.75)$$

We can calculate the sum of the last terms by introducing the quantities

$$l_i^a = q_a - 1 - m_{n_a-i}^a ,$$

and noting that then

$$0 \leq l_1^a < l_2^a < \dots < l_{n_a}^a < q_a , \quad (6.76)$$

$$\sum_{\text{all allowed } m_i^a} \sum_{a,i} \left(m_i^a + \frac{1}{2} \right) = N \prod_a \binom{q_a}{n_a} - \sum_{\text{all allowed } l_i^a} \sum_{i,a} \left(l_i^a + \frac{1}{2} \right) , \quad (6.77)$$

where we used that $\sum_a n_a q_a = N$. As l_i^a and m_i^a satisfy the same conditions, equation (6.77) simply implies that

$$\sum_{\text{all possible } m_i^a} \sum_i \left(m_i^a + \frac{1}{2} \right) = \sum_{\text{all possible } l_i^a} \sum_i \left(l_i^a + \frac{1}{2} \right) = \frac{N}{2} \binom{q_a}{n_a} .$$

Using this last equality, we see that the number of states (6.75) is given by

$$d_{\{n_a, q_a\}} = (I - N) \prod_a \binom{q_a}{n_a} = (I - \sum_a n_a q_a) \prod_a \binom{q_a}{n_a} . \quad (6.78)$$

So, we indeed find back the result we derived using attractor tree arguments: the degeneracy is that of the corresponding halo, multiplied by $\langle \Gamma_1, \Gamma_2 \rangle + N\langle \Gamma_1, \Gamma_\star \rangle = I - N$.

Counting all the different degeneracies for all possible partitions of a given total halo charge $N\Gamma_\star$, gives rise to the following generating function:

$$\begin{aligned}
 \mathcal{Z}(q) = \sum_N D_N q^N &= \sum_{\{n_a\} \{q_a\}} (I - \sum_a n_a q_a) \prod_a \binom{q_a}{n_a} q^{n_a q_a} \\
 &= (I - q\partial_q) \prod_{q_a} \left[\sum_{n_a} \binom{q_a}{n_a} q^{n_a q_a} \right] \\
 &= (I - q\partial_q) \prod_k (1 + q^k)^k. \tag{6.79}
 \end{aligned}$$

Using this generating function, we can estimate the large N growth of D_N . This turns out to be of the form $\log D_N \sim N^{2/3}$, modulo logarithmic corrections. Note that, although we find an exponential number of states, the $N^{2/3}$ scaling of the entropy is far less than the expected horizon area from supergravity for a black hole with charges $I/4 < N < I/2$, which is of the order N (for $N < I/4$ no single centered black hole exists with this total charge [30]). It would, however, be extremely interesting to do a similar counting for scaling solutions ($N \geq I/2$), which do admit single center black hole realizations, and compare this to the black hole entropy. This will be the subject of the next section.

6.5 SCALING SOLUTIONS AND FUZZBALLS

In the previous section, the solution space associated with a D6- $\overline{\text{D}6}$ pair (with the intersection product $I = \langle \Gamma_6, \Gamma_6 \rangle$) surrounded by a “halo” of N D0’s was quantized in the *non-scaling* regime, and the entropy was determined to grow as $S \sim N^{2/3}$. Non-scaling implies that $N < I/2$ whereas scaling solutions satisfy $N > I/2$.

Earlier arguments in the literature [169, 30] have suggested that scaling solutions carry vastly more entropy and may account for a large fraction of the black hole entropy. Here, we will see that this is not the case, at least for this large class of solutions. Rather, we will see that the (leading) entropy coming from these solutions matches that of free gravitons in AdS_3 . The change in the leading degeneracy between the non-scaling and scaling regime seems to precisely take into account a bound on possible BPS quantum numbers [17], $\tilde{h} \leq c/24$.

6.5.1 D6- $\overline{\text{D}6}$ -D0 CRUSH AND ITS QUANTIZATION

The scaling regime of the D6- $\overline{\text{D}6}$ -D0 system is physically relevant as it is conjectured to correspond to the geometric manifestation of D4-D0 black hole states [118]. As discussed in the previous section, for the purpose of counting the degeneracy one can study the system at the wall of threshold stability [64]. This can be done thanks to the independence of the scaling solutions from the moduli at infinity. In the following, the threshold point is assumed throughout all the calculations.

The difference between the polytopes associated to the dipole halo in the scaling and non-scaling case resides in two important modifications:

- In the scaling case $N > I/2$, the D0's angles θ_a do not span the whole range $[0, \pi/2]$. There is a lower bound on the possible θ_a 's as j defined in (6.62) is positive by definition, which leads to a non-trivial constraint as $\sum_a q_a = N > I/2$ in the scaling case.
- For D0 centers that carry a D0 charge $q_a > I/2$, the facet $x_a = q_a$ is not part of the polytope anymore.

Note that $j \sim 0$ corresponds to the scaling point. Notice also that, strictly speaking j never becomes zero as this corresponds to D6 and $\overline{\text{D}6}$ sitting on top of each other. However, we are going to include the point $j = 0$ in the following to compactify our polytope.

So, our polytope in the case of scaling dipole halo, neglecting for the moment the possibility of having centers that carry the same D0 charge, is given by

$$-j \leq y \leq j, \quad 0 \leq x_a \leq \text{Min} \left\{ q_a, \frac{I}{2} \right\}, \quad (6.80)$$

where y and x_a are defined in (6.69). Notice that the constraint:

$$j = \frac{I}{2} - \sum_a x_a \geq 0, \quad (6.81)$$

is implied by the first inequality in (6.80). The quantization goes through the same steps as before. Taking the right orbifold version of the naive polytope above, one ends up with the following constraints on (half-)integers $(m, \{m_{i_a}^a\})$ using (6.29)

$$0 \leq m_1^a < m_2^a < \dots < m_{n_a}^a < q_a; \forall a, \quad \sum_{a,i} \left(m_i^a + \frac{1}{2} \right) \leq \frac{I-1}{2} \quad (6.82)$$

$$- \left[\frac{I-1}{2} - \sum_{a,i} \left(m_i^a + \frac{1}{2} \right) \right] \leq m + \frac{1}{2} \leq \left[\frac{I-1}{2} - \sum_{a,i} \left(m_i^a + \frac{1}{2} \right) \right] \quad (6.83)$$

where i_a labels the n_a centers that carry the same charge q_a . We wish to make two observations at this point:

- The constraints on (half-)integers $(m, \{m_{i_a}^a\})$ that we got here are similar to the ones in the non-scaling case (6.74) except for an extra condition, which is the second inequality in (6.82). The latter is a consequence of the first inequality in the same equation (6.82). However, since it implies a non-trivial condition, and it is necessary for the consistency of the counting, we should treat it on the same footing as the other constraints. That is why we included it above as part of the constraints.
- The upper bound in the first inequality of (6.82) should be $\text{Min}\{q_a, \frac{I}{2}\}$, and not q_a . However, a little thought reveals that keeping it as it is written in (6.82) will not alter the counting of states, which will be the subject of the next subsection.

6.5.2 NOT ENOUGH STATES

The complication in the scaling regime arises because of the second constraint in equation (6.82). To proceed, let us introduce the quantity

$$M = \sum_{a,i} \left(m_i^a + \frac{1}{2} \right), \quad (6.84)$$

where M takes both integer and half-integer values. Using that the m_i^a are the discrete analogues of the classical $q_a \cos \theta_a$, the interpretation of M is as the amount of angular momentum carried by the D0 centers (which by the geometry is always opposite in direction to the angular momentum carried by the D6 $\bar{D}6$ pair):

$$M = \frac{I-1}{2} - J. \quad (6.85)$$

Such an equality implies that M is bounded by $1/2 \leq M \leq (I-1)/2$. It is not hard to find the following approximate generating function

$$\mathcal{Z}(q, y) = \sum_{N,M}^{\infty} d_{N,M} q^N y^M = (I - 2y\partial_y) \prod_{k \geq 1, 0 \leq l \leq k} \left(1 + q^k y^{l-1/2} \right), \quad (6.86)$$

where N corresponds to the total D0 halo charge, and M stands for the value of (6.85). The word approximate generating function reflects the fact that the actual degeneracy is given by:

$$D_{N,I} = \sum_{M=1/2}^{M=(I-1)/2} d_{N,M}, \quad (6.87)$$

and not $d_{N,I}$ as is familiar from the usual definition of a generating function. Since we are interested in the leading behavior of the entropy, it will be enough to maximize $d_{N,M}$ with respect to M . This is like going from the canonical to the micro-canonical ensemble, which is a valid transition for large quantum numbers. For a fixed M , we get the following entropy for $M, N \gg 1$

$$S(N, M) \sim (\alpha M [N - M])^{1/3} \quad (6.88)$$

where $\alpha = \frac{3}{4} \zeta(3)$. Maximizing $S(N, M)$ over M in the range $0 < M < I/2$, we find that

$$S(N) = \begin{cases} \left(\alpha \frac{N^2}{4}\right)^{1/3} & \text{if } N \leq I \\ \left(\alpha \frac{I}{2}(N - \frac{I}{2})\right)^{1/3} & \text{if } I \leq N \end{cases} \quad (6.89)$$

A surprising and physically interesting behavior is that, entropy is dominated by $M \sim I/2$ in the case $N > I$ which corresponds to $j \sim 0$ i.e. the scaling point. This suggests that, for large enough D0 charge, most of the states of the scaling dipole halo correspond to the D0 charges localized deep inside the throat. Such a behavior suggests that, there is a phase transition where for a large enough D0 charge, a single centered black hole dominates over a multi-center solution following our proposal to identify scaling solutions as potential black hole states. It will be very interesting to study this observation in more detail.

Another intriguing observation is that, in the regime of charges where we trust supergravity $N \gg I \gg 1$, the entropy above looks asymptotically the same as the horizon area of the corresponding black hole except that, we have a wrong power: $1/3$ instead of $1/2$. This raises the following question: “*do we need to include other solutions with the same asymptotic charges –probably even solutions not belonging to the class of multi-center black holes of $\mathcal{N} = 2$ four dimensional supergravity that we are considering– or is this the best that supergravity can do?*” To answer this question, we will give below an approximate upper bound on the number of BPS states that we can get from supergravity.

6.5.3 BEYOND SUPERGRAVITY?

The approach we will take to get an estimate of the degrees of freedom contained in ‘supergravity’, is to exploit the fact that both the D4D0 black hole and the D6 $\bar{D}6$ D0 systems and generalizations can be studied in asymptotically AdS space by the decoupling limit of [64]. Here, we will do a counting of states with the same total charge but in the limit of vanishing backreaction. The advantage of this calculation is that, in this limit where the supergravity fields can be treated as free excitations around a fixed $\text{AdS}_3 \times S^2 \times \text{CY}_3$ background, the BPS states arrange themselves as

chiral primary multiplets of the (0,4) superconformal isometry group and hence, allow us to do a precise calculation of **all** supergravity states with a given total D4-D0 charge. As was shown in detail in e.g. [172], it is most convenient to KK-reduce the eleven-dimensional supergravity fields on the compact $S^2 \times \text{CY}_3$ space to fields living on AdS_3 , where CY_3 is the Calabi-Yau threefold. Note that we will assume the size of the CY_3 to be much smaller than that of the S^2 so that we will only consider the massless spectrum on the Calabi-Yau, while keeping track of the full tower of massive harmonic modes on the sphere. In this case, all states arrange themselves in a set of harmonic towers of chiral primaries, fully determined by the isometries and the original field content, and all BPS states can be enumerated directly using these algebraic constraints.

Following [64], we are looking for the number of states with these CFT quantum numbers

$$L_0 = N, \quad \bar{L}_0 = \frac{I}{4}, \quad J_3 = -J. \quad (6.90)$$

One recognizes the states as the Ramond ground states as expected for BPS states. The calculation of the KK-spectrum on AdS_3 is however most naturally phrased in the NS sector. The map between the two sectors, R and NS, is called “*spectral flow*” [173]. After performing the spectral flow in the rightmoving sector, the charges (6.90) become (see e.g [64] for some details)

$$L_0 = N, \quad \bar{L}_0 = \frac{I}{2} - J, \quad J_3 = \frac{I}{2} - J = M, \quad (6.91)$$

where in the last equation we used (6.85). As expected, our BPS states manifest themselves in the NS sector as chiral primaries, satisfying the condition $\bar{L}_0 = J_3$. The well known unitarity bound [173] on the R-charge of chiral primaries translates itself into a bounded range for the four-dimensional angular momentum:

$$0 \leq J \leq \frac{I}{2} \quad (6.92)$$

Using the identification of M and L_0 , the analogue of the generating function (6.86) is

$$Z = \text{Tr}_{\text{NS}} q^{L_0} y^{\bar{L}_0}. \quad (6.93)$$

To calculate the degeneracies we are interested in, we need to enumerate the possible BPS states. As we have only supersymmetry on the right, there are no BPS constraints on the left, and hence, the leftmoving fields can be descendants of any highest weight states. On the right we have $N = 4$ supersymmetry and the BPS states have to be chiral primaries of a given weight. As a consequence, and as was shown in detail in e.g [172], [174], [175], the full spectrum arranges itself in several towers of the form

$$\{s, \tilde{h}_{min}\} = \bigoplus_{n \geq 0} \bigoplus_{\tilde{h} \geq \tilde{h}_{min}} (L_{-1})^n |\tilde{h} + s\rangle_L \otimes |\tilde{h}\rangle_R, \quad (6.94)$$

5d origin	number	$\{s, \tilde{h}_{min}\}$ -towers
hyper-multiplets	$2h^{1,2} + 2$	$\{\frac{1}{2}, \frac{1}{2}\}$
vector-multiplets	$h^{1,1} - 1$	$\{0, 1\}$ and $\{1, 1\}$
gravity-multiplet	1	$\{-1, 2\}, \{0, 2\}, \{1, 1\}$ and $\{2, 1\}$

Table 6.1: Summary of the spectrum of chiral primaries on AdS_3 .

where $|h\rangle_L$ are highest weight states of weight h of the leftmoving Virasoro algebra, and $|\tilde{h}\rangle_R$ are weight \tilde{h} chiral primaries of the rightmoving $\mathcal{N} = 4$ super-Virasoro algebra. Strictly speaking, we should include also descendants of $|h\rangle_L$ under the global $\mathcal{N} = 4$ superconformal algebra. We are not going to do so in the following, since it will only change the leading behavior of the entropy with an overall numerical factor. We should also include the so-called “singleton representation” but, their contribution is subleading, and hence, we will ignore them also (see e.g. [28]).

Each field of the five-dimensional supergravity gives rise to such a tower under KK-reduction, where essentially \tilde{h} labels the different spherical harmonics, while n labels momentum excitations in AdS_3 . It was shown in [172], [174], [175] that given the precise field content of a particular $\mathcal{N} = 1$ supergravity in five dimensions, the reduction on a two-sphere gives the set of towers shown in table 6.1. For each such tower the partition function (6.93) has the following form (the total partition function is the product of those):

$$Z_{\{s, \tilde{h}_{min}\}} = \prod_{n \geq 0} \prod_{m \geq 0} (1 - y^{m+\tilde{h}_{min}} q^{n+m+\tilde{h}_{min}+s})^{(-1)^{2s+1}}. \quad (6.95)$$

Following the same steps as above (section 6.5.2), one gets the following entropy

$$S \sim (M(N - M))^{1/3}. \quad (6.96)$$

This has the same wrong exponential as we found before (6.89). This suggests that we need extra degrees of freedom beyond the once obtainable from supergravity. We will further discuss the implication of this estimate in the conclusions.

6.6 LARGE SCALE QUANTUM EFFECTS

Although it has long been understood how to account for the number of black hole microstates in string theory [16], this has generally been done in a dual field theory making it difficult to address some fundamental questions in black hole quantum mechanics, such as information loss via Hawking radiation. For some microscopic black holes (such as those discussed in chapter 3), the ability to dualize to an FP

system has allowed for a more detailed analysis of the structure of the microstates. For these black holes, it has been argued [33] that the average microstate is a highly quantum superposition of states with the corresponding spacetime a wildly fluctuating “fuzzball”. The very interesting part of this claim is that, these fluctuations extend over a region of spacetime circumscribed by the putative black hole horizon. The “metrics” corresponding to the states in the superposition are all very different within the region which would be enclosed by a horizon in the naive black hole solution, but, they settle down very quickly to the same metric outside the horizon. Thus, the remarkable claim of [33] is that the generic state in the black hole ensemble has quantum fluctuations over a large region of spacetime reaching all the way to the black hole horizon.

Unfortunately, the black hole discussed in [33] is microscopic and has no horizon in supergravity (without higher derivative corrections); it would thus be very desirable to be able to demonstrate this type of behavior in a system with a macroscopic black hole. In [56] an attempt was made to do exactly this. Scaling multi-center solutions can classically form arbitrarily deep throats that become infinitely deep in the strict $\lambda \rightarrow 0$ limit, where the coordinate separation of the centers vanishes. We expect, however, that quantum effects will prohibit us from localizing the centers arbitrarily close together and will thus, effectively cap off the throat (see picture 6.3). we can trace this back to the fact that the symplectic form, and hence the quantum exclusion principle, is not renormalized as we increase g_s to interpolate between quiver quantum mechanics and gravity. So, even though gravitational effects increase the depth of the throat as it forms, the phase space volume stays very small. Thus, gravitational back-reaction essentially blows up these quantum effects to a macroscopic scale. This is important not only because it is reminiscent of the large scale quantum fluctuations of the D1-D5 black hole, but, also because a smooth geometry with an infinite throat would be hard to understand in the context of AdS/CFT for the following reason. Solution spaces with a scaling point persist and continue to exhibit scaling behavior even after we take a decoupling limit making all the solutions asymptotically $\text{AdS}_3 \times S^2$. This is problematic as general arguments suggest that an infinitely deep throat in a smooth geometry that is asymptotically AdS would imply a continuous spectrum in the CFT [176]. Thus, it is comforting that the analysis of [56] reveals the infinite throat to be an artifact of the classical limit. Indeed, this is precisely the kind of phenomenon that was suggested in [108].

Before discussing this phenomena in more detail let us note some caveats. The states defined by quantizing the scaling solutions spaces are not necessarily generic black hole microstates. In fact, the discussion in the previous section suggests that such states require including additional stringy degrees of freedom in the phase space, so they may not reflect the behavior of the actual black hole ensemble. Also, the symplectic form was computed in the gauge theory and extended to gravity

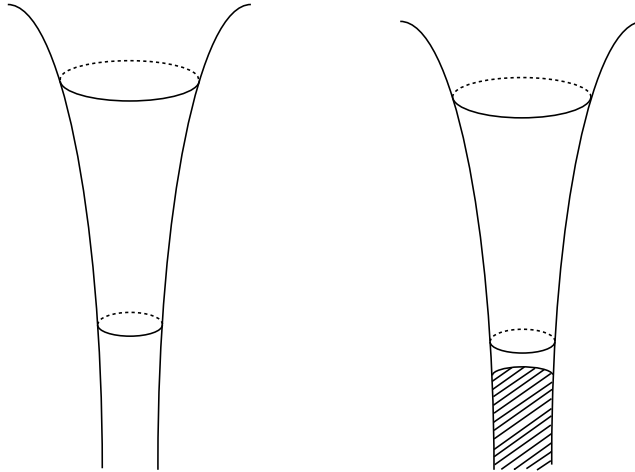


Figure 6.3: (Left) The infinite throat of the naive black hole geometry. **(Right)** An effectively cupped off throat because of the large spread of the wave function (hashed area) that localizes as much as possible down the naive infinite throat.

via a supersymmetric non-renormalization theorem; it would be more insightful to have a direct supergravity computation of the symplectic form. These caveats notwithstanding, it is remarkable that these solutions exhibit quantum structure on a large scale even though they are smooth with a small curvature everywhere.

What is actually determined in [56] is the effective minimum distance between the centers at the scaling point. Specifically, a three center solution similar to the one described in section 6.3.2 with a pure fluxed D6- $\bar{D}6$ pair and a single D0 with charge “ $-N$ ” is considered in its state that is localized as much as possible down the throat, and the expectation value of the harmonic H_0 and the D6-D0 separation is computed. The latter is shown to be of order $\epsilon \sim N/I \geq 1/2$, implying that the centers cannot be localized arbitrarily close to each other so an infinite throat never forms. Rather, the geometry is effectively capped off at a scale set by the D0-D6 distance (see picture 6.3).

While the computation above is heuristic in many ways it yields two very important qualitative lessons. The first is that quantization of these solution spaces as phase spaces resolves several classical paradoxes such as infinitely deep throats and also clarifies the issue of bound states (see [56] for a discussion of this). More importantly, however, it demonstrates that classical solutions may be invalid even though they do not suffer from large curvature scales or singularities. This is an important

point so let us explore it further.

In this particular system the phase space structure of the supergravity theory can be related to that of quiver quantum mechanics by a non-renormalization theorem. In the latter, the scaling solutions (at weak coupling) are analogous to electron-monopole bound states. Heisenberg uncertainty implies that the minimum inter-center distance is of order $x_{ij} \sim \hbar$. Moreover, because the solution space is a *phase space* rather than a configuration space, the coordinates are conjugate to other coordinates rather than velocities, so it is not possible to localize all coordinate directions with arbitrary precision by constructing delta-function states. Thus this quantity will have a large variance so $\delta x_{ij}/x_{ij} \sim 1$ for very small x_{ij} . At weak coupling this is nothing more than the standard uncertainty principle and is not particularly surprising.

What is surprising is that this behavior persists even once gravity becomes strong and the centers backreact stretching the infinitesimal coordinate distance between them to a macroscopic metric distance. Moreover, in this regime, the depth of the throat is extremely sensitive to the precise value of x_{ij} (see [176] for a numerical example), thus, the large relative value of δx_{ij} translates into wildly varying depths for the associated throat. The associated expectation values for any component of the metric have an extremely large variance $\delta g/g$ and so cannot possibly correspond to good semi-classical states. It is somewhat unusual to have classical configurations that cannot be well approximated by semi-classical states (i.e. those with low variance) but here, this can be seen to follow from the very small phase space volume this class of classical solutions occupy [108].

Part IV

Conclusion and Discussion

CHAPTER 7

CONCLUSIONS

In the following, we will try to summarize the important lessons that we learned while applying the fuzzball ideas to the D1-D5 and $\mathcal{N} = 2$ four-dimensional supergravity 1/2-BPS black holes. We will also discuss some open issues and possible future directions of research.

7.1 SO FAR SO GOOD

The application of the fuzzball ideas to the D1-D5 and $\mathcal{N} = 2$ four-dimensional 1/2-BPS black holes has taught us many interesting lessons. Before discussing the most important ones, let us point out some potential misconceptions that may arise when talking about fuzzball ideas. The first one among these misconception is to litterally identify smooth geometries with the microstates of black holes. As we have seen explicitly, smooth geometries, as classical solutions define points in the phase space of a theory (since a coordinate and a momentum define a history and hence a solution; see section 2.3 for more details) which is isomorphic to the solution space. In combination with a symplectic form, the phase space defines the Hilbert space of the theory upon quantization. While it is not clear that direct phase space quantization is the correct way to quantize gravity in its entirety, this procedure when applied to the BPS sector of the theory, seems to yield meaningful results that are consistent with AdS/CFT.

As always in quantum mechanics, it is not possible to write down a state that corresponds to a point in phase space. The best we can do is to construct a state which is localized in one unit of phase space volume near a point. We will refer to such

states as coherent states. Very often, but not always, the limit in which supergravity becomes a good approximation corresponds exactly to the classical limit of this quantum mechanical system, and in this limit coherent states localize at a point in phase space (see chapter 4). It is in this sense, and only in this sense, that smooth geometries can correspond to microstates. Clearly, coherent states are very special states, and a generic state will *not* admit a description in terms of a smooth geometry.

To define our black hole states, we quantized a restricted set of supergravity solutions that preserve the same amount of supersymmetries. But such a restriction of quantization does raise the question of its validity. In some instances, a subspace of the solution space corresponds to a well defined symplectic manifold and is hence a phase space in its own right. Quantizing such a space defines a Hilbert space which sits in the larger Hilbert space of the full theory. Under some favorable circumstances, the resulting Hilbert space may be physically relevant because a subspace of the total Hilbert space can be naturally identified with this smaller Hilbert space. That is, there is a one-to-one map between states in the Hilbert space generated by quantizing a submanifold of the phase space and states in the full Hilbert space whose support is localized close to this submanifold.

For instance, in determining BPS states we can imagine imposing BPS constraints on the Hilbert space of the full theory, generated by quantizing the full solution space, and expect that the resulting states will be supported primarily on the locus of points that corresponds to the BPS phase space; that is, the subset of the solution space corresponding to classical BPS solutions. It is therefore possible to first restrict the phase space to this subspace and then quantize it in order to determine the BPS sector of the Hilbert space.

Another lesson we uncovered was that, string scale curvature and large quantum fluctuations are not confined to the region around the singularity. For example the $\mathcal{N} = 2$ four dimensional 1/2-BPS black holes do show signs of large quantum fluctuations, see section 6.6. Such a behavior will generally appear whenever there are some regions of phase space where the density of states is too low to localize a coherent state at a particular point as follows. Recall that the symplectic form effectively discretizes the phase space into \hbar -sized cells. Since a quantum state can be localized at most in one such cell, it is not possible to localize any state to a particular point within the cell. Hence all states that belong to the same cell should be treated as describing the same quantum state, where, the possible differences between the former states are attributed to quantum fluctuations. One then naturally concludes that in general all the points in a given cell should correspond to classical solutions that are essentially indistinguishable from each other at large scales. It is possible, however, for a cell to contain solutions to the equation of motion that *do* differ from each other at very large scales. In such situations, the size of quantum fluctuations

that differentiate between different points in this cell turns out to be macroscopic.

Thus, even though the black hole solution satisfies the classical equations of motion all the way to the singularity, this does not necessarily imply that this solution will correspond to a good semi-classical state with very small quantum fluctuations, once quantum effects are taken into account.

7.2 LOOKING TO THE FUTURE

On top of the lessons we learned from our study of a class of BPS black holes that emerge in string theory, we stumbled also on some puzzles that clearly need further investigation. The first puzzle has to do with the mismatch of the number of states with the entropy of $\mathcal{N} = 2$ four-dimensional 1/2-BPS black holes, that we found using either the quantization of a special class of black hole states, or free excitations of the fields of a particular $\mathcal{N} = 1$ five-dimensional supergravity estimate (section 6.5). Such a mismatch raises the following question: can we account for the missing states by looking at other classes of supergravity solutions? Or by going higher in dimensions like ten or even eleven dimensions? Or is this the best supergravity can do? As things stand right now, we do not know the answer to such questions. The only certain thing is that if we include all closed strings states, we should recover the right entropy. Unfortunately, we do not know how to proceed in this direction for the moment. However, we are inclined to believe that most probably, supergravity will not be able to offer enough states to account for the entropy of these class of black holes.

If we really need stringy states, one cannot help himself but wonder what is the content of the fuzzball proposal in such a situation. A possibility would be that the fuzzball proposal is the statement that the closed string description of a generic microstate of a black hole, while possibly highly stringy and quantum in nature, has interesting structure that extends all the way to the horizon of the naive black hole solution, and is well approximated by the black hole geometry outside the horizon.

More precisely, the naive black hole solution is argued to correspond to a thermodynamical ensemble of pure states. The *generic* constituent state will not have a good geometrical description in classical supergravity; it may be plagued by regions with string-scale curvature and may suffer large quantum fluctuations. These, however, are not restricted to the region near the singularity but extend all the way to the horizon of the naive geometry. This is important as it might shed light on information loss via Hawking radiation from the horizon as near horizon processes would now encode information about this state that, in principle, distinguishes it from the ensemble average.

On the conceptual level, one would like to understand what possible concrete predictions one can make in the fuzzball framework. As an example, it will be very interesting to understand what will an observer falling into a black hole see. At present, we cannot answer this question. The fuzzball picture of a black hole does suggest that the observer will gradually thermalize once the horizon has been passed, but the rate of thermalization remains to be computed. It would be interesting to do this and to compare it to recent suggestions that black holes are the most efficient scramblers in nature [177, 178, 179].

Part V

Appendices

APPENDIX A

SQUEEZED STATES AND NEGATIVE ENERGY DENSITY

The horizon vacuum in Hawking calculation belongs to a special kind of states called “*squeezed states*” [42]. Their importance for us resides in that they may exhibit negative energy densities, which is important for black hole evaporation. In the following, we are going to review some of their properties that we will be needing in the bulk of the thesis. For more detailed study of their properties see [180] for example.

A.1 SQUEEZED STATES

In the following, we are going to restrict ourselves to a single mode. A general squeezed state takes the form [181, 182, 183]

$$|z, \xi\rangle = D(z) S(\xi) |0\rangle , \quad (\text{A.1})$$

where $D(z)$ is the displacement operator

$$D(z) = \exp(z a^\dagger - z^* a) = e^{-|z|^2/2} e^{z a^\dagger} e^{-z^* a} = e^{|z|^2/2} e^{-z^* a} e^{z a^\dagger} , \quad (\text{A.2})$$

and $S(\xi)$ is the squeeze operator

$$S(\zeta) = \exp\left[\frac{1}{2} (\zeta^* a^2 - \zeta(a^\dagger)^2)\right] . \quad (\text{A.3})$$

It is easy to prove that $D(z)$ and $S(\xi)$ satisfy

$$D^\dagger(z) a D(z) = a + z , \quad (\text{A.4})$$

$$D^\dagger(z) a^\dagger D(z) = a^\dagger + z^* , \quad (\text{A.5})$$

$$S^\dagger(\zeta) a S(\zeta) = a \cosh |\zeta| - a^\dagger e^{i\theta} \sinh |\zeta| , \quad (\text{A.6})$$

$$S^\dagger(\zeta) a^\dagger S(\zeta) = a^\dagger \cosh |\zeta| - a e^{-i\theta} \sinh |\zeta| , \quad (\text{A.7})$$

where $\zeta = |\zeta| e^{i\theta}$. When $\zeta = 0$, we have the familiar coherent state, so in a way, the squeezed states are a generalization of them. Actually for ζ real ($\theta = 0$), they saturate the uncertainty inequality

$$(\Delta x)^2 (\Delta p)^2 = |1 + i \sin \theta \sinh 2|\zeta||^2 . \quad (\text{A.8})$$

A.2 NEGATIVE ENERGY DENSITY

The other extreme case occurs when $z = 0$, and is called the “*squeezed vacuum*”. This is precisely the state of the Hawking radiation field (section 1.3.2). It turns out that these states always have a negative energy density somewhere in spacetime. In flat spacetime one finds for real ζ

$$\mathcal{H} = \frac{1}{2} \omega + \sinh |\zeta| (\sinh |\zeta| - \cosh |\zeta| [2\omega x^2 - 1]) , \quad (\text{A.9})$$

which is clearly negative for large enough x

$$\mathcal{H} < \frac{1}{2} \omega (1 - 4 \sinh^2 |\zeta| x^2) \quad \text{For } x^2 > \frac{1}{2\omega} . \quad (\text{A.10})$$

However, when integrated over the whole space one finds that

$$\langle H \rangle = \frac{1}{2} \omega + \sinh^2 |\zeta| . \quad (\text{A.11})$$

APPENDIX B

A QUICK TRIP IN TEN DIMENSIONS

In this appendix, we will collect some facts about ten dimensional $\mathcal{N} = 2$ supergravity theories and some of their important properties. We start by reviewing the action of the two types, type-IIA and type-IIB. Then the solution describing a D-brane will be relayed. At the end, some formulas describing the action of T and S-duality on background fields will be given.

This appendix should not be taken as an introduction of any sort to the above mentioned subjects. The reader is already assumed to have some elementary knowledge of string theory. For background material one can consult standard books on string theory e.g. [184, 185, 186].

B.1 TEN-DIMENSIONAL SUPERGRAVITY

There are two types of $\mathcal{N} = 2$ supergravity in ten dimensions that describe the low energy effective action of type-II string theories. The field content of these supergravity theories is the massless spectrum of the associated superstring theory. We summarize the field content in table B.1 below to set up notation.

Type	Neveu-Schwarz (NS-NS)	Ramond-Ramond (R-R)
Type-II.A	$G_{\mu\nu}$ (graviton), ϕ (dilaton), $B_{\mu\nu}$	$C_\mu, C_{\mu\nu\rho}; H^{(0)}$ (non propagating)
Type-II.B	$G_{\mu\nu}$ (graviton), ϕ (dilaton), $B_{\mu\nu}$	$C, C_{\mu\nu}, C_{\mu\nu\rho\tau}$

Table B.1: The massless spectrum of type-II string theories. The fields $B, C^{(n)}$ are form field potentials. NS-NS and R-R stand for two of the four possible sectors in closed superstrings.

B.1.1 TYPE-IIA SUPERGRAVITY

The massless spectrum of type-IIA superstring contains the graviton and its two superpartners that have opposite chiralities. In addition to these fields, the bosonic fields include also the dilaton and the B-field coming from the NS-NS sector, the different p-forms coming from the R-R sector, namely $C^{(1)}$ and $C^{(3)}$ (see the table B.1). The effective action has the following bosonic part (the wedge product is understood):

$$\begin{aligned}
 S_{II.A} = & S_{NS} + S_R + S_{CS}, \\
 S_{NS} = & \frac{1}{2\kappa_0^2} \int d^{10}x (-G)^{1/2} e^{-2\phi} \left[R + 4(\nabla\phi)^2 - \frac{1}{2}(H^{(3)})^2 \right] \\
 S_R = & -\frac{1}{4\kappa_0^2} \int d^{10}x (-G)^{1/2} \left[(G^{(2)})^2 + (G^{(4)})^2 \right] \\
 S_{CS} = & -\frac{1}{4\kappa_0^2} \int B^{(2)} dC^{(3)} dC^{(3)}.
 \end{aligned} \tag{B.1}$$

where S_{NS} is the contribution of the NS-NS sector, S_R comes from the R-R sector, S_{CS} is a Chern-Simons term, $G_{\mu\nu}$ is the metric, ϕ is the dilaton, $H^{(3)} = dB^{(2)}$ is the field strength of the NS-NS 2-form, while the R-R field strengths are $G^{(2)} = dC^{(1)}$, and $G^{(4)} = dC^{(3)} + H^{(3)} \wedge C^{(1)}$.

B.1.2 TYPE-IIB SUPERGRAVITY

This theory is chiral as the two gravitinos, the super-partners of the graviton, have the same chirality. The bosonic field content of this theory differs from the previous one in the R-R sector. Here, one has the following p-form potentials: a scalar $C^{(0)}$, $C^{(2)}$, and $C^{(4)}$ (see table B.1). Strictly speaking, we do not have a satisfactory action due to the self-duality of the field strength of $C^{(4)}$. We are going to implement this condition at the level of the equations of motion as an extra constraint. In this case,

the action reads:

$$\begin{aligned}
 S_{II.B} &= S_{NS} + S_R + S_{CS} \\
 S_{NS} &= \frac{1}{2\kappa_0^2} \int d^{10}x (-G)^{1/2} e^{-2\phi} \left[R + 4(\nabla\phi)^2 - \frac{1}{2}(H^{(3)})^2 \right] \\
 S_R &= -\frac{1}{4\kappa^2} \int d^{10}x (-G)^{1/2} \left\{ \frac{1}{12}(G^{(3)} - C^{(0)}H^{(3)})^2 + (dC^{(0)})^2 + \frac{1}{2}(G^{(5)})^2 \right\} \\
 S_{CS} &= -\frac{1}{4\kappa_0^2} \int C^{(4)} H^{(3)} G^{(3)}. \tag{B.2}
 \end{aligned}$$

Now, $G^{(3)} = dC^{(2)}$ and $G^{(5)} = dC^{(4)} + \frac{1}{2}H^{(3)}C^{(2)} + \frac{1}{2}B^{(2)}G^{(3)}$. Remember that we are imposing the self-duality condition on $G^{(5)}$ by hand $G^{(5)} = *G^{(5)}$.

A point worth mentioning here is that, in the actions above the gravity part (the term proportional to the Ricci scalar R) is not of the canonical form; there is an extra $\exp(-2\phi)$ multiplying it. The frame these actions are written in is called the “*string frame*”. One can go to the “*Einstein frame*” with the canonical action for gravity by rescaling the metric by an appropriate power of $\exp(\phi)$ ($\exp(-\phi/2)$ in ten dimensions).

B.2 D-BRANES IN SUPERGRAVITY

D-brane can be seen as extended hypersurfaces where open strings can end. We will be calling them, as is custom in string theory, D p -branes where p stands for the spatial extension of the D-brane. Type-IIA (IIB) string theory include in its spectrum D0, D2, D4, D6, D8 (respectively, D(-1), D1, D3, D5, D7, D9) branes.

A D p -brane is massive and charged under the R-R $(p+1)$ -form $C^{(p+1)}$. Due to these properties, the presence of a D-brane will generate a non-trivial geometry. Taking into account such modification in the geometry is called “*backreacting*” the D-brane. There is another important property that these D-branes enjoy. In weakly coupled string theory, the so called “*probe approximation*”, it can be checked that straight D-branes preserve half of the total 32 possible supersymmetries in ten dimensions i.e. they are 1/2-BPS solutions. Since supersymmetry is robust, they should, and indeed they do, preserve the same amount of supersymmetry when the string coupling constant is increased [187].

B.2.1 ELECTRIC AND MAGNETIC D-BRANES

Before spelling out the supergravity solution describing a Dp-brane, there is a small subtlety that we should take care of first. In the following, we set $B = 0$. From the point of view of the field strengths G of the R-R forms C described in table B.1, there are two kinds of D-branes: “electrically” charged and “magnetically” charged D-branes. This choice of naming will be clear in a moment. The R-R forms $C^{(n)}$ can be seen as a higher dimensional generalization of the Maxwell field A_μ . Let us revisit the four dimensional Maxwell theory in the language of forms. The field strength $F = dA$ satisfies the following equation:

$$dF = 0, \quad d * F = *j \quad (\text{B.3})$$

where $*$ is the Hodge dual, and j is a current due to charged particles under A . Let us call these charges electrically charged particles. An example is an electron. In the vacuum $j = 0$, the field $\tilde{F} = *F$ satisfies the same equations as F . One can wonder if there are charged particles under a “dual” gauge field \tilde{A} defined such that $d\tilde{A} = \tilde{F}$. If such a particle exists then, \tilde{F} will satisfy the same equations as F in (B.3). These new particles are described as being magnetically charged under the original field A . An example is the hypothetical monopole.

This story generalizes to the R-R forms. In this case, for the R-R form $C^{(p+1)}$, the magnetic D-brane is a D(8-p)-brane. In the following, when dealing with only the magnetic D(8-p)-brane, we will use the dual field $C^{(9-p)}$ instead of the original one $C^{(p+1)}$ in the action (B.1.1) or (B.1.2).

B.2.2 THE BACKREACTION Dp-BRANE

In looking for the solution corresponding to a Dp-brane, the only surviving part of the actions (B.1) and (B.2) is the NS-NS common part without the B-field and the kinetic term of the associated $C^{(p+1)}$ form:

$$S = \frac{1}{2\kappa_0^2} \int d^{10}x (-G)^{1/2} \left(e^{-2\phi} [R + 4(\nabla\phi)^2] - \frac{1}{2} dC^{(p+1)} \wedge *dC^{(p+1)} \right) \quad (\text{B.4})$$

Calling the coordinates along the brane x^μ and the ones transverse to it y^α , the solution describing the Dp-branes turns out to be:

$$ds^2 = H_p^{-1/2}(y) \eta_{\mu\nu} dx^\mu dx^\nu + H_p^{1/2}(y) \delta_{\alpha\beta} dy^\alpha dy^\beta \quad (\text{B.5})$$

$$e^{2\phi} = g_s^2 H_p^{(3-p)/2}(y), \quad C^{(p+1)} = \frac{1 - H_p(y)}{g_s} d\text{vol} \quad (\text{B.6})$$

where $H_p(y)$ is a harmonic function in the transverse space.

B.3 T AND S DUALITIES

In the following we are going to touch upon two important dualities that will be of use in the third chapter of the thesis; T and S dualities. The first one relates the two types of closed string theory. The other, however, is a relation between strongly and weakly coupled type-IIB string theory.

B.3.1 T-DUALITY AND BUSCHER RULES

Studying the spectrum of perturbative bosonic closed string theory on $\mathbb{R}^{1,8} \times S^1$ reveals that it is invariant under sending the radius of S^1 to its inverse. Such a duality is called “T-duality” and generalizes to closed superstrings with a surprise: type-IIA is mapped to type-IIB and vice versa.

On the level of supergravity, T-duality requires a $U(1)$ isometry direction on which it is performed. Its action on the background fields is given by “Buscher rules” [188, 189, 190, 191]

$$\begin{aligned} \tilde{g}_{yy} &= \frac{1}{g_{yy}}, & e^{2\tilde{\phi}} &= \frac{e^{2\phi}}{g_{yy}}, & \tilde{g}_{\mu y} &= \frac{b_{\mu y}}{g_{yy}}, & \tilde{b}_{\mu y} &= \frac{g_{\mu y}}{g_{yy}} \\ \tilde{g}_{\mu\nu} &= g_{\mu\nu} - \frac{g_{y\mu} g_{y\nu} - b_{y\mu} b_{y\nu}}{g_{yy}}, & \tilde{b}_{\mu\nu} &= b_{\mu\nu} - \frac{b_{y\mu} g_{y\nu} - g_{y\mu} b_{y\nu}}{g_{yy}} & (B.7) \\ \tilde{C}_{\mu\dots\nu\alpha y}^{(n)} &= C_{\mu\dots\nu\alpha}^{(n-1)} - (n-1) \frac{C_{[\mu\dots\nu|y}^{(n-1)} g_{|\alpha]y}}{g_{yy}} \\ \tilde{C}_{\mu\dots\nu\alpha\beta}^{(n)} &= C_{\mu\dots\nu\alpha\beta y}^{(n+1)} + n C_{[\mu\dots\nu\alpha}^{(n-1)} b_{\beta]y} - n(n-1) \frac{C_{[\mu\dots\nu|y}^{(n-1)} b_{|\alpha|y} g_{|\beta]y}}{g_{yy}} \end{aligned}$$

where y is the $U(1)$ isometry direction, the tilde stand for the T-dual fields, $g_{\mu\nu}$ is the metric, $b_{\mu\nu}$ is the b-field, ϕ is the dilaton, and $C_{\mu\dots\nu}^{(n)}$ is a R-R n -form.

B.3.2 TYPE-IIB AND S-DUALITY

Looking back at the massless spectrum of type-IIB string theory (table B.1), we see a striking resemblance between the NS-NS and R-R fields: both of them contain a scalar (dilaton ϕ vs R-R zero-form $C^{(0)}$), and a two-form field (B-field $b_{\mu\nu}$ vs R-R two-form $C^{(2)}$). This observation raises the following question “*Can we map these fields between themselves or is it just a coincidence?*” It turns out that the answer to this question is yes, and this is due to an $SL(2, \mathbb{Z})$ symmetry that type-IIB string theory enjoys [192, 193]. Actually an $SL(2, \mathbb{R})$ symmetry is already visible in the classical

type-IIB supergravity low energy action (B.2), which is believed to be broken to its discrete version $SL(2, \mathbb{Z})$ once quantum and non-perturbative effects are included. The type-IIB effective action can be recast in an $SL(2, \mathbb{R})$ duality invariant way using the following field redefinition

$$\tau = C^{(0)} + ie^{-\phi} \quad (B.8)$$

and combining the two two-forms $b_{\mu\nu}$ and $C^{(2)}$ in an $SL(2, \mathbb{Z})$ doublet. The new field τ then transforms in a fractional way.

$$\tau \longrightarrow \frac{a\tau + b}{c\tau + d}, \quad \text{with } \begin{pmatrix} a & b \\ c & d \end{pmatrix} \in SL(2, \mathbb{Z}) \quad (B.9)$$

What interests us is a special duality transformation that goes under the name of “S-duality”. Its effect on type-IIB fields is the following

Field Transformations	Interpretation
$\tau \rightarrow -1/\tau$	mixing of the dilaton ϕ and the zero-form $C^{(0)}$
$\begin{cases} b_{\mu\nu} \rightarrow -C^{(2)} \\ C^{(2)} \rightarrow b_{\mu\nu} \\ C^{(4)} \rightarrow C^{(4)} \end{cases}$	$\begin{cases} \text{F1-string} \leftrightarrow \text{D1-brane} \\ \text{NS5 brane} \leftrightarrow \text{D5-brane} \\ \text{D3-brane changes into itself.} \end{cases}$

In the case where there is no D(-1)-brane ($C^{(0)} = 0$), the first part of the transformation becomes $\phi \rightarrow -\phi$, which amounts to taking the string coupling constant $g_s = e^\phi$ to its inverse. In this case the S-duality is just a weak/strong coupling duality.

APPENDIX C

THE D1-D5 GENERATING FUNCTION

When evaluating the different effective geometries (3.8) in the fourth chapter, one is led to computing the functions in (4.17). The latter can be evaluated once the following generating function is known

$$f_v = \frac{Q_5}{4\pi^2 L} \int d^4 u \int_0^L ds \int_{d,\bar{d}} f(d, \bar{d}) \frac{e^\alpha e^{i\mathbf{u} \cdot (\mathbf{x} - \mathbf{F}(s)) + i\mathbf{v} \cdot \mathbf{F}'(s)}}{|\mathbf{u}|^2}, \quad (\text{C.1})$$

where the constant e^α is due to normal ordering (section 4.2.2). To evaluate α one starts with the expression of $\mathbf{F}(s)$ in terms of oscillators (3.19), then uses the identity

$$e^{\alpha c^\dagger} e^{\beta c} = e^{-\alpha\beta} e^{\beta c} e^{\alpha c^\dagger}, \quad (\text{C.2})$$

valid for any operators c and c^\dagger satisfying $[c, c^\dagger] = \mathbb{I}$. One finds that

$$\alpha = \sum_k \left(\frac{|\mathbf{u}|^2 \mu^2}{2k} + \frac{2\pi^2 k \mu^2 |\mathbf{v}|^2}{L^2} \right). \quad (\text{C.3})$$

The relation between the functions in (4.17) and the generating function (C.1) is easily found to be

$$f_5(\mathbf{x}) = 1 + f_v(\mathbf{x})|_{v=0}, \quad f_1(\mathbf{x}) = 1 - \partial_{v^i} \partial_{v^i} f_v(\mathbf{x})|_{v=0}, \quad A_i(\mathbf{x}) = -i \partial_{v^i} f_v(\mathbf{x})|_{v=0}. \quad (\text{C.4})$$

In the following, we are going to evaluate f_v in two special cases. The first case is a pure state describing an excited single rotating frequency mode, useful for the geometries discussed in sections 4.2.2 and 4.6. The second case is the generic thermodynamical ensemble, relevant for sections 4.3 and 4.4.

C.1 SIMPLE PHASE SPACE DENSITIES

It turns out that all our phase space densities $f_{d, \bar{d}}$ that we will be dealing with in the fourth chapter take the following simple form

$$f_{d, \bar{d}} = \prod_{k, \pm} f^{(k^\pm)}(|d_k^\pm|^2), \quad (\text{C.5})$$

where $d_k^\pm = (d_k^1 \pm id_k^2)\sqrt{2}$. There is another contribution coming from the 34-plane which looks exactly the same as the expression above. Such contribution will be implicit in the following as we can always reconstruct it given the 12-plane contribution. This form of the phase space density allows us to simplify the expression of f_v in (C.1) as follows. First, one Fourier transforms the \mathbf{x} dependence using

$$\frac{1}{|\mathbf{x}|^2} = \frac{1}{4\pi^2} \int d^4u \frac{e^{i\mathbf{u}\cdot\mathbf{x}}}{|\mathbf{u}|^2}. \quad (\text{C.6})$$

Then, using that the operators c_k^\dagger commute with the operators c_l for different modes ($k \neq l$), one can rewrite (C.1) as

$$\begin{aligned} f_v = & \frac{Q_5}{4\pi^2 L} \int d^4u \frac{e^{i(\sum_k u^\pm x^\mp)}}{|\mathbf{u}|^2} \int_0^L ds \prod_k e^{\alpha_k} \\ & \prod_{\pm} \int_{d_k, \bar{d}_k} f^{(k^\pm)}(|d_k^\pm|) e^{-iu^\pm \gamma_k (d_k^\mp e^{ik\frac{2\pi}{L}s} + \bar{d}_k^\mp e^{-ik\frac{2\pi}{L}s}) - v^\pm \lambda_k (d_k^\mp e^{ik\frac{2\pi}{L}s} - \bar{d}_k^\mp e^{-ik\frac{2\pi}{L}s})}, \end{aligned} \quad (\text{C.7})$$

where α_k is the restriction of α (C.3) to the k^{th} oscillator, $a^\pm = (a^1 \pm ia^2)/\sqrt{2}$, and:

$$\gamma_k = \frac{\mu}{\sqrt{2k}}, \quad \lambda_k = \frac{\pi\mu}{L} \sqrt{2k}. \quad (\text{C.8})$$

Next, integrating over all possible values of the complex numbers d_k^\pm allows us to absorb the s -dependent phase, in the expression above, in the definition of d_k^\pm . By doing so, the integration over s is easily performed leaving

$$f_v = \frac{Q_5}{4\pi^2} \int d^4u \frac{e^{i(u^\pm x^\mp)}}{|\mathbf{u}|^2} \prod_k e^{\alpha_k} \int_{d_k, \bar{d}_k} f^{(k^\pm)}(|d_k^\pm|) e^{-\sigma_k^\pm d_k^\mp + \bar{d}_k^\mp d_k^\mp}, \quad (\text{C.9})$$

where we introduced the following quantities:

$$\sigma_k^\pm = \lambda_k v^\pm + i \gamma_k u^\pm, \quad \bar{\sigma}_k^\pm = \lambda_k v^\mp - i \gamma_k u^\mp. \quad (\text{C.10})$$

Once again, by redefining the phase of d_k^\pm appropriately, we can integrate over them leaving us with the expression:

$$f_v = \frac{Q_5}{2\pi^2} \int d^4u \frac{e^{i(u^\pm x^\mp)}}{|\mathbf{u}|^2} \prod_k e^{\alpha_k} \int |d_k^\pm| d|d_k^\pm| f^{(k^\pm)}(|d_k^\pm|) J_0(2|d_k^\pm| |\sigma_k^\mp|), \quad (\text{C.11})$$

where $J_0(x)$ is the Bessel function of the first kind, and

$$2\alpha_k = \gamma_k^2 |\mathbf{u}_{12}|^2 + \lambda_k^2 |\mathbf{v}_{12}|^2 , \quad (\text{C.12})$$

$$|\sigma_k^\pm|^2 = \alpha_k \pm \frac{1}{2} \left(\frac{2\pi}{L} \right) \mu^2 (u^1 v^2 - u^2 v^1) . \quad (\text{C.13})$$

This is as far as we can get for these class of phase space densities. Let us now discuss our specific examples.

C.2 THE MONOCHROMATIC STATE

In the following, we restrict ourselves to the 12-plane as the contribution from the other directions is trivial. The simplest state that describes a rotation (3.11) is

$$|\psi\rangle = [(a_q^+)^{\dagger}]^J |0\rangle . \quad (\text{C.14})$$

The state so constructed describes a circular profile following (4.26). Its associated phase space density $f_{d, \bar{d}}$ can easily be evaluated to be (see (4.16, 4.14) and (4.34))

$$f(d, \bar{d}) = e^{-|d_q^+|^2} \frac{|d_q^+|^{2J}}{J!} \prod_{k \neq q^+} e^{-|d_k|^2} . \quad (\text{C.15})$$

We have dropped the delta function (4.21) here and expect (C.15) to be valid for large values of J . It is therefore better thought of as a semiclassical profile rather than the full quantum profile.

In evaluating f_v (C.11), we distinguish two cases

In the case $k \neq q^+$ In this case, $f_{d, \bar{d}}^{(k)}$ is given by $\exp(-|d_k^\pm|^2)$ which leads upon integration over $|d_k^\pm|$ to

$$I_k = \frac{1}{2} e^{-|\sigma_k^\pm|^2} . \quad (\text{C.16})$$

In the case $k = q^+$ In this case, the phase space density is given by

$$e^{-|d_q^+|^2} \frac{|d_q^+|^{2J}}{J!} ,$$

which leads, upon integration over $|d_q^+|$ using (4.36), to

$$I_{q^+} = \frac{1}{2} e^{-|\sigma_q^-|^2} L_J(|\sigma_q^-|^2) , \quad (\text{C.17})$$

where $L_J(x)$ is the Laguerre polynomial of order J .

Putting everything together we end up with

$$\begin{aligned} f_v(\mathbf{x}) &= \frac{Q_5}{4\pi^2 L} \int d^4 u \frac{e^{i(u^\pm x^\mp)}}{|\mathbf{u}|^2} L_J \left(\frac{\mu^2}{2k} \left[\left(\frac{2\pi}{L} k v^1 + u^2 \right)^2 + \left(\frac{2\pi}{L} k v^2 - u^1 \right)^2 \right] \right) \\ &= Q_5 L_J \left(\frac{\mu^2}{2k} \left[\left(\frac{2\pi}{L} k v^1 - i\partial_2 \right)^2 + \left(\frac{2\pi}{L} k v^2 + i\partial_1 \right)^2 \right] \right) \frac{1}{|\mathbf{x}|^2}, \end{aligned} \quad (\text{C.18})$$

where the last equation is seen as a formal expression.

C.3 THE GENERIC THERMODYNAMICAL ENSEMBLE

Another important class of examples is the generic thermodynamical ensemble discussed in section 4.4. In this case, the phase space density reads (4.52), restricting once again to the 12-plane,

$$f_k(d, \bar{d}) = (1 - e^{-\beta_k^+})(1 - e^{-\beta_k^-}) e^{-(1 - e^{-\beta_k^+})|d_k^+|^2 - (1 - e^{-\beta_k^-})|d_k^-|^2}. \quad (\text{C.19})$$

Plugging this expression in (C.11), then performing the $|d_k^\pm|$ integral gives

$$\begin{aligned} f_v &= \frac{Q_5}{4\pi^2} \int d^4 u \frac{e^{i\mathbf{u}\mathbf{x}}}{|\mathbf{u}|^2} \exp \left(-\frac{\mu^2}{8} \left[\mathcal{D}|\mathbf{u}|^2 + \left(\frac{2\pi}{L} \right)^2 \mathcal{N}|\mathbf{v}|^2 \right] \right) \\ &\quad \exp \left(\frac{\mu^2}{2} \left(\frac{2\pi}{L} \mathcal{J} [u^1 v^2 - u^2 v^1 + u^3 v^4 - u^4 v^3] \right) \right), \end{aligned} \quad (\text{C.20})$$

where:

$$\mathcal{N} = 2 \sum_k k \left(\frac{e^{-\beta_k^+}}{1 - e^{-\beta_k^+}} + \frac{e^{-\beta_k^-}}{1 - e^{-\beta_k^-}} \right), \quad (\text{C.21})$$

$$\mathcal{J} = j_{12} = j_{34} = \sum_k \left(\frac{e^{-\beta_k^+}}{1 - e^{-\beta_k^+}} - \frac{e^{-\beta_k^-}}{1 - e^{-\beta_k^-}} \right), \quad (\text{C.22})$$

$$\mathcal{D} = 2 \sum_k \frac{1}{k} \left(\frac{e^{-\beta_k^+}}{1 - e^{-\beta_k^+}} + \frac{e^{-\beta_k^-}}{1 - e^{-\beta_k^-}} \right). \quad (\text{C.23})$$

One can rewrite the expression (C.20) in a formal way as

$$f_v = Q_5 e^{-\frac{\mu^2}{8} \left(\frac{2\pi}{L} \right)^2 \mathcal{N}|\mathbf{v}|^2} e^{-i \frac{\mu^2}{2} \left(\frac{2\pi}{L} \right) \mathcal{J} [v^2 \partial_1 - v^1 \partial_2 + v^4 \partial_3 - v^3 \partial_4]} \frac{1 - e^{-\frac{\mu^2}{\mathcal{D}} x^2}}{x^2}. \quad (\text{C.24})$$

APPENDIX D

CALABI-YAU MANIFOLDS AND STRING COMPACTIFICATION

In this appendix, we are going to describe Calabi-Yau manifolds and the compactification on them in the case they are six dimensional. We will refer to the latter as Calabi-Yau threefolds. The emphasis will be on the low energy field content while the construction of the resulting effective action will be carried out in the fifth chapter (section 5.1).

D.1 FROM KÄHLER TO CALABI-YAU MANIFOLDS

Before being able to define a Calabi-Yau manifold, we need first to understand what a Kähler manifold is? the answer to this question requires the notion of complex structure. The material discussed here can be found in many places, see for example [194, 163, 195, 196].

Complex Structure Given a $2m$ -dimensional manifold M , a complex structure is an endomorphism of the tangent bundle $J : TM \rightarrow TM$, that squares to $J^2 = -\mathbb{I}_{2m \times 2m}$, and whose Nijenhuis tensor $N : TM \times TM \rightarrow TM$, defined by:

$$N[X, Y] = [X, Y] + J[JX, Y] + J[X, JY] - [JX, JY], \quad (\text{D.1})$$

where $[\cdot, \cdot]$ is the Lie bracket, vanishes. The existence of a complex structure allows us to introduce complex coordinate $z^i, \bar{z}^{\bar{i}}$, where locally J takes the form

$$J = -i dz^i \otimes \frac{\partial}{\partial z^i} + i d\bar{z}^{\bar{i}} \otimes \frac{\partial}{\partial \bar{z}^{\bar{i}}} \equiv -i dz^i \otimes \partial_i + i d\bar{z}^{\bar{i}} \otimes \bar{\partial}_{\bar{i}}. \quad (\text{D.2})$$

Hermitian Metric Given a complex manifold with complex structure J , a Hermitian metric g is a metric that satisfies

$$g(JX, JY) = g(X, Y) . \quad (\text{D.3})$$

Locally, it can be written as

$$g = g_{i\bar{j}} dz^i \otimes d\bar{z}^j + g_{\bar{i}j} d\bar{z}^i \otimes dz^j . \quad (\text{D.4})$$

Kähler Form Given a Hermitian metric g , we can associate to it a Kähler form ω defined locally by

$$\omega = \frac{i}{2} g_{i\bar{j}} dz^i \wedge d\bar{z}^j . \quad (\text{D.5})$$

Kähler Manifold A complex manifold is Kähler if the Kähler form ω is closed $d\omega = 0$, which implies that ω is harmonic. In this situation the metric, called the “Kähler metric”, takes the following local form

$$g_{i\bar{j}} = \partial_i \bar{\partial}_{\bar{j}} \mathcal{K} . \quad (\text{D.6})$$

\mathcal{K} is called the “Kähler potential”, and it is not unique because the equation above is invariant under

$$\mathcal{K} \longrightarrow \mathcal{K} + f(z) + \bar{f}(\bar{z}) . \quad (\text{D.7})$$

Ricci Form In the case of a Kähler manifold, the only non-vanishing component of the Ricci tensor is $R_{i\bar{j}}$ given by

$$R_{i\bar{j}} = -\partial_i \partial_{\bar{j}} \ln \sqrt{g} , \quad (\text{D.8})$$

where $g = \det g_{i\bar{j}}$. This allows us to define a closed real two-form, the “Ricci form”, as

$$\mathcal{R} = i R_{i\bar{j}} dz^i \wedge d\bar{z}^j . \quad (\text{D.9})$$

One can check that the Ricci form defined above is closed. However it is not exact, which implies that it defines a non-trivial class called the “first Chern class”. The latter is invariant under smooth changes of the metric $g \rightarrow g + \delta g$.

Calabi-Yau Manifold A Calabi-Yau manifold is a compact Ricci flat Kähler manifold. Ricci flat means that the associated Ricci tensor vanishes. This turns out to be equivalent to either of the two requirements:

- There exists a nowhere vanishing holomorphic $(n, 0)$ -form Ω .
- The holonomy of the Kähler manifold is a subgroup of $\text{SU}(n)$

where n is the complex dimension of our Calabi-Yau.

D.2 COHOMOLOGY OF CALABI-YAU MANIFOLDS

The existence of a complex structure allows us to introduce complex coordinates, as well as a refinement of the notion of p-forms. In this case, we have a double grading of forms; the “ (p, q) -forms” α . Locally, they can be written as:

$$\alpha^{(p,q)} \sim \alpha_{i_1 \dots i_p \bar{j}_1 \dots \bar{j}_q} dz^{i_1} \wedge \dots \wedge dz^{i_p} \wedge d\bar{z}^{\bar{j}_1} \wedge \dots \wedge d\bar{z}^{\bar{j}_q}. \quad (\text{D.10})$$

Such a refinement allows for the study of “*Dolbeault cohomology*”. Remember that “de Rham cohomology” is defined using the exterior derivative d , that maps a p -form to a $(p + 1)$ -form, as follows. The p^{th} cohomology group is the set of closed p -forms α (i.e. $d\alpha = 0$) modulo exact ones (i.e. $\alpha = d\beta$). In the same spirit, one defines now an exterior derivative $\bar{\partial}$ that maps a (p, q) -form to a $(p, q + 1)$ -form. The Dolbeault (p, q) -cohomology is defined similar to the de Rham one except that one uses $\bar{\partial}$ instead of d .

In deriving the four-dimensional effective action, the dimensions $h^{p,q}$ of (p, q) -cohomologies fix the four dimensional field content (see section D.3.2 below). On top of specifying the moduli space of Calabi-Yau deformations, they also encode information about the different form fields (RR and the NS B-field) after reduction. In the case of a simply connected Calabi-Yau threefold, cohomology dimensions can be collected in the following Hodge diamond.

$$\begin{array}{ccccccccc}
 & & h^{0,0} & & & & 1 & & \\
 & h^{1,0} & & h^{0,1} & & & 0 & & 0 \\
 h^{2,0} & & h^{1,1} & & h^{0,2} & & h^{1,1} & & 0 \\
 h^{3,0} & h^{2,1} & & h^{1,2} & & h^{0,3} & = & 1 & h^{1,2} & h^{1,2} & 1 \\
 h^{3,1} & & h^{2,2} & & h^{1,3} & & h^{1,1} & & 0 \\
 h^{3,2} & & h^{2,3} & & & & 0 & & 0 \\
 & h^{3,3} & & & & & 1 & & . \\
 \end{array} \quad (\text{D.11})$$

D.3 COMPACTIFICATION

We have seen that consistency of perturbative superstrings fixes the spacetime dimension to be ten. However, we can do physics in lower dimensions by compactifying the unwanted dimensions [197, 198]. We will restrict ourselves to the compactification of type-IIA supergravity on Calabi-Yau threefolds. For general cases see for example [199, 200], and also [201] for quick ideas about the procedure. For other approaches to get lower dimensional physics see e.g. [202].

D.3.1 SOME GENERAL REMARKS ON COMPACTIFICATION

Before getting down to the actual Calabi-Yau compactification, let us pause for a moment and discuss some general properties of compactification.

THE KALUZA-KLEIN TOWER

To get acquainted with compactification, let us take the simple theory of a massless scalar field Φ on spacetime that is a direct product of a circle S^1 of radius R with Minkowski spacetime \mathcal{M} that we are living in. Let us denote by y the coordinate on S^1 , and by x^μ the coordinates on \mathcal{M} . We start by decomposing Φ in a complete basis of functions on S^1 . In this case one gets

$$\Phi(x, y) = \sum_{n \in \mathbb{Z}} \phi_n(x) e^{i n y / (2\pi R)} \quad (\text{D.12})$$

Using this expansion, the field equation $\square \Phi = 0$ can equivalently be rewritten as a collection of infinitely many equations of the form

$$(\square_{\mathcal{M}} - \mu_n^2) \phi_n(x) = 0; \quad \mu_n = n / (2\pi R) \quad (\text{D.13})$$

One recognizes these equations as the field equations of massive scalar fields in \mathcal{M} with masses μ_n . At low energies and for small enough $R \ll 1$, we can forget about the massive tower of fields, called the “Kaluza-Klein (KK in short) tower”, and study the effective action of the resultant massless field ϕ_0 .

In general, every massless field will be accompanied by its own KK-tower, where the role of R will be played by some typical scale in the compact space. We will be dealing with small compact spaces to suppress the contributions of the massive KK-tower to the effective action of the massless fields.

THE METRIC REDUCTION AND NON-ABELIAN GAUGE FIELDS

In the following, we are going to study the reduction of the metric g_{MN} on a smooth compact manifold. To keep the discussion as general as possible, let us call y^α the coordinates of the compact manifold X , and x^μ the coordinates of the non-compact part \mathcal{M} . Let us further suppose that the compact space \mathcal{M} has an isometry group G . Such isometries are characterized by Killing vectors $\xi_a^\alpha(y)$, where a is the adjoint index of the group G . Under these assumptions, the most general form of the metric g_{MN} takes the form:

$$ds^2 = h_{\alpha\beta}(x) (dy^\alpha - A_\mu^\alpha(x) \xi_a^\alpha(y) dx^\mu) \left(dy^\beta - A_\nu^\beta(x) \xi_b^\beta(y) dx^\nu \right) + g_{\mu\nu}(x) dx^\mu dx^\nu. \quad (\text{D.14})$$

After reduction, the following fields emerge

- A metric $g_{\mu\nu}$ which gives rise to gravity.
- Several scalars coming from $h_{\alpha\beta}(x)$. Knowing the number of these scalars is the non-trivial part in this reduction.
- (Non-)Abelian gauge fields A_μ^a with gauge group G , the latter is equal to the isometry group of the compact manifold.

We are interested in Calabi-Yau threefold compactification. Let us investigate its isometries. Remember that a Killing vector κ satisfies

$$\nabla_\alpha \kappa_\beta + \nabla_\beta \kappa_\alpha = 0 , \quad (\text{D.15})$$

where ∇_α is the covariant derivative of our Calabi-Yau X . Hitting both sides of the equality by ∇^α , then using the Ricci flatness property of Calabi-Yau's leads to

$$\int \sqrt{g} \kappa^\beta \nabla^\alpha \nabla_\alpha \kappa_\beta = 0 , \quad (\text{D.16})$$

where g is the determinant of the Calabi-Yau metric $g_{\alpha\beta}$. This implies that κ is a covariantly constant vector, hence a singlet under the holonomy group. Such a vector does not exist in the case where the holonomy group of the Calabi-Yau is exactly $SU(3)$: the 6 of $SO(6)$ (vectors) transform as $3 + \bar{3}$ of $SU(3)$. In the following, we will be working with simply connected Calabi-Yau threefolds. The holonomy group of the latter is exactly $SU(3)$. This means that the ten-dimensional metric will not give rise to gauge fields after reduction.

FORMS AND (CO)HOMOLOGY

Until now, we have dealt with the metric and scalar fields. The remaining bosonic fields are form-fields. In the absence of fluxes, every n -form $C^{(n)}$ can always be written globally as

$$C^{(n)} = \bigoplus_{0 \leq p \leq n} C_X^{(p)}(y) C_{\mathcal{M}}^{(n-p)}(x) , \quad (\text{D.17})$$

where the subscript stands for the space in which the components of the form live in. Using this decomposition, the field equation $\Delta C^{(n)} = 0$ reduces to

$$\Delta_X C^{(p)} = 0 , \quad \Delta_{\mathcal{M}} C^{(n-p)} = 0 , \quad p = 0, 1, \dots, n . \quad (\text{D.18})$$

In other words we get $(n-p)$ -forms living in \mathcal{M} , with degeneracy given by the number of independent solutions of the first equation above, $\Delta_X C^{(p)} = 0$. In differential geometry, this equation specifies the p -cohomology of the manifold X (See for example [194]).

KILLING SPINORS AND THE SURVIVAL OF SUPERSYMMETRY

Since we will be dealing with bosonic solutions, preserving supersymmetry amounts to the existence of a Killing spinor. Such spinors guarantee the consistency of setting the fermions to zero with supersymmetry transformations. The defining equation of a Killing spinor takes the following schematic form

$$\delta\psi = (\Gamma \cdot \nabla + \Gamma \cdot \text{fluxes}) \epsilon = 0 \quad (\text{D.19})$$

where ∇_α is the covariant derivative and fluxes stand for possible form fluxes. Using the ansatz $\epsilon = \xi \otimes \varepsilon$ where ξ lives in the internal part of the geometry, and satisfies –due to (D.19)–

$$(\nabla_\alpha + \Gamma \text{fluxes}|_{int\alpha}) \xi \equiv \mathcal{O}_\alpha \xi = 0 \quad (\text{D.20})$$

Such an equation admits a solution if

$$[\mathcal{O}_\alpha, \mathcal{O}_\beta] \xi = (R_{\alpha\beta\gamma\delta} \Gamma^{\gamma\delta} + [\Gamma \cdot \text{fluxes}]_{\rho\sigma}) \xi = 0 \quad (\text{D.21})$$

which can be translated to constraints on the holonomy of the internal space. This is a necessary condition to have some unbroken supersymmetry after compactification. In the case of Calabi-Yau threefolds, only one quarter of the original supersymmetry survives the compactification, leading to an effective action with $\mathcal{N} = 2$ supersymmetry in four dimensions.

D.3.2 TYPE-IIA ON A CALABI-YAU

It is time to discuss our compactification. First, let us remind ourselves about the field content of type-IIA ten-dimensional supergravity. We will restrict ourselves to the bosonic part as the fermions will be added by the requirement of supersymmetry. The ten-dimensional fields are: the NS-NS fields (graviton g_{MN} , b-field b_{MN} and the dilaton ϕ), and the R-R forms (C_M and C_{MNP}). The reduction of the dilaton and forms is already done, we need just to select the appropriate information from (D.11). The only remaining task is the metric reduction. We have already done half of the work (metric + no vectors). Let us then deal with the scalar part. These are the deformations of the Calabi-Yau metric that preserve, to first order, the Ricci flatness condition. The most general metric perturbation reads

$$\delta g = \delta g_{ij} dz^i dz^j + \delta g_{i\bar{j}} dz^i d\bar{z}^j + c.c., \quad (\text{D.22})$$

where *c.c* means complex conjugate terms. The first perturbation δg_{ij} does not respect the $(1,1)$ decomposition of the metric (D.4), and turns out to describe deformations of the complex structure. Using the unique $(3,0)$ -form Ω and the inverse of

the metric $g^{i\bar{j}}$, the Ricci flatness condition implies that the form $\xi_{i\bar{j}k} = \Omega_{i\bar{j}l} g^{l\bar{k}} \delta g_{\bar{k}l}$ is harmonic. This means that the complex structure deformations give rise to $h^{1,2}$ complex scalar fields. The second perturbation $\delta g_{i\bar{j}}$, on the contrary, respects the $(1, 1)$ decomposition of the metric (D.4). It turns out that they describe the deformation of the Kähler form. Once again, Ricci flatness implies that $\delta g_{i\bar{j}}$ is harmonic. This means that the Kähler deformations lead to $h^{1,1}$ real scalars.

In the language of $\mathcal{N} = 2$ multiplets and concentrating on the bosonic content only, the reduction of type-IIA on a Calabi-Yau threefold gives rise to

- One supergravity multiplet: $g_{\mu\nu}$ and one particular linear combination of C_μ and $C_{\mu i\bar{j}}$.
- One universal hypermultiplet: C_{ijk} , ϕ and $b_{\mu\nu}$.
- $h^{1,1}$ vectormultiplets: $(b_{i\bar{j}} + i \delta g_{i\bar{j}})$ and a linear combination of the one-forms C_μ and $C_{\mu i\bar{j}}$ except the one that belongs to the supergravity multiplet.
- $h^{1,2}$ hypermultiplets: δg_{ij} and $C_{i\bar{j}k}$.

APPENDIX E

ADDING FERMIONS

The aim of this appendix is to study the structure of $(\det \partial_i \partial_j \mathcal{K})^{-1/2}$ that enters in the measure (6.25), where \mathcal{K} is given by (6.20). Already a simplification emerges due to (6.21). A careful look at this formula reveals that the only non trivial piece is $\sqrt{\partial_i \partial_j g}$ where g is given by (6.18). Our main result is

$$\det \partial_i \partial_j g = \left(\prod_{j=1}^m \frac{1}{l_j} \right) A(l) , \quad (\text{E.1})$$

where $A(l)$ is a homogeneous polynomial of order $m - n$ in the l_a (given by (6.17)) with coefficients such that for no Delzant polytopes it will contain an overall l_a factor. We will prove this in two steps. First, we will evaluate the relevant determinant to show the form (E.1) explicitly. In the second step, we explain the properties of $A(l)$, namely, that it has no poles nor contains an overall l_j factor.

E.1 CALCULATING THE DETERMINANT

It is straightforward to check, using (6.18, 6.17), that

$$\partial_i \partial_j g = \frac{1}{2} \sum_{a=1}^m \frac{m_a c_{ai} m_a c_{aj}}{l_a} = \frac{1}{2} (C^T \cdot L^{-1} \cdot C)_{ij} , \quad (\text{E.2})$$

with $C_{ai} = m_a c_{ai}$ an $m \times n$ matrix, and $L_{ab} = l_a \delta_{ab}$ an $m \times m$ matrix, which makes $C^T L^{-1} C$ a square $n \times n$ matrix. Since we are interested in the zeros and the pole structure of such a determinant, we are going to neglect over all numerical factors

in the following. The easiest way to evaluate such a determinant is to re-express it in terms of a larger symmetric $(n+m) \times (n+m)$ matrix D given by

$$D_{\alpha\beta} = \begin{cases} L_{ab} & \text{for } \alpha, \beta = 1, \dots, m. \\ C_{ai} & \text{for } \alpha = 1, \dots, m, \beta = m+1, \dots, m+n. \\ 0 & \text{for } \alpha, \beta = m+1, \dots, m+n. \end{cases} \quad (\text{E.3})$$

Now using that L is diagonal and $\det(\partial_i \partial_j g) = \det D / \det L$, it is easy to show that

$$\det(C^T L^{-1} C) = \left(\prod_{j=1}^m l_j^{-1} \right) \left(\sum_S l^S (\det C_S)^2 \right), \quad (\text{E.4})$$

which has the same structure as (E.1). In the second factor, the sum is over all different subsets $S \subset \{1, \dots, m\}$ with $m-n$ elements, i.e. $\#S = m-n$. Furthermore, we use the shorthand $l^S := \prod_{a \in S} l_a$. Finally, there is the definition of the $n \times n$ matrix C_S . Note that C was an $m \times n$ matrix, C_S is now defined as the matrix C but with the a_1, \dots, a_{m-n} 'th rows removed where $S = \{a_1, \dots, a_{m-n}\}$.

E.2 PROPERTIES OF $A(l)$

In the following, we are going to show that $A(l) = \sum_S l^S (\det C_S)^2$ has no poles nor does it contain an overall l_a factor. As is clear from its definition, $A(l)$ is a homogeneous polynomial of order $m-n$ in x^i , and hence has no pole in x^i . Let us now turn to the second property. Without loss of generality, let us show the absence of an overall factor l_1 . A moment thought translates such property to the non vanishing of at least one $\det C_{\tilde{S}}$ with $1 \notin \tilde{S}$, which can be shown using some basic properties of C and $C_{\tilde{S}}$.

By the definition of the C_S , all the $C_{\tilde{S}}$ include the first row of C , given by c_{1i} . Furthermore, using the geometric interpretation of c_{ai} below (6.14), the statement $\exists \tilde{S}_* \mid \det C_{\tilde{S}_*} \neq 0$ translates to: “there exists a set of $(n-1)$ vectors among the m different normals \vec{c}_a that together with \vec{c}_1 form a basis of \mathbb{R}^n ”. We will use the notation \vec{c}_α for these n vectors and now show their existence.

Pick one of the vertices that is a corner of the facet orthogonal to \vec{c}_1 and let's call it v_1 . As the polytopes of our interest are Delzant, there are exactly n edges \vec{e}_α meeting in the vertex v_1 , that furthermore form a basis of \mathbb{R}^n . Now, the different facets meeting in v_1 each lie in a subspace generated by a set of $(n-1)$ of the n edges e_α . So, we find n facets that all meet in the vertex v_1 . Let us label the n normals to these facets as \vec{c}_α , by their definition they can be labelled such that they satisfy $\vec{e}_\alpha \cdot \vec{c}_\beta \sim \delta_{\alpha\beta}$. So, we see that the \vec{c}_α form a basis of \mathbb{R}^n that includes \vec{c}_1 , which concludes the proof i.e. we now know that $\det C_{\tilde{S}_*} \neq 0$ for $(C_{\tilde{S}_*})_{ai} = c_{\alpha i}$.

APPENDIX F

THE THREE-CENTER SOLUTION SPACE

In this appendix, we will analyze some properties of the moduli space of three-center solutions. Our starting point will be the set of equations (6.37), which we will rewrite as follows

$$\begin{aligned}\frac{a}{x} - \frac{b}{y} &= c_2 - c_1 . \\ \frac{b}{y} - \frac{c}{z} &= c_3 - c_2 . \\ \frac{c}{z} - \frac{a}{x} &= c_1 - c_3 .\end{aligned}\tag{F.1}$$

Here a, b, c represent the inner products $\langle \Gamma_a, \Gamma_b \rangle$, x, y, z are the lengths of the three sides of the triangle spanned by \vec{x}_a , and $c_2 - c_1 = \langle h, \Gamma_1 \rangle$ etc. The constants c_a are not uniquely fixed, as we shift them by a fixed amount without modifying the above equations. Still, expressing things in terms of c_a allows for a somewhat more symmetric treatment.

The first important remark is that up to an $SO(3)$ rotation, x, y, z uniquely determine the solution. In other words, the quotient of the solution space by $SO(3)$ is precisely the set of solutions x, y, z of (F.1).

Second, we should keep in mind that x, y, z are the sides of a triangle, i.e. they should be nonnegative numbers that satisfy the triangle inequality $x + y \geq z$ and its cyclic permutations.

In our discussion of the solution space quantization, the size of angular momentum

will play an important role, as we will use it as a coordinate on the solution space. In terms of the variables used in (F.1), the norm of the angular momentum is given by (see (5.43))

$$J^2 = -\frac{1}{4} (x^2(c_2 - c_1)(c_1 - c_3) + y^2(c_3 - c_2)(c_2 - c_1) + z^2(c_1 - c_3)(c_3 - c_2)) . \quad (\text{F.2})$$

We would in particular like to know whether $|J|$ is a good single-valued coordinate on the solution space, and what range of values it takes.

It is easy to write down the general solution to (F.1) in terms of a single free parameter λ :

$$x = \frac{a}{\lambda - c_1}, \quad y = \frac{b}{\lambda - c_2}, \quad z = \frac{c}{\lambda - c_3} . \quad (\text{F.3})$$

This is the general solution if a, b, c are not equal to zero. If all three are zero, or two out of three are zero, there are either no solutions to (F.1) or the space of solutions is at least two-dimensional. In either case, the symplectic form becomes degenerate and most likely these solution spaces do not give rise to BPS states. Finally, if one of a, b, c is zero, say $a = 0$, then either there are no solutions or one finds a fixed value for y, z from (F.1), while x is not constrained by (F.1). However, x is constrained by the triangle inequalities so that the solution space becomes

$$a = 0, \quad b \neq 0, \quad c \neq 0, \quad \Rightarrow y, z \text{ fixed}, \quad |y - z| \leq x \leq y + z . \quad (\text{F.4})$$

We now continue with the case where a, b, c are not equal to zero so that the solutions are of the form (F.3). We again need to distinguish a few cases. The most degenerate case is when $c_1 = c_2 = c_3$. Then either the moduli space is empty or one-dimensional, but in the latter case, the angular momentum vanishes identically everywhere on the solution space, and thus, the symplectic form is trivially degenerate.

The next case is a, b, c nonzero and two of the c_i equal to each other. Using the permutation symmetry of (F.1) and the possibility to simultaneously change the signs of a, b, c, c_i, λ , we can distinguish three different cases: (i) $c_3 > c_1 = c_2$ and $a, b, c > 0$, (ii) $c_1 = c_2 > c_3$ and $a, b, c > 0$, and (iii) $c_3 > c_1 = c_2$, $a, b > 0$ and $c < 0$. Positivity of x, y, z requires that $\lambda \in I_1 = (c_3, \infty)$ for cases (i),(ii) and $\lambda \in I_1 = (c_1, c_3)$ in case (iii). Next we denote by I_2 the set of solutions of the triangle inequalities

$$\frac{a+b}{\lambda - c_1} > \frac{c}{\lambda - c_3} > \frac{|a-b|}{\lambda - c_1} . \quad (\text{F.5})$$

It is easy (though somewhat tedious) to see that $I_1 \cap I_2$ is either empty, an interval of the form $[\lambda_-, \lambda_+]$, an interval of the form $[\lambda_-, \infty)$, an interval of the form $(c_1, \lambda_+]$, or an interval (c_1, ∞) . The endpoints λ_+ and λ_- always correspond to a point where a triangle inequality is saturated. The interval extends all the way to infinity only

if $a + b > c > |a - b|$, i.e. when a, b, c satisfy triangle inequalities, which can only happen in case (i) and (ii). In these cases, there is a scaling throat with $x, y, z \rightarrow 0$. Actually, this can possibly also happen when $a + b = c$ or $c = |a - b|$. The interval starts at c_1 only if we are in case (ii) or (iii) and $a = b$, and in this case the solution space includes configurations where a center can move off to infinity.

From the point of view of angular momentum, the case where one of the centers moves away to infinity (e.g. $x, y \rightarrow \infty$) can be viewed as a case where the triangle inequalities $x + z \geq y$ and $y + z \geq x$ are both saturated. Therefore, in all cases we have analyzed so far, the solution space contained just a single connected component described by a single interval of possible values of λ , and at the endpoints of the interval either one has a scaling solution with vanishing angular momentum, or a solution that saturates at least one triangle inequality. Whenever this happens, we always find that

$$|J|^2 = \frac{1}{4}(\pm a + \pm b + \pm c)^2, \quad (\text{F.6})$$

for suitable choices of the signs, as can be seen easily e.g. from (5.42).

It remains to analyze the generic case with all c_i different from each other. Up to an overall sign flip and a permutation, there are two cases, which are (iv) $c_1 < c_2 < c_3$ and $a, b, c > 0$ and (v) $c_1 < c_2 < c_3$ and $a, b > 0, c < 0$. Positivity of x, y, z in case (iv) implies $\lambda > c_3$ and implies $c_2 < \lambda < c_3$ in case (v). The main problem is to analyze the triangle inequalities. They can be analyzed qualitatively by sketching $x + y - z$, $x - y + z$ and $-x + y + z$ as a function of λ . We know that each of these functions can have at most two zeroes as a function of λ , and we know its behavior near the three poles at $\lambda = c_1, c_2, c_3$. We will skip the details, but one finds that the moduli space consists of at most two components, each of which corresponds to a certain interval of possible values of λ . At the boundaries of each interval a triangle inequality is saturated. Notice that in case (iv) one of the components can be of the form $[\lambda_-, \infty)$. This is possible whenever a, b, c themselves satisfy triangle inequalities. If this happens, at $\lambda = \infty$ there is a scaling solution.

To summarize, the solution space in all cases consists of at most two components, corresponding to two intervals of possible values of λ . At the endpoints of the interval some triangle inequality is saturated. This can include configurations where one of the centers moves off to infinity (cases (ii) and (iii) above, with $a = b$), and scaling solutions where $\lambda \rightarrow \infty$ (cases (i), (ii) and (iv) with a, b, c obeying triangle inequalities).

Finally, we would like to show that J^2 is a good coordinate on each component of the moduli space of solutions to (F.1). In order to do so, we compute $dJ^2/d\lambda$. According to (F.3), $dx/d\lambda = -x^2/a$ and similarly for y, z . If we differentiate (F.2), use these relations, and finally replace c_i by the left hand side of the original equations (F.1),

we obtain

$$2 \frac{dJ^2}{d\lambda} = \frac{x^3}{a} \left(\frac{a}{x} - \frac{b}{y} \right) \left(\frac{c}{z} - \frac{a}{x} \right) + \frac{y^3}{b} \left(\frac{b}{y} - \frac{c}{z} \right) \left(\frac{a}{x} - \frac{b}{y} \right) + \frac{z^3}{c} \left(\frac{c}{z} - \frac{a}{x} \right) \left(\frac{b}{y} - \frac{c}{z} \right). \quad (\text{F.7})$$

We rewrite this as

$$-2abcxyz \frac{dJ^2}{d\lambda} = n_0 a^2 + n_1 a + n_2 = n_0 \left(a + \frac{n_1}{2n_0} \right)^2 + \frac{4n_2 n_0 - n_1^2}{4n_0}, \quad (\text{F.8})$$

with n_0, n_1, n_2 certain a -independent polynomials. The right hand side of (F.8) is positive if n_0 and $4n_2 n_0 - n_1^2$ are positive. By explicit computation we find

$$\begin{aligned} n_0 &= \left(z^2 b + \frac{cy}{2z} (x^2 - y^2 - z^2) \right)^2 + \frac{c^2 y^2}{4z^2} \theta, \\ 4n_2 n_0 - n_1^2 &= b^2 c^2 x^2 (bz - cy)^2 \theta, \end{aligned} \quad (\text{F.9})$$

where

$$\theta = (x + y + z)(x + y - z)(x - y + z)(-x + y + z). \quad (\text{F.10})$$

Since $\theta > 0$ if all triangle inequalities are satisfied, we have indeed shown that J^2 is a monotonous function of λ and that J^2 is a good coordinate on each component of the solution space.

BIBLIOGRAPHY

- [1] S. W. Hawking, *Particle Creation by Black Holes*, *Commun. Math. Phys.* **43** (1975) 199–220.
- [2] P. K. Townsend, *Black holes*, gr-qc/9707012.
- [3] J. M. Bardeen, B. Carter and S. W. Hawking, *The Four laws of black hole mechanics*, *Commun. Math. Phys.* **31** (1973) 161–170.
- [4] S. W. Hawking, *Black Holes and Thermodynamics*, *Phys. Rev.* **D13** (1976) 191–197.
- [5] R. Emparan and H. S. Reall, *A rotating black ring in five dimensions*, *Phys. Rev. Lett.* **88** (2002) 101101 [hep-th/0110260].
- [6] H. Elvang, R. Emparan, D. Mateos and H. S. Reall, *Supersymmetric black rings and three-charge supertubes*, *Phys. Rev.* **D71** (2005) 024033 [hep-th/0408120].
- [7] G. 't Hooft, *Dimensional reduction in quantum gravity*, gr-qc/9310026.
- [8] L. Susskind, *The World as a hologram*, *J. Math. Phys.* **36** (1995) 6377–6396 [hep-th/9409089].
- [9] J. M. Maldacena, *The large n limit of superconformal field theories and supergravity*, *Adv. Theor. Math. Phys.* **2** (1998) 231–252 [hep-th/9711200].
- [10] S. W. Hawking, *Breakdown of Predictability in Gravitational Collapse*, *Phys. Rev.* **D14** (1976) 2460–2473.
- [11] S. D. Mathur, *What Exactly is the Information Paradox?*, arXiv:0803.2030 [hep-th].
- [12] R. Penrose, *Gravitational collapse: The role of general relativity*, *Riv. Nuovo Cim.* **1** (1969) 252–276.
- [13] R. M. Wald, *Gravitational collapse and cosmic censorship*, gr-qc/9710068.

Bibliography

- [14] P. S. Joshi, *Cosmic Censorship: A Current Perspective*, gr-qc/0206087.
- [15] B. de Wit, *Black Hole Entropy, talk given during the Postgraduate AIO/OIO School (THEP)* (2006) Driebergen, the Netherlands.
- [16] A. Strominger and C. Vafa, *Microscopic origin of the bekenstein-hawking entropy*, *Phys. Lett.* **B379** (1996) 99–104 [hep-th/9601029].
- [17] J. M. Maldacena and A. Strominger, *Ads(3) black holes and a stringy exclusion principle*, *JHEP* **12** (1998) 005 [hep-th/9804085].
- [18] J. M. Maldacena, *Black holes in string theory*, hep-th/9607235.
- [19] D. Youm, *Black holes and solitons in string theory*, *Phys. Rept.* **316** (1999) 1–232 [hep-th/9710046].
- [20] E. T. Akhmedov, *Black hole thermodynamics from the point of view of superstring theory*, *Int. J. Mod. Phys.* **A15** (2000) 1–44 [hep-th/9711153].
- [21] R. D'Auria and P. Fre, *BPS black holes in supergravity: Duality groups, p-branes, central charges and the entropy*, hep-th/9812160.
- [22] T. Mohaupt, *Black hole entropy, special geometry and strings*, *Fortsch. Phys.* **49** (2001) 3–161 [hep-th/0007195].
- [23] A. W. Peet, *TASI lectures on black holes in string theory*, hep-th/0008241.
- [24] J. R. David, G. Mandal and S. R. Wadia, *Microscopic formulation of black holes in string theory*, *Phys. Rept.* **369** (2002) 549–686 [hep-th/0203048].
- [25] L. Susskind and J. Lindesay, *An introduction to black holes, information and the string theory revolution: The holographic universe*, . Hackensack, USA: World Scientific (2005) 183 p.
- [26] A. Dabholkar, F. Denef, G. W. Moore and B. Pioline, *Precision counting of small black holes*, *JHEP* **10** (2005) 096 [hep-th/0507014].
- [27] B. Pioline, *Lectures on black holes, topological strings and quantum attractors*, *Class. Quant. Grav.* **23** (2006) S981 [hep-th/0607227].
- [28] P. Kraus, *Lectures on black holes and the ads(3)/cft(2) correspondence*, hep-th/0609074.
- [29] L. Andrianopoli, R. D'Auria, S. Ferrara and M. Trigiante, *Extremal black holes in supergravity*, *Lect. Notes Phys.* **737** (2008) 661–727 [hep-th/0611345].
- [30] F. Denef and G. W. Moore, *Split states, entropy enigmas, holes and halos*, hep-th/0702146.

Bibliography

- [31] A. Sen, *Black Hole Entropy Function, Attractors and Precision Counting of Microstates*, 0708.1270.
- [32] O. Lunin and S. D. Mathur, *Ads/cft duality and the black hole information paradox*, *Nucl. Phys.* **B623** (2002) 342–394 [hep-th/0109154].
- [33] O. Lunin and S. D. Mathur, *Statistical interpretation of bekenstein entropy for systems with a stretched horizon*, *Phys. Rev. Lett.* **88** (2002) 211303 [hep-th/0202072].
- [34] S. D. Mathur, *A proposal to resolve the black hole information paradox*, *Int. J. Mod. Phys.* **D11** (2002) 1537–1540 [hep-th/0205192].
- [35] O. Lunin, S. D. Mathur and A. Saxena, *What is the gravity dual of a chiral primary?*, *Nucl. Phys.* **B655** (2003) 185–217 [hep-th/0211292].
- [36] S. D. Mathur, *The fuzzball proposal for black holes: An elementary review*, *Fortsch. Phys.* **53** (2005) 793–827 [hep-th/0502050].
- [37] S. D. Mathur, *The quantum structure of black holes*, *Class. Quant. Grav.* **23** (2006) R115 [hep-th/0510180].
- [38] I. Bena and N. P. Warner, *Black holes, black rings and their microstates*, hep-th/0701216.
- [39] K. Skenderis and M. Taylor, *The fuzzball proposal for black holes*, 0804.0552.
- [40] V. Balasubramanian, J. de Boer, S. El-Showk and I. Messamah, *Black Holes as Effective Geometries*, *Class. Quant. Grav.* **25** (2008) 214004 [0811.0263].
- [41] T. Jacobson, *Introduction to quantum fields in curved spacetime and the Hawking effect*, gr-qc/0308048.
- [42] L. H. Ford, *Quantum field theory in curved spacetime*, gr-qc/9707062.
- [43] W. G. Unruh, *Origin of the Particles in Black Hole Evaporation*, *Phys. Rev.* **D15** (1977) 365–369.
- [44] W. G. Unruh, *Notes on black hole evaporation*, *Phys. Rev.* **D14** (1976) 870.
- [45] T. Jacobson, *Thermodynamics of space-time: The Einstein equation of state*, *Phys. Rev. Lett.* **75** (1995) 1260–1263 [gr-qc/9504004].
- [46] T. Elster, *VACUUM POLARIZATION NEAR A BLACK HOLE CREATING PARTICLES*, *Phys. Lett.* **A94** (1983) 205–209.
- [47] B. P. Jensen, J. McLaughlin and A. C. Ottewill, *Renormalized electromagnetic stress tensor for an evaporating black hole*, *Phys. Rev.* **D43** (1991) 4142–4144.

Bibliography

- [48] S. J. Gates, M. T. Grisaru, M. Rocek and W. Siegel, *Superspace, or one thousand and one lessons in supersymmetry*, *Front. Phys.* **58** (1983) 1–548 [hep-th/0108200].
- [49] P. C. West, *Introduction to supersymmetry and supergravity*, . Singapore, Singapore: World Scientific (1990) 425 p.
- [50] J. Wess and J. Bagger, *Supersymmetry and supergravity*, . Princeton, USA: Univ. Pr. (1992) 259 p.
- [51] I. L. Buchbinder and S. M. Kuzenko, *Ideas and methods of supersymmetry and supergravity: A Walk through superspace*, . Bristol, UK: IOP (1995) 640 p.
- [52] S. R. Coleman and J. Mandula, *ALL POSSIBLE SYMMETRIES OF THE S MATRIX*, *Phys. Rev.* **159** (1967) 1251–1256.
- [53] Y. A. Golfand and E. P. Likhtman, *Extension of the Algebra of Poincare Group Generators and Violation of p Invariance*, *JETP Lett.* **13** (1971) 323–326.
- [54] E. Witten, *Constraints on Supersymmetry Breaking*, *Nucl. Phys.* **B202** (1982) 253.
- [55] N. Seiberg and E. Witten, *Electric - magnetic duality, monopole condensation, and confinement in $N=2$ supersymmetric Yang-Mills theory*, *Nucl. Phys.* **B426** (1994) 19–52 [hep-th/9407087].
- [56] J. de Boer, S. El-Showk, I. Messamah and D. V. d. Bleeken, *Quantizing $N=2$ Multicenter Solutions*, 0807.4556.
- [57] A. Dabholkar, *Exact counting of black hole microstates*, *Phys. Rev. Lett.* **94** (2005) 241301 [hep-th/0409148].
- [58] A. Dabholkar, R. Kallosh and A. Maloney, *A stringy cloak for a classical singularity*, *JHEP* **12** (2004) 059 [hep-th/0410076].
- [59] A. Sen, *How does a fundamental string stretch its horizon?*, *JHEP* **05** (2005) 059 [hep-th/0411255].
- [60] A. Dabholkar, F. Denef, G. W. Moore and B. Pioline, *Exact and Asymptotic Degeneracies of Small Black Holes*, *JHEP* **08** (2005) 021 [hep-th/0502157].
- [61] A. Sen, *Stretching the horizon of a higher dimensional small black hole*, *JHEP* **07** (2005) 073 [hep-th/0505122].
- [62] D. Gaiotto, A. Strominger and X. Yin, *New connections between 4d and 5d black holes*, *JHEP* **02** (2006) 024 [hep-th/0503217].
- [63] M. C. N. Cheng, *More bubbling solutions*, *JHEP* **03** (2007) 070 [hep-th/0611156].

Bibliography

- [64] J. de Boer, F. Denef, S. El-Showk, I. Messamah and D. Van den Bleeken, *Black hole bound states in $AdS_3 \times S^2$* , arXiv:0802.2257 [hep-th].
- [65] N. Iizuka and M. Shigemori, *A note on d1-d5-j system and 5d small black ring*, *JHEP* **08** (2005) 100 [hep-th/0506215].
- [66] L. F. Alday, J. de Boer and I. Messamah, *What is the dual of a dipole?*, *Nucl. Phys.* **B746** (2006) 29–57 [hep-th/0511246].
- [67] R. Emparan, *Rotating circular strings, and infinite non-uniqueness of black rings*, *JHEP* **03** (2004) 064 [hep-th/0402149].
- [68] K. Copsey and G. T. Horowitz, *The role of dipole charges in black hole thermodynamics*, *Phys. Rev.* **D73** (2006) 024015 [hep-th/0505278].
- [69] O. Lunin and S. D. Mathur, *Metric of the multiply wound rotating string*, *Nucl. Phys.* **B610** (2001) 49–76 [hep-th/0105136].
- [70] V. Balasubramanian, P. Kraus and M. Shigemori, *Massless black holes and black rings as effective geometries of the d1-d5 system*, *Class. Quant. Grav.* **22** (2005) 4803–4838 [hep-th/0508110].
- [71] A. Dabholkar, N. Iizuka, A. Iqbal and M. Shigemori, *Precision microstate counting of small black rings*, *Phys. Rev. Lett.* **96** (2006) 071601 [hep-th/0511120].
- [72] A. Dabholkar, N. Iizuka, A. Iqbal, A. Sen and M. Shigemori, *Spinning strings as small black rings*, *JHEP* **04** (2007) 017 [hep-th/0611166].
- [73] V. Balasubramanian, J. de Boer, V. Jejjala and J. Simon, *The library of babel: On the origin of gravitational thermodynamics*, *JHEP* **12** (2005) 006 [hep-th/0508023].
- [74] H. Lin, O. Lunin and J. M. Maldacena, *Bubbling ads space and 1/2 bps geometries*, *JHEP* **10** (2004) 025 [hep-th/0409174].
- [75] S. Mathur, *The fuzzball paradigm for black holes: FAQ*, <http://www.physics.ohio-state.edu/~mathur/faq.pdf>.
- [76] V. Balasubramanian, B. Czech, V. E. Hubeny, K. Larjo, M. Rangamani and J. Simon, *Typicality versus thermality: An analytic distinction*, *Gen. Rel. Grav.* **40** (2008) 1863–1890 [hep-th/0701122].
- [77] P. Dedecker, *Calcul des variations, formes différentielles et champs géodésiques*, Geometrie différentielle, Colloq. Intern. du CNRS LII, Strasbourg (1953) 17–34.
- [78] S. Raju, *Counting giant gravitons in $ads(3)$* , arXiv:0709.1171 [hep-th].

Bibliography

- [79] C. Crnkovic and E. Witten, *Covariant description of canonical formalism in geometrical theories*, . Print-86-1309 (PRINCETON).
- [80] G. J. Zuckerman, *Action principles and global geometry*, . Print-89-0321 (YALE).
- [81] J. Lee and R. M. Wald, *Local symmetries and constraints*, *J. Math. Phys.* **31** (1990) 725–743.
- [82] B. Julia and S. Silva, *On covariant phase space methods*, hep-th/0205072.
- [83] L. Maoz and V. S. Rychkov, *Geometry quantization from supergravity: The case of 'bubbling ads'*, *JHEP* **08** (2005) 096 [hep-th/0508059].
- [84] R. L. Arnowitt, S. Deser and C. W. Misner, *The dynamics of general relativity*, gr-qc/0405109.
- [85] F. Denef, *Quantum quivers and hall/hole halos*, *JHEP* **10** (2002) 023 [hep-th/0206072].
- [86] S. T. Ali and M. Englis, *Quantization methods: A guide for physicists and analysts*, *Rev. Math. Phys.* **17** (2005) 391–490 [math-ph/0405065].
- [87] A. Donos and A. Jevicki, *Dynamics of chiral primaries in $ads(3) \times s^{**3} \times t^{**4}$* , *Phys. Rev.* **D73** (2006) 085010 [hep-th/0512017].
- [88] V. S. Rychkov, *D1-d5 black hole microstate counting from supergravity*, *JHEP* **01** (2006) 063 [hep-th/0512053].
- [89] M. Blau, *Symplectic geometry and geometric quantization*, .
<http://www.blau.itp.unibe.ch/lecturesGQ.ps.gz>.
- [90] A. Echeverria-Enriquez, M. C. Munoz-Lecanda, N. Roman-Roy and C. Victoria-Monge, *Mathematical foundations of geometric quantization*, *Extracta Math.* **13** (1998) 135–238 [math-ph/9904008].
- [91] W. G. Ritter, *Geometric quantization*, math-ph/0208008.
- [92] M. Hillery, R. F. O'Connell, M. O. Scully and E. P. Wigner, *Distribution functions in physics: Fundamentals*, *Phys. Rept.* **106** (1984) 121–167.
- [93] G. Mandal, S. Raju and M. Smedback, *Supersymmetric Giant Graviton Solutions in AdS_3* , *Phys. Rev.* **D77** (2008) 046011 [arXiv:0709.1168 [hep-th]].
- [94] A. A. Tseytlin, *Harmonic superpositions of M-branes*, *Nucl. Phys.* **B475** (1996) 149–163 [hep-th/9604035].

Bibliography

- [95] J. P. Gauntlett, D. A. Kastor and J. H. Traschen, *Overlapping Branes in M-Theory*, *Nucl. Phys.* **B478** (1996) 544–560 [hep-th/9604179].
- [96] T. Mohaupt, *Black holes in supergravity and string theory*, *Class. Quant. Grav.* **17** (2000) 3429–3482 [hep-th/0004098].
- [97] O. Lunin, J. M. Maldacena and L. Maoz, *Gravity solutions for the d1-d5 system with angular momentum*, hep-th/0212210.
- [98] C. G. Callan, J. M. Maldacena and A. W. Peet, *Extremal Black Holes As Fundamental Strings*, *Nucl. Phys.* **B475** (1996) 645–678 [hep-th/9510134].
- [99] A. Dabholkar, J. P. Gauntlett, J. A. Harvey and D. Waldram, *Strings as Solitons and Black Holes as Strings*, *Nucl. Phys.* **B474** (1996) 85–121 [hep-th/9511053].
- [100] A. A. Tseytlin, *Generalised chiral null models and rotating string backgrounds*, *Phys. Lett.* **B381** (1996) 73–80 [hep-th/9603099].
- [101] M. Taylor, *General 2 charge geometries*, *JHEP* **03** (2006) 009 [hep-th/0507223].
- [102] I. Kanitscheider, K. Skenderis and M. Taylor, *Fuzzballs with internal excitations*, *JHEP* **06** (2007) 056 [arXiv:0704.0690 [hep-th]].
- [103] K. Skenderis and M. Taylor, *Fuzzball solutions and D1-D5 microstates*, *Phys. Rev. Lett.* **98** (2007) 071601 [hep-th/0609154].
- [104] I. Kanitscheider, K. Skenderis and M. Taylor, *Holographic anatomy of fuzzballs*, *JHEP* **04** (2007) 023 [hep-th/0611171].
- [105] E. P. Wigner, *On the quantum correction for thermodynamic equilibrium*, *Phys. Rev.* **40** (1932) 749–760.
- [106] L. F. Alday, J. de Boer and I. Messamah, *The gravitational description of coarse grained microstates*, *JHEP* **12** (2006) 063 [hep-th/0607222].
- [107] K. Larjo, *On the existence of supergravity duals to d1-d5 cft states*, *JHEP* **07** (2007) 041 [arXiv:0705.4433 [hep-th]].
- [108] S. D. Mathur, *Black hole size and phase space volumes*, arXiv:0706.3884 [hep-th].
- [109] V. Balasubramanian, J. de Boer, E. Keski-Vakkuri and S. F. Ross, *Supersymmetric conical defects: Towards a string theoretic description of black hole formation*, *Phys. Rev.* **D64** (2001) 064011 [hep-th/0011217].
- [110] J. M. Maldacena and L. Maoz, *De-singularization by rotation*, *JHEP* **12** (2002) 055 [hep-th/0012025].

Bibliography

- [111] V. Jejjala, O. Madden, S. F. Ross and G. Titchener, *Non-supersymmetric smooth geometries and D1-D5-P bound states*, *Phys. Rev.* **D71** (2005) 124030 [hep-th/0504181].
- [112] V. Cardoso, O. J. C. Dias, J. L. Hovdebo and R. C. Myers, *Instability of non-supersymmetric smooth geometries*, *Phys. Rev.* **D73** (2006) 064031 [hep-th/0512277].
- [113] E. G. Gimon, T. S. Levi and S. F. Ross, *Geometry of non-supersymmetric three-charge bound states*, *JHEP* **08** (2007) 055 [arXiv:0705.1238 [hep-th]].
- [114] S. Giusto, S. F. Ross and A. Saxena, *Non-supersymmetric microstates of the D1-D5-KK system*, *JHEP* **12** (2007) 065 [arXiv:0708.3845 [hep-th]].
- [115] B. D. Chowdhury and S. D. Mathur, *Radiation from the non-extremal fuzzball*, arXiv:0711.4817 [hep-th].
- [116] D. Gaiotto, A. Simons, A. Strominger and X. Yin, *D0-branes in black hole attractors*, hep-th/0412179.
- [117] D. Gaiotto, A. Strominger and X. Yin, *Superconformal black hole quantum mechanics*, *JHEP* **11** (2005) 017 [hep-th/0412322].
- [118] F. Denef, D. Gaiotto, A. Strominger, D. Van den Bleeken and X. Yin, *Black hole deconstruction*, hep-th/0703252.
- [119] B. de Wit, P. G. Lauwers and A. Van Proeyen, *Lagrangians of N=2 Supergravity - Matter Systems*, *Nucl. Phys.* **B255** (1985) 569.
- [120] I. Bena and N. P. Warner, *One ring to rule them all ... and in the darkness bind them?*, *Adv. Theor. Math. Phys.* **9** (2005) 667–701 [hep-th/0408106].
- [121] K. Behrndt, A. H. Chamseddine and W. A. Sabra, *BPS black holes in $N = 2$ five dimensional AdS supergravity*, *Phys. Lett.* **B442** (1998) 97–101 [hep-th/9807187].
- [122] F. Denef, *Supergravity flows and d-brane stability*, *JHEP* **08** (2000) 050 [hep-th/0005049].
- [123] B. Bates and F. Denef, *Exact solutions for supersymmetric stationary black hole composites*, hep-th/0304094.
- [124] V. Balasubramanian, E. G. Gimon and T. S. Levi, *Four Dimensional Black Hole Microstates: From D-branes to Spacetime Foam*, *JHEP* **01** (2008) 056 [hep-th/0606118].
- [125] P. S. Aspinwall, *Compactification, geometry and duality: $N = 2$* , hep-th/0001001.

Bibliography

- [126] T. Mohaupt, *Supersymmetric black holes in string theory*, *Fortsch. Phys.* **55** (2007) 519–544 [hep-th/0703035].
- [127] S. Ferrara, R. Kallosh and A. Strominger, *$N=2$ extremal black holes*, *Phys. Rev.* **D52** (1995) 5412–5416 [hep-th/9508072].
- [128] M. Huebscher, P. Meessen and T. Ortin, *Supersymmetric solutions of $N = 2$ $d = 4$ SUGRA: The whole ungauged shebang*, *Nucl. Phys.* **B759** (2006) 228–248 [hep-th/0606281].
- [129] P. Candelas and X. de la Ossa, *MODULI SPACE OF CALABI-YAU MANIFOLDS*, *Nucl. Phys.* **B355** (1991) 455–481.
- [130] M. Bodner, A. C. Cadavid and S. Ferrara, *(2,2) vacuum configurations for type IIA superstrings: $N=2$ supergravity Lagrangians and algebraic geometry*, *Class. Quant. Grav.* **8** (1991) 789–808.
- [131] T. W. Grimm and J. Louis, *The effective action of type IIA Calabi-Yau orientifolds*, *Nucl. Phys.* **B718** (2005) 153–202 [hep-th/0412277].
- [132] A. Strominger, *Yukawa Couplings in Superstring Compactification*, *Phys. Rev. Lett.* **55** (1985) 2547.
- [133] A. Strominger, *SPECIAL GEOMETRY*, *Commun. Math. Phys.* **133** (1990) 163–180.
- [134] B. Craps, F. Roose, W. Troost and A. Van Proeyen, *What is special Kaehler geometry?*, *Nucl. Phys.* **B503** (1997) 565–613 [hep-th/9703082].
- [135] J. Louis, J. Sonnenschein, S. Theisen and S. Yankielowicz, *Non-perturbative properties of heterotic string vacua compactified on $K3 \times T^{*2}$* , *Nucl. Phys.* **B480** (1996) 185–212 [hep-th/9606049].
- [136] K. Behrndt *et. al.*, *Classical and quantum $N=2$ supersymmetric black holes*, *Nucl. Phys.* **B488** (1997) 236–260 [hep-th/9610105].
- [137] M. Billo *et. al.*, *The 0-brane action in a general $D = 4$ supergravity background*, *Class. Quant. Grav.* **16** (1999) 2335–2358 [hep-th/9902100].
- [138] K. p. Tod, *All Metrics Admitting Supercovariantly Constant Spinors*, *Phys. Lett.* **B121** (1983) 241–244.
- [139] K. P. Tod, *More on supercovariantly constant spinors*, *Class. Quant. Grav.* **12** (1995) 1801–1820.
- [140] S. Ferrara and R. Kallosh, *Supersymmetry and Attractors*, *Phys. Rev.* **D54** (1996) 1514–1524 [hep-th/9602136].

Bibliography

- [141] S. Ferrara, G. W. Gibbons and R. Kallosh, *Black holes and critical points in moduli space*, *Nucl. Phys.* **B500** (1997) 75–93 [hep-th/9702103].
- [142] G. W. Moore, *Attractors and arithmetic*, hep-th/9807056.
- [143] G. W. Moore, *Arithmetic and attractors*, hep-th/9807087.
- [144] M. Shmakova, *Calabi-yau black holes*, *Phys. Rev.* **D56** (1997) 540–544 [hep-th/9612076].
- [145] G. Lopes Cardoso, B. de Wit, J. Kappeli and T. Mohaupt, *Stationary BPS solutions in $N = 2$ supergravity with R^{**2} interactions*, *JHEP* **12** (2000) 019 [hep-th/0009234].
- [146] K. Behrndt, D. Lust and W. A. Sabra, *Stationary solutions of $N = 2$ supergravity*, *Nucl. Phys.* **B510** (1998) 264–288 [hep-th/9705169].
- [147] F. Denef, *On the correspondence between D-branes and stationary supergravity solutions of type II Calabi-Yau compactifications*, hep-th/0010222.
- [148] F. Denef, *(Dis)assembling special Lagrangians*, hep-th/0107152.
- [149] P. Berglund, E. G. Gimon and T. S. Levi, *Supergravity microstates for bps black holes and black rings*, *JHEP* **06** (2006) 007 [hep-th/0505167].
- [150] I. Bena and N. P. Warner, *Bubbling supertubes and foaming black holes*, *Phys. Rev.* **D74** (2006) 066001 [hep-th/0505166].
- [151] L. Grant, L. Maoz, J. Marsano, K. Papadodimas and V. S. Rychkov, *Minisuperspace quantization of 'bubbling ads' and free fermion droplets*, *JHEP* **08** (2005) 025 [hep-th/0505079].
- [152] G. M. Tuynman, *QUANTIZATION: TOWARDS A COMPARISON BETWEEN METHODS*, *J. Math. Phys.* **28** (1987) 2829–2840.
- [153] T. Banks, W. Fischler, S. H. Shenker and L. Susskind, *M theory as a matrix model: A conjecture*, *Phys. Rev.* **D55** (1997) 5112–5128 [hep-th/9610043].
- [154] S. Sethi and M. Stern, *The structure of the D0-D4 bound state*, *Nucl. Phys.* **B578** (2000) 163–198 [hep-th/0002131].
- [155] J. Polchinski, *M-theory and the light cone*, *Prog. Theor. Phys. Suppl.* **134** (1999) 158–170 [hep-th/9903165].
- [156] J. de Boer, S. El-Showk, I. Messamah and D. V. d. Bleeken, *To appear*, .
- [157] A. Cannas da Silva, *Symplectic Toric Manifolds*, .
<http://www.math.ist.utl.pt/~acannas/Books/toric.pdf>.

Bibliography

- [158] V. Guillemin, *Kaehler structures on toric varieties*, *J. Differential Geometry* **40** (1994) 285–309.
- [159] M. Abreu, *Kahler geometry of toric manifolds in symplectic coordinates*, 2000. <http://www.citebase.org/abstract?id=oai:arXiv.org:math/0004122>.
- [160] E. Lerman and S. Tolman, *Hamiltonian torus actions on symplectic orbifolds and toric varieties*, 1995. <http://www.citebase.org/abstract?id=oai:arXiv.org:dg-ga/9511008>.
- [161] M. Abreu, *Kaehler metrics on toric orbifolds*, *J. Differential Geometry* **58** (2001) 151–187.
- [162] T. Delzant, *Hamiltoniens périodiques et images convexes de l'application moment*, *Bull. Soc. Math. France* **116** (1988) 315–339. no. 3.
- [163] K. Hori *et. al.*, *Mirror symmetry*, . Providence, USA: AMS (2003) 929 p.
- [164] A. P. C. and E. F., *Supergravity solitons. 1. General framework*, *Phys. Rev. D* **37** (1988) 338.
- [165] P. C. Aichelburg and F. Embacher, *Supergravity solitons. 4. Effective soliton interaction*, *Phys. Rev. D* **37** (1988) 2132.
- [166] I. Vaisman, *Super-Geometric Quantization*, *Acta Math.* **64** (1995) 153–170.
- [167] H. B. Lawson, Jr. and M.-L. Michelsohn, *Spin geometry*, vol. 38 of *Princeton Mathematical Series*. Princeton University Press, Princeton, NJ, 1989.
- [168] P. Griffiths and J. Harris, *Principles of Algebraic Geometry*, . Wiley Classics Library. John Wiley and Sons, Inc. 1987.
- [169] I. Bena, C.-W. Wang and N. P. Warner, *Mergers and typical black hole microstates*, *JHEP* **11** (2006) 042 [[hep-th/0608217](https://arxiv.org/abs/hep-th/0608217)].
- [170] R. Dijkgraaf, *Fields, strings, matrices and symmetric products*, [hep-th/9912104](https://arxiv.org/abs/hep-th/9912104).
- [171] C. Vafa and E. Witten, *A Strong coupling test of S duality*, *Nucl. Phys. B* **431** (1994) 3–77 [[hep-th/9408074](https://arxiv.org/abs/hep-th/9408074)].
- [172] J. de Boer, *Six-dimensional supergravity on $S^{*2}3 \times AdS(3)$ and 2d conformal field theory*, *Nucl. Phys. B* **548** (1999) 139–166 [[hep-th/9806104](https://arxiv.org/abs/hep-th/9806104)].
- [173] W. Lerche, C. Vafa and N. P. Warner, *Chiral Rings in $N=2$ Superconformal Theories*, *Nucl. Phys. B* **324** (1989) 427.

Bibliography

- [174] A. Fujii, R. Kemmoku and S. Mizoguchi, *D = 5 simple supergravity on $AdS(3) \times S(2)$ and $N = 4$ superconformal field theory*, *Nucl. Phys.* **B574** (2000) 691–718 [hep-th/9811147].
- [175] D. Kutasov, F. Larsen and R. G. Leigh, *String theory in magnetic monopole backgrounds*, *Nucl. Phys.* **B550** (1999) 183–213 [hep-th/9812027].
- [176] I. Bena, C.-W. Wang and N. P. Warner, *Plumbing the abyss: Black ring microstates*, arXiv:0706.3786 [hep-th].
- [177] P. Hayden and J. Preskill, *Black holes as mirrors: quantum information in random subsystems*, *JHEP* **09** (2007) 120 [0708.4025].
- [178] H.-C. Kim, J.-W. Lee and J. Lee, *Does Information Rule the Quantum Black Hole?*, 0709.3573.
- [179] Y. Sekino and L. Susskind, *Fast Scramblers*, *JHEP* **10** (2008) 065 [0808.2096].
- [180] H. P. Yuen, *Two photon coherent states of the radiation field*, *Phys. Rev.* **A13** (1976) 2226–2243.
- [181] D. Stoler, *Equivalence classes of minimum uncertainty packets*, *Phys. Rev.* **D1** (1970) 3217–3219.
- [182] D. Stoler, *Equivalence classes of minimum-uncertainty packets. ii*, *Phys. Rev.* **D4** (1971) 1925–1926.
- [183] D. Stoler, *Generalized coherent states*, *Phys. Rev.* **D4** (1971) 2309–2312.
- [184] J. Polchinski, *String theory. Vol. 1 and 2: Superstring theory and beyond*, . Cambridge, UK: Univ. Pr. (1998).
- [185] M. B. Green, J. H. Schwarz and E. Witten, *SUPERSTRING THEORY. VOL. 1 and 2*, . Cambridge, Uk: Univ. Pr. (1987). (Cambridge Monographs On Mathematical Physics).
- [186] K. Becker, M. Becker and J. H. Schwarz, *String theory and M-theory: A modern introduction*, . Cambridge, UK: Cambridge Univ. Pr. (2007) 739 p.
- [187] M. J. Duff, R. R. Khuri and J. X. Lu, *String solitons*, *Phys. Rept.* **259** (1995) 213–326 [hep-th/9412184].
- [188] T. H. Buscher, *A Symmetry of the String Background Field Equations*, *Phys. Lett.* **B194** (1987) 59.
- [189] T. H. Buscher, *Path Integral Derivation of Quantum Duality in Nonlinear Sigma Models*, *Phys. Lett.* **B201** (1988) 466.

Bibliography

- [190] E. Bergshoeff, C. M. Hull and T. Ortin, *Duality in the type II superstring effective action*, *Nucl. Phys.* **B451** (1995) 547–578 [hep-th/9504081].
- [191] P. Meessen and T. Ortin, *An $Sl(2, \mathbb{Z})$ multiplet of nine-dimensional type II supergravity theories*, *Nucl. Phys.* **B541** (1999) 195–245 [hep-th/9806120].
- [192] C. M. Hull and P. K. Townsend, *Unity of superstring dualities*, *Nucl. Phys.* **B438** (1995) 109–137 [hep-th/9410167].
- [193] E. Witten, *String theory dynamics in various dimensions*, *Nucl. Phys.* **B443** (1995) 85–126 [hep-th/9503124].
- [194] M. Nakahara, *Geometry, topology and physics*, . Boca Raton, USA: Taylor and Francis (2003) 573 p.
- [195] T. Eguchi, P. B. Gilkey and A. J. Hanson, *Gravitation, Gauge Theories and Differential Geometry*, *Phys. Rept.* **66** (1980) 213.
- [196] B. R. Greene, *String theory on Calabi-Yau manifolds*, hep-th/9702155.
- [197] T. Kaluza, *On the Problem of Unity in Physics*, *Sitzungsber. Preuss. Akad. Wiss. Berlin (Math. Phys.)* **1921** (1921) 966–972. English Translation HUPD-8401.
- [198] O. Klein, *Quantum theory and five-dimensional theory of relativity*, *Z. Phys.* **37** (1926) 895–906.
- [199] M. J. Duff, B. E. W. Nilsson and C. N. Pope, *Kaluza-Klein Supergravity*, *Phys. Rept.* **130** (1986) 1–142.
- [200] D. Bailin and A. Love, *KALUZA-KLEIN THEORIES*, *Rept. Prog. Phys.* **50** (1987) 1087–1170.
- [201] M. J. Duff, *Kaluza-Klein theory in perspective*, hep-th/9410046.
- [202] J. M. Overduin and P. S. Wesson, *Kaluza-Klein gravity*, *Phys. Rept.* **283** (1997) 303–380 [gr-qc/9805018].

Bibliography

SUMMARY

Throughout the history of physics, trying to demystify puzzles and paradoxes was always an efficient way to uncover new faces of nature. This thesis deals with the mysterious black holes and their paradoxes. Solving the latter is believed to be an important window into the mystic theory of “*Quantum Gravity*”. In the following, we will try to give a quick taste of what has been done in this thesis.

THE ENIGMATIC BLACK HOLES

Black holes are among the physical objects that are both extensively studied and not fully understood. Since the theoretical prediction of their existence, they have always shown non-expected behavior. The classical side of their story reached its apogee with the “*no-hair theorem*” and the “*laws of black hole mechanics*”. The latter suggests that the black hole could behave like a thermodynamical object –at least at the level of formulas– provided we identify its horizon area (surface gravity) with entropy (respectively, temperature). However, the no-hair theorem (implying a vanishing black hole entropy) and the fact that black holes are black (no radiation) confined the similarity with thermodynamics to the level of formulas. A totally unexpected development in the physics of black holes occurred when Hawking studied quantum fields in the black hole background. This study revealed a new face of black holes: a “*white face*”. It turns out that black holes are not completely black as they Hawking radiate as follows. A particle anti-particle pair is produced near the horizon where the particle escapes to infinity as radiation whereas the anti-particle falls behind the horizon.

The discovery of the white face of black holes opened a Pandora box of paradoxes whose resolutions were the center of an ongoing effort for over three decades now. These paradoxes are:

- **The entropy paradox:** With the discovery of black holes radiation, the thermodynamical nature of black holes was promoted from a resemblance at the

level of formulas to a physical equivalence. In such equivalence, the black hole horizon area is identified with its entropy which led to the following two paradoxes. First of all, the no-hair theorem clearly prohibits any black hole entropy, hence, clashes with the thermodynamical nature of black holes. Secondly, the entropy being extensive would naturally be associated to a volume rather than an area as is the case of the black hole entropy.

- **Information loss paradox:** It turns out that the black hole loses its mass through radiation. The end result of radiation, baring some caveats related to trans-Planckian physics, is the complete evaporation of black holes. Since the radiated particle is correlated with the anti-particle that fell behind the horizon, such a complete evaporation of black holes results in the destruction of a part of the information leading to information loss.
- **Black hole singularity** On the contrary to the other paradoxes of black holes, this one has nothing to do with the semi-classical treatment of quantum gravity. Each black hole has a singularity where the curvature blows up. We do not know for the moment how to formulate physics laws near such region.

The thermodynamical nature of black holes on the other hand suggests that, black hole geometry could be an effective description of an underlying microscopic system. This is in the same spirit as thermodynamics is an effective description of an underlying complex microscopic system, a well established paradigm in statistical physics. Investigating such possible description of black holes in the fuzzball scenario was the main subject of this thesis.

THE UNORTHODOX FUZZBALL IDEA

Driven by the search for a better understanding of the D1-D5 system, the so called “*small black hole*”, in the framework of AdS/CFT duality, Mathur and collaborators were led to suggest an unorthodox idea that was called the “*fuzzball proposal*”. In this proposal, the black hole is conjectured to be an effective description of an exponentially large number of smooth geometries with the same asymptotic charges as the black hole. These smooth geometries are usually called “*black hole states*”, although they are not quantum states in the usual sense. In favorable circumstances, these smooth geometries are geometric manifestations of the coherent states of the underlying black hole microscopic system. The black hole states geometries only differ significantly from the naive black hole geometry in a compact region of space-time delimited by a surface dubbed the “*stretched horizon*”. Outside such a surface, all the black hole states geometries settle very quickly to the naive black hole geometry in such a way to avoid differences in measurements done with respect to either

the naive black hole geometry or a black hole state geometry.

Let us take a look at what has the fuzzball idea to say about the black hole paradoxes mentioned above.

- **The fuzzball and the entropy paradox:** In the fuzzball proposal, the number of black hole states gives, in principle, the statistical explanation of the black hole entropy. What is missing to complete the picture is a satisfactory explanation of the second part of the entropy paradox i.e. the entropy being proportional to the horizon area.
- **The fuzzball and information loss paradox:** Since the black hole states geometries are smooth, the information is not lost. The incident quantum gets trapped in the complicated black hole state geometry for a long time, but eventually escapes to infinity in a process similar to Hawking radiation. The fuzzball also predicts large quantum fluctuations of horizon size giving a possible explanation to why the semi-classical treatment breaks down.
- **The fuzzball and black hole singularity:** In the fuzzball scenario, the singularity is not there in the first place as black hole states geometries are smooth. It only emerges in the effective description of the black hole states.

What actually has been done in this thesis is the concrete realization of the idea that black holes are an effective description of some underlying microscopic system in the fuzzball scenario in some simple systems: the D1-D5 system and the 1/2-BPS black holes of the four-dimensional $\mathcal{N} = 2$ supergravity.

THE ELEGANT D1-D5 SYSTEM

The D1-D5 system turned out to be a very successful testing ground of the fuzzball ideas. Due to its simple supergravity solution, averaging over geometries was possible. By choosing appropriately the weights of the D1-D5 smooth geometries, we managed to construct average geometries that asymptotically look like the five-dimensional small black hole and small black ring. The word “small” refers to the vanishing horizon area of these black objects when restricting to the five-dimensional supergravity. Black ring, on the other hand, stands for a black object solution with horizon topology $S^2 \times S^1$ instead of S^3 , the horizon topology of a black hole. These are five-dimensional solutions, and they are the first solutions that violated the no-hair theorem as they have an extra non-conserved charge dubbed the “dipole” charge. The latter is invisible at infinity, but, nevertheless does enter in the first law of black ring mechanics.

The effective geometry that we got differs from the corresponding naive black object

geometry by an exponentially suppressed term that renders the geometry smooth at the would be singularity for the naive geometry. We have also uncovered a version of the no-hair theorem, where, we found that generically the effective geometry depends only on three charges, the mass and angular momentum both visible at infinity and a “dipole” charge that sets the size of the “core” of the geometry.

We have also found that we cannot associate weights to the D1-D5 smooth geometries in such a way to get an effective geometry into a conical defect metric with an arbitrary opening angle, except of the form “ $2\pi/n$ ” where n is an integer.

TOWARDS DOWNTOWN BLACK HOLES

Although the D1-D5 system allowed for different successful checks of some of the fuzzball ideas, it can be argued that it is too “good” to address real black hole physics questions. This is essentially due to the vanishing of its horizon area and the fact that this system is BPS with eight preserved supercharges. Since realistic black holes are out of technical reach at the moment, we opted in this thesis to make small steps towards such black holes. We chose to deal with BPS black holes with fewer preserved supersymmetries, four in our case. In doing so, we could hope also to study black holes with a macroscopically large horizon as such black holes belong to these class of BPS solutions.

It turns out that on top of the single centered black hole solutions, the $\mathcal{N} = 2$ four-dimensional supergravity admits 1/2-BPS multi-center solutions that are essentially a bound state of black holes. In this thesis we described a quantization procedure of these solutions. Such a quantization allowed us to count the number of BPS states related to the external degrees of freedom of these solutions. Although, the quantization was carried out only for a restricted class of multi-center solutions that share the same mathematical properties, this class includes interesting multi-center solutions that were argued to be the geometric manifestation of the D0-D4 black hole states. Unfortunately, the entropy that we got after counting the number of states of these geometries was far less than the horizon area of the D0-D4 black hole. We believe that such mismatch is due to the limitation of supergravity. In other words, we conjecture that to account for the entropy of these class of black holes we need stringy degrees of freedom. We have also given a free field estimate of an upper bound on the number of states accessible in super gravity which scales precisely like our wrong entropy.

We have also managed to check in a simple case that quantum fluctuations of the 1/2-BPS solutions of $\mathcal{N} = 2$ four-dimensional supergravity are enhanced and can be macroscopically large.

SAMENVATTING

De geschiedenis van de natuurkunde leert ons dat het ophelderen van schijnbare puzzels en paradoxen een uitstekende manier is om nieuwe kanten van de natuur te leren kennen. Dit proefschrift beschrijft zwarte gaten en de daaraan gerelateerde puzzels en paradoxen, waarvan de oplossing ons belangrijke informatie kan opleveren in de mysterieuze theorie die we “*kwantumzwaartekracht*” noemen. In dit hoofdstuk geven we een kort overzicht van de inhoud van dit proefschrift.

HET ENIGMA VAN ZWARTE GATEN

Zwarre gaten zijn één van die fysische objecten die zowel uitgebreid bestudeerd als slecht begrepen zijn. Het theoretisch onderzoek aan zwarte gaten heeft sinds de voorspelling van hun bestaan tot diverse verrassingen geleid. De klassieke kant van hun verhaal bereikte een hoogtepunt met de zogeheten “*geen-haar stelling*” en de “*wetten van de mechanica van zwarte gaten*”. Die laatsten suggeren dat het zwarte gat zich misschien wel als een thermodynamisch object zou kunnen gedragen – in ieder geval op het niveau van deze formules – als we de oppervlakte van de horizon met de entropie en de oppervlaktezwaartekracht met de temperatuur identificeren. Aan de andere kant impliceren de geen-haar stelling (leidend tot een entropie die identiek nul is) en het idee dat zwarte gaten ‘zwart’ zijn (dus geen straling uitzenden) dat de analogie met de thermodynamica niet dieper zou kunnen zijn dan het niveau van deze formules. Een totaal onverwachte ontwikkeling in de studie van zwarte gaten ontstond echter toen Hawking kwantumveldentheorie in de zwart-gat achtergrond bestudeerde. Zijn studie liet een nieuw gezicht van zwarte gaten zien: een “*wit gezicht*”. Het bleek dat zwarte gaten niet totaal zwart waren, maar Hawking-straling uitzenden. Dat werkt als volgt: een deeltje-antideeltje-paar wordt geproduceerd achter de horizon, en terwijl het deeltje uit het zwarte gat ontsnapt verdwijnt het antideeltje achter de horizon van het zwarte gat.

De ontdekking van de witte kant van zwarte gaten opende een doos van Pandora van

paradoxen die de focus is van een nu al dertig jaar durende studie. Deze paradoxen zijn:

- **De paradox van de entropie:** Met de ontdekking van Hawking-straling werd de thermodynamische natuur van zwarte gaten gepromoveerd van een oppervlakkige gelijkenis op het niveau van de formules tot een een fysische equivalentie. De oppervlakte van het zwarte gat wordt nu geïdentificeerd met diens entropie, maar dit leidt tot de volgende twee paradoxen. Allereerst verbiedt de geen-haar stelling dat zwarte gaten entropie hebben en dit botst met de thermodynamische natuur van zwarte gaten. Ten tweede is de entropie een extensieve grootheid die daarom natuurlijkerwijs evenredig zou moeten zijn met het volume in plaats van met de oppervlakte van het zwarte gat.
- **De paradox van informatieverlies:** Het blijkt dat het zwarte gat zijn massa verliest door de Hawking-straling. Het eindpunt van dit proces is de complete verdamping van het zwarte gat, tenminste op details gerelateerd aan fysica voorbij de Planck-schaal na. Omdat het uitgezonden deeltje gecorreleerd is met het antideeltje dat in het zwarte gat verdween leidt zo'n complete verdamping van het zwarte gat echter tot het vernietigen van een deel van de informatie en dus tot informatieverlies.
- **De singulariteit van het zwarte gat:** In tegenstelling tot de bovenstaande paradoxen heeft deze niets te maken met de semiklassieke benadering van kwantumzwaartekracht. Elk zwart gat heeft een singulariteit waar de kromming divergeert. Op dit moment weten we niet hoe we natuurkundige wetten kunnen formuleren in de buurt van zo'n gebied...

De thermodynamische natuur van zwarte gaten suggereert dat de geometrie van het zwarte gat wel eens een effectieve beschrijving zou kunnen zijn van een onderliggend microscopisch systeem, net zoals in de statistische fysica waar de thermodynamische wetten precies zo'n effectieve beschrijving zijn van een complex microscopisch systeem. Het hoofdonderwerp van dit proefschrift was het onderzoeken van zo'n mogelijke beschrijving in het "fuzzball" scenario.

HET ONORTHODOXE FUZZBALL-SCENARIO

Gemotiveerd door de zoektocht naar een beter begrip van het D1-D5 systeem, een zogeheten "*klein zwart gat*", en in het kader van de AdS/CFT dualiteit, kwamen Mathur et al. met het onorthodoxe "*fuzzball-scenario*". Hun bewering is dat het zwarte gat een effectieve beschrijving is van een exponentieel aantal 'gladde' geometrieën met dezelfde asymptotische ladingen als het zwarte gat. Deze gladde geometrieën worden normaal gesproken de 'toestanden' van het zwarte gat genoemd,

hoewel het geen kwantumtoestanden zijn in de gebruikelijke zin van het woord. In gunstige omstandigheden zijn deze geometrieën manifestaties van coherente toestanden van het onderliggende microscopische systeem van het zwarte gat. De geometrieën verschillen alleen significant van de zwart-gat geometrie in een compact gebied van de ruimtetijd, begrensd door een oppervlak dat de “*uitgerekte horizon*” wordt genoemd. Buiten dit oppervlak lijken alle toestandsgeometrieën al heel snel op de zwart-gat geometrie, zodat de resultaten van metingen gedaan in beide geometrieën niet van elkaar verschillen.

Laten we nu bestuderen wat het fuzzball-scenario te zeggen heeft over de hierboven vermelde paradoxen.

- **Fuzzballs en de paradox van de entropie:** In het fuzzball-scenario geeft het aantal zwart-gat toestanden in principe de statistische verklaring van de entropie van het zwarte gat. In deze beschrijving ontbreekt echter nog een afdoende verklaring van het tweede deel van de paradox van de entropie, namelijk het feit dat de entropie evenredig is met de oppervlakte van de horizon.
- **Fuzzballs en de paradox van informatieverlies:** Omdat de toestandsgeometrieën glad zijn is er geen informatieverlies. Het invallende deeltje is lange tijd gevangen in een gecompliceerde toestandsgeometrie, maar ontsnapt uiteindelijk naar oneindig via een proces dat vergelijkbaar is met Hawking-straling. Het fuzzball-idee voorspelt ook grote kwantumfluctuaties in de grootte van de horizon, wat mogelijk verklaart waarom de semiklassieke benadering hier niet toereikend is.
- **Fuzzballs en de singulariteit van het zwarte gat:** In het fuzzball-scenario is de singulariteit in beginsel afwezig omdat de toestandsgeometrieën glad zijn. De singulariteit is een emergent fenomeen dat verschijnt door de effectieve beschrijving van de toestanden van het zwarte gat.

In dit proefschrift wordt, binnen het fuzzball-scenario, het idee dat zwarte gaten een effectieve beschrijving zijn van een onderliggend microscopisch systeem uitgewerkt voor enkele simpele systemen: het D1-D5 systeem en de 1/2-BPS zwarte gaten in vier-dimensionale supergravitatie.

HET ELEGANTE D1-D5 SYSTEEM

Het D1-D5 systeem bleek een erg succesvolle basis om het fuzzball-idee te testen. Vanwege de eenvoud van de oplossing van de supergravitatie-vergelijkingen was het mogelijk om over geometrieën te middelen. Door geschikte gewichten van de gladde D1-D5 geometrieën te kiezen konden we gemiddelde geometrieën construeren die asymptotisch lijken op het kleine vijf-dimensionale zwarte gat en de zwarte ring.

Het woord “klein” betekent hier dat de oppervlakte van de horizon van deze zwarte objecten nul is als men zich beperkt tot vijfdimensionale supergravitatie. De zwarte ring, daarentegen, is een zwart object waarbij de topologie van de horizon $S^2 \times S^1$ is, in tegenstelling tot een zwarte gat met een horizontopologie van S^3 . Dit zijn vijf-dimensionale oplossingen en het zijn de eerste oplossingen die de geen-haar stelling schenden, omdat zij een extra niet-behouwen “dipool”-lading hebben die, hoewel onzichtbaar vanaf oneindig, voorkomt in de eerste wet van de mechanica van zwarte gaten.

De effectieve geometrie die we verkregen verschilt van de naïeve zwart-gat geometrie door een exponentieel smalle term die zorgt dat de geometrie glad blijft waar anders de singulariteit zou ontstaan. We hebben ook een versie van de geen-haar stelling ontdekt en we vonden dat de effectieve geometrie in het algemeen afhangt van slechts drie ladingen, de massa en het impulsmoment (beiden zichtbaar vanaf oneindig) en een “dipool”-lading die de grootte van de “kern” van de geometrie bepaalt.

We hebben ook gevonden dat we geen gewichten aan het D1-D5 systeem kunnen toekennen zodanig dat de effectieve geometrie een conisch defect vertoont met een een willekeurige openingshoek, behalve als deze $2\pi/n$ bedraagt, met n een integer.

DE WEG NAAR ALLEDAAGSE ZWARTE GATEN

Hoewel het D1-D5 systeem verschillende succesvolle toetsen van het fuzzball-scenario heeft doorstaan, kan men zich voorstellen dat het te “goed” is om de vragen van de fysica van echte zwarte gaten te beantwoorden. Dit is met name omdat de oppervlakte van de horizon identiek nul is, alsmede het feit dat dit systeem BPS is en acht behouden superladingen heeft. Omdat een analoge beschrijving van realistische zwarte gaten technisch momenteel niet haalbaar is, kozen we er in dit proefschrift voor om te beginnen met een kleine stap in deze richting. We hebben ervoor gekozen om BPS zwarte gaten te beschrijven met minder, namelijk vier, behouden superladingen. Deze aanpak staat ons toe om zwarte gaten te bestuderen met een macroscopische oppervlakte van de horizon, omdat zulke zwarte gaten in deze klasse van BPS-oplossingen voorkomen.

Het blijkt dat vierdimensionale $\mathcal{N} = 2$ supergravitatie niet alleen 1/2-BPS oplossingen heeft die een enkel zwart gat beschrijven, maar ook zogeheten “multi-centered” oplossingen die gezien kunnen worden als gebonden toestanden van meerdere zwarte gaten. In dit proefschrift beschreven we een procedure voor de kwantisatie van deze oplossingen. Met deze kwantisatie konden we het aantal BPS toestanden tellen dat gerelateerd is aan de externe vrijheidsgraden van deze oplossingen. Hoewel

Samenvatting

alleen een bepaalde klasse van deze multi-centered oplossingen is gekwantiseerd, namelijk die met zekere mathematische eigenschappen, bevat deze klasse interessante multi-centered oplossingen die men met de geometrische vorm van de D0-D4 zwart-gat toestanden kan associëren. Helaas was de entropie die we verkregen door het tellen van het aantal toestanden van deze geometrieën veel minder dan de oppervlakte van de horizon van het D0-D4 zwarte gat. Wij denken dat het verschil te verklaren is door de beperkte geldigheid van supergravitatie, en dus dat er snaar-achtige vrijheidsgraden nodig zijn om de entropie van deze zwarte gaten microscopisch te verklaren. We hebben ook een vrij-veld schatting gegeven van de bovengrens van het aantal toestanden dat in supergravitatie gevonden kan worden en deze komt precies overeen met onze “verkeerde” entropie.

We hebben ook in een simpel geval geverifieerd dat kwantumfluctuaties van de 1/2-BPS oplossingen van vierdimensionale $\mathcal{N} = 2$ supergravitatie versterkt kunnen worden tot macroscopische afmetingen.

ACKNOWLEDGEMENTS

Deepest appreciation to my supervisor Jan de Boer for his guidance, diligence, and helpful advises throughout my stay as a PhD student here in Amsterdam, for without him and his help I would not have made it this far. I am also very grateful for all the time and effort he spent reading thoroughly, commenting and giving very helpful tips and insights from the very first draft of this thesis.

Many thanks to my collaborators: Luis Fernando Alday, Vijay Balasubramanian, Frederik Denef, Sheer El-Showk, and Dieter Van den Bleeken; working with you was both stimulating and productive.

I am grateful to Marika Taylor and Bernard de Wit for comments on an earlier version of this thesis.

Special thanks to Sheer El-Showk, Lotte Hollands, and Amir-Kian Kashani-Poor for useful discussions and clarifications about different mathematical and physical notions. I am also grateful to Xerxes Arsiwalla, Iosif Bena, Micha Berkooz, Joost Hoogeveen, Ingmar Kanitscheider, Jan Manschot, Suresh Nampuri, Kyriakos Papadodimas, Balt van Rees, and Masaki Shigemori for all the instructive and constructive physics discussions.

I am also indebt to all the members of ITFA, university of Amsterdam in the years 2004-2009, for the friendly, warm and stimulating environment, thanks a lot. Special thanks to Leo Kampmeijer, Meidert van der Meulen, and Balt van Rees for making my stay in Amsterdam fun. Thank you also for the different Dutch-English translations.

Among people mentioned above, Balt and Sheer thanks for being my paramimfs. Also thanks for the Dutch translation of the summary of this thesis, Balt.

Last but not least, I am very grateful to my family who was very supportive and encouraging even beings leagues away. Thanks for my parents for keeping faith in me, my brother Moussaab for spending time helping me out with English details.

Acknowledgements

My big family, you have been a constant source of support and encouragement, to all of you: Thanks a lot.

And to all of you whom I did not mention, know that you were not nor will you be forgotten for all the help you gave me.